MODELING OF THE LINEAR VISCOELASTIC RESPONSE OF POLYMER MODIFIED ASPHALT BINDERS AT INTERMEDIATE AND HIGH TEMPERATURES

by

Fariborz Gahvari

Dissertattion submitted to the Faculty of the Virginia Polytechnic Institute and State University in partial fulfillment of the requirements for the degree of

Doctor of Philosophy
in
Civil Engineering

APPROVED:

Imad L. Al-Qadi, Associate Professor
of Civil Engineering, Chairman

David A. Dillard, Professor of
Engineering Science and Mechanics

Donald R. Drew, W. Thomas
Rice Professor of Civil Engineering

Surot Thangjitham, Associate Professor
of Engineering Science and Mechanics

Richard D. Walker, Professor of
Civil Engineering

April 1996

Blacksburg, Virginia

Keywords: Asphalt, Polymer, Viscoelasticity

MODELING OF THE LINEAR VISCOELASTIC RESPONSE OF POLYMER MODIFIED ASPHALT BINDERS AT INTERMEDIATE AND HIGH TEMPERATURES

by

Fariborz Gahvari

Imad L. Al-Qadi, Chairman

Civil Engineering

(ABSTRACT)

An experimental study was conducted to characterize the dynamic mechanical properties of polymer modified asphalt binders at intermediate and high service temperatures. A typical paving grade asphalt and seven different elastomeric modifiers were used. The modifiers, representing a wide variety of random copolymers and thermoplastic block copolymers, were blended with asphalt at three concentration levels to yield a total of twenty one mixes. The effect of short term aging was simulated by the rolling thin film oven test (RTFOT) procedure. A dynamic shear rheometer with parallel plate configuration was used to conduct the dynamic mechanical tests at frequencies between 0.06 to 188.5 rad/s and temperatures ranging from 5 to 75° C. After establishing the linear viscoelastic range of response through performing stress sweeps, a series of frequency sweeps was carried out. Investigation of the resulting isothermal response curves indicated that simple time-temperature superposition is applicable, and dynamic master curves can be constructed by empirical superposition.

Effects of polymer type, polymer content, and aging treatment on the behavior of dynamic master curves and relaxation spectra were studied. Feasibility of using the current mathematical models of frequency dependence to characterize the experimental dynamic master curves of modified binders was investigated. These models were generally found inadequate in representing the behavioral complexities of modified binders.

To address this inadequacy, two new analytical expressions were developed to represent the dynamic storage shear modulus and dynamic loss shear modulus of polymer modified asphalts. The predictive capability of the developed equation for storage modulus is high for moduli below 10^8 Pa. The developed model for loss modulus was found to be accurate over the entire range of measured moduli. A procedure for application of these models to practical engineering problems was presented.

The measured shift factor data was used to study the dependency of the viscoelastic response on temperature variations. It was observed that this dependency is dominated by the asphalt phase. Within the studied range of temperatures, the WLF equation with universal constants was found to be adequate in describing the temperature dependence of response.

Dedication

This dissertation is dedicated to my parents Aghajan and Mariette Gahvari.

Acknowledgments

The author would like to express his gratitude to the chairman of his committee, Dr. Imad L. Al-Qadi for his support and encouragement. Thanks are also due to the committee members, Drs. David A. Dillard, Donald R. Drew, Surot Thangjitham, and Richard D. Walker for their helpful comments.

The author would like to extend his deep appreciation to his parents (to whom this dissertation is dedicated), and to his brothers and sisters for their love and support, without which, this work would have never seen the light of day.

Table of Contents

List of Figures

List of Tables

Chapter 1
Introduction

1.1. Background

Highways are a major component of the world's infrastructure. In United States, more than 94% of the surfaced roads are covered with flexible pavements (FHWA, 1990). These pavements experience a variety of distresses including cracking, permanent deformation (rutting), stripping, and raveling. In recent years, increasing traffic volumes, heavier axle loads, and higher tire pressures have dramatically aggravated the problem. Each year, millions of dollars are spent for repair, maintenance and rehabilitation of premature distressed pavements. Design and construction of roads with longer service lives have always drawn the attention of engineers. Selecting appropriate highway materials considering climatic and loading conditions can significantly contribute to the fulfillment of this goal and optimize the life-cycle costs of pavements.

Hot mix asphalt (HMA) is a mixture of asphalt binder and aggregate. Therefore, its performance is a function of properties and interaction of these two materials. However, in a number of cases, the asphalt binder plays the major role in the mix performance. For instance, it is documented that asphalt binder is fundamentally responsible for mix fracture under thermally induced stresses (Hills, 1974). Thus, the low temperature characteristics of the mix are predominantly controlled by the binder. Although permanent deformation

of flexible pavements has a more complicated mechanism and is a function of several variables in the HMA layer as well as underlying layers, the significance of binder properties in rut resistance has been stressed by many investigators (Jacobs, 1981; Speer *et al.*, 1963; Tada, 1985). These facts highlight the importance of studying the rheological properties of asphalt binders and attempt to improve them.

For several decades, blending different types of asphalt was the only way to obtain desirable properties. In recent years, advances in polymer technology and increasing use of polymers in different branches of industry, has brought up another opportunity for pavement engineers, i.e., the polymer modification of asphalt cements. In literature, there have been up to 22 suggested benefits attributed to modifying asphalts with polymers (Lewandowski, 1994). Improved rut resistance, decreased thermal and fatigue cracking potential, enhanced stripping resistance and reduced temperature susceptibility are among the suggested advantages of polymer modification of asphalts.

On the effectiveness of polymer modification on performance improvement of asphalt cements, there is no consensus among different investigators. While significant improvement in permanent deformation resistance due to polymer modification has been emphasized by many researchers (Fleckenstein *et al.*, 1992; Srivastava *et al.*, 1992; Khosla, 1991; Little, 1992), others report no considerable reduction in rut depth (Al Dhalaan *et al.*, 1992) and, in some cases, adverse effects on performance resulted from adding polymers (Brown *et al.*, 1992). Similarly, other binder associated problems such as

temperature susceptibility, aging effect, thermal and fatigue cracking resistance, etc., have been controversially discussed. This stems from several facts, part of which can be summarized as follows:

1. Drawing conclusions based on small scale laboratory experiments, i.e., limited number of tests, polymer-asphalt combinations, etc.
2. Selecting wrong polymeric modifiers for specific distress types.
3. Adopting testing methods which do not address the distress mechanism precisely.
4. Failure in establishing correlation between laboratory results and field performance.
5. Most importantly, lack of rational understanding of the behavior of polymer modified asphalt as a viscoelastic material and making inappropriate research approaches.

1.2. Problem Statement

Asphalt cement has a complicated behavior. It acts as a viscous fluid at elevated temperatures, a viscoelastic material above the glass transition temperature (Wada and Hirose, 1960), and a brittle elastic material at extremely low temperatures (Goodrich, 1991). Incorporating polymer into asphalt results in a new material which exhibits even more complexity in behavior.

Efficient application of a viscoelastic material without characterizing its response over a wide range of temperature and loading time (frequency) is not possible. A number of

mathematical models have been proposed to represent the time (frequency) dependency and temperature dependency of straight asphalts (Jongepier and Kuilman, 1969, 1970; Dobson, 1969; Dickinson and Witt, 1974; Christensen and Anderson, 1992), however, no models have been developed to describe the linear viscoelastic response of polymer modified asphalt binders.

1.3. Objectives

The objectives of this research are first characterizing the linear viscoelastic response of polymer modified asphalt binders at intermediate and high service temperatures, and over a wide range of frequencies. Secondly, developing mathematical models to represent the frequency dependence of response. Thirdly, proposing a procedure for complete characterization of response based on a limited number of dynamic measurements. Finally, investigating the temperature dependence of response and applicability of classical models.

1.4. Scope

To achieve the objectives of this study, dynamic mechanical analysis was conducted on asphalt-polymer blends at frequencies between 0.06 to 188.5 rad/s and temperatures ranging from 5 to 75° C. Several mixes were prepared using one viscosity graded asphalt cement and seven different polymeric modifiers. The modifiers were thermoplastic block copolymers and random copolymers which are most commonly used in industry. The

selected polymers represent a wide range of chemical structures and mechanical and physical properties. Each polymer was blended with asphalt cement at three different concentration levels. The effect of short term aging on the rheological properties of binders was simulated by the Rolling Thin Film Oven Test (RTFOT) procedure in accordance with ASTM D 2872 (Annual Book of ASTM Standards, 1991).

This study is restricted to the linear range of response. In order to establish the linear viscoelastic range of response, stress sweeps were performed over the entire range of temperatures and at selected frequencies. Based on the results, frequency sweeps were carried out at all temperatures. The primary results of frequency sweeps, i.e., the isothermal graphs of dynamic storage shear modulus and dynamic loss shear modulus versus frequency were obtained. Time-temperature superposition principle was applied to develop master curves of dynamic moduli over several decades of reduced frequency. Characterization of response was possible by interpretation of the dynamic master curves. Two mathematical models were proposed to describe the frequency dependence of response. The models were evaluated and validated through rigorous statistical analyses.

During the course of developing master curves, the amount of shift factors were measured and plotted against temperature as a measure of temperature dependence of response. The applicability of a classical model of temperature dependence to the shift factor data was investigated.

A procedure was developed to characterize the response based on three dynamic measurements at a single temperature. The feasibility of the proposed procedure was assessed. It was concluded that for most engineering purposes, the proposed mathematical models and characterization procedure can represent the response with reasonable accuracy.

This dissertation is comprised of six chapters. General description of the structure of asphalt and polymeric modifiers, an overview of the linear viscoelastic theory with applications to asphalt binders, and discussion of the current research on straight and modified asphalts including the approach to the modeling problem are presented in Chapter 2. Chapter 3 describes the materials and instruments used in this study, explains the experimental program in detail, and elaborates the process of acquisition and primary analysis of data. In Chapter 4, after explanation of inadequacies of the current mathematical models, two new analytical expressions for frequency dependence are introduced, the characteristics and limitations of proposed models are described, observations on temperature dependence of response are presented, and applicability of a classical model to this dependency is investigated. Furthermore, in this chapter, a procedure for practical application of the proposed models based on a limited number of dynamic measurements is outlined. Chapter 5 presents the evaluation and validation of proposed models by means of various statistical methods, and assessment of the proposed characterization procedure through comparison between predicted and measured data.

Chapter 6 contains the summary, findings and conclusions of this study along with recommendations for further research.

Chapter 2
Present State of Knowledge

2.1. Introduction

Asphalt is one of the oldest binders used in the human's history. The unique adhesive and waterproofing features of asphalt cement has been the basis of its use for roofing and paving purposes. Flexible pavements, while providing a smooth and comfortable surface for users should be flexible enough to withstand the vehicle loads without fracture of the surface, and rigid enough to resist excessive deflections. Asphalt cement can affect the desirable properties of the hot mix asphalt layers of flexible pavements.

For years, studying the properties of asphalt as a traditional binder was possible through conventional tests which were mostly empirical in nature. Complexity in the behavior of asphalt which stems from its complicated composition, necessitates more sophisticated testing and analysis techniques. This need is particularly more pronounced when advanced materials like polymers are introduced to asphalt to improve its properties.

Prior to any attempt to characterize the behavior of a composite material, a thorough understanding of the structure and properties of its components is necessary. Furthermore, the theories that describe this behavior should be well understood. The main objectives of this chapter are the description of the structure of asphalt and polymers used

in this study, an overview of some aspects of the linear viscoelastic theory, and finally, a discussion of the current research on the rheology of asphalt binders.

2.2. Asphalt Cement

2.2.1. Nature of Asphalt Cement

Rhelogical properties of asphalt cement are closely related to its chemical composition. Therefore, to better understand the asphalt behavior, an overview of the microstructure of this material is necessary.

Asphalt cement is basically composed of hydrocarbon molecules, along with small percentages of sulfur, nitrogen and oxygen. The last three elements are called heteroatoms and may have considerable effects on asphalt properties. In addition to heteroatoms, some heavy metals such as nickel and vanadium may exist in very small amounts (Halstead, 1985).

A large variety of molecular structures are found in asphalt. Therefore, a thorough identification and classification of all these structures is an extremely difficult task. As an alternative, the asphalt constituents are commonly grouped in generic fractions based on polarity and solubility. On this basis, asphalt is considered to be comprised of three fractions: asphaltenes, resins and oil. Asphaltenes are high-polar high molecular weight

hydrocarbons surrounded by moderately polar aromatic molecules and dispersed in the continuous non-polar oily phase. Resins are semi-solid fraction acting as a peptizing agent which keeps the asphaltene molecules from coagulation (Krebs and Walker, 1971).

This explanation is based on the traditional colloidal (micellular) model for asphalt microstructure (Nellensteyn, 1923). According to this model, the degree of effectiveness of resins in keeping asphaltene fraction dispersed in oil can highly affect the rheology of asphalt. Asphalt cements containing highly peptized asphaltenes generally exhibit Newtonian behavior, while non-Newtonian flow is usually the characteristic of asphalts with low dispersed asphaltenes (Roberts *et al.*, 1991). Furthermore, the physical properties of asphalt is a function of the relative proportion of fractions. Figure 2.1 shows the schematic of colloidal model.

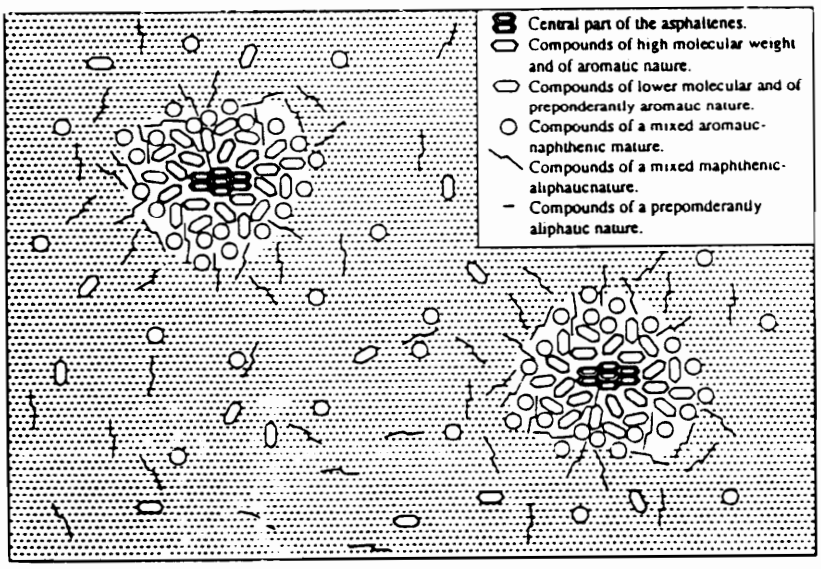

Figure 2.1. Schematic of Colloidal Model for Asphalt Cement (After SHRP, 1990)

Another model for asphalt microstructure which has recently been suggested (Anderson *et al.*, 1991) is the dispersed polar fluid model and accounts for some important features of the viscoelastic behavior of asphalt. According to this model, molecules of varying size and polar functionality are continuously distributed in a fluid phase. Interaction of the molecules through various levels and types of bonding is considered to be the source of viscoelastic nature of asphalt cement.

2.2.2. Conventional Asphalt Cement Tests

A number of testing methods have been traditionally used to characterize the physical properties, consistency and aging of asphalt cements. Temperature susceptibility parameters of asphalt are derived based on the results of penetration and viscosity tests. Furthermore, these tests have served as the basis for traditional grading systems of asphalt. Softening point of asphalt as a consistency measure has been widely used in Europe for specification purposes. Of particular interest, is the effects of aging on the rheological properties of asphalt. This section presents a summary of the conventional consistency and aging tests.

2.2.2.1. Consistency Tests

Penetration test is a strictly empirical measure of consistency of asphalt. According to ASTM D 5 (Annual Book of ASTM Standards, 1991), penetration is defined as the

amount of penetration of a standard needle loaded with a 100 g weight in the asphalt sample for 5 seconds. Test is usually performed at 25° C. However, other temperatures with different needle loads and penetration times may be used as well.

Absolute viscosity is measured in accordance with ASTM D 2171 (Annual Book of ASTM Standards, 1991) using a U-shaped capillary tube viscometer. Asphalt at a temperature of 60° C is poured into the large tube of viscometer, and rises in the capillary tube under application of vacuum. The measured time of flow between two successive timing marks on the capillary tube is multiplied by the calibration factor of viscometer to yield the viscosity of asphalt in units of poises. Absolute viscosity provides basis for a widely used asphalt grading system. Based on the viscosity grading system, the paving grade asphalts are classified into six groups of AC-2.5, AC-5, AC-10, AC-20, AC-30 and AC-40, where the numbers refer to the viscosity of original binder in units of 100 poises.

According to ASTM D 2170 (Annual Book of ASTM Standards, 1991), kinematic viscosity test is performed at 135° C. A cross-armed viscometer is used, and asphalt flows in the capillary tube due to gravity force rather than vacuum application. Other than this, the procedure is similar to the absolute viscosity test. Kinematic viscosity is usually defined in units of centistokes.

Softening point is an empirical test which is performed in accordance with ASTM D 36 (Annual Book of ASTM Standards, 1991). It measures a temperature at which the

asphalt phase changes from semi-solid to liquid. At softening point, the asphalt sample placed in a brass ring, can no longer support the weight of a steel ball, and consequently flows.

The viscoelastic behavior of asphalt binders is more complicated to be described by simple traditional measures of consistency such as penetration and softening point. Viscosity at 60° C and 135° C, although a fundamental rheological parameter, is not capable of characterizing the response with respect to varying shear rates, loading times and temperatures. Dynamic mechanical analysis is currently the most efficient method to provide complete rheological data on asphalt binders.

2.2.2.2. Aging Tests

Short term aging of asphalt cement usually takes place in the mixing plant and during hauling and lay-down of HMA. Furthermore, asphalt cement undergoes a long term aging during the service life of flexible pavements. Aging can significantly affect the rheological properties of asphalt. The effect of aging is mostly pronounced in increasing the stiffness and viscosity, and decreasing the penetration value.

There are two standard test methods to simulate the short term aging of asphalt, namely thin film oven test (TFOT), and rolling thin film oven test (RTFOT). According to ASTM D 1754 (Annual Book of ASTM Standards, 1991), in the thin film oven test a thin circular

film of asphalt is aged for 5 hours on a rotating shelf inside an oven maintained at 163° C. The rolling thin film oven test, which is performed in accordance with ASTM D 2872 (Annual Book of ASTM Standards, 1991), is a variation of the previous test. In this test, a certain amount of asphalt is poured in a bottle and placed on a rotating rack inside an oven maintained at 163° C. While rotating, a hot air jet with a specified discharge is blown into the sample. The testing time is 75 minutes.

Long term aging of asphalt is simulated by a pressurized aging vessel (PAV). According to AASHTO PP1 (AASHTO Provisional Standards, 1994), a specified thickness of residue from the RTFOT or TFOT is placed in standard TFOT pans and aged at the specified temperature for 20 hours in a vessel pressurized with air to 2.10 MPa. Aging temperature is selected based on the grade of asphalt.

The aged asphalt obtained from any of these three procedures can be further tested to detect changes in viscosity, penetration and stiffness or complex moduli.

2.3. Polymers

Polymers are large chain-type molecules formed by conjunction of small chemical units, called monomers. Polymers used in the asphalt industry can be classified based on different criteria (King and King, 1986; Lewandowski, 1994). One method is classifying them in two general categories: elastomers and plastomers. The mechanism of resistance

to deformation is different between elastomeric and plastomeric polymers. The load-deformation behavior of elastomers is similar to that of a rubber band, i.e., increasing tensile strength with increased elongation and ability to recover to the initial state after removal of load. Under a given load, elastomers deform faster than plastomers and recover elastically after withstanding large strains. Plastomers, on the other hand, exhibit high early strength but are less flexible and more prone to fracture under large strains compared to elastomers (King and King, 1986).

Major elastomeric modifiers are: styrene-butadiene-styrene (SBS), styrene-isoprene-styrene (SIS), styrene-ethylene/butylene-styrene (SEBS), and styrene-butadiene rubber (SBR). Plastomerics include: ethylene-vinyl-acetate (EVA), polyvinylchloride (PVC), and polyethylene/polypropylene.

In this study, only elastomeric modifiers are addressed. The reasons for this selection is discussed in Chapter 3 of this dissertation. The molecular structure and mechanical properties of two widely used categories of elastomeric modifiers, namely thermoplastic block copolymers (thermoplastic elastomers) and random copolymers will be briefly discussed in the following section.

2.3.1. Thermoplastic Block Copolymers

Thermoplastic block copolymers are produced through a programmed process of reacting monomers together. There are three general structures for block copolymers. The most common, is a triblock linear structure A-B-A, where A is a thermoplastic end-block such as polystyrene and B is a rubbery mid-block like polybutadiene or polyisoprene. Examples of triblock copolymers are styrene-butadiene-styrene (SBS) and styrene-isoprene-styrene (SIS). By hydrogenation of the rubbery mid-block, another version of these copolymers can be generated, i.e., styrene-ethylene/butylene-styrene (SEBS) and styrene-ethylene/propylene-styrene (SEPS). This structure represents a two-phase system in which the rubbery mid-block forms a continuous phase of three-dimensional elastomeric network containing the dispersed end-block phase (Holden *et al.*, 1969). The second structure is a radial or branched system of $(A\text{-}B)_n$ type; $(SB)_n$ and $(SI)_n$ are examples of this system. The third structure is a linear diblock A-B type; SB, SEP and SEB represent the famous copolymers of this type.

The process of synthesizing these copolymers is a rather complicated one. First, through anionic polymerization, a polystyrene block of desired molecular weight is created. Then, a rubbery mid-block (isoprene or butadiene) is polymerized on the existing polystyrene block resulting in a diblock unit. Finally, by means of various coupling agents, the diblocks are linked together to form triblock or radial copolymers (Collins and Mikols, 1985). Figure 2.2 shows a schematic of this procedure.

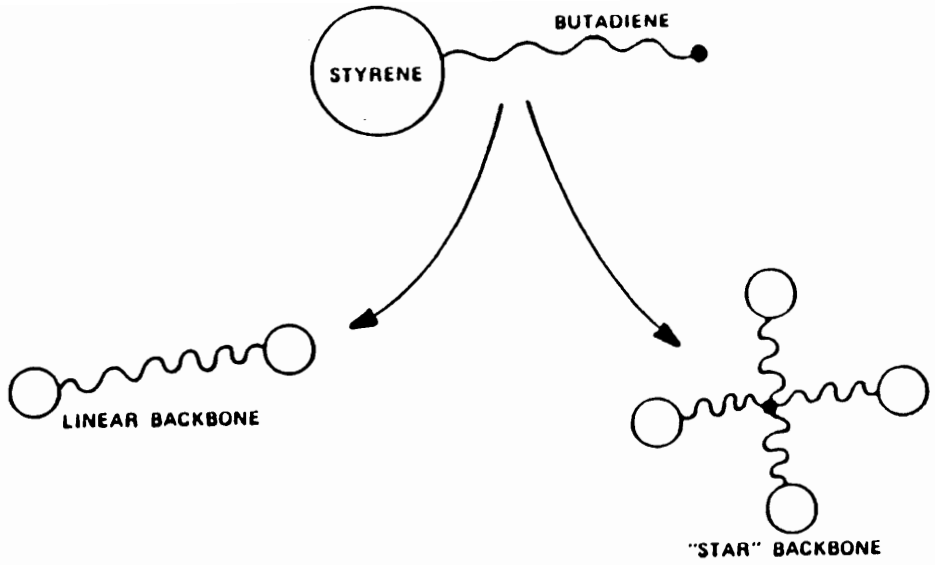

Figure 2.2. Backbone Structure of Thermoplastic Block Copolymers (After Collins and Mikols, 1985)

Due to thermodynamic incompatibility between polystyrene end-blocks and rubbery mid-block, the former are associated in rigid domains. At temperatures below the glass transition temperature of polystyrene (100° C), these "rigid" domains act as physical cross-links connected by rubbery "springs", i.e., a three dimensional rubbery system. When heated to temperatures above 100° C, the rigid domains soften and in the presence of shear, polymer can be incorporated into asphalt. After cooling, the process is reversed, i.e., the rigid domains and the network reform and impart elasticity and tensile strength to the blend (Collins and Mikols, 1985; Shuler *et al.*, 1987). Figure 2.3 illustrates a schematic of the morphology of block copolymers.

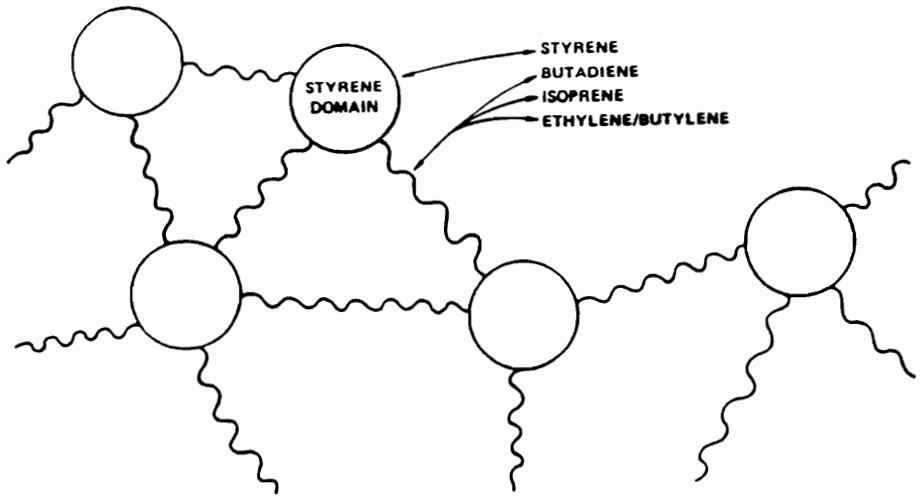

Figure 2.3. Morphology of Block Copolymers (After Collins and Mikols, 1985)

It should be noted that the block lengths and weight fractions of styrene and rubber can significantly affect the mechanical properties and performance of the resulting block copolymer. It has been shown that increasing styrene/rubber ratio results in increasing moduli and ultimate tensile strength and decreased flexibility of copolymer (Holden *et al.*, 1969). At higher styrene contents, polystyrene becomes the continuous matrix and rubber forms the dispersed phase resulting in a copolymer which shows neither the thermoplasticity of polystyrene nor the elastomeric properties of rubber (Bishop and Davison, 1969). Figure 2.4 shows the stress strain curve for SBS copolymers containing various styrene fractions.

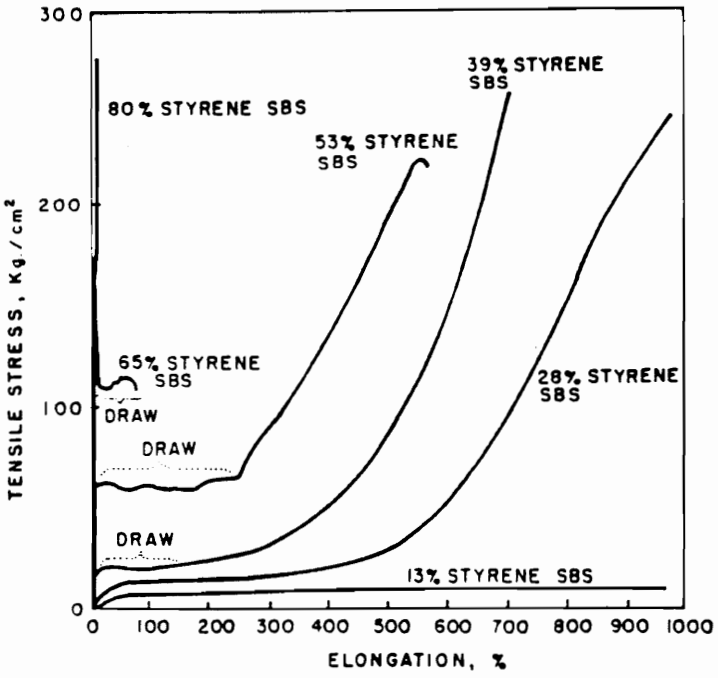

Figure 2.4. Stress-Strain Curves (at 5 cm/min) for SBS Copolymers of Various Styrene Contents (After Holden *et al.*, 1969)

2.3.2. Random Copolymers

Unlike block copolymers, random copolymers are synthesized by statistical placement of the monomer units along the chain backbone (Noshy and McGrath, 1977). An example is styrene-butadiene rubber (SBR) which is formed by randomly reacting styrene and butadiene together. This is an easier and more economical method compared to the block copolymerization process. Random copolymers are homogeneous systems which exhibit characteristics between two extremes of the reacting monomers. Therefore, behavior of

SBR is somewhere between the flexibility of butadiene and stiffness of styrene, and is a function of relative proportion of these two. In contrast to block copolymers, random copolymers do not create a network and have a single-phase morphology.

2.4. Overview of the Linear Viscoelastic Theory

Strain response of a linear elastic material to an arbitrary stress input is not time dependent and is in phase with the applied stress. In other words, under a constant suddenly applied load, an elastic material will deform instantaneously, maintains constant deformation, and upon removal of the load returns to its initial configuration. On the other hand, in a linear viscous material, the strain response is time dependent and out of phase with respect to the stress input. If subjected to a constant instantaneous load, the viscous material does not show immediate response, undergoes an increasing deformation with constant rate, and when the load is removed will maintain its deformed shape.

A linear viscoelastic material exhibits a response between the two extremes of linear elastic and linear viscous responses, i.e., a time dependent behavior which includes components of both elastic and viscous behaviors. When a sudden load is applied to a viscoelastic material and is kept constant with respect to time, the material may or may not show an instantaneous deformation response, but will undergo an increasing deformation with time. Depending on the nature of material, this deformation may continue infinitely

or approach a limit, and upon removal of the load part or all of deformation will be recovered.

The behavior of viscoelastic materials including asphalt binders can be characterized by transient or dynamic response, a brief explanation of each will follow.

2.4.1. Relaxation Response

Relaxation describes the time dependent stress response of a viscoelastic material to a constant sudden strain. The applied strain can be shown as the following:

$$\varepsilon(t) = \hat{\varepsilon} H(t) \tag{2. 1}$$

where,

$\varepsilon(t)$ = uniaxial applied strain,

$\hat{\varepsilon}$ = strain magnitude,

t = loading time, s, and

$H(t)$ = unit step function defined by:

$$H(t) = \begin{cases} 1 & t \geq 0 \\ 0 & t < 0. \end{cases}$$

Under such strain, the resulting stress can be defined by the following equation:

$$\sigma(t) = \hat{\varepsilon} E(t) \tag{2. 2}$$

where,

$\sigma(t)$ = uniaxial stress output, Pa, and

$E(t)$ = relaxation modulus, Pa.

In the non-linear range of response, relaxation modulus is a function of both time and stress magnitude, i.e., $E = E(t, \hat{\sigma})$. Under shear strain, the shear relaxation modulus, $G(t)$, will represent the response.

2.4.2. Creep Response

In creep tests, a constant sudden stress is applied to material, and the resulting strain is monitored over time. The stress input can be defined as follows:

$$\sigma(t) = \hat{\sigma} H(t) \tag{2. 3}$$

where,

$\sigma(t)$ = uniaxial applied stress, Pa,

$\hat{\sigma}$ = stress magnitude, Pa,

and the remaining parameters are as defined before. Then, strain output can be described by the following equation:

$$\varepsilon(t) = \hat{\sigma} D(t) \tag{2. 4}$$

where,

$\varepsilon(t)$ = uniaxial strain output, and

$D(t)$ = creep compliance, Pa^{-1}.

In shear loading mode, the shear creep compliance, $J(t)$, will represent the creep response.

In the literature related to asphalt, use is usually made of stiffness modulus which is defined as the inverse of creep compliance:

$$S(t) = \frac{1}{D(t)} \tag{2. 5}$$

where, $S(t)$ = stiffness modulus, Pa.

At extremely short loading times, and at equilibrium, stiffness modulus and relaxation modulus are identical, i.e.,

$$S(t) = E(t) \qquad \text{for } t \to 0 \text{ and } t \to \infty \tag{2. 6}$$

At intermediate loading times, however, the two functions yield different quantities.

2.4.3. Dynamic Response

Viscoelastic behavior can be best characterized by dynamic mechanical analysis. Dynamic tests may be performed in stress controlled or strain controlled modes. In the stress controlled tests, a sinusoidal stress is applied to the sample and the resulting strain is monitored with time. Application of strain controlled tests requires a sinusoidal strain input and monitoring the stress output with time.

Considering the strain controlled mode, it is convenient to define the applied strain as the real part of a complex strain:

$$\varepsilon^* = \hat{\varepsilon} e^{i\omega t} = \hat{\varepsilon}(\cos\omega t + i \sin\omega t) \tag{2. 7}$$

$$\varepsilon(t) = \hat{\varepsilon} \cos\omega t \tag{2. 8}$$

where,

ε^* = complex strain,

$\varepsilon(t)$ = applied strain,

$\hat{\varepsilon}$ = applied strain amplitude,

t = time, s, and

ω = frequency, rad/s.

Similarly, with a complex notation, the stress output can be considered as the real part of a complex stress:

$$\sigma^* = \hat{\sigma} e^{i(\omega t + \delta)} = \hat{\sigma}[\cos(\omega t + \delta) + i \sin(\omega t + \delta)] \quad (2.\ 9)$$

$$\sigma(t) = \hat{\sigma} \cos(\omega t + \delta) \quad (2.\ 10)$$

where,

σ^* = complex stress,

$\sigma(t)$ = stress output, Pa,

$\hat{\sigma}$ = stress output amplitude, Pa, and

δ = phase angle, rad.

As mentioned earlier, in an elastic material, the applied strain and resulting stress are always in phase, i.e., $\delta = 0$ rad. In a viscous material, on the other hand, strain lags

behind stress by $\frac{\pi}{2}$ rad, i.e., $\delta = \frac{\pi}{2}$ rad. The phase angle of a viscoelastic material is always between these two extremes: $0 < \delta < \frac{\pi}{2}$.

The dynamic complex modulus can be defined as the ratio of complex stress to complex strain:

$$E^*(i\omega) = \frac{\sigma^*}{\varepsilon^*} = \frac{\hat{\sigma}}{\hat{\varepsilon}} e^{i\delta} \tag{2. 11}$$

where, $E^*(i\omega)$ = dynamic complex modulus.

The dynamic complex modulus can be conveniently resolved into two components:

$$E^*(i\omega) = E'(\omega) + iE''(\omega) \tag{2. 12}$$

where,

$E'(\omega)$ = dynamic storage modulus, Pa, and

$E''(\omega)$ = dynamic loss modulus, Pa.

$E'(\omega)$ and $E''(\omega)$ represent the in phase and out of phase components of complex modulus, respectively. Furthermore, the absolute value of complex modulus can be computed as follows:

$$\left|E^*(i\omega)\right| = \sqrt{\left[E'(\omega)\right]^2 + \left[E''(\omega)\right]^2} = \frac{\hat{\sigma}}{\hat{\varepsilon}} \tag{2. 13}$$

Comparing equations (2. 10), (2. 11) and (2. 12), and through simple mathematical manipulation it can be shown that

$$E' = \left|E^*\right|\cos\delta \tag{2. 14}$$

$$E'' = \left|E^*\right|\sin\delta \tag{2. 15}$$

$$\tan\delta = \frac{E''}{E'} \tag{2. 16}$$

where $\tan\delta$ is called loss tangent and is a measure of relative energy dissipation.

Similar equations may be derived in case of stress controlled mode:

$$D^*(i\omega) = \frac{\varepsilon^*}{\sigma^*} = \frac{\hat{\varepsilon}}{\hat{\sigma}} e^{-i\delta} \tag{2. 17}$$

$$D^*(i\omega) = D'(\omega) - iD''(\omega) \tag{2. 18}$$

$$\tan\delta = \frac{D''}{D'} \tag{2. 19}$$

where,

$D^*(i\omega)$ = dynamic complex compliance,

$D'(\omega)$ = dynamic storage compliance, Pa^{-1}, and,

$D''(\omega)$ = dynamic loss compliance, Pa^{-1}.

In dynamic mechanical analysis in shear mode, the moduli G^*, G', G'', and the compliances J^*, J', J'' represent the response. In the course of this dissertation and for simplicity, the term "complex modulus" is used to refer to the "absolute value of complex modulus". Figure 2.5 shows the schematic of a typical dynamic mechanical analysis along with the related equations.

In Figure 2.6, typical master curves of storage shear modulus and loss shear modulus for an asphalt-polymer blend are illustrated on a log-log scale. At short loading times (high frequencies), storage modulus and relaxation modulus are almost equal (Ferry, 1980):

$$G(t) \cong G'(\omega)\Big|_{\omega \to \frac{1}{t}} \tag{2. 20}$$

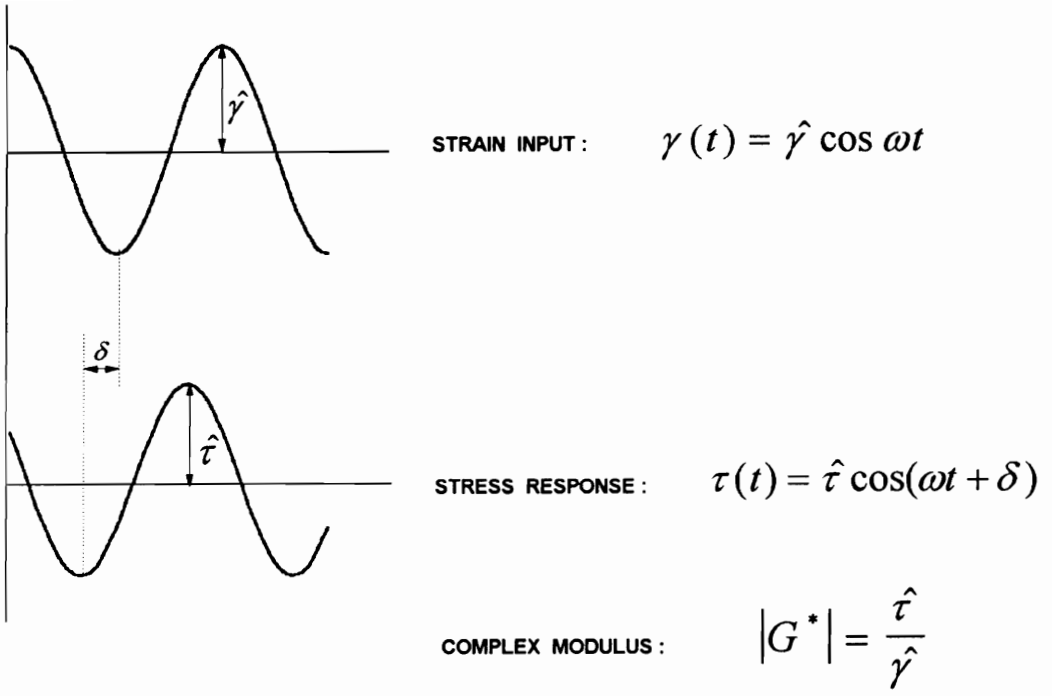

Figure 2.5. Schematic of a Typical Dynamic Mechanical Analysis in Shear Mode

Furthermore, in many polymers, the relaxation modulus at short times approaches a limiting glassy modulus of the order of 10^9 Pa which represents the rigidity of molecular bonds (Ferry, 1980). The same conclusion holds true for asphalt cements and has been stated by several researchers (Brodnyan *et al.*, 1960; Christensen and Anderson, 1992; Dobson, 1969). At very low frequencies, the complex modulus is almost completely made up of the loss modulus, i.e., $|G^*| \cong G''$. In this region as observed in Figure 2.6, the slope of loss modulus curve approaches unity and the binder exhibits viscous behavior.

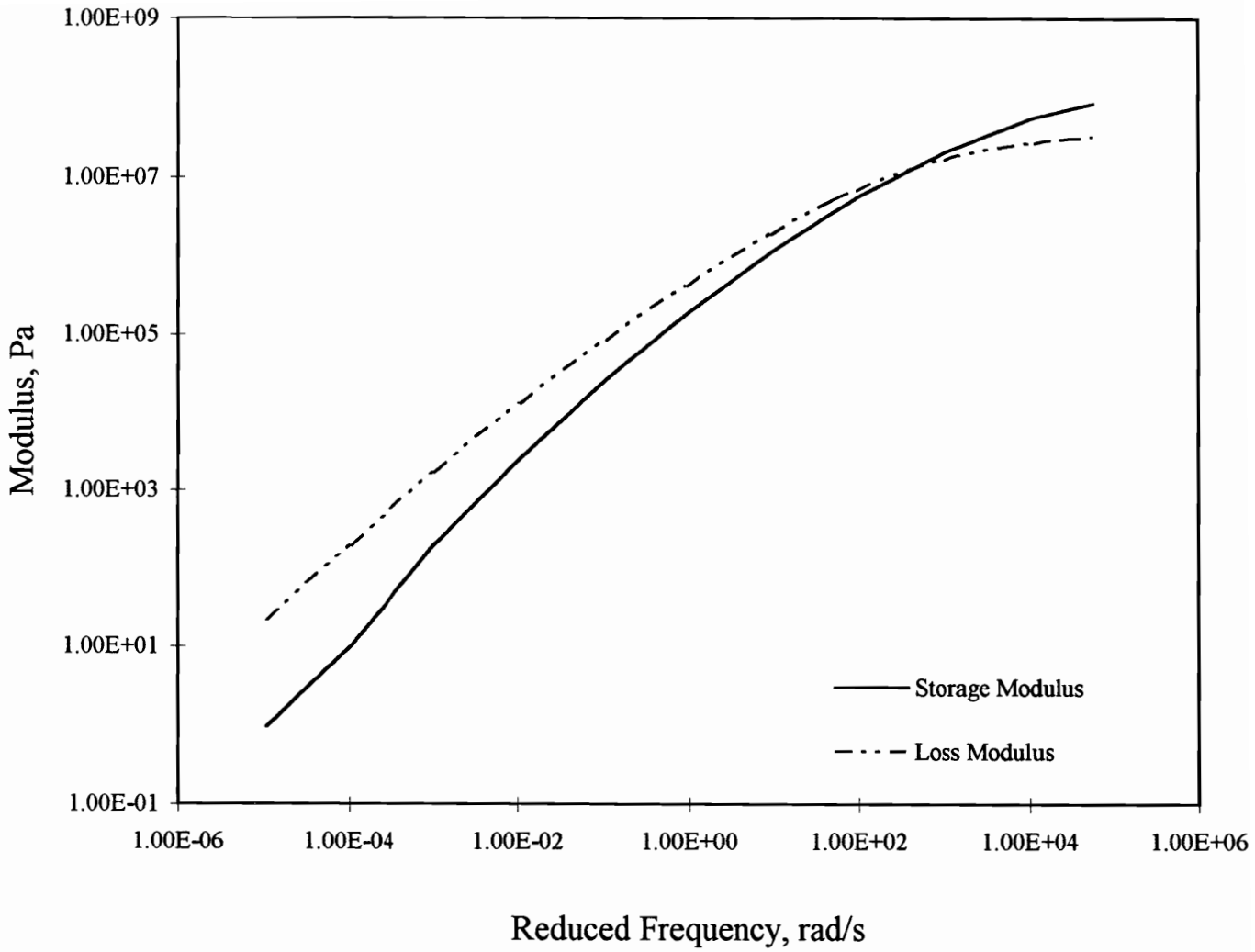

Figure 2.6. Dynamic Storage Shear Modulus and Loss Shear Modulus as a Function of Frequency

2.4.4. Relaxation Spectrum

Relaxation spectrum can be interpreted as a density function representing the moduli over time. All of the other viscoelastic functions can be derived from relaxation spectrum. Furthermore, the relaxation spectrum can be used as a basic approach to mathematical modeling of viscoelastic response (Jongepier and Kuilman, 1970). Closed form solutions for derivation of relaxation spectrum from dynamic viscoelastic functions are extremely complicated. However, use can be made of approximate interrelations among linear viscoelastic functions to derive expressions for relaxation spectrum. An approximation of this type has been given by Ninomiya and Ferry (1959):

$$H(\tau) = \frac{G'(a\omega) - G'(\omega/a)}{2\ln a} - \frac{a^2}{(a^2-1)^2} \frac{G'(a^2\omega) - G'(\omega/a^2) - 2G'(a\omega) + 2G'(\omega/a)}{2\ln a}\Bigg|_{\frac{1}{\omega}=\tau} \tag{2. 21}$$

where,

$H(\tau)$ = relaxation spectrum, Pa,

$G'(\omega)$ = storage modulus, Pa, and

a = a constant greater than unity, selected so that $0.2 \leq \log a \leq 0.4$.

A similar equation has been presented in the same reference for calculating the spectrum from loss modulus data:

$$H(\tau)=\frac{2}{\pi}\left\{G''(\omega)-\frac{a}{(a-1)^2}\left[G''(a\omega)+G''(\omega/a)-2G''(\omega)\right]\right\}\Bigg|_{\frac{1}{\omega}=\tau} \tag{2. 22}$$

where $G''(\omega)$ = loss modulus, Pa.

Tschoegl (1989) provides second order approximations based on the slope of storage modulus:

$$H(\tau)=\frac{dG'(\omega)}{d\ln\omega}+\frac{1}{2}\frac{d^2G'(\omega)}{d(\ln\omega)^2}\Bigg|_{\frac{1}{\omega}=\sqrt{2}\tau} \tag{2. 23}$$

$$H(\tau)=\frac{dG'(\omega)}{d\ln\omega}-\frac{1}{2}\frac{d^2G'(\omega)}{d(\ln\omega)^2}\Bigg|_{\frac{1}{\omega}=\frac{\tau}{\sqrt{2}}} \tag{2. 24}$$

Equations (2. 23) and (2. 24) correspond to the positive and negative slopes of $H(\tau)$, respectively. First order approximate relations based on the slope of loss modulus are provided as well, and can be applied to the positive and negative slope regions of $H(\tau)$ curves, respectively:

$$H(\tau)=\frac{2}{\pi}\left[G''(\omega)+\frac{dG''(\omega)}{d\ln\omega}\right]\Bigg|_{\frac{1}{\omega}=\sqrt{3}\tau} \tag{2. 25}$$

$$H(\tau)=\frac{2}{\pi}\left[G''(\omega)-\frac{dG''(\omega)}{d\ln\omega}\right]\Bigg|_{\frac{1}{\omega}=\frac{\tau}{\sqrt{3}}} \tag{2. 26}$$

Several other approximations with various degrees of accuracy can be found in literature. From a practical point of view, the method of Ninomiya and Ferry (1959) is superior to the others, since it depends on the values of moduli rather than their time derivatives, and the moduli can readily be obtained from experiments.

2.4.5. Time-Temperature Superposition Principle

Viscoelastic response is both time (frequency) dependent and temperature dependent. In other words, in dynamic mechanical analysis, the amount of moduli and loss tangents are simultaneous functions of frequency and temperature. Characterization of response is not possible unless plots of viscoelastic functions are extended over several decades of frequency. Performing dynamic mechanical tests over wide ranges of frequency is not practical. Therefore, it is highly desirable to extend the frequency scale of a given viscoelastic measurement which has been taken over a limited frequency range.

Leaderman (1943) was among the first to emphasize that for a wide variety of amorphous polymers, time (frequency) dependency and temperature dependency are separable. This resulted from the observation that viscoelastic response curves obtained at different temperatures were identical and differed only in their location along the time (frequency) axis. The same observation was independently made by Tobolosky and Eyring (1943), and led to introducing the time-temperature superposition principle (Andrews *et al.*, 1948; Tobolosky, 1956). According to this principle, viscoelastic data at any temperature can be translated to another temperature by a simple multiplicative transformation of the time scale, i.e., change of temperature is equivalent to a shift of the logarithmic time scale.

This principle, also called method of reduced variables (Ferry, 1980) is applicable to a class of polymeric materials generally known as thermorheologically simple (Schwarzl and Staverman, 1952). Many non-crystalline homopolymers and homogeneous copolymers (such as random copolymers) belong to this category. Furthermore, asphalt cements are recognized as thermorheologically simple materials (Brodnyan *et al.*, 1960; Wada and Hirose, 1960; Dickinson and Witt, 1974). Time (frequency)-temperature superposition principle can be mathematically expressed as follows:

$$F(T_1,\omega) = F(T_2,\omega / a_T) \qquad (2.27)$$

where,

$F(T_1, \omega)$ = value of viscoelastic function at temperature T_1 and frequency ω,

$F(T_2, \omega / a_T)$ = value of viscoelastic function at temperature T_2 and frequency ω / a_T,

and

a_T = horizontal shift factor, a function of T_1 and T_2.

To apply the time-temperature superposition principle, first dynamic mechanical tests are performed at several selected temperatures and over a limited range of frequencies. Next, the test data at all temperatures for one of the viscoelastic functions (modulus, compliance, or loss tangent) are plotted against frequency. Finally, the curve corresponding to one of temperatures is selected as reference, and the other curves are shifted along the frequency axis to partially overlap and form a continuous and smooth curve. The resulting curve extends over a wide range of frequencies and is called a master curve. The amount of shift required for each curve to fit the master curve, a_T, is a measure of temperature dependency of response. A graphical illustration of the time-temperature superposition is presented in Figure 2.7.

According to Ferry (1980), application of time-temperature superposition principle requires three conditions. First, shapes of adjacent response curves should exactly match. Secondly, shift factor for all viscoelastic functions must be unique. Finally, the variations of shift factors with temperature should follow a rational pattern which is compatible with experience. The latter condition will be discussed in more detail in Chapter 4.

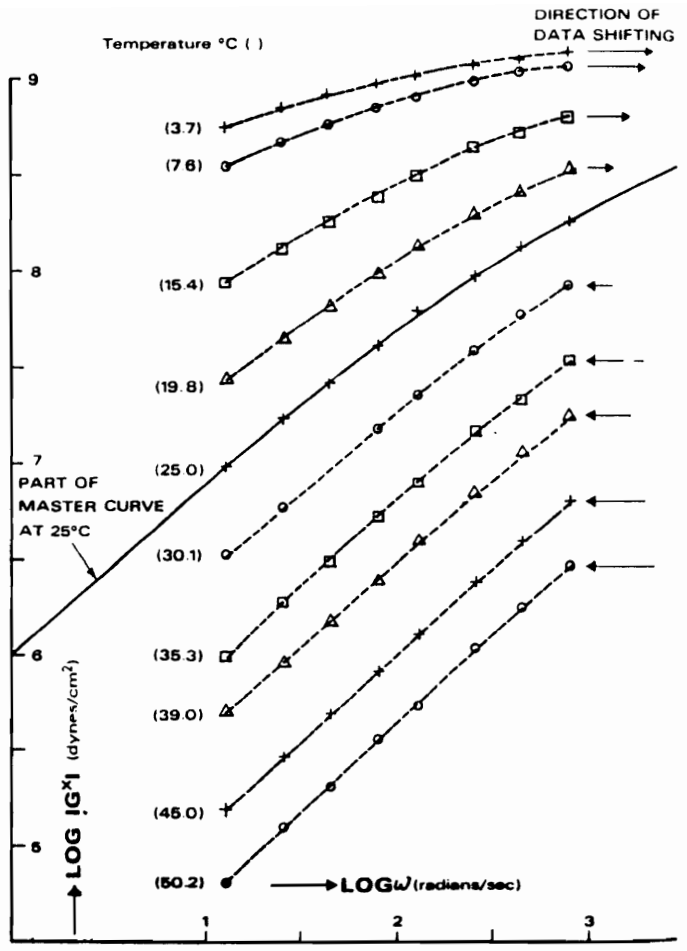

Figure 2.7. Graphical Presentation of Time-Temperature Superposition Principle (After Dickinson and Witt, 1974)

From a micro-rheological point of view, in a thermorheologically simple material, a change of temperature results in a change in the speed of molecular processes, while the sequence of molecular events remains unchanged. In thermorheologically complex

materials, however, not only the speed, but the sequence of molecular processes changes with temperature (Schwarzl and Staverman, 1952).

2.4.6. Thermorheological Simplicity Versus Thermorheological Complexity

The underlying assumption in validity of time-temperature superposition principle for thermorheologically simple materials is that all relaxation times are equally affected by a change in temperature. In other words, the ratio of any relaxation time at a certain temperature to the same relaxation time at another temperature remains constant for the entire range of relaxation times. This can be shown by the following:

$$\frac{\tau_i(T)}{\tau_i(T_r)} = a_T \tag{2. 28}$$

where,

τ_i = ith relaxation time at temperature T or reference temperature T_r, and

a_T = shift factor from temperature T to reference temperature T_r.

The fact that viscoelastic response curves of thermorheologically simple materials can be brought into superposition by a simple shift along the logarithmic frequency axis stems from the above assumption.

If the behavior of material is thermorheologically complex, however, coincidence of mechanical response curves can not be possible by a simple translation along the time or frequency axis. In this class of materials, equation (2. 28) does not hold true and shift factor is a function of time or frequency in addition to temperature (Fesko and Tschoegl, 1971). Superposition in this case is possible only on a point to point basis. This is shown in Figure 2.8 where typical creep compliance curves at two temperatures are plotted versus time. This figure clearly shows that for this class of materials, the value of shift factor depends not only on temperature, but also on time.

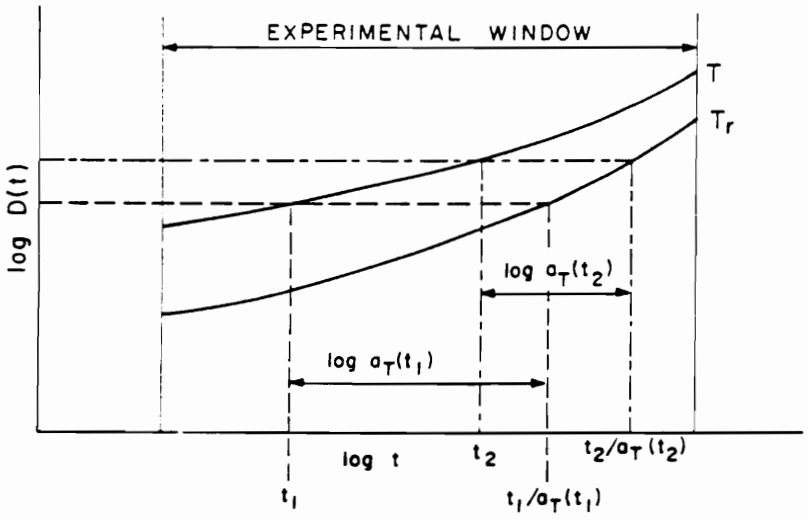

Figure 2.8. Superposition Along Time Axis for Thermorheologically Complex Materials (After Fesko and Tschoegl, 1971)

As mentioned in the preceding section, single-phase systems such as homopolymers exhibit the qualitative features of thermorheological simplicity. Even random copolymers such as SBR have a single transition between those of styrene and butadiene, hence, can be categorized as thermorheologically simple. In heterophase systems, however, the constituents have different temperature dependence and as a result, the material shows multiple transitions corresponding to those of constituents. In these systems the relaxation mechanism of each phase is associated with a distinct distribution of relaxation times. Therefore, heterophase systems are inherently thermorheologically complex. Block copolymers, polymer blends, and asphalt-polymer mixes are examples of heterophase systems. Temperature dependence of this class of materials is extremely complex and has not been completely understood as yet.

Application of time-temperature superposition to heterophase systems has been the subject of extensive research by Tschoegl and co-workers (Fesko and Tschoegl, 1971; Lim *et al.*, 1971; Cohen and Tschoegl, 1973; Fesko and Tschoegl, 1974; Cohen and Tschoegl, 1976; Tschoegl and Cohen, 1978). These studies resulted in development of a model for shift factors of a two-phase material when the dynamic mechanical properties and temperature dependence of the constituent phases are known. Furthermore, a new method for representation of time and temperature dependence of mechanical response functions - contour map method - was proposed. These subjects as well as general treatment of time-temperature superposition in thermorheologically complex materials will be further discussed below.

It can be shown that for a thermorheologically complex material (Fesko and Tschoegl, 1971)

$$\left(\frac{\partial \log F(t)}{\partial \log t}\right)_T = \left(\frac{\partial \log F[t/a_T(t)]}{\partial \log t/a_T(t)}\right)_{T_r}\left[1-\left(\frac{\partial \log a_T(t)}{\partial \log t}\right)_T\right] \qquad (2.\ 29)$$

where,

F = viscoelastic function (modulus, compliance, etc.), and

a_T = time-dependent shift factor.

Equation (2. 29) expresses that on a log-log scale, the slope of isothermal segment of the response curve at any loading time equals the slope of shifted curve to the reference temperature multiplied by a factor representing the effect of time on shift factor. For a thermorheologically simple material, shift factor is not time-dependent. Thus, the last term in brackets cancels and equation (2. 29) reduces to

$$\left(\frac{\partial \log F(t)}{\partial \log t}\right)_T = \left(\frac{\partial \log F(t/a_T)}{\partial \log t/a_T}\right)_{T_r} \qquad (2.\ 30)$$

which represents the well-known fact of equality of slopes of isothermal segments and the master curve at corresponding loading times.

Similar to equation (2. 29), another equation was developed for slope of $F(T)$ with respect to T at constant time (Fesko and Tschoegl, 1971):

$$\left(\frac{\partial \log a_T(t)}{\partial T}\right)_t = -\left(\frac{\partial F(T)}{\partial T}\right)_t \left(\frac{\partial F[t/a_T(t)]}{\partial \log t/a_T(t)}\right)^{-1}_{T_r} \tag{2. 31}$$

Equation (2. 31) can not be integrated, thus, it is not applicable in practice. To predict the shift function of a two-phase system based on the temperature shift factors of each constituent phase (which are assumed to be individually thermorheologically simple), use was made of a model proposed by Takayanagi (1965). According to this model, the two phases are assumed to be connected partly in series and partly in parallel. Assumption of series coupling results in additive compliances, and parallel connection leads to additive moduli. In either case, an equation similar to the following can be derived (Fesko and Tschoegl, 1974):

$$\log a_T(t) = n_1(t)\log a_{T1} + n_2(t)\log a_{T2} \tag{2. 32}$$

with

$$n_1(t) + n_2(t) = 1 \tag{2. 33}$$

where,

a_{T1} and a_{T2} = shift factors corresponding to phases 1 and 2, respectively, and

$n_1(t)$ and $n_2(t)$ = time-dependent weighting factors.

$n_1(t)$ and $n_2(t)$ are complicated functions of relaxation or retardation spectrum of respective phases, and are proportional to the weight fraction of each phase. These functions have different forms based on the viscoelastic function in consideration. For example, in case of storage compliance, $D'(\omega)$, they can be derived from the following equations (Fesko and Tschoegl, 1971):

$$n_1(\omega) = \left. \frac{w_1 L_1(\tau)}{w_1 L_1[\tau / a_T(\omega)] + w_2 L_2[\tau / a_T(\omega)]} \right|_{\tau = \frac{1}{\omega}} \tag{2. 34}$$

$$n_2(\omega) = \left. \frac{w_2 L_2(\tau)}{w_1 L_1[\tau / a_T(\omega)] + w_2 L_2[\tau / a_T(\omega)]} \right|_{\tau = \frac{1}{\omega}} \tag{2. 35}$$

where,

L_1 and L_2 = first approximation to retardation spectrum for phases 1 and 2, respectively, and

w_1 and w_2 = weight fractions of phases 1 and 2, respectively.

Thus, equation (2. 32) yields different composite shift factors for $D(t)$, $D'(\omega)$, $D''(\omega)$, etc. Such a conclusion is quite rational for a thermorheologically complex material.

It results from equations (2. 32) through (2. 35) that if the values of viscoelastic functions and their temperature dependence are known for individual phases, the temperature dependence of the two-phased system can readily be evaluated. This allows for construction of a master curve for a thermorheologically complex two-phase material.

Time or temperature dependence of thermorheologically simple materials is usually presented by isothermal or isochronal measurements, i.e., plots of viscoelastic response functions versus logarithmic time (frequency) at fixed temperature, or versus temperature at fixed time. For thermorheologically complex materials, due to the previously mentioned facts this method of presentation may result in misleading information. Consequently, a third method has been proposed for simultaneous presentation of time and temperature dependency of this class of materials (Cohen and Tschoegl, 1976; Tschoegl and Cohen, 1978). In this method, a contour map tracing the loci of points of constant response as a function of logarithmic time and temperature is constructed. These contour maps can provide insight into the complicated time-temperature relations of thermorheologically complex materials. A contour map of this type which was developed for the loss compliance of an SBS triblock copolymer is shown in Figure 2.9.

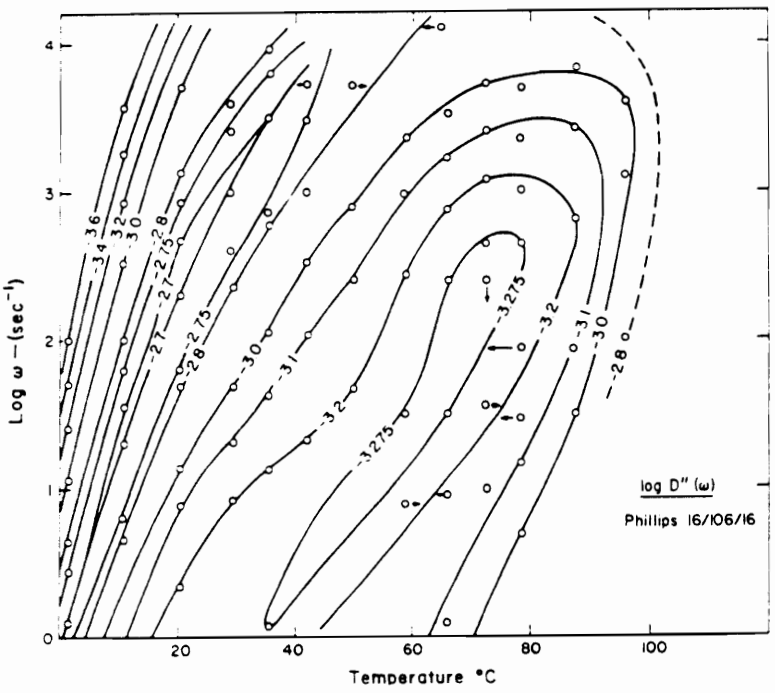

Figure 2.9. Contour Map of Logarithmic Loss Compliance as a Function of Temperature and Logarithmic Frequency for an SBS Sample (After Cohen and Tschoegl, 1976)

2.5. Current Research on Straight and Modified Asphalts

The idea of using rubberized asphalt in construction of flexible pavements dates back to 1902, when a French company installed the first test road of this type (Thompson, 1979). By 1930's several rubberized asphalt paved test roads were constructed by the British and French (Lewandowski, 1994). However, polymer modification of asphalt cements was not promoted to a research subject area until late 1970's. Commercial introduction of

thermoplastic rubbers in the late 1960's and increasing use of this category of polymers in the asphalt industry afterwards, was an important incentive for establishing numerous laboratory and field research projects in this area.

During the past 15 years, a large number of papers have been published regarding studies on the application, behavior and performance related problems of polymer modified asphalt binders. Some of the studies have addressed the microstructure of asphalt-polymer blends, compatibility issues, and asphalt-polymer interaction (Brule *et al.*, 1988; Collins *et al.*, 1991; Hesp and Woodhams, 1992; King and King, 1986; Kraus and Hall, 1983; Shuler *et al.*, 1987). Several research projects have concentrated on the performance of polymer modified binders and mixes related to specific distress mechanisms in pavements such as cracking and rutting (Al Dhalaan, 1992; Brown *et al.*, 1992; Fleckenstein *et al.*, 1992; Jew *et al.*, 1986; Jew and Woodhams, 1986; Khosla, 1991; Little, 1992; Serfass *et al.*, 1992; Stock and Arand, 1993; Tayebali *et al.*, 1992). The effects of aging on the rheological behavior and temperature susceptibility parameters of modified binders have been investigated as well (Anderson *et al.*, 1992; Collins and Bouldin, 1992; Muncy *et al.*, 1987; Srivastava *et al.*, 1992).

Dynamic mechanical analysis has been one of the techniques used in many of the previously mentioned studies. However, no effort has been made so far to reduce the dynamic mechanical data on a wide range of modified binders into the framework of

mathematical models. Very few studies have attempted to approach the problem through characterizing some aspects of the viscoelastic response.

Collins *et al.* (1991) studied the dynamic mechanical properties of SBS, SBR and EVA modified asphalts at a range of intermediate to high temperatures. They suggested that for all the blends and over the entire range of temperatures, the Arrhenius function provided a suitable fit for the temperature dependency of shift factors. However, this suggestion was not accompanied with any further elaboration or presentation of actual shift factor data. Some limited observations were made on the variations of loss and storage moduli with frequency through interpretation of master curves. Existence of a plateau in some storage modulus curves was attributed to the possible formation of a polymeric network in the blend. A similar conclusion had been previously drawn by Goodrich (1988).

Anderson *et al.*, (1992) utilized different testing methods to study the rheological properties of asphalt emulsions modified with SBS, SBR and neoprene. Dynamic mechanical tests were performed at temperatures ranging from -35 to 60° C. Construction of master curves led to the conclusion that polymer modification extends the relaxation process to longer times. However, no quantitative measure of shift in the relaxation spectra was established. The values of adjusted shift factors were fitted to the WLF equation (Williams *et al.*, 1955) at temperatures above the glass transition temperature, T_g. Below T_g, an Arrhenius function was proposed to characterize the temperature dependency of response.

Stock and Arrand (1993) investigated the rheology of 6 different binders modified with a range of elastomeric to plastomeric modifiers. Dynamic mechanical properties of these binders were determined over a limited range of temperatures and frequencies. In describing the frequency dependence of response, they used the model developed by Dobson (1969) and derived the model constants based on their experimental data. However they did not attempt to develop a new mathematical model.

As mentioned before, during the late 1960's and early 1970's, some analytical expressions were established to characterize the frequency dependence and temperature dependence of viscoelastic response of asphalt cements (Jongepier and Kuilman, 1969, 1970; Dobson, 1969; Dickinson and Witt, 1974). Recently, Christensen and Anderson (1992) have proposed another mathematical model for this purpose. All of these models have been developed based on experimental studies on straight asphalts and none of them has addressed the response of polymer modified binders. However, in order to gain an understanding of the approach to modeling problem, it is useful to review these models. In the remaining part of this section, a brief description of the models will be presented.

2.5.1. Jongepier and Kuilman's Model

Jongepier and Kuilman (1969, 1970) derived their mathematical model for frequency dependence of asphalt binders based on the assumption of a log normal distribution for relaxation times. The relaxation spectrum was defined as follows:

$$H(\tau) = \frac{G_g}{\beta\sqrt{\pi}} \exp - \left(\frac{\ln \tau / \tau_m}{\beta} \right)^2 \qquad (2.\ 36)$$

where,

β = width of the distribution function,

τ_m = time constant, s, defined by $\frac{\eta_0}{G_g} e^{-\frac{\beta^2}{4}}$,

η_0 = Newtonian viscosity, Pa.s, and

G_g = glassy modulus, Pa.

The glassy modulus is defined as the limiting value of storage modulus at extremely high frequencies and is expressed by the following equation:

$$G_g = \int_{-\infty}^{+\infty} H(\tau) d \ln \tau \qquad (2.\ 37)$$

Based on this distribution function and using the Ninomiya and Ferry's approach (1959), the following equations were derived for the storage and loss moduli, respectively:

$$G'(x) = \frac{G_g}{\beta\sqrt{\pi}} \exp - \left[\frac{\beta (x - 1/2)}{2} \right]^2 \times \int_0^{\infty} \exp - \left(\frac{u}{\beta} \right)^2 \frac{\cosh(x + 1/2)u}{\cosh u} du \qquad (2.\ 38)$$

$$G''(x) = \frac{G_g}{\beta\sqrt{\pi}} \exp -\left[\frac{\beta(x-1/2)}{2}\right]^2 \times \int_0^{\infty} \exp -\left(\frac{u}{\beta}\right)^2 \frac{\cosh(x-1/2)u}{\cosh u} du \qquad (2.39)$$

where the transformations u and x are defined as follows:

$$u = \ln \omega\tau \text{ , and } x = \frac{2}{\beta^2} \ln \omega_r \qquad (2.40)$$

where ω_r is a dimensionless reduced frequency defined by

$$\omega_r = \frac{\omega\eta_0}{G_g} \qquad (2.41)$$

Through performing dynamic mechanical tests on a wide variety of asphalts, the authors concluded that the variations in relaxation spectrum strictly result from the changes in width parameter β. Therefore, they introduced β as a rational parameter for characterizing asphalt binders. Furthermore, they observed a strong correlation between β and the composition of asphalt, i.e., the asphaltene content. Comparison between the experimental master curves of moduli and those developed by the model, showed that with increasing β values there is a tendency to a wider transition from the viscous asymptote to the glassy asymptote of response. In other words, the response of asphalt cements with large β values is less frequency dependent.

On describing the temperature dependency of response, the authors used the WLF equation (Williams *et al.*, 1955):

$$\log a_T = -\frac{C_1(T - T_s)}{C_2 + (T - T_s)} \tag{2. 42}$$

where,

a_T = shift factor,

T_s = reference temperature, °K or °C, and

C_1 and C_2 = experimental constants.

They stated that for constants C_1 and C_2 to be worth mentioning, T_s should be selected to have a physical significance. However, through dilatometric glass transition temperature (T_g) measurements, they realized that use of T_g as the reference temperature does not result in a universal set of constants in the WLF equation. They concluded that the glass transition temperature is not an appropriate parameter to describe the temperature dependence of asphalt cement. Defining T_s as an equi-viscous temperature, i.e., a temperature at which asphalts have a certain viscosity, resulted in varying sets of C_1 and C_2 constants for different asphalt types.

Mathematical complexity of the equations developed for frequency dependence of response, makes their practical application quite difficult. As stated by the authors, the

width parameter β although strongly related to the viscoelastic behavior, is not suitable for rapid characterization of asphalt.

2.5.2. Dobson's Model

Development of Dobson's model (1969) for frequency dependence of asphalt was directly based on describing the master curves of complex modulus and loss tangent as a function of frequency. The resulting equation defines the relative frequency in terms of relative modulus:

$$\log \omega_r = \log G_r - \frac{1}{b}\left[\log(1-G_r^b) + \frac{20.5 - G_r^{-b}}{230.3}\right] \qquad \text{for } G_r > 10^{-\frac{1.02}{b}} \tag{2. 43}$$

where,

$$\omega_r = \frac{\eta_0 \omega a_T}{G_g} \tag{2. 44}$$

$$G_r = \frac{|G^*|}{G_g} \tag{2. 45}$$

b = a parameter describing the width of relaxation spectrum.

Although b was defined as the width parameter for relaxation spectrum, no further explanation was made and it is not clear what type of distribution function it refers to. It was stated that b can be looked at as a shear susceptibility parameter and is related to the penetration index.

Based on experimental observations, the following relationship between complex modulus and loss tangent for values of $\tan\delta < 9.5$ was proposed:

$$\frac{d\log|G^*|}{d\log\omega} = \frac{\tan\delta}{(1+\tan\delta)(1-0.01\tan\delta)} \tag{2. 46}$$

On temperature dependency of response, Dobson relied on the WLF equation to describe the shift factors. He confirmed the previous findings of Brodnyan (1960) that for $T - T_s > -20$, the WLF equation with universal constants can fit the shift factor data. However, at lower temperatures the equation overestimates the shift factors. Therefore, his version of the WLF equation consists of two pairs of constants for temperatures below and above the reference temperature:

$$\log a_T = \frac{-12.5(T-T_s)}{142.5+(T-T_s)} \qquad T - T_s < 0 \tag{2. 47}$$

$$\log a_T = \frac{-8.86(T-T_s)}{101.6+(T-T_s)} \qquad T - T_s > 0 \tag{2. 48}$$

Dobson did not specify a certain reference temperature, but like Jongepier and Kuilman stated that T_s should be an equi-viscous temperature for asphalts.

2.5.3. Dickinson and Witt's Model

Dickinson and Witt (1974), based on dynamic mechanical data on 14 different asphalt cements, developed two analytical expressions for complex modulus and phase angle in terms of frequency. The following equation was proposed for modulus:

$$\log G_r = \frac{1}{2}\left[\log \omega_r - \sqrt{(\log \omega_r)^2 + (2\beta)^2}\right] \qquad (2.49)$$

where G_r and ω_r have the same definitions as before. This is the equation of a hyperbola whose asymptotes, $\log G_r = \log \omega_r$, and $\log G_r = 0$, indicate the viscous and elastic extremes of response, respectively. The shear susceptibility parameter, β, varies based on composition and aging condition of asphalt.

The mathematical expression for phase angle is as follows:

$$\delta = \delta' + \frac{\pi - 2\delta'}{4}\left[1 - \frac{\log \omega_r}{\sqrt{(\log \omega_r)^2 + (2\beta)^2}}\right] \qquad (2.50)$$

where δ' is a small angle (less than 3°) which is assigned to the glassy modulus.

Based on these two equations, Dickinson and Witt computed the values of storage and loss moduli and developed the relaxation spectra. They observed that the spectra were not symmetrical with respect to the maximum value, i.e., the spectra were not consistent with the Jongepier and Kuilman's assumption of log normal distribution for relaxation times.

Dickinson and Witt used the Dobson's version of WLF equation to describe the temperature dependency of their experimental data. Based on the two sets of constants proposed by Dobson, they estimated the reference temperature for the range of studied asphalts.

2.5.4. Christensen and Anderson's Model

Christensen and Anderson (1992) performed dynamic mechanical analysis on the eight SHRP core asphalts. The mathematical model describing the frequency dependence of response was derived based on a logistic distribution function for the resulting relaxation spectra. The following equations were proposed to define the complex moduli and phase angels in terms of frequency:

$$|G^*(\omega)| = G_g\left[1+\left(\frac{\omega_c}{\omega}\right)^{\frac{\log 2}{R}}\right]^{-\frac{R}{\log 2}} \tag{2. 51}$$

$$\delta(\omega) = \frac{90}{1+\left(\frac{\omega}{\omega_c}\right)^{\frac{\log 2}{R}}} \tag{2. 52}$$

where,

ω_c = crossover frequency, rad/sec, and

R = rheological index defined by $\log\left(\frac{G_g}{|G^*(\omega)|}\right)\Big|_{\omega=\omega_c}$.

The parameters ω_c and R in this model have considerable physical significance. The crossover frequency, ω_c, represents a frequency at which δ = 45°. Several empirical observations have confirmed that this frequency usually coincides with the intersection of glassy and viscous asymptotes of the modulus master curve. Therefore, ω_c can be regarded as a location parameter on the master curve. The rheological index, R, on the other hand, is a shape parameter for the master curve and represents the width of relaxation spectrum. Asphalts characterized by larger R values exhibit wider relaxation spectrum.

Compared to the previous models, this model has a simpler shape. However, through comparison between the experimental data and those generated by the model, the authors observed some discrepancy for moduli below about 10^5 Pa. In other words, use of model is strictly suitable for characterizing the response at intermediate and high ranges of modulus.

Unlike previous models for temperature dependency of shift factors which were restricted to the use of WLF equation, the authors have made use of the Arrhenius function as well. At temperatures lower than a certain limit (designated by defining temperature), an Arrhenius function defined by the following equation was used to characterize the temperature dependency of asphalt:

$$\log a_T = \frac{H_a}{2.303\,\mathrm{R}}\left(\frac{1}{T} - \frac{1}{T_d}\right) \qquad (2.52)$$

where,

H_a = activation energy for flow below T_d, J/mol,

R = ideal gas constant, 8.314 J/mol.°K, and

T_d = defining temperature, °K or °C.

At temperatures above T_d, the WLF equation was found to yield reasonable values for shift factors. It was suggested that there is a strong correlation between the defining

temperature, T_d, and the glass transition temperature, T_g. However, no explicit relationship between these two was established.

2.6. Need for Further Research on Polymer Modified Asphalt Binders

The models described in the previous sections, have all been developed based on dynamic mechanical data on straight asphalts. The frequency dependence models, although successful in describing the shape of master curves, are either mathematically complex, or have some limitations in the application range. Furthermore, some aspects of the viscoelastic response of polymer modified binders resulting from formation of new molecular structures can not be described by expressions which are strictly developed for straight asphalts. Limitations of these models and their shortcomings in characterizing polymer modified binders will be further discussed in Chapter 4.

Thermorheological simplicity of straight asphalts has been emphasized by several researchers (Brodnyan *et al.*, 1960; Wada and Hirose, 1960; Dickinson and Witt, 1974). However, applicability of simple time-temperature superposition to dynamic mechanical data on polymer modified binders as heterophase systems is not certain at this point. This subject will be thoroughly elaborated in Chapter 3. Furthermore, application of WLF equation in describing the temperature dependence of modified asphalts will be investigated in Chapters 4 and 5.

Chapter 3
Research Approach

In order to achieve the objectives of this study, an experimental program was designed. After selection of the appropriate materials, several asphalt-polymer blends were prepared. Dynamic mechanical analysis was conducted to collect the necessary data. The data were further processed and analyzed to develop analytical models describing the response.

3.1. Selection of Materials

3.1.1. Asphalt Cement

Chemical composition and microstructure of asphalt cement can significantly influence its rheological properties. Chemical composition of petroleum asphalt is a function of crude source and distillation process. Wide variety of the crude sources in the United States and other parts of the world and technical differences in distillation of crude oil in several refining plants result in numerous chemical compositions of asphalts available in the market.

In the early stages of this research, efforts were made to obtain asphalt samples with the desirable chemical compositions in terms of potential compatibility with polymers. To achieve this goal, several oil companies were contacted and a number of asphalt samples

were obtained. Reluctance of the companies in providing information about the composition of their products, made this a difficult task. Finally, it was decided to use a typical paving grade asphalt which according to the results of elution-adsorption chromatography (Corbett, 1969) could well present the desirable composition. The AC-20 paving grade asphalt cement was supplied by the Amoco Oil Company. Tables 3.1 and 3.2 show the results of conventional tests and Corbett analysis on the asphalt sample, respectively (Amoco, 1995).

Table 3.1. Conventional Test Results for AC-20 Sample

	Unaged Condition	Residue of Thin Film Oven Test
Specific Gravity	1.037	
Penetration at 25° C, 0.1 mm	66	40
Absolute Viscosity at 60° C, poise	2054	4232
Kinematic Viscosity at 135° C, cSt	437	

Table 3.2. Results of Corbett Analysis on Asphalt Cement

Asphaltenes	14.0-14.3%
Polar Aromatics	13.2-19.0%
Naphtene Aromatics	51.2-53.4%
Saturates	14.5-18.0%
Unrecovered	1.1-1.3%

3.1.2. Polymers

A brief overview of the polymeric modifiers was presented in Chapter 2. In selection of polymers for this study, two major factors were considered:

1. The extent of use in asphalt industry: The results of this study are intended to have practical applications in the asphalt modification technology. Therefore, choice of polymers should be primarily based on the extent to which they are used in the industry. Presently, the elastomeric polymers are more commonly used compared to the plastomeric modifiers.

2. Capability of being mixed and processed in the laboratory: Selected polymers should be capable of being processed with respect to the available laboratory equipment. Preparing plastomerically modified asphalt binders requires more sophisticated

instruments including high shear blenders. Elastomeric modifiers, on the other hand, can be blended with asphalt at lower shear stress applications.

Regarding the above facts, elastomeric polymers were considered more suitable for this study. The polymeric modifiers were to be selected to represent a wide range of molecular structures, physical and mechanical properties, and application purposes. Therefore, a total of 7 polymers were used: 2 SBR random copolymers, 2 SBS linear block copolymers, 2 SEBS linear block copolymers, and 1 $(SB)_n$ branched copolymer. The block copolymers were supplied by the Shell Chemical Company. The random copolymers were manufactured by Goodyear Company and supplied by the Textile Rubber & Chemical Company.

Tables 3.3 and 3.4 show the typical properties of thermoplastic block copolymers and random copolymers used in this study (Shell Chemical Company, 1992; Textile Chemical and Rubber Company, 1992).

3.2. Instrument

Dynamic mechanical tests were performed using a Bohlin stress controlled dynamic shear rheometer with parallel plate configuration (Bohlin, 1990). At sub-ambient temperatures, due to high stiffness of asphalt binder, high shear stresses are required to achieve a certain strain level. This is generally possible by using a small-diameter rotating plate. Therefore,

Table 3.3. Typical Properties of Thermoplastic Block Copolymers at 23° C

Trade Name	Kraton D-1101	Kraton D-4141	Kraton G-1652	Kraton G-1654X	Kraton D-1184
Designation	S	D	G	X	N
Structure	Linear SBS	Linear SBS	Linear SEBS	Linear SEBS	Radial $(SB)_n$
Physical Form	Porous Pellet	Porous Pellet	Powder	Powder	Porous Pellet
Placticizer Oil Content, %w	0	29	0	0	0
Specific Gravity	0.94	0.93	0.91	0.92	0.94
Brookfield Viscosity at 25° C, cps	4000	1000	1350	370	20000
Tensile Strength, Pa (ASTM D 412)	31700	19000	31050	24150	27600
300% Modulus, Pa (ASTM D 412)	2760	1720	4830	6210	5520
Elongation, % (ASTM D 412)	880	1300	500	700	820
Styrene/Butadiene Ratio	31/69	31/69	29/71	31/69	30/70

Table 3.4. Typical Properties of Random Copolymers

Trade Name	UP 7289	UP 2897
Designation	P	C
Physical Form	Emulsion	Emulsion
Solid Content, %	68	68
Specific Gravity	0.95	0.95
pH	10.0	10.0
Brookfield Viscosity, cps	1300	1300
Styrene/Butadiene Ratio	24/76	24/76

an 8 mm diameter plate was used for performing tests at temperatures between 5 to 35° C. Tests at temperatures above 35° C were performed using a 25 mm diameter plate. To maintain a specified constant temperature during tests, the samples were completely immersed in temperature controlled water. A pump-equipped water bath circulated the water around the specimen throughout the tests. Operation of the rheometer and temperature control unit, along with data acquisition and analysis were controlled by a personal computer.

The operation of dynamic shear rheometer is based on the general theory of dynamic mechanical analysis as described in Chapter 2. A disk-shaped binder specimen is mounted

between two circular plates. The upper plate can rotate around a vertical axis, while the lower plate is fixed. The specimen is subjected to a specified shear stress at a certain frequency through application of a torque to the upper plate. The response is monitored by measurement of the angular deflection of the sample. The storage and loss moduli are then computed as follows (Bohlin, 1990):

$$G' = \frac{2h}{\pi R^4} \frac{|T_D^*| \cos\phi + I\omega^2 |\theta^*|}{|\theta^*|} \tag{3. 1}$$

$$G'' = \frac{2h}{\pi R^4} \frac{|T_D^*| \sin\phi}{|\theta^*|} \tag{3. 2}$$

where,

h = sample thickness, m,

R = sample radius, m,

T_D^* = complex output torque, N.m,

θ^* = complex angular deflection of sample, rad,

I = system inertia, kg.m,

ω = angular frequency, rad/sec, and

ϕ = raw phase angle, rad, composed of the actual phase angle and the phase angle between the output torque and sample torque.

Calculation of $|G^*|$ and $\tan\delta$ will then be possible by means of equations (2. 13) and (2. 16).

3.3. Preparation of Blends

The 19 liter container of asphalt received from Amoco company was placed in an oven maintained at $140\pm5°$ C for approximately 5 hours. During this time, the asphalt was stirred periodically to ensure uniformity. Then, it was poured in several one liter cans. The cans were sealed and stored at room temperature to be used in preparing the blends.

Polymers G and X were supplied by the manufacturer in form of a fine uniform powder which is suitable for mixing with asphalt due to the high surface area of particles. Polymers D, S, and N, however, had a particle size of approximately 3 mm. Any attempt for blending asphalt with polymer particles of this size can result in extended mixing times, which in addition to excessive use of laboratory equipment and time may lead to adverse effects such as undesirable oxidation of the mix. Therefore, prior to mixing, the particle size of these three polymers was reduced using a laboratory granulator. The ground polymer was then passed through a # 16 sieve to obtain finer and more uniform particles.

Mixing was performed using a Lightnin Labmaster laboratory mixer, model L1UO3. The mixer had varied mixing and computer interfacing capabilities. The quantitative characterization of mixing parameters including speed, power input, and pumping capacity

as measured by the impeller generated flow was possible. The mixer was capable of operating at speeds ranging from 50 to 1800 rpm. A three blade propeller-paddle with 5 cm blade diameter was used along with the mixer.

All polymers were blended with the asphalt cement at three different concentration levels. For polymer C, the concentration levels were 2, 3, and 4% by weight of the asphalt. All other polymers were blended at 3, 4, and 5%. Therefore, a total of 21 mixes were prepared.

Asphalt-polymer blends were prepared according to the following procedure. The one liter can of asphalt was placed in an oven preheated to 140° C. After becoming sufficiently soft, the asphalt was stirred and approximately 400 g of it was transferred to a 1000 ml glass beaker. The beaker was placed in a heating mantle to maintain a constant temperature throughout mixing. Depending on the polymer type, mixing temperature was ranging from 163 to 177° C. To avoid the adverse effects of excessive heat during mixing, two thermocouple probes were used to monitor the temperature. The first one which was installed between the beaker and heating mantle, controlled the power input. The second probe was placed inside the beaker to directly measure the binder temperature.

The mixer shaft was placed directly at the center of the beaker, with the propeller 1/3 of the depth from the bottom. With the mixer operating at 100 rpm, the asphalt was heated to the desired temperature. When the target temperature was reached inside the beaker,

the required amount of polymer was added very slowly, i.e., over a 30 minute period of time. This was to avoid possible agglomeration in case of block copolymer powders, and to give sufficient time for evaporation of water in case of SBR latex. During that period, the mixer speed was increased to 400 rpm at three consecutive steps.

The main mixing cycle started after addition of the entire amount of polymer. At this point, the speed was increased to 800-1000 rpm, and mixing was continued for approximately 1 hour for SBR latex, and between 3 to 10 hours for block copolymers to obtain a uniform blend. The beaker was then transferred to an oven maintained at 163° C and allowed to stay for approximately one hour. If no obvious signs of phase separation between polymer and asphalt were observed, the blend was poured in several 30 ml cans. The cans were sealed and stored at room temperature for further testing.

3.4. Aging Treatment

Immediately after preparation of a blend, 4 samples of 35 g were poured in special bottles, and aged in accordance with the RTFOT procedure, ASTM D 2872 (Annual Book of ASTM Standards, 1991). The aged samples were transferred to 30 ml cans and stored at ambient temperature for further testing.

3.5. Designation of Binders

Each asphalt-polymer combination is designated by a four-character code. The first character, A, refers to the asphalt type, i.e., Amoco AC-20. The second character, U or R, refers to the aging condition of binder; U stands for unaged condition, and R designates the RTFOT residue. The third character denotes the polymer type according to Tables 3.3 and 3.4. The last character, shows the polymer concentration percentage, i.e., 2, 3, 4, or 5. For example, AUN4 denotes a blend of asphalt with 4% polymer N (radial SB_n) in unaged condition, and ARN4 designates the RTFOT residue of the same binder. The straight asphalt in unaged and aged conditions is shown by AU00 and AR00, respectively.

3.6. Dynamic Mechanical Analysis

3.6.1. Stress Sweeps

Dynamic mechanical tests were performed at eight temperatures ranging from 5 to 75° C with increments of 10° C. Prior to performing frequency sweeps, it was imperative to ensure that all measurements would be taken in the linear viscoelastic range of response. To establish the linear range for each asphalt-polymer combination in aged and unaged conditions, stress sweeps were performed at all temperatures and at selected frequencies. At 15° C and higher temperatures, frequencies of 3.142, 6.283, and 9.425 rad/s were used. Stress sweeps at 5° C, were usually performed at a frequency of 0.063 rad/s. This

was due to the relatively high stiffness of the binders at this temperature. Within the linear range of response, the values of viscoelastic functions such as G' or G'' are independent of the applied stress amplitude. In the non-linear region, however, the moduli will decrease with increasing stresses.

In the course of performing the stress sweeps, it was observed that due to gradual variations of moduli, drawing an exact line between the linear and non-linear regions is not possible. Therefore, the dividing line between two regions was arbitrarily defined as a resulting strain at which the amount of moduli drops to 95% of its initial value. This concept is graphically presented in Figure 3.1.

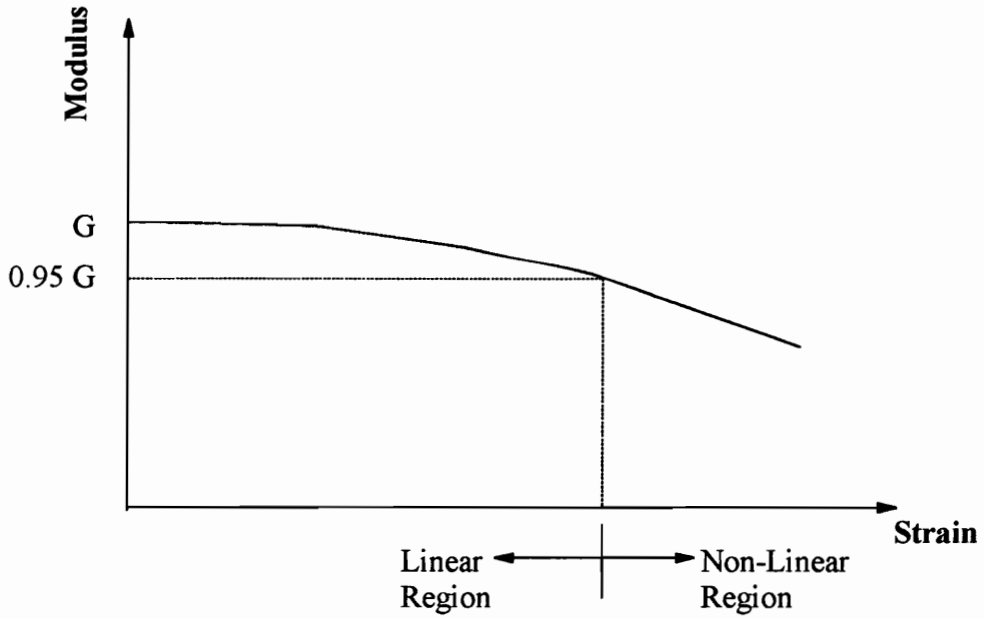

Figure 3.1. Definition of Linear and Non-Linear Ranges of Response

It should be noted that particularly at temperatures below 25° C, due to high stiffness of the modified binder and limited strain generation capability of the rheometer, no decrease in the value of moduli could be observed over the entire range of applied stresses. This means that at these temperatures, even at the highest possible generated strain, the sample was still within its linear range. Therefore, based on the results of stress sweeps on all samples, it was decided to conduct the frequency sweeps at a uniform set of target strains for all asphalt-polymer combinations. These strains are shown in Table 3.5. They are well within the linear range of response as established by stress sweeps, and are below the values stated by AASHTO TP5 (AASHTO Provisional Standards, 1994) for straight asphalts.

Table 3.5. Target Strains for Frequency Sweeps

Test Temperature, °C	Target Strain, %
5	0.8
15	1
25	2
35	3
45	6.5
55 and more	9

3.6.2. Frequency Sweeps

Upon completing the stress sweeps and establishing the target strains, frequency sweeps were performed on all samples in the unaged and aged conditions, and over the entire range of temperatures. A total of 34 frequencies ranging from 0.063 to 188.496 rad/s were used.

For the 8 mm diameter plate and before starting measurements, the apparatus with specimen in place were allowed to equilibrate at 45° C for approximately 30 minutes. This procedure assured sufficient bond between the specimen and confining plates, and improved the repeatability of measurements. The test temperature was then progressively lowered in intervals of 10° C, and at each target temperature, a frequency sweep was carried out in ascending order of frequencies. The procedure continued until data had been obtained at the lowest temperature of interest, i.e., 5° C.

Measurements with 25 mm diameter plate always started at 45° C. In a similar manner, test temperature was successively increased in intervals of 10° C, and frequency sweeps were performed in ascending order at each target temperature up to 75° C.

All tests were performed in replicas. To ensure the independence of replicas, specimens were taken from different sample cans. The number of independent replicas varied for

different specimens. A detailed discussion of repeatability of dynamic mechanical measurements and associated sources of errors follows.

3.6.3. Repeatability of Dynamic Mechanical Tests on Polymer Modified Asphalts

Results of dynamic mechanical tests on asphalt cements in general, and polymer modified asphalts specifically are sometimes prone to poor repeatability. Among several factors that may contribute to this problem, the following can be mentioned:

1. Effect of temperature: Dynamic moduli of asphalt binders are highly sensitive to variations of temperature. During the tests, it was realized that temperature fluctuations as low as ±0.5° C could result in up to 15% change in the complex modulus values. The temperature control unit of the rheometer was capable of maintaining temperatures within ±0.1° C which conforms to the requirements of AASHTO TP5 (AASHTO Provisional Standards, 1994). It should be noted that in addition to high accuracy of temperature control unit, it is highly imperative to allow the specimens a sufficient period of time to reach a thermal equilibrium state. Prior to running each test, the specimen was allowed to equilibrate at the specified test temperature for a period of time not shorter than 30 minutes. This period is long enough to eliminate any possibility of a temperature gradient within the small thickness of specimen.

2. Effect of specimen preparation method: Asphalt specimens for dynamic mechanical tests with parallel plate geometry can be prepared in two different ways. The first method is prefabricating the specimen with specified thickness and diameter using a silicone rubber mold, and mounting it between the two measuring plates. Although the specimens produced by this method have the exact desired geometry, due to lack of sufficient bond between the material and parallel plates specially at low temperatures, risk of slippage during test can be considerably high. In the second method, after adjusting the desired gap between the plates, the melted asphalt is poured on the lower plate. With upper plate in place, the specimen is trimmed between two confining plates. According to equations (3. 1) and (3. 2), the measured dynamic moduli are inversely proportional to the fourth power of the radius of specimen. Therefore, slightest deviation from the desired diameter, can result in significant errors in the measured moduli. Regarding the fact that trimming the elastomerically modified binder with a hot spatula is extremely difficult, this procedure can be looked upon as a major source of variability in results.

In the early stage of experimental work, both 8 mm and 25 mm diameter specimens were prefabricated using silicone rubber molds. The high level of variability in results of tests on 8 mm diameter specimens, specially at temperatures below 25° C, led to the conclusion that slippage may had been a source of error. Therefore, 8 mm diameter specimens were no longer prefabricated, and method of direct preparation was used thereafter. However, generating repeatable data on prefabricated 25 mm diameter specimens was continued successfully.

3. Compliance error: Compliance error is a result of transferring the angular deflection generated by motor into the force transducer instead of the specimen. This problem usually occurs at extremely low temperatures, i.e., when the stiffness of binder is considerably high compared to the system stiffness. Considering the fact that no tests were performed at temperatures below 5° C, the compliance problem is not expected to have been a major source of variability in this work.

4. Effect of steric hardening: Storing asphalt at ambient temperatures for extended period of time is usually followed by formation of a new structure within the binder as a result of molecular associations. This phenomenon, usually referred to as steric or thixotropic hardening (Roberts *et al.*, 1991) can lead to increased complex modulus over time. Steric hardening is reversible through heat application. Heating the binder to 160-170° C can break the newly formed molecular bonds and restore the structure of binder to its initial status.

Dynamic tests were usually performed a few days, and occasionally a few weeks after preparation of blends. This period of time was long enough to allow for steric hardening of binder, and hence erroneous measurements. Therefore, prior to preparing a specimen for test, the sample container was placed in an oven maintained at 163° C for approximately 15 minutes, and binder was rigorously stirred. This procedure proved to be effective in reducing the effects of steric hardening.

5. Effect of factors associated with testing procedure: During the period of experimental work, it was observed that results of dynamic mechanical tests on asphalt binders were highly sensitive to all aspects of specimen preparation and testing procedure. Variations in temperature of parallel plates before placing and trimming the specimen, sequence of performing frequency sweeps (ascending or descending order of applied frequencies), sequence of exposing the specimen to the desired temperature (increasing or decreasing towards the target value), and several other factors all proved to have significant effects on results. In order to minimize the sources of variability of this type, efforts were made to follow a uniform testing protocol throughout the entire course of experiments.

6. Effect of instrument calibration: Calibration of rheometer can be changed over time. To reduce the effect of calibration change on the repeatability of results, this factor was periodically checked by testing polybutene. This oil which is supplied by Cannon Company and used as a certified viscosity standard to check the calibration of capillary viscometers at 60° C, can also be used to check the calibration of dynamic shear rheometer. At this temperature, the dynamic viscosity of polybutene is highly independent of frequency, and approaches the steady state viscosity. Therefore, The calibration of rheometer was verified on a monthly basis by means of comparing the measured dynamic viscosity of oil at 60° C with the Newtonian viscosity stated by the manufacturer.

3.6.4. Results

The primary results of frequency sweeps are the values of dynamic shear storage and loss modulus on the entire range of applied frequencies. In general, depending on experiment type, either storage modulus or loss modulus may be a more reliable measurement in certain regions of frequency and/or temperature. Over the range of temperatures used in this study, the loss modulus measurements were more reliable and their spacing were preferred to storage modulus results. For each asphalt-polymer combination, multiple graphs of loss modulus versus frequency at the eight test temperatures were developed and plotted on a log-log scale. As an example, Figure 3.2 shows a multiple graph of this type which was constructed for ARG5.

In Section 2.4.6, it was stated that polymer modified asphalts are heterophase systems. In these materials, the constituent phases generally have different temperature dependence, and their relaxation mechanisms are associated with distinct distribution of relaxation times. Therefore, polymer modified asphalts are considered to be thermorheologically complex in nature. It was discussed that for this category of materials, the mechanical response curves could not be brought into coincidence with a simple shift along the logarithmic frequency axis, and that different viscoelastic functions have different shift factors. Application of time-temperature superposition principle to these materials generally requires decomposition of contribution of individual mechanisms to the overall response, and determination of time-temperature relationship for each contribution

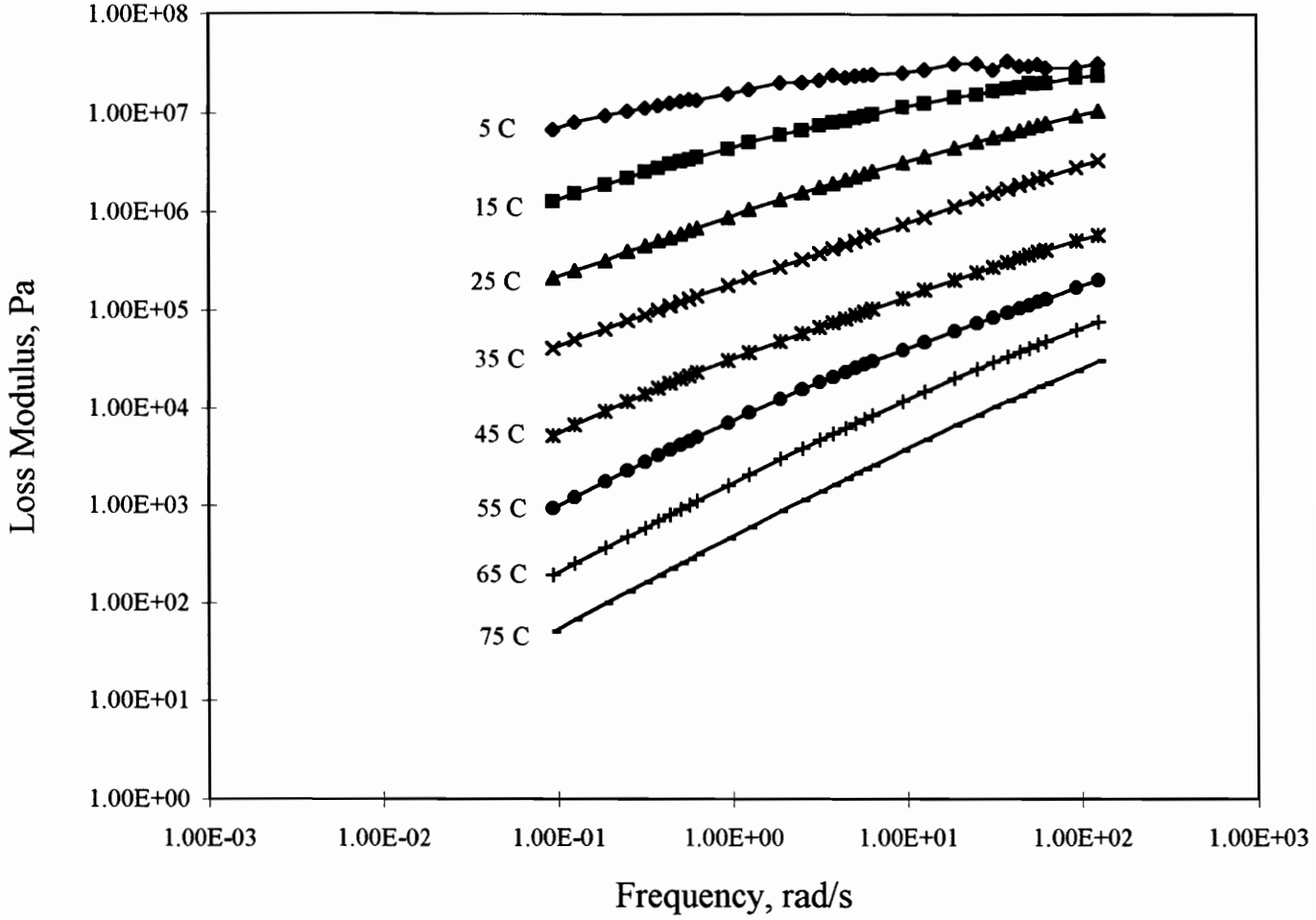

Figure 3.2. Dynamic Loss Shear Modulus Versus Frequency at 8 Test Temperatures for ARG5

separately (Fesko and Tschoegl, 1974).

During analysis of data, it was realized, however, that for all asphalt-polymer blends the isothermal loss modulus response curves could indeed be brought into superposition with a simple translation along the frequency axis. Furthermore, the resulting horizontal shift factors could smoothly superpose the other response function i.e., storage modulus as well. To interpret this phenomenon a few possibilities may be argued.

A heterophase system may fulfill the requirements for simple superposition if the constituent phases have similar transitions. No glass transition temperature measurement was possible in this study. However, depending on the composition and aging condition, several researchers have reported glass transition temperatures ranging from -4° C to -38° C for paving grade asphalts (Wada and Hirose, 1960; Schmidt and Santucci, 1966; Petersen *et al.*, 1992). The upper glass transition temperature of the block copolymers used in this study is almost 100° C which corresponds to the glass transition of polystyrene blocks. Therefore, in the studied asphalt polymer blends, the two dominant viscoelastic transitions are expected to be separated by roughly 120° C, i.e., no similarity of response between the two phases. It should be noted, on the other hand, that as observed in Figure 3.2, the experimental window in this study is limited to almost 3.5 decades of logarithmic frequency. The wide separation of the two transitions and the relative smallness of experimental window brings up another possibility, i.e., actual lack of superposition which is not clearly apparent within the experimental range. Such an

undetectable lack of superposition has been reported for isothermal segments of dynamic compliances of other thermorheologically complex materials (Cohen and Tschoegl, 1976).

The final possibility to be discussed, is domination of temperature dependence of the asphalt phase in asphalt-polymer blends. Study of the collected shift factor data for straight asphalt and asphalt-polymer blends depicts no anomalies or abrupt changes due to addition of polymers. In fact, over the entire range of temperatures, the variations of shift functions corresponding to blends with different polymer types and concentration levels are slight. According to equation (2. 32), in a two-phase system contributions of individual phases to the composite shift function is represented by weighting factors n_1 and n_2. Exact determination of these factors can be extremely difficult. However, according to equations (2. 34) and (2. 35), they are proportional to the weight functions of each phase. In the studied blends, the polymer fractions make up 1.96% to 4.76% of the weight of total mix. This can affect the overall values of n_1 and n_2, causing the weighting factor of the asphalt phase appreciably exceed that of the polymer phase. If this is the case, within the experimental regions of temperature and frequency, the behavior of blend may be assumed to be dominated by the asphalt phase. Hence, although being a heterophase system, the isothermal response curves would admit simple translation along the logarithmic frequency scale.

Whatever the source, regarding the admissibility of simple translation, the master curves of dynamic loss shear modulus were developed by empirical superposition. For this

purpose, the isothermal curve corresponding to 25° C was considered the reference, and all other isothermal segments were shifted along the frequency axis to obtain a unique smooth curve. Shifting the data was accomplished using a spread sheet and through several trial and errors to find the best possible coincidence. The resulting shift factors from this procedure were then applied to the corresponding storage modulus data to superpose the respective isothermal curves.

Dynamic storage and loss shear modulus master curves for the entire modified binders are presented in Appendix A. As an example, storage modulus, loss modulus, and loss tangent master curves for ARG5 are shown in Figures 3.3 and 3.4, respectively.

The amount of shift required by each isothermal curve to fit the dynamic master curve (horizontal shift factor, a_T) was recorded for each binder and plotted against temperature on a semi-log scale. These plots are presented in Appendix B. Figure 3.5 illustrates the shift function for ARG5.

Due to interdependency between viscoelastic functions, plotting two of the four functions $|G^*|$, G', G'', and $\tan\delta$ will be sufficient for complete characterization of response.

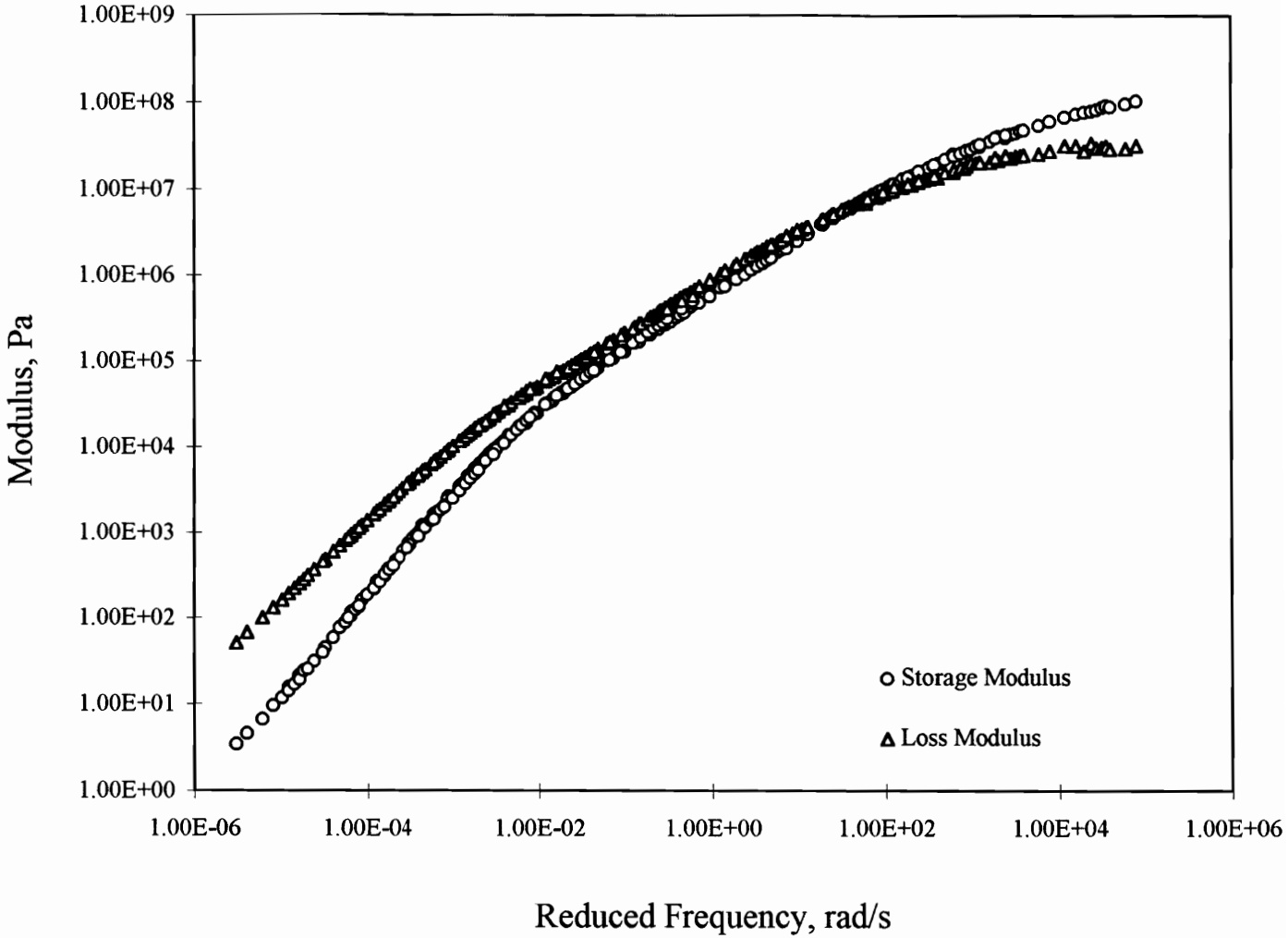

Figure 3.3. Dynamic Storage Modulus and Loss Modulus Master Curves for ARG5

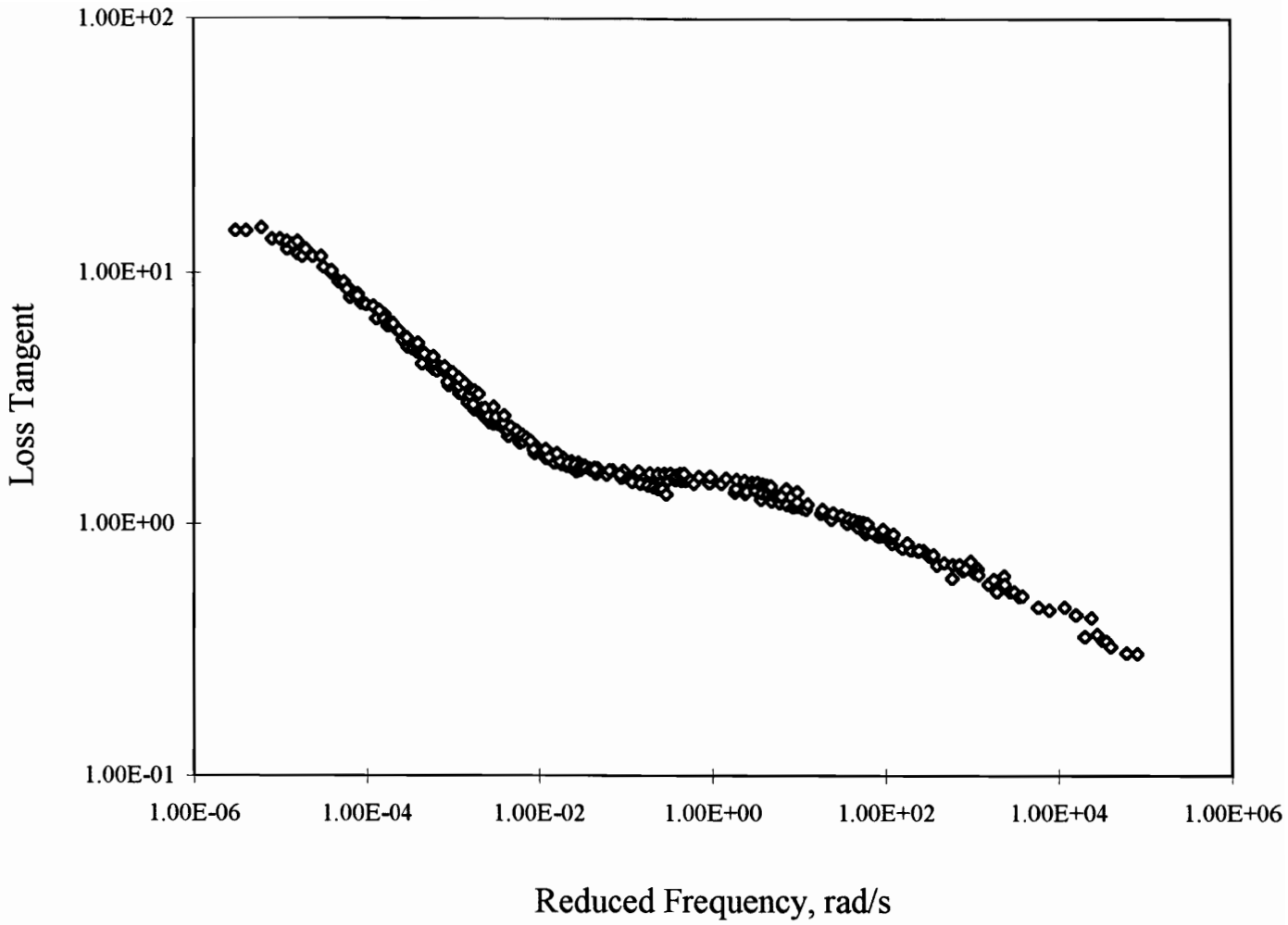

Figure 3.4. Loss Tangent Master Curve for ARG5

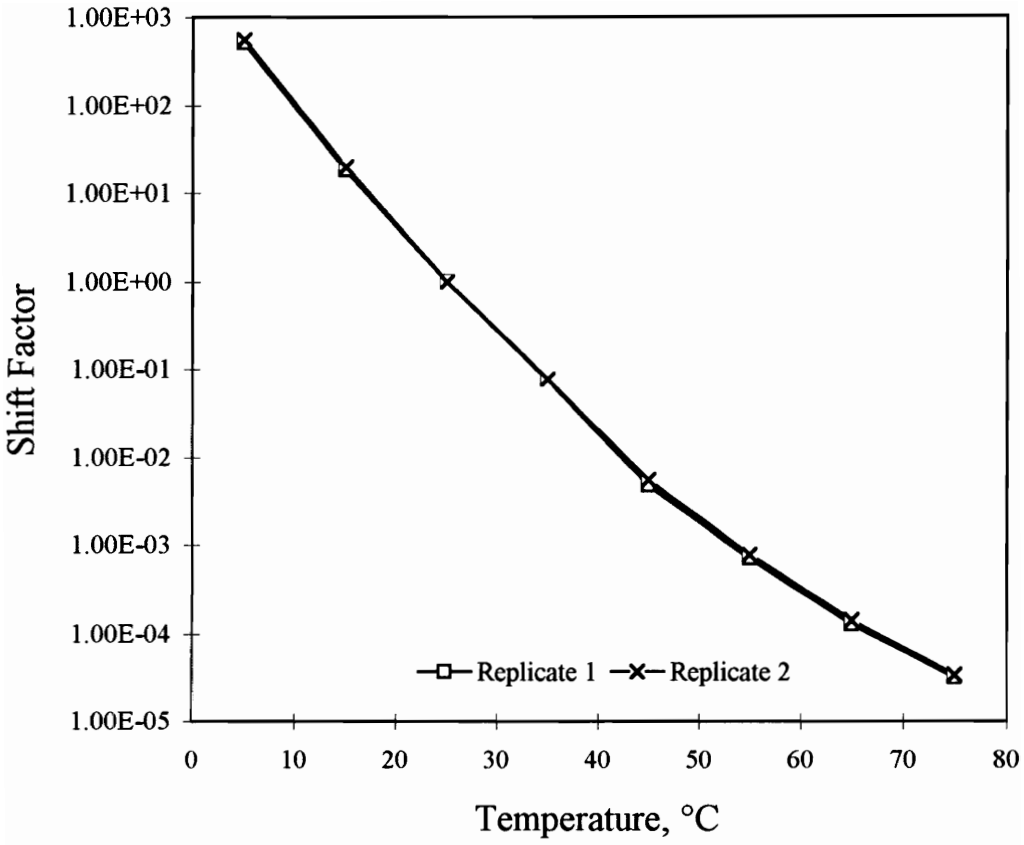

Figure 3.5. Shift Factors for ARG5

Chapter 4

Development of Mathematical Models for Frequency Dependence and Investigation of Temperature Dependence of Response

4.1. Background

During the primary analysis of dynamic tests data, several master curves were constructed. Furthermore, using the mathematical models described in Chapter 2, the corresponding analytical master curves were developed and compared to the experimental curves. In most cases, considerable discrepancies were observed between the experimental results and data generated by the mathematical models. Although the degree of disagreement between results was variable based on both the model and experimental data sets, the deviations were generally large enough to make the use of models questionable.

Figure 4.1 shows the experimental complex modulus master curve for ARX5, along with the results based on Christensen and Anderson's model for the same binder with rheological index, R=1.846, and crossover frequency, ω_c=101.2 rad/s. Although for values of complex modulus above 10^5 Pa, agreement between the model and experimental data is reasonably good, it can be easily observed that for lower values of modulus, the model always underestimates the actual data. Such a trend is quite expected, since as stated by the authors, use of this model is strictly suitable for a range of complex moduli

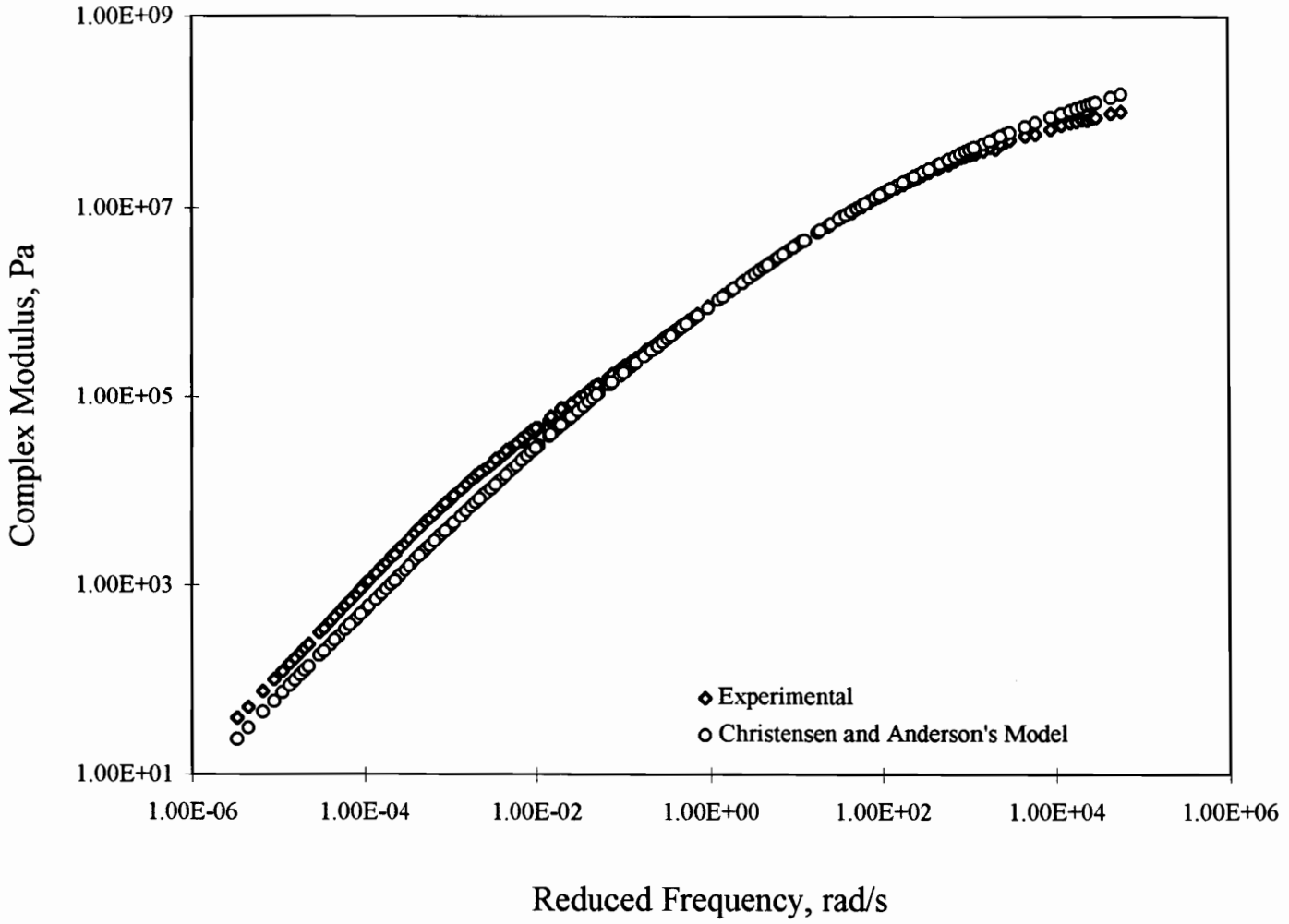

Figure 4.1. Comparison between Measured Complex Moduli of ARX5 and Results of Christensen and Anderson's Model with R=1.846 and Cross-Over Frequency of 101.2 rad/s

above 10^5 Pa. At intermediate and high temperatures, the complex modulus values for polymer modified binders usually extend from 10 Pa to orders of 10^8 Pa. This can be observed over the entire dynamic master curves presented in Appendix A. Therefore, one can directly deduce that use of this model can result in underestimated values for almost 60% of the modulus range. This fact, as well as some deficiencies in the proposed mathematical expression for loss tangent which will be discussed below, indicates that the model, although theoretically sound, is somewhat nebulous in describing the frequency dependence of polymer modified asphalts.

One interesting feature of the viscoelastic response of polymer modified asphalts, is the presence of a plateau in the loss tangent master curves. This region which can be seen in Figure 3.4, is observed on the loss tangent master curves of SBS, SEBS, and $(SB)_n$ modified binders with as low as 3% polymer content. Although not present in case of binders with up to 5% SBR content, the plateau may be expected at higher concentration levels. This phenomenon, which to the knowledge of author has not been reported for straight asphalts, can be attributed to the formation of a polymeric network within the binder. A major shortcoming of the models described in Chapter 2 is their inability to characterize the loss tangent master curves of polymer modified asphalts, especially the plateau regions.

Except the Jongepier and Kuilman's equations for loss and storage moduli which are derived from the assumed function for relaxation spectrum, all other models rely on some

approximate interrelationships between viscoelastic functions. For instance, the mathematical equations for loss tangent data in both Dickinson and Witt's, and Christensen and Anderson's models have been derived based on the following approximate formula:

$$\delta(\omega) = \frac{\pi}{2} \frac{d \log |G^*(\omega)|}{d \log \omega} \qquad (4.1)$$

Equations of this type are approximations to the integral transform relationships between the real and imaginary parts of harmonic response functions, generally known as Kronig-Kramers relations (1926, 1927).

As can be seen, equation (4. 1) defines a correlation between the phase angle and slope of the complex modulus curve on a log - log plot. Despite the fact that accuracy of this approximation has been stated by other investigators (Booij and Thoone, 1982; Booij and Palmen, 1982) as well, studying the behavior of dynamic master curves of several modified binders proved that this equation does not hold true for these materials. As an example, the experimental loss tangent master curve for ARX5, along with the results of Dickinson and Witt's model are plotted in Figure 4.2. Disagreement between the two graphs over several decades of frequency is quite noticeable.

In developing his frequency dependence model for straight asphalts, Dobson (1969)

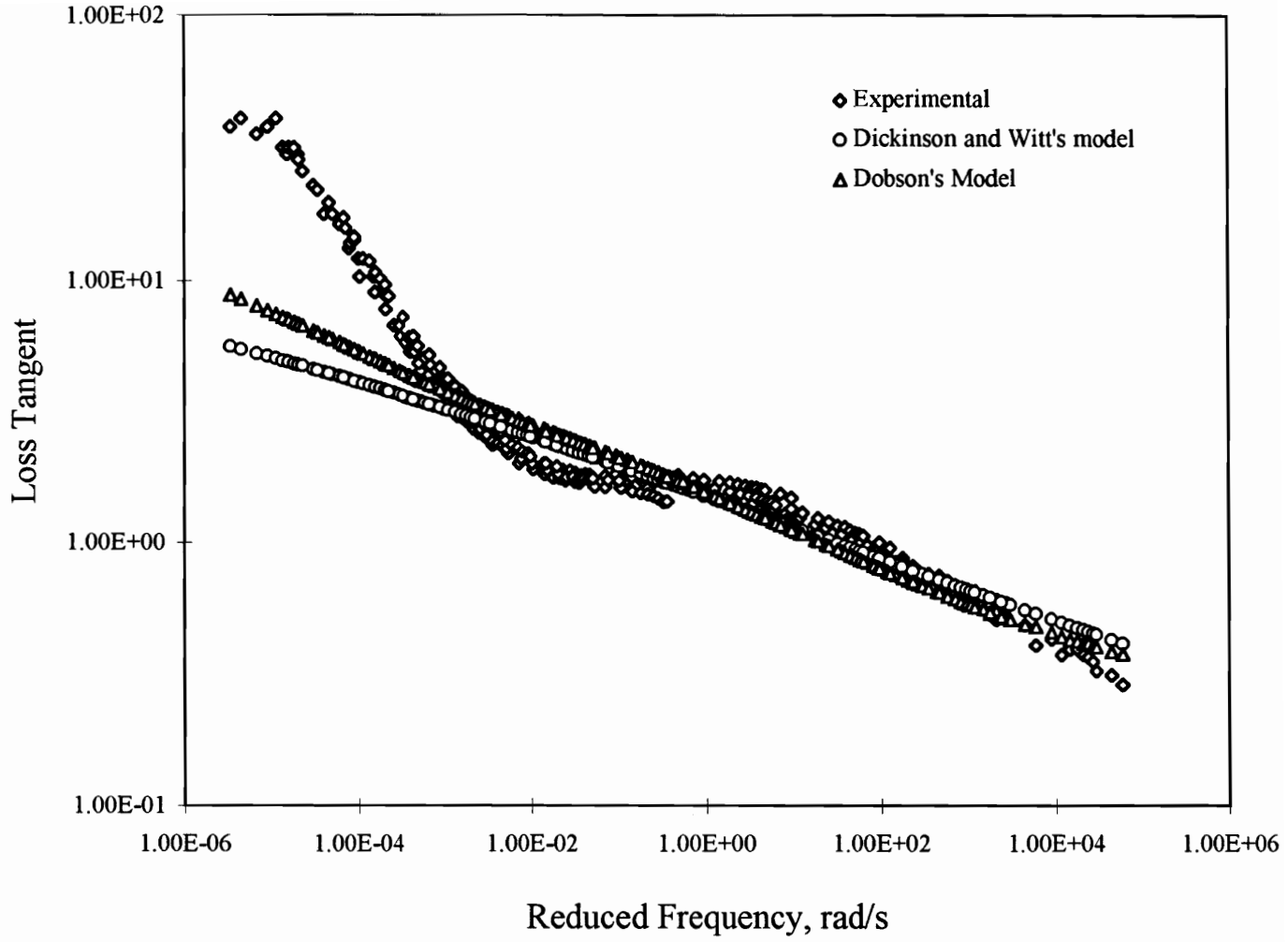

Figure 4.2. Comparison between Measured Loss Tangent for ARX5, Dickinson and Witt's, and Dobson's Fits

defined the following linear relationship between $\log(1+\tan\delta)$ and $\log|G^*|$:

$$\log(1+\tan\delta) = -b\log\frac{|G^*|}{G_g} \qquad (4.2)$$

where b represents the width of relaxation spectrum. Examination of dynamic data for a wide range of modified binders clearly showed that such a linear relationship does not hold true. As an example, in Figure 4.3 the complex modulus data for ARX5 are plotted versus $1+\tan\delta$ on a log - log scale. Obviously, the relationship between these two is of a third degree polynomial type rather than a linear one. The same conclusion was confirmed for several other asphalt-polymer blends. Therefore, it can be expected that Dobson's model is not capable of representing the frequency dependence of loss tangent data for modified binders. This conclusion can be observed in Figure 4.2, where the results of Dobson's model for ARX5 are compared to the measured loss tangent values.

4.2. Development of Mathematical Models for Storage and Loss Moduli

After developing the dynamic master curves for all asphalt-polymer blends, several distribution functions were examined to characterize the frequency dependence of complex modulus data. Weibull distribution function, logistic equation, Gompertz growth model, Mitcherlich equation and inverse polynomial function were among different models which were used for this purpose. It was found that none of these models could provide

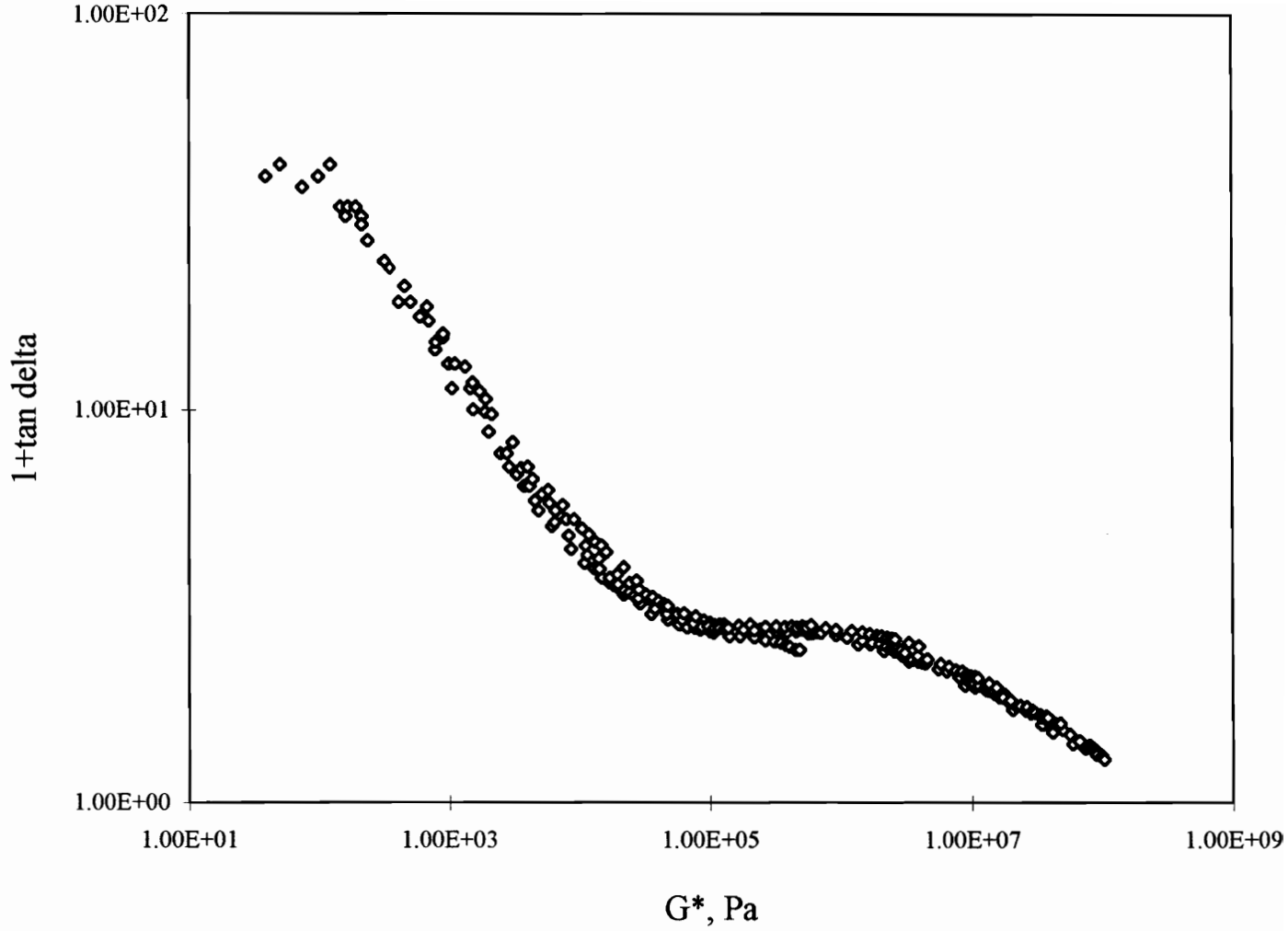

Figure 4.3. Examination of Dobson's Approximate Interrelationship between Viscoelatic Functions for ARX5

an acceptable fit to the complex modulus data. The models were either suffering from lack of agreement to experimental data at certain frequency ranges, or did not satisfy the boundary conditions at one or both extremes of the frequency range. Furthermore, efforts were made to derive an analytical expression for loss tangent data from the above models and based on various approximate interrelationships between viscoelastic functions.

Examination of almost all approximate relationships found in literature proved that these equations generally failed to represent the collected dynamic data on polymer modified asphalts. By further investigation of data, it was realized that storage modulus and loss modulus master curves could be characterized by a modified Mitcherlich equation and a hyperbolic function, respectively. A detailed description of the models is presented below.

4.2.1. Mathematical Expression for Storage Modulus

As described in Section 2.4.3, at very low frequencies the storage modulus is almost zero and the complex modulus is totally comprised of the loss modulus. At extremely high frequencies, on the other hand, the storage modulus approaches a limiting glassy value, and the slope of storage modulus curve in this region is zero. Investigation of the entire dynamic storage modulus master curves indicated that variation of storage modulus between these two extremes follows an exponential pattern which can be described by the Mitcherlich's law of diminishing returns (1909). According to this law, the rate of increase in value of certain functions is proportional to the difference between the

maximum asymptotical and actual values of the function. For variations of storage modulus versus frequency on a log - log scale, this can be expressed by the following equation:

$$\frac{d\log G'(\omega)}{d\log\omega} = p(\log G_g - \log G') \tag{4. 3}$$

where,

$G'(\omega)$ = storage modulus, Pa,

ω = reduced frequency, rad/s,

G_g = glassy modulus, Pa, and

p = proportionality factor.

The proposed mathematical model for storage modulus is obtained by solving the differential equation (4. 3) and can be written as follows:

$$\log G'(\omega) = \log G_g\left[1-\left(\frac{e^{-l}}{\omega^{\log e}}\right)^p\right] \tag{4. 4}$$

where,

l = location parameter for the master curve = $\log\frac{1}{\omega}\Big|_{G'=1}$.

This equation can be written in an alternative form:

$$\log G'(\omega) = \log G_g\left[1 - \exp(-p(\log\omega + l))\right] \qquad (4.\ 5)$$

Equation (4. 5) furnishes a smooth transition between the two extremes of response which conforms to the experimental data. At extremely low frequencies, this equation yields a value of $G' = 0$. At high frequencies, the boundary condition $G' \to G_g$ is satisfied. Therefore, according to equation (4. 3), the slope of log of storage modulus with respect to log of frequency approaches zero, which should be the case.

In equation (4. 5), the parameter l indicates the log of reciprocal frequency when the value of log of storage modulus equals zero. In other words, l marks the intersection point of plot of the storage modulus curve with the reciprocal frequency axis on a log - log scale and hence, can be considered as a location parameter for the master curve. Study of the collected storage modulus data shows that l is a function of the polymer type, polymer concentration level, and aging condition of the binder. Increasing polymer content usually tends to increase l. A similar trend can be observed due to the effect of short term aging of binder.

Parameter p determines the rate at which the storage modulus curve approaches the glassy asymptote. In general, SBR modified asphalts exhibit lower p values than asphalts modified by block copolymers. Although a strong function of polymer type, within the

studied range of polymer contents, p does not appear to be highly correlated to the polymer concentration level. Comparison between the storage modulus master curves of different modified binders before and after aging treatment shows that values of p generally increase due to the aging effect.

As a graphical presentation of the degree of agreement between the experimental data and those generated by the proposed model, Figure 4.4 shows the experimental storage modulus master curve for ARP4, as well as results of equation (4. 5). This plot clearly depicts that the frequency dependence of storage modulus can be best characterized by the proposed model for moduli below 10^8 Pa. Above this value, equation (4. 5) tends to overestimate the modulus. A similar trend can be observed for other asphalt-polymer combinations. This subject will be further discussed in Chapter 5. It should be noted, however, that the values of storage modulus for modified binders used in this study, even at the lowest temperatures (or equivalent highest frequencies) do not exceed 10^8 Pa. Therefore, within the range of applied frequencies and temperatures, the proposed model for storage modulus can reasonably fit the experimental data. The accuracy of model at intermediate frequencies will be discussed in Chapter 5.

4.2.2. Mathematical Expression for Loss Modulus

The proposed mathematical function for characterizing the frequency dependence of loss modulus is a hyperbolic equation:

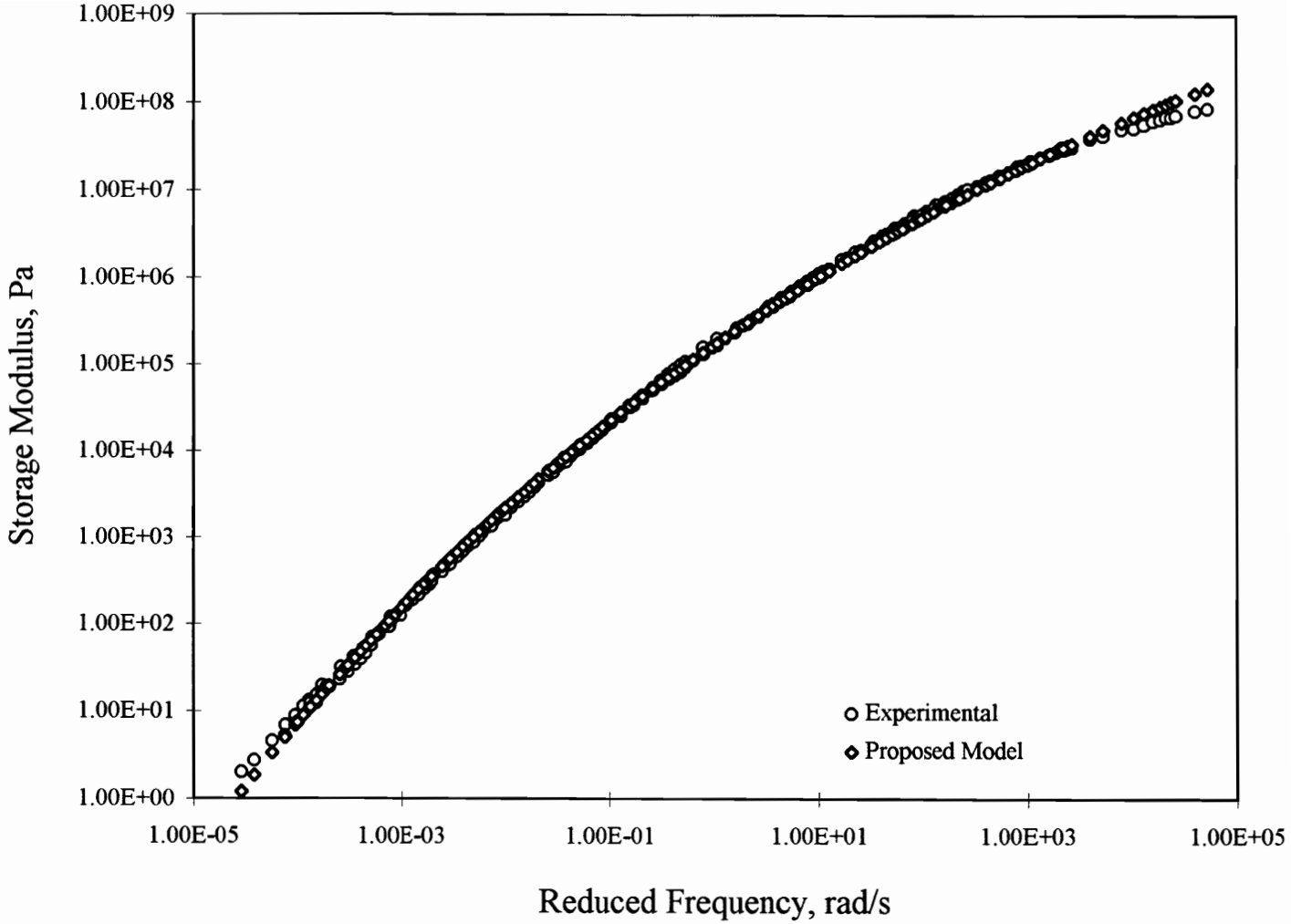

Figure 4.4. Comparison between the Measured Storage Modulus for ARP4 and Results of the Proposed Model

$$\log G''(\omega) = (\log G''_{\max} + d) - \sqrt{(\log \omega - \log \omega_d)^2 + d^2} \qquad (4.\ 6)$$

where,

$G''(\omega)$ = loss modulus, Pa

ω = reduced frequency, rad/s,

$G''_{\max}$ = peak value of loss modulus, Pa,

d = half length of the transverse axis, Pa, and

ω_d = location parameter for the master curve, rad/s = $\omega|_{G''=G''_{\max}}$.

Equation (4. 6) represents one arm of a rectangular hyperbola centered at $(\log \omega_d, \log G''_{\max} + d)$ on the $\log \omega - \log G''$ coordinate system. At low frequencies, the hyperbola approaches an asymptote whose equation is given by

$$\log G''(\omega) = (\log \omega - \log \omega_d) + (\log G''_{\max} + d) \qquad (4.\ 7)$$

This is the equation of a line with a slope of unity on the same coordinate system which represents the viscous asymptote of response. Graphs of equations (4. 6) and (4. 7) are shown in Figure 4.5. Geometrical meanings of the various model constants are shown in this figure as well.

The constant ω_d is the location parameter for the loss modulus master curve and indicates the frequency at which, loss modulus reaches the peak value. Investigation of

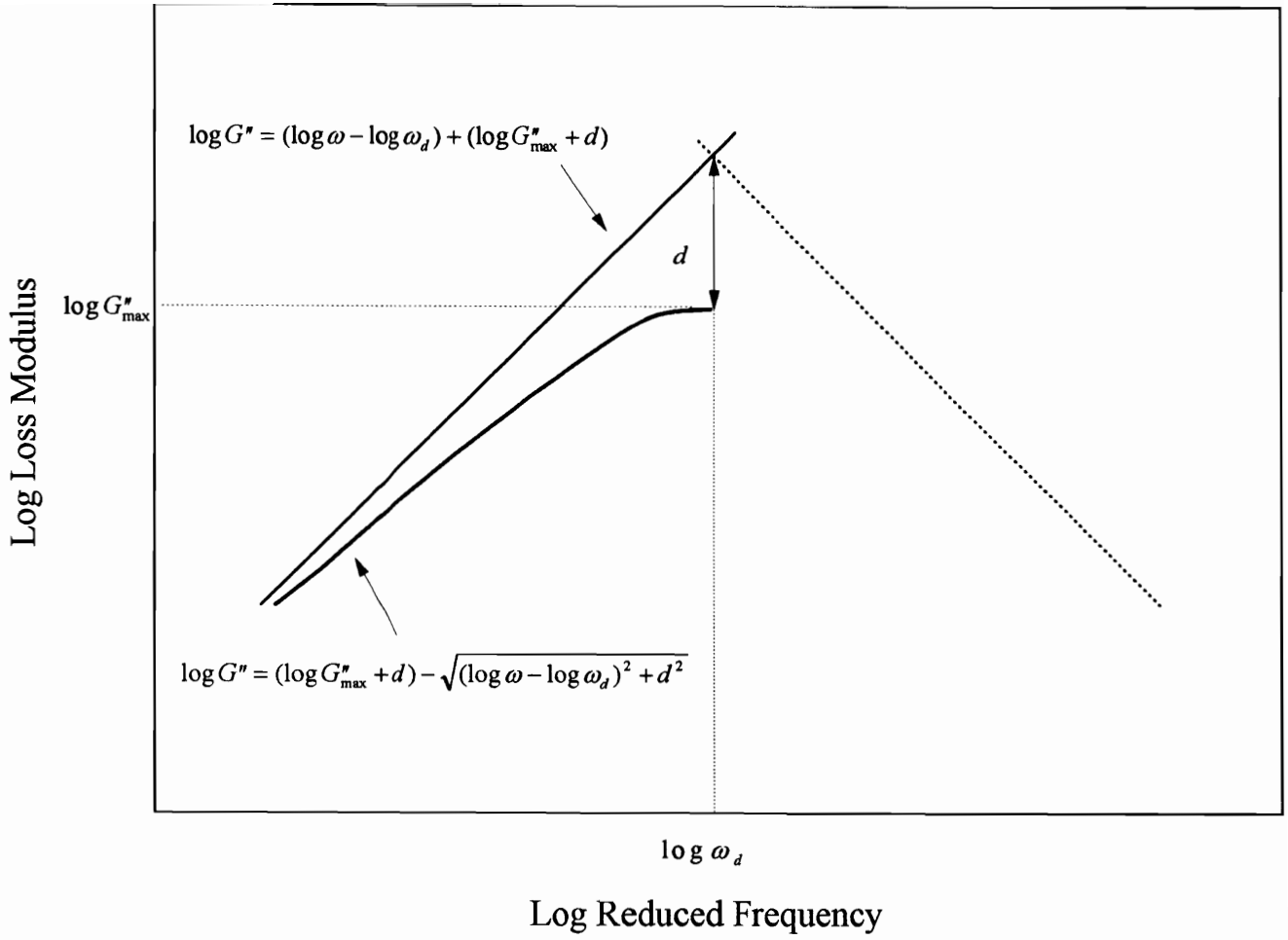

Figure 4.5. Graphical Presentation of the Proposed Model for Loss Modulus

the loss modulus master curves shows that the ω_d value changes with the polymer type. Binders modified by block copolymers have higher ω_d values compared to SBR modified asphalts. Increasing polymer contents can generally result in a slight increase in ω_d. On the contrary, with a constant polymer content, aging treatment usually causes a backward shift in ω_d value.

The parameter d is the vertical distance between the center of hyperbola and the maximum of loss modulus curve on the log modulus axis. Similar to constant β in Dickinson and Witt's model, d can be considered as a shape factor for the loss modulus master curve. For asphalt-polymer blends with higher d values, the transition between the viscous asymptote and peak value is more gradual. Therefore, the loss modulus master curve has smaller slope, and for a range of moduli, extends over more decades of reduced frequency. This fact is shown in Figure 4.6, where the loss modulus master curves for AUP5 with $d = 3.462$, and AUS5 with $d = 5.859$ are plotted. This figure can illustrate the effect of polymer type on the d value as well. In general, with equal concentration levels, blends containing block copolymers possess considerably higher d values than blends with random copolymers. Furthermore, short term aging of binder results in significant increase in the d value.

Addition of polymer to asphalt generally results in larger dispersion in the relaxation process. In other words, polymer modification leads to extension of the relaxation phenomenon to larger periods of time. This is well manifested in the shape of several

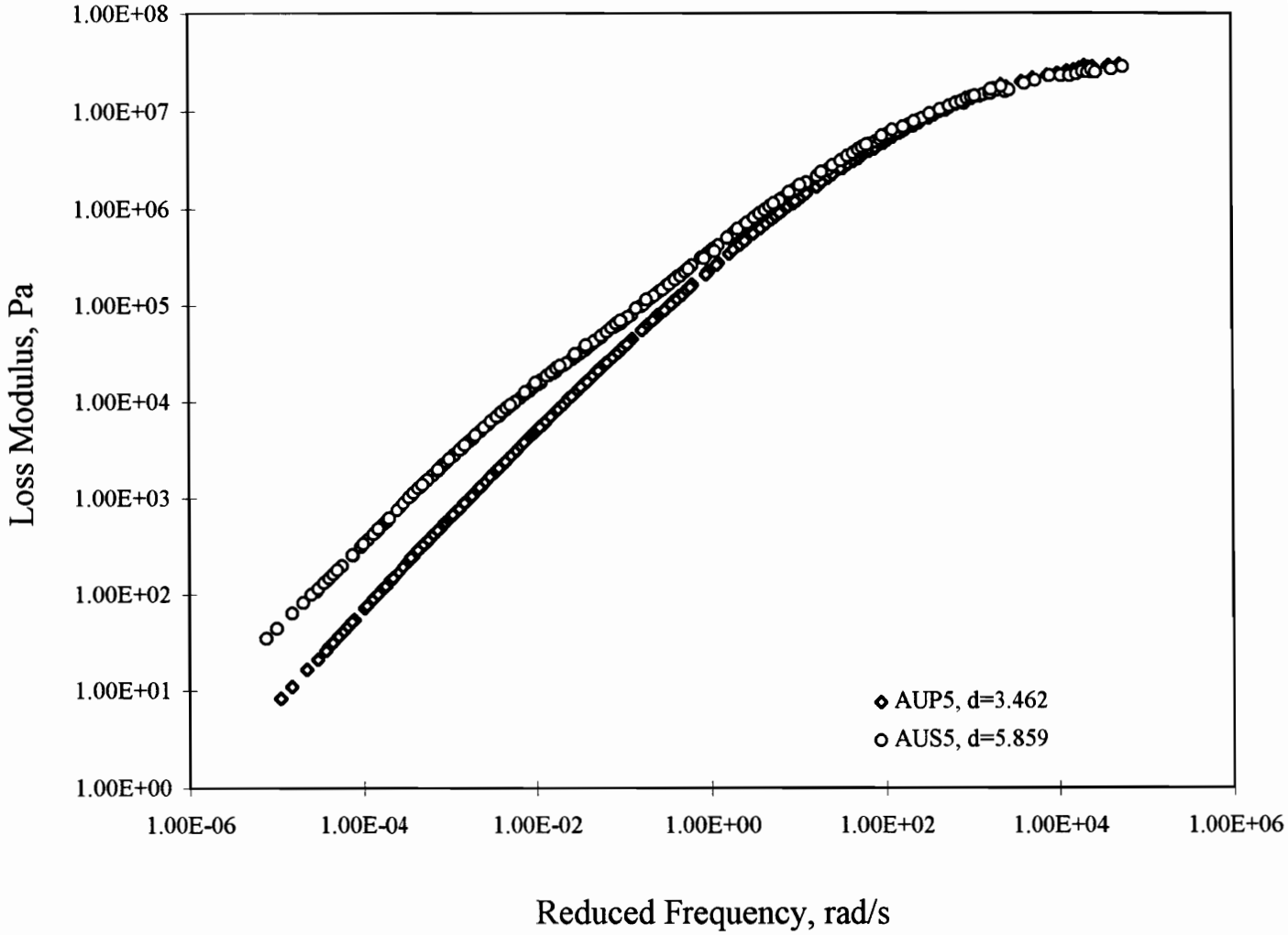

Figure 4.6. Effect of d Value on the Shape of Dynamic Loss Modulus Master Curves

relaxation spectra developed for asphalt-polymer blends. As an example, the relaxation spectra for ARS3 with $d = 4.927$, and ARS5 with $d = 6.508$ are plotted in Figure 4.7. As observed on this graph, increasing polymer content is accompanied with decreasing slope of the curve over almost the entire range of relaxation times, i.e., a broader relaxation spectrum. Considering the fact that for all asphalt-polymer blends the d value increases with increase in polymer content, another interpretation for d value may be attained. Parameter d can be considered to be proportional to the width of relaxation spectrum. Within the experimental range, increasing polymer contents result in broader relaxation spectra.

The peak value of loss modulus, G''_{max}, is a characteristic of the base asphalt. Addition of polymer, and aging treatment do not appear to appreciably influence this parameter. For all asphalt-polymer blends, a G''_{max} value of approximately $10^{7.5}$ Pa was measured.

The proposed model for frequency dependence of loss modulus fits the experimental data over the entire range of reduced frequencies with a high degree of accuracy. Figure 4.8 illustrates the experimental loss modulus master curve for ARP4 along with results of the proposed model. The accuracy of model will be further discussed in Chapter 5. It should be noted that within the temperature range used in this study, the resulting loss modulus master curves are not extended beyond the G''_{max} value, i.e., no experimental data is available to demonstrate the behavior of curves above ω_d. On the other hand, the graph of equation (4. 6) is symmetric with respect to the line $\log\omega = \log\omega_d$. In general, the loss

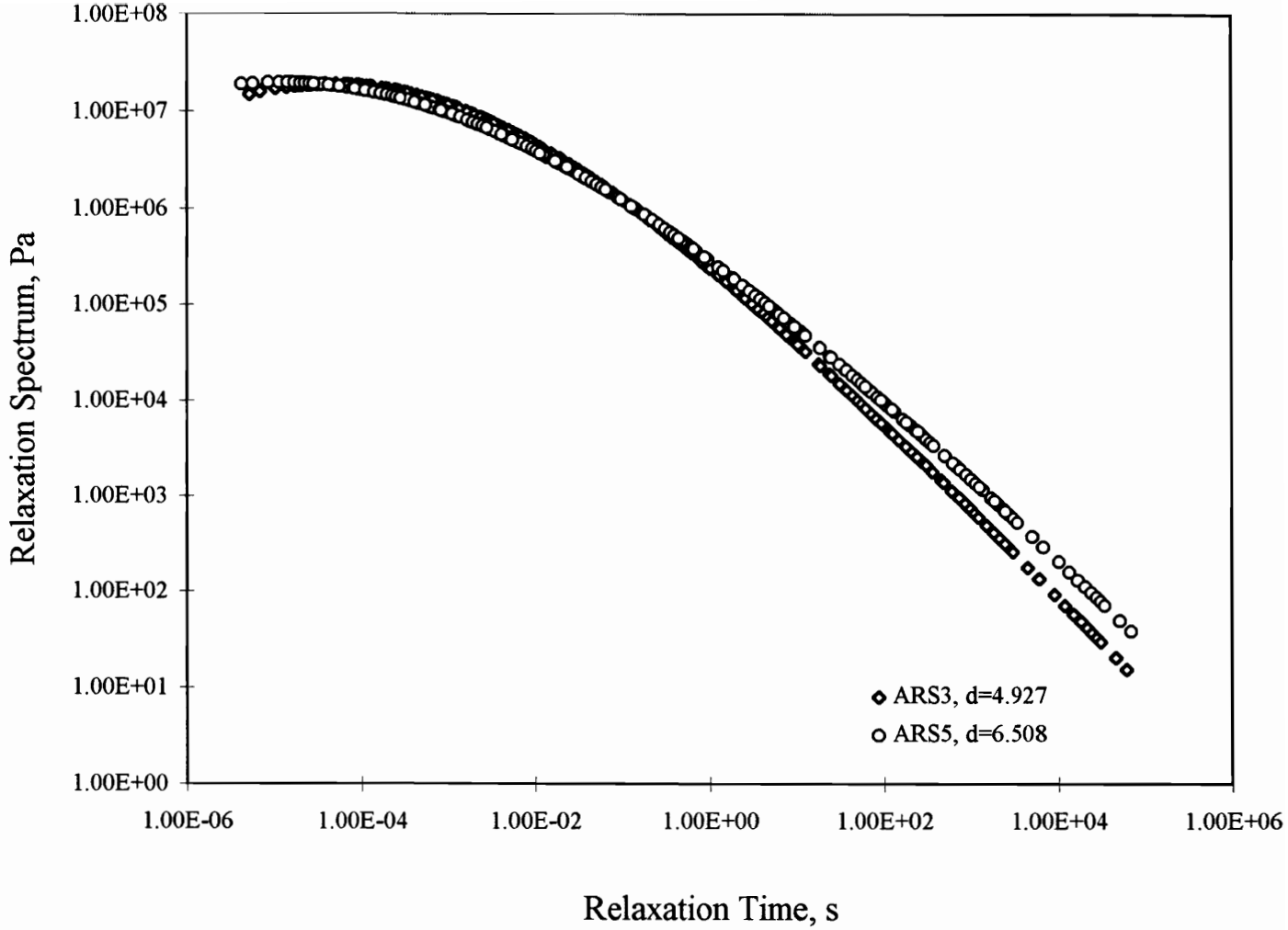

Figure 4.7. Effect of d Value on the Shape of Relaxation Spectrum

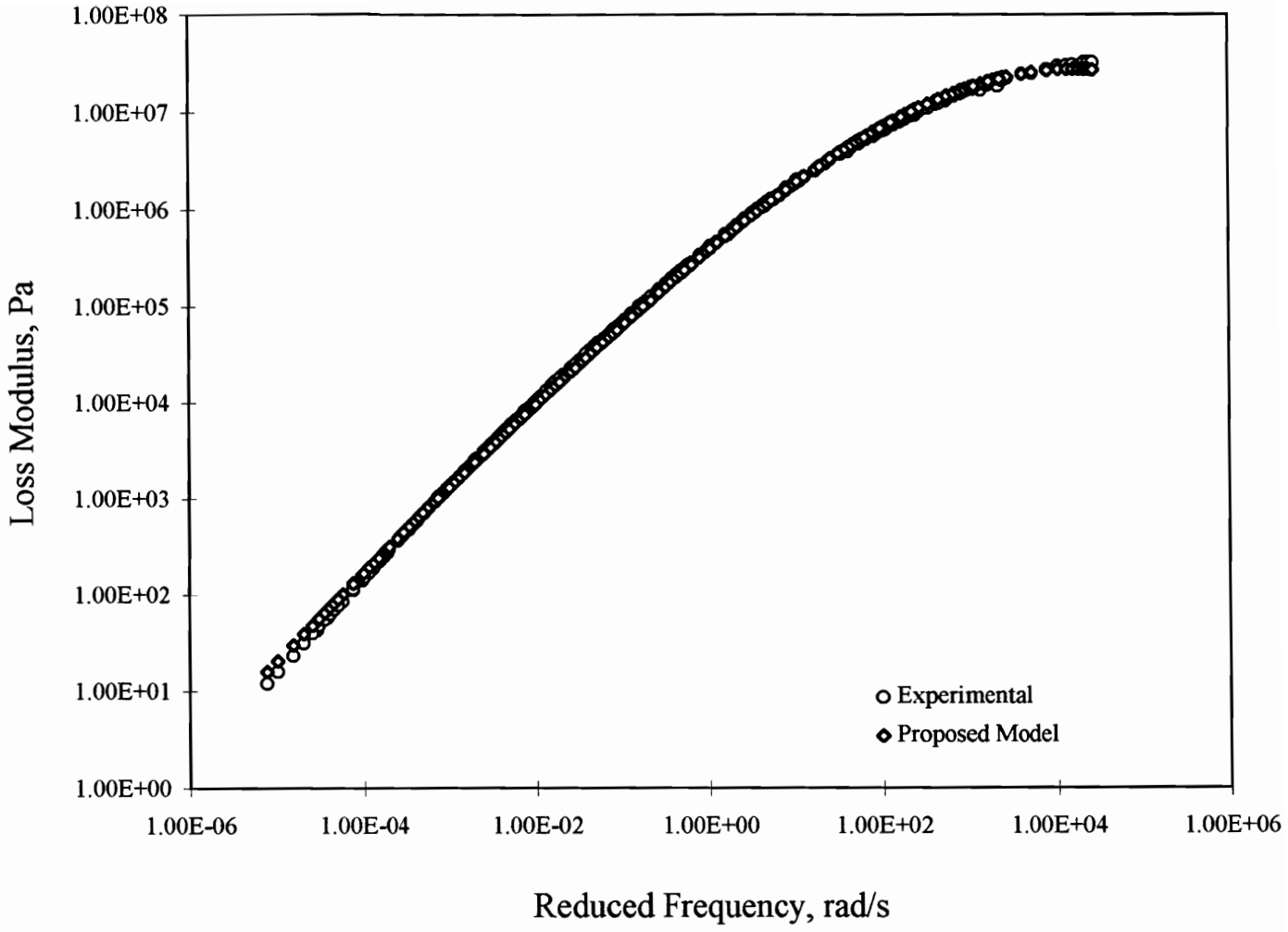

Figure 4.8. Comparison between the Measured Loss Modulus for ARP4 and Results of the Proposed Model

modulus master curve is not expected to have a symmetrical shape with respect to the peak point. Therefore, use of this model is restricted to the specified range, and care should be exercised in any attempt for extrapolation of loss modulus using the equation.

As stated in the previous sections, a major drawback of the existing frequency dependence models for straight asphalts, is their inability to characterize the loss tangent master curves of modified binders, specifically the plateau regions. The loss tangent function derived from equations (4. 5) and (4. 6) is capable of providing acceptable fit to the measured data. As an example, in Figure 4.9 the loss tangent values for ARG5 as derived from equations (4. 5) and (4. 6) are compared to the measured data. From this figure, it is apparent that formation of plateau at frequencies ranging from 0.01 to 10 rad/s is reflected in the results of proposed models. Agreement between the calculated and experimental points over other regions of reduced frequency is reasonable as well. Similar conclusions were obtained for several other modified binders.

4.3. Investigation of Temperature Dependence of Response

In Chapter 2, it was stated that efforts have been made by several investigators to describe the temperature dependence of straight asphalts using the WLF equation with universal or modified constants. This function as described by equation (2. 42), although initially derived as an empirical relationship, can be justified on theoretical ground based on the free volume theory. According to this theory, the external (total) volume of a liquid, V, is

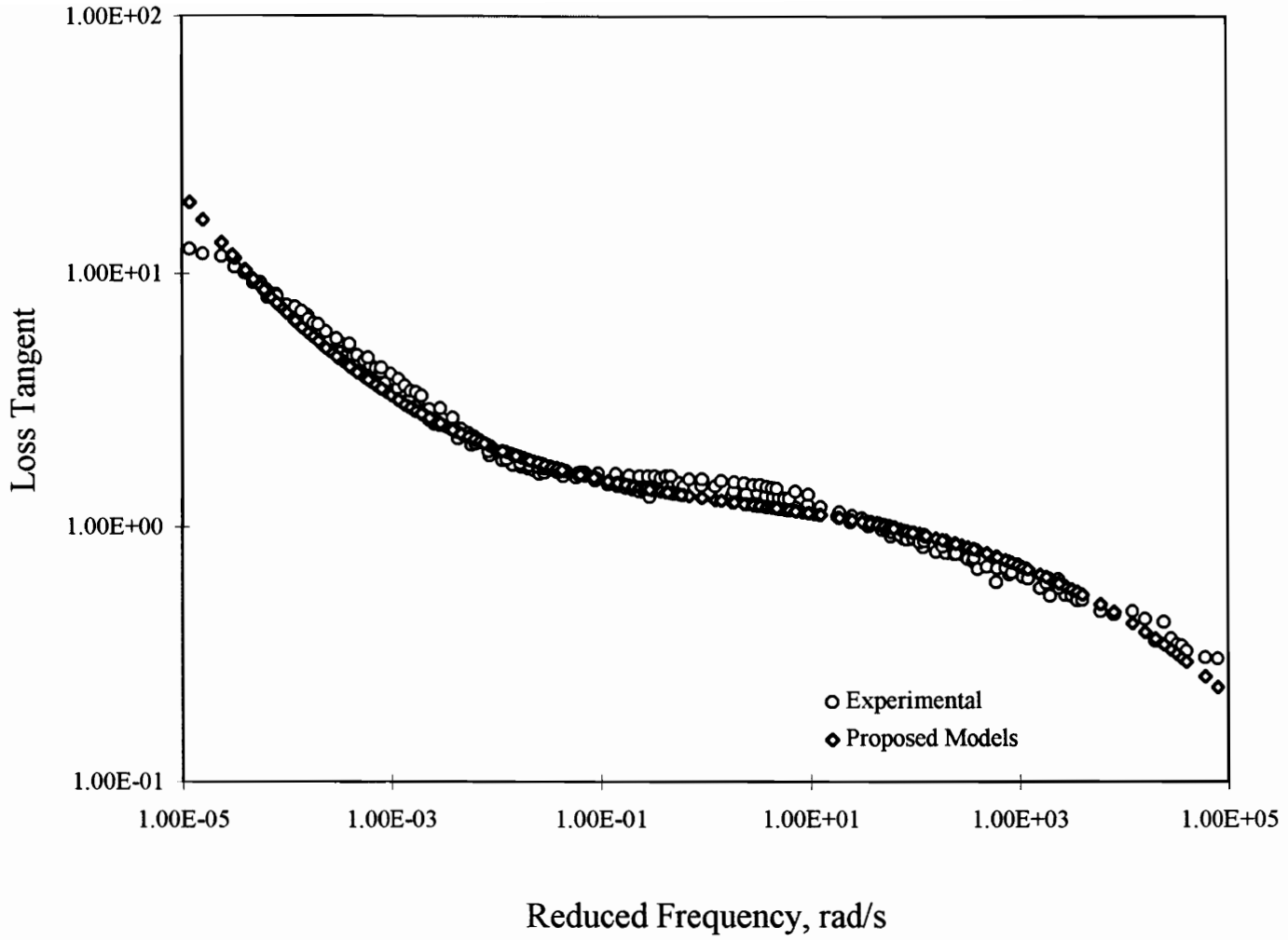

Figure 4.9. Comparison between the Measured Loss Tangent for ARG5 and Results of the Proposed Models

considered to be comprised of an occupied volume, V_0, and a free volume, V_f. The fractional free volume, f, is defined as the ratio of specific free volume to specific total volume:

$$f = \frac{v_f}{v} \tag{4. 8}$$

where,

f = fractional free volume,

v_f = specific free volume, cm^3/g, and

v = specific external volume, cm^3/g.

Above glass transition temperature, T_g, the fractional free volume linearly increases with corresponding increase in temperature. This relationship can be defined by the following equation (Ferry, 1980):

$$f(T) = f(T_g) + \Delta\alpha(T - T_g) \tag{4. 9}$$

where,

$f(T)$ = fractional free volume at temperature T,

$f(T_g)$ = fractional free volume at glass transition temperature T_g, and

$\Delta\alpha$= difference between the coefficients of thermal expansion above and below T_g.

According to Doolittle and Doolittle (1957), the steady-state viscosity of low molecular weight liquids can be related to their fractional free volume using the following equation:

$$\eta = Ae^{B(\frac{1}{f}-1)} \tag{4. 10}$$

where,

η = steady-state viscosity, Pa.s, and

A and B = empirical constants.

By re-writing equation (4. 10) at temperatures T and T_g, one can obtain

$$\frac{\eta(T)}{\eta(T_g)} = e^{B\left[\frac{1}{f(T)}-\frac{1}{f(T_g)}\right]} \tag{4. 11}$$

Furthermore, the ratio of steady-state viscosities at two different temperatures is equal to the ratio of associated relaxation times. Thus, equation (4. 11) can be reduced to

$$\log a_T = \log\frac{\tau(T)}{\tau(T_g)} = \log\frac{\eta(T)}{\eta(T_g)} = \frac{B}{2.303}\left[\frac{1}{f(T)}-\frac{1}{f(T_g)}\right] \tag{4. 12}$$

where,

a_T = shift factor, and

τ = relaxation time, s.

Substituting equation (4. 9) in equation (4. 12) yields

$$\log a_T = \frac{-\frac{B}{2.303 f(T_g)}(T - T_g)}{\frac{f(T_g)}{\Delta\alpha} + (T - T_g)} \tag{4. 13}$$

By comparing equation (4. 13) to the WLF equation, the following relationships can be established between the parameters of this equation and coefficients C_1 and C_2 of the WLF equation:

$$C_1 = \frac{B}{2.303 f(T_g)} \tag{4. 14}$$

$$C_2 = \frac{f(T_g)}{\Delta\alpha} \tag{4. 15}$$

For a majority of polymeric systems the values of $f(T_g)$, $\Delta\alpha$, and B have been reported to be 0.025, 4.8×10^{-4}° K^{-1}, and 1, respectively (Ferry, 1980). Substituting these values in equations (4. 14) and (4. 15) yields the universal constants of C_1 = 17.44 and C_2 = 51.6° K which had been previously reported on an empirical basis (Williams *et al.*, 1955). The

reference temperature in WLF can always be converted to another temperature. In this case the constants C_1 and C_2 will change accordingly. In another approximation, if the reference temperature is considered to be an adjustable parameter about 50° C above T_g, a new pare of constants will be obtained, i.e., C_1 = 8.86 and C_2 = 101.6° K (Williams *et al.*, 1955).

Therefore, the practical importance of the WLF equation is that when the glass transition temperature or another temperature closely related to T_g is used as the reference temperature, the temperature dependence of a wide variety of amorphous polymers and low molecular weight organic liquids can be described by a single set of parameters, i.e., universal constants.

In the primary analysis of temperature dependence of modified binders, the shift factor values were obtained through reduction of data to 25° C. Since this temperature does not carry any level of physical significance, any attempt to fit the measured shift factor data to the WLF equation using 25° C as the reference temperature, will result in a different set of constants for each binder which provides no insight into the temperature dependence relations. However, if the reference temperature, T_s, for each sample is appropriately selected, then the shift factor data for different binders can be fitted to the WLF equation with universal constants. This is equivalent to matching the experimental plot of $\log a_T$ versus T-25 to the plot of equation (2. 42) with universal constants C_1 = 8.86 and C_2 =

101.6° K, through application of horizontal and vertical translations, and can be mathematically presented as

$$\log a_T = \frac{-8.86(T - T_s)}{101.6 + (T - T_s)} - \log b \qquad (4.\ 16)$$

where,

a_T = experimentally measured shift factor,

T_s = reference temperature, ° C, and

b = vertical translation factor.

Therefore, by using the observed shifts for each binder and performing non-linear least squares based on equation (4. 16), the values of reference temperature, T_s, and b can be determined. This analysis was performed for all modified binders. The results, along with a rigorous evaluation of the fit will be presented in Chapter 5. It should be mentioned at this point, that for all samples tested, the WLF equation provided excellent fit to the experimental data over the entire range of temperatures. No deviations from WLF fit such as those reported by Brodnyan *et al.* (1960) or Dobson (1969) were observed. This may be attributed to the fact that the range of applied temperatures in this study is well above the anticipated glass transition temperature of the binders. Application of WLF equation is generally restricted to temperatures above T_g (Williams *et al.*, 1955). Below this value,

other models such as Arrhenius function can be used to describe the temperature dependence of mechanical properties.

Since no glass transition temperature measurement was possible in this study, it is not clear how the estimated reference temperatures from the WLF equation relate to the glass transition temperature of modified binders. However, limited observations can be made on the estimated T_s values. First, addition of polymer to the base asphalt appears to have a slight increasing effect on the estimated reference temperature. Secondly, for all binders the estimated reference temperature of the RTFOT residue is higher than that of the unaged binder. Aging is generally known to increase the asphaltene content of asphalt binders and decrease the oily fraction (Krebs and Walker, 1971). Dilatometric glass transition temperature measurements have shown that T_g always becomes higher with increase in asphaltene content (Wada and Hirose, 1960). Therefore, the increase in estimated T_s due to aging can be attributed to an increase in the associated glass transition temperature. This can prove that the resulting reference temperatures from WLF equation with universal constants are in fact related to the glass transition temperatures. However, no quantitative measure for this relationship can be established at this point.

As a final conclusion, one can state that within the range of temperatures used in this study, the WLF equation with universal constants is indeed adequate to describe the temperature dependence of polymer modified asphalts.

4.4. Proposed Procedure for Characterization of Response

Characterization of viscoelastic response of binders is usually possible by developing dynamic master curves over several decades of reduced frequency. Construction of the dynamic master curves requires performing frequency sweeps at various temperatures, taking a considerable number of modulus measurements, analyzing the data, and finally, reducing the data to a single curve. This process is quite cumbersome and time-consuming.

A major practical application of the proposed models for frequency dependence, is providing a method for complete characterization of the viscoelastic response of binder by means of a limited number of measurements. Using this method, three modulus measurements at a single temperature can yield sufficient information to characterize the response of binder over a wide range of frequencies. The procedure is outlined below.

In order to construct a dynamic master curve, it is necessary to take three measurements at three different frequencies at a certain temperature. Each measurement consists of determination of storage modulus and loss modulus at the test frequency. Substituting the measured values of $G'(\omega)$ at three frequencies in equation (4. 5) yields a system of three simultaneous equations which can be solved in terms of model coefficients log G_g, p, and l. The same procedure can be followed using the measured $G''(\omega)$ values at three test frequencies to compute the parameters $\log G''_{\max}$, d, and $\log \omega_d$ from equation (4. 6). Once

the model coefficients are obtained, the values of storage modulus and loss modulus at any other frequencies may be calculated from equations (4. 5) and (4. 6).

The only drawback of this system is the necessity of solving three simultaneous equations derived from equation (4. 5) which are transcendental in terms of model constants. There is no closed form solution to equations of this type. However, they can be solved using numerical methods such as Newton's or secant procedures. The algorithms for these methods can be found in most commercially available mathematical software packages.

It should be kept in mind that parameters l in equation (4. 5) and $\log\omega_d$ in equation (4. 6) are temperature dependent. Therefore, graphs of these equations will represent the dynamic master curves at the test temperature. However, since shape of master curves at all temperatures is exactly the same, curves for other temperatures can be generated by shifting the base curve along the frequency axis. In order to find the shift value, it is necessary to evaluate the location parameters l, and $\log\omega_d$ at desired temperature. Regarding the fact that other model coefficients are not temperature dependent, the location parameters can be evaluated by taking a single modulus measurement at the desired temperature.

Once the location parameters at two different temperatures are determined, the reference temperature, T_s, in WLF equation can be easily evaluated. Therefore, no further

measurements are required and the response is completely characterized over the entire range of frequencies and temperatures. Determination of the model constants using the proposed procedure will be further discussed in Chapter 5.

Chapter 5
Evaluation and Validation of Proposed Models

The proposed models for frequency dependence of response are evaluated in this chapter. Validity of the models, in general, is thoroughly investigated. Rigorous statistical analyses are conducted to evaluate the accuracy of models. The proposed characterization procedure outlined in Chapter 4 is discussed in more detail. Furthermore, suitability of the WLF fit to the observed shift factor data is assessed.

In order to accomplish these objectives, first, the various model coefficients were estimated using non-linear least squares method. An analysis of mean squared error of prediction was then performed to verify the validity of proposed models. As another means for validation of models, the relaxation spectra were derived from both proposed mathematical equations, and were compared to each other using statistical test techniques. To evaluate the proposed characterization method, the model constants were determined using this procedure, and the resulting moduli at certain frequencies were compared to the observed data. Finally, the reference temperatures in WLF equation were estimated using non-linear least squares, and suitability of fits were evaluated by performing a lack of fit analysis.

All statistical analyses in this chapter have been performed using SAS software package available on the Virginia Tech Computing Center mainframe .

5.1. Estimation of Model Coefficients Using Non-Linear Least Squares

The proposed mathematical equations for storage and loss moduli were fit to the experimental data using non-linear least squares method. For all asphalt-polymer combinations in aged and unaged conditions, the entire measured data was used to determine the parameters of loss modulus equation (approximately 250 data points in each curve). For the storage modulus equation, however, due to uncertainty in storage modulus measurements at high temperatures and low frequencies, the first ten measurements of modulus at T = 75° C (corresponding to frequencies 0.0628 rad/s through 0.5655 rad/s) were discarded from the analysis. It should be noted that within the range of discarded data, the storage modulus usually makes up less than 1% of the magnitude of complex modulus. Therefore, omission of this data would not have any adverse effect on the accuracy of prediction. In case of straight asphalt, at T = 75° C the behavior is completely viscous and storage modulus measurements are not much meaningful. For this reason, in determination of parameters of the storage modulus equation for straight asphalt, the entire frequency sweep data at this temperature was discarded.

In estimation of the model constants in this analysis, only the first replica of measured data was utilized. The second replicate data sets were used for validation of models through the analysis of mean squared error of prediction, discussed in the following section. As examples of the fitting procedure, the SAS input and output data files for non-

linear least squares fit of ARP5 results to the proposed storage modulus and loss modulus equations are presented in Appendices C and D, respectively.

The results of non-linear least square analysis for the proposed storage and loss modulus models are summarized in Tables 5.1 and 5.2, respectively. The tables contain the estimated parameter values, the corresponding asymptotic standard error (s), coefficient of determination (r^2), mean squared error (MSE), and total degrees of freedom (DF).

Despite the fact that in all cases coefficients of determination are very large and approaching unity, this is not necessarily an indication of adequacy of models. In general, a very large r^2 value may be accompanied by a large mean squared error, implying a poor fit. Therefore, the MSE values were obtained. Smallness of MSE provides a better means for evaluation of fits.

In Chapter 2, it was stated that the value of glassy modulus for most polymeric materials and asphalt cements is of the order of 10^9 Pa. According to Table 5.1, the estimated values for glassy modulus in most cases are considerably larger than the expected limiting value, therefore they are not physically meaningful. Nevertheless, within the specified range of temperatures (intermediate and high relative to pavement), this fact does not undermine the predictive capability of the proposed model. The proposed model can estimate the storage modulus within this temperature range accurately. Hence, use of

Table 5.1. Estimated Parameters for the Proposed Storage Modulus Model from Least Squares

Binder	l (1/rad/s)	s (l) (1/rad/s)	p	s (p)	log G_g (Pa)	s (log G_g) (Pa)	r^2	MSE	DF
AUC2	3.801	0.0083	0.116	0.0018	12.957	0.1355	0.999110	0.004331	237
AUC3	4.011	0.0082	0.108	0.0016	13.423	0.1344	0.999304	0.003129	238
AUC4	4.271	0.0090	0.093	0.0015	14.411	0.1570	0.999407	0.002405	238
ARC2	4.342	0.0084	0.138	0.0016	11.445	0.0786	0.999287	0.003184	238
ARC3	4.543	0.0084	0.126	0.0014	11.885	0.0808	0.999434	0.002376	238
ARC4	4.652	0.0096	0.116	0.0014	12.218	0.0929	0.999444	0.002138	238
AUP3	3.983	0.0104	0.116	0.0021	12.925	0.1521	0.998772	0.005782	246
AUP4	4.193	0.0112	0.114	0.0020	12.824	0.1476	0.998851	0.005082	243
AUP5	4.349	0.0129	0.110	0.0022	12.886	0.1613	0.998651	0.005732	246
ARP3	4.575	0.0105	0.132	0.0018	11.598	0.0907	0.999063	0.004027	246
ARP4	4.599	0.0093	0.130	0.0015	11.639	0.0802	0.999313	0.002832	246
ARP5	4.704	0.0094	0.133	0.0015	11.388	0.0708	0.999376	0.002427	246
AUD3	4.005	0.0079	0.144	0.0017	11.202	0.0799	0.999151	0.003937	246
AUD4	4.125	0.0086	0.138	0.0017	11.322	0.0838	0.999175	0.003493	246
AUD5	4.222	0.0139	0.166	0.0029	10.127	0.0948	0.997718	0.009119	245

Table 5.1. Estimated Parameters for the Proposed Storage Modulus Model from Least Squares (continued)

Binder	l (1/rad/s)	s (l) (1/rad/s)	p	s (p)	log G_g (Pa)	s (log G_g) (Pa)	r^2	MSE	DF
ARD3	4.497	0.0083	0.162	0.0016	10.353	0.0535	0.999280	0.002996	246
ARD4	4.608	0.0105	0.163	0.0019	10.193	0.0601	0.999009	0.003782	246
ARD5	4.701	0.0122	0.165	0.0021	10.015	0.0644	0.998729	0.004633	246
AUS3	4.413	0.0105	0.145	0.0019	10.910	0.0794	0.998981	0.004100	246
AUS4	4.671	0.0121	0.139	0.0019	10.975	0.0842	0.998934	0.004006	246
AUS5	5.462	0.0194	0.106	0.0020	12.147	0.1350	0.998769	0.003715	246
ARS3	5.037	0.0122	0.155	0.0018	10.330	0.0621	0.998999	0.003672	246
ARS4	5.239	0.0169	0.150	0.0023	10.310	0.0786	0.998430	0.005222	246
ARS5	5.759	0.0215	0.128	0.0022	10.831	0.0971	0.998416	0.004635	246
AUG3	4.121	0.0082	0.165	0.0019	10.495	0.0622	0.998999	0.004870	246
AUG4	4.710	0.0117	0.155	0.0020	10.365	0.0695	0.998846	0.004425	246
AUG5	5.221	0.0231	0.150	0.0031	10.282	0.1040	0.997180	0.009051	246
ARG3	4.658	0.0087	0.179	0.0017	9.913	0.0454	0.999187	0.003399	246
ARG4	5.032	0.0104	0.176	0.0017	9.764	0.0452	0.999102	0.003435	246
ARG5	5.696	0.0131	0.154	0.0016	10.068	0.0477	0.999231	0.002440	246

Table 5.1. Estimated Parameters for the Proposed Storage Modulus Model from Least Squares (continued)

Binder	l (1/rad/s)	s (l) (1/rad/s)	p	s (p)	log G_g (Pa)	s (log G_g) (Pa)	r^2	MSE	DF
AUX3	5.283	0.0214	0.083	0.0022	14.580	0.2549	0.998484	0.005146	245
AUX4	5.321	0.0130	0.108	0.0014	12.311	0.0970	0.999366	0.002118	246
AUX5	5.680	0.0209	0.093	0.0019	13.149	0.1675	0.998812	0.003657	246
ARX3	5.081	0.0110	0.159	0.0017	10.196	0.0525	0.999180	0.003024	246
ARX4	5.225	0.0164	0.171	0.0025	9.834	0.0660	0.998195	0.006352	246
ARX5	5.396	0.0218	0.166	0.0031	9.866	0.0839	0.997167	0.009689	246
AUN3	4.590	0.0124	0.129	0.0020	11.467	0.1029	0.998852	0.004390	246
AUN4	5.644	0.0200	0.084	0.0018	13.947	0.1913	0.998982	0.003034	246
AUN5	6.291	0.0174	0.085	0.0000	13.286	0.0177	0.998111	0.004942	246
ARN3	4.927	0.0190	0.164	0.0031	10.036	0.0933	0.997184	0.010537	246
ARN4	5.431	0.0214	0.143	0.0026	10.447	0.0957	0.997915	0.006525	246
ARN5	6.240	0.0200	0.108	0.0017	11.700	0.0974	0.999107	0.002460	246
AU00	3.605	0.0131	0.124	0.0030	12.795	0.2021	0.997611	0.011992	224
AR00	4.165	0.0075	0.160	0.0015	10.799	0.0567	0.999394	0.002736	223

Table 5.2. Estimated Parameters for the Proposed Loss Modulus Model from Least Squares

Binder	d (Pa)	s (d) (Pa)	logω_d (rad/s)	s (logω_d) (rad/s)	logG''_{max} (Pa)	s (logG''_{max}) (Pa)	r^2	MSE	DF
AUC2	2.881	0.0251	4.253	0.0224	7.430	0.0083	0.999765	0.000795	248
AUC3	3.036	0.0239	4.280	0.0212	7.432	0.0078	0.999795	0.000636	248
AUC4	3.430	0.0168	4.519	0.0150	7.456	0.0055	0.999924	0.000235	248
ARC2	3.533	0.0381	4.153	0.0303	7.451	0.0101	0.999484	0.001583	248
ARC3	3.758	0.0337	4.243	0.0269	7.452	0.0090	0.999649	0.001066	248
ARC4	3.963	0.0295	4.370	0.0232	7.412	0.0076	0.999758	0.000709	248
AUP3	2.990	0.0264	4.203	0.0225	7.451	0.0081	0.999705	0.000932	256
AUP4	3.213	0.0302	4.182	0.0250	7.401	0.0087	0.999642	0.001119	253
AUP5	3.462	0.0271	4.282	0.0222	7.399	0.0076	0.999743	0.000807	256
ARP3	3.720	0.0350	4.107	0.0265	7.449	0.0086	0.999529	0.001413	256
ARP4	3.867	0.0368	4.219	0.0283	7.444	0.0092	0.999545	0.001350	256
ARP5	4.078	0.0359	4.229	0.0267	7.423	0.0084	0.999576	0.001183	256
AUD3	3.557	0.0351	4.477	0.0297	7.485	0.0104	0.999619	0.001169	256
AUD4	3.779	0.0394	4.549	0.0333	7.439	0.0116	0.999583	0.001244	256
AUD5	4.444	0.0571	4.779	0.0467	7.474	0.0158	0.999337	0.001824	255

Table 5.2. Estimated Parameters for the Proposed Loss Modulus Model from Least Squares (continued)

Binder	d (Pa)	s (d) (Pa)	logω_d (rad/s)	s (logω_d) (rad/s)	logG''_{max} (Pa)	s (logG''_{max}) (Pa)	r^2	MSE	DF
ARD3	4.148	0.0428	4.286	0.0323	7.453	0.0102	0.999447	0.001593	256
ARD4	4.594	0.0499	4.471	0.0371	7.444	0.0116	0.999380	0.001655	256
ARD5	4.949	0.0554	4.590	0.0405	7.420	0.0124	0.999329	0.001743	256
AUS3	4.152	0.0383	4.534	0.0302	7.461	0.0099	0.999579	0.001133	256
AUS4	4.603	0.0455	4.656	0.0353	7.482	0.0114	0.999552	0.001239	256
AUS5	5.859	0.0544	5.059	0.0395	7.469	0.0120	0.999593	0.001002	256
ARS3	4.927	0.0464	4.349	0.0325	7.443	0.0096	0.999463	0.001425	256
ARS4	5.614	0.0551	4.647	0.0380	7.459	0.0110	0.999444	0.001403	256
ARS5	6.508	0.0671	4.907	0.0442	7.465	0.0123	0.999369	0.001466	256
AUG3	3.695	0.0429	4.305	0.0340	7.498	0.0114	0.999375	0.001950	256
AUG4	4.729	0.0561	4.511	0.0415	7.434	0.0128	0.999258	0.002032	256
AUG5	6.041	0.0936	4.930	0.0648	7.516	0.0189	0.998687	0.003133	256
ARG3	4.500	0.0553	4.238	0.0392	7.497	0.0118	0.999078	0.002553	256
ARG4	5.157	0.0633	4.260	0.0422	7.440	0.0119	0.998968	0.002689	256
ARG5	6.409	0.0775	4.598	0.0486	7.474	0.0129	0.998973	0.002430	256

Table 5.2. Estimated Parameters for the Proposed Loss Modulus Model from Least Squares (continued)

Binder	d (Pa)	s (d) (Pa)	$\log\omega_d$ (rad/s)	s ($\log\omega_d$) (rad/s)	$\log G''_{max}$ (Pa)	s ($\log G''_{max}$) (Pa)	r^2	MSE	DF
AUX3	4.722	0.0205	4.790	0.0161	7.560	0.0052	0.999914	0.000237	255
AUX4	5.103	0.0330	4.709	0.0244	7.513	0.0075	0.999788	0.000556	256
AUX5	5.557	0.0356	4.870	0.0258	7.528	0.0078	0.999797	0.000529	256
ARX3	5.090	0.0516	4.360	0.0354	7.463	0.0103	0.999351	0.001696	256
ARX4	5.591	0.0708	4.442	0.0471	7.488	0.0132	0.998957	0.002619	256
ARX5	6.015	0.0804	4.582	0.0528	7.515	0.0146	0.998860	0.002819	256
AUN3	4.440	0.0419	4.714	0.0338	7.491	0.0113	0.999621	0.001058	256
AUN4	5.760	0.0465	5.155	0.0348	7.538	0.0109	0.999716	0.000731	256
AUN5	7.161	0.0895	5.474	0.0615	7.551	0.0179	0.999270	0.001674	256
ARN3	5.077	0.0550	4.487	0.0388	7.455	0.0115	0.999316	0.001820	256
ARN4	5.889	0.0618	4.679	0.0417	7.448	0.0118	0.999338	0.001578	256
ARN5	6.734	0.0464	4.857	0.0296	7.470	0.0080	0.999703	0.000679	256
AU00	2.659	0.0307	4.142	0.0269	7.450	0.0100	0.999563	0.001479	256
AR00	3.359	0.0383	3.998	0.0294	7.477	0.0098	0.999347	0.002037	256

equation (4. 5) should be restricted to storage moduli below 10^8 Pa. This model is not capable of predicting low temperature storage modulus values.

5.2. Validation of the Proposed Models

Statistical measures such as r^2 or MSE are useful in reflecting the degree of agreement between a model and the data set from which it was developed. However, they provide no information as to the potential degree of effectiveness of the model against independent data sets. Model validation involves assessing the adequacy of model with respect to future observations. In validation of a model, in addition to precision (repeatability), the bias of prediction should be addressed. A variety of methods may be used to verify the validity of a model. A simple procedure is re-determination of model coefficients based on an independent data set, and comparison between the two coefficient sets in terms of consistency.

Another method combines the variance of prediction with bias to yield a single measure of predictive capability of model. This measure is called mean squared error of prediction (MSEP). The equation for MSEP can be written as follows (Rawlings, 1988):

$$MSEP = \frac{(n^* - 1)s^2(\delta_i)}{n^*} + (\bar{\delta})^2 \qquad (5.\ 1)$$

where,

δ_i = difference between independent observations and predicted values from the model for the ith validation case,

s^2 = variance,

$\bar{\delta}$ = average of δ_i values, and

n^* = number of cases in the independent (validation) data set.

The first term in equation (5. 1) represents the variance term, and the second one indicates the bias term. Substituting the value of $s^2(\delta_i)$ in equation (5. 1) yields

$$MSEP = \frac{\sum \delta_i^2}{n^*} \tag{5. 2}$$

Therefore, MSEP can be simply defined as the average squared difference between the response variable in independent data set and prediction of the model derived from the model building data set.

In order to check the validity of proposed models of frequency dependence, an analysis of MSEP was performed. For this purpose, after determination of model constants based on the first replica of measured data, the second replica was considered to be the independent or validation data set. Therefore, using the model developed based on the first replica, the moduli were predicted for each frequency in the second replica, and the

differences between predicted values and observed values of the second replica were computed. Average of squared differences in each case yields the corresponding MSEP.

Results of this analysis on proposed models for storage modulus and loss modulus are summarized in Tables 5.3 and 5.4, respectively. The tables include the values of MSEP and n^* for each binder. In general, the magnitude of MSEP is an indication of the predictive capability of the model. The less the MSEP, the higher the adequacy of model against independent sets of data. Extremely small values of MSEP in Tables 5.3 and 5.4 describes the potential validity of proposed models with respect to future data sets.

5.3. Evaluation of Relaxation Spectra Based on Proposed Models

The proposed mathematical models for frequency dependence are two independent equations with no common parameters. In reality, however, the real and imaginary parts of harmonic response functions (in this case, storage and loss moduli, respectively) are interrelated through integral transforms. If the analytical expressions derived for different viscoelastic functions are legitimate, they should all generate a unique distribution of relaxation times. Therefore, to verify the validity of proposed models despite their lack of apparent interdependency, the relaxation spectra for all modified binders were derived once based on the proposed equation for storage modulus, and once based on the analytical model for loss modulus. The approximation of Ninomiya and Ferry (1959) represented by equations (2. 21) and (2. 22) was used for this purpose, and the resulting spectra were checked for coincidence. In all cases, a high degree of agreement between

Table 5.3. Evaluation of Mean Squared Error of Prediction for the Proposed Storage Modulus Model

Binder	MSEP	n*	Binder	MSEP	n*	Binder	MSEP	n*
AUC2	0.008122	238	**ARD3**	0.006496	246	**AUX3**	0.009278	246
AUC3	0.006646	238	**ARD4**	0.004160	246	**AUX4**	0.002600	246
AUC4	0.007816	238	**ARD5**	0.019005	246	**AUX5**	0.004940	246
ARC2	0.002093	238	**AUS3**	0.005662	246	**ARX3**	0.006427	246
ARC3	0.006072	238	**AUS4**	0.011239	246	**ARX4**	0.006609	246
ARC4	0.005376	238	**AUS5**	0.004487	246	**ARX5**	0.007951	246
AUP3	0.011530	246	**ARS3**	0.003452	246	**AUN3**	0.004086	246
AUP4	0.005208	245	**ARS4**	0.004136	246	**AUN4**	0.004324	246
AUP5	0.005192	246	**ARS5**	0.003883	246	**AUN5**	0.004772	246
ARP3	0.009425	246	**AUG3**	0.005237	246	**ARN3**	0.009732	246
ARP4	0.004753	246	**AUG4**	0.007048	246	**ARN4**	0.008619	246
ARP5	0.004110	246	**AUG5**	0.007798	246	**ARN5**	0.003222	246
AUD3	0.005825	246	**ARG3**	0.003863	246	**AU00**	0.060365	224
AUD4	0.006046	246	**ARG4**	0.003887	246	**AR00**	0.004390	224
AUD5	0.012707	246	**ARG5**	0.009862	246			

Table 5.3. Evaluation of Mean Squared Error of Prediction for the Proposed Loss Modulus Model

Binder	MSEP	n*	Binder	MSEP	n*	Binder	MSEP	n*
AUC2	0.001691	248	**ARD3**	0.003185	256	**AUX3**	0.001165	256
AUC3	0.001148	248	**ARD4**	0.002144	256	**AUX4**	0.000836	256
AUC4	0.002349	248	**ARD5**	0.004021	256	**AUX5**	0.000802	256
ARC2	0.001380	248	**AUS3**	0.001715	256	**ARX3**	0.003652	256
ARC3	0.002536	248	**AUS4**	0.001958	256	**ARX4**	0.002616	256
ARC4	0.001760	248	**AUS5**	0.001637	256	**ARX5**	0.003493	256
AUP3	0.001587	256	**ARS3**	0.001697	256	**AUN3**	0.000940	256
AUP4	0.001781	255	**ARS4**	0.001653	256	**AUN4**	0.000740	256
AUP5	0.001352	256	**ARS5**	0.002151	256	**AUN5**	0.001397	256
ARP3	0.004475	256	**AUG3**	0.002330	256	**ARN3**	0.001845	256
ARP4	0.001533	256	**AUG4**	0.002558	256	**ARN4**	0.002276	256
ARP5	0.002653	256	**AUG5**	0.002748	256	**ARN5**	0.001352	256
AUD3	0.001890	256	**ARG3**	0.002911	256	**AU00**	0.003163	256
AUD4	0.002507	256	**ARG4**	0.002687	256	**AR00**	0.002537	256
AUD5	0.001476	256	**ARG5**	0.003180	256			

the two spectra was observed. In essence, except for the highest and lowest extremes of relaxation times, the resulting spectra perfectly coincided. As an example, this coincidence is shown in Figure 5.1 where the relaxation spectra derived based on proposed equations are plotted for AUS5.

To examine the possibility of significant statistical differences between the two spectra despite the visual agreement, a set of statistical tests were conducted. For each binder, the average of differences between pairs of relaxation spectrum values, $\bar{d}$, was computed. The null hypothesis $H_0 : \bar{d} = 0$ was then tested against the alternative hypothesis $H_a : \bar{d} \neq 0$. To test the hypothesis, the t statistic was computed in each case according to the following equation:

$$t = \frac{\bar{d} - 0}{\frac{s}{\sqrt{n}}} \tag{5. 3}$$

where,

s = standard deviation, and

n = degrees of freedom.

The large number of degrees of freedom for a complete relaxation spectrum data set (approximately 260), makes the interpretation of resulting t statistic somewhat difficult.

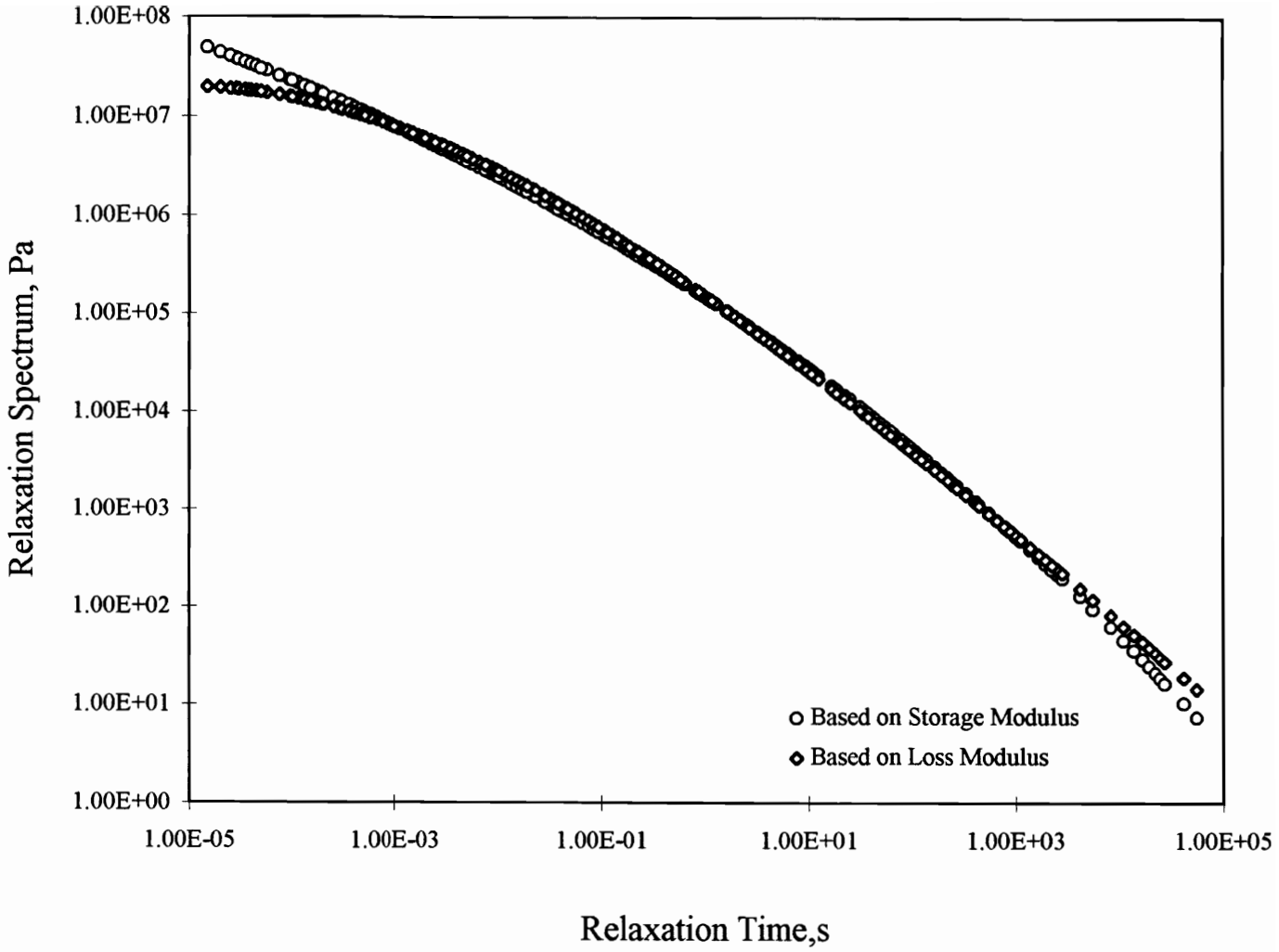

Figure 5.1. Comparison between Relaxation Spectra of AUS5 Derived From Proposed Equations for Storage Modulus and Loss Modulus

Therefore, only 41 equally spaced points on the log relaxation time scale were chosen for each test. The test results including the values of $\bar{d}$, s, and t statistic for each binder are summarized in Table 5.5. Degrees of freedom in all cases equal 40. Assuming a probability of type I error, α= 5%, the critical t (t_{cr}) for a two sided test with 40 degrees of freedom is found to be 2.021. The results of hypothesis tests showed that $|t| < t_{cr}$ for all cases except for AUN5 and AUD5 with t values slightly off the limit. Therefore, the null hypothesis is accepted, i.e., there is no difference between the two relaxation spectra derived from equations of storage modulus and loss modulus. This ensures that the proposed models for storage and loss moduli result in a unique distribution of relaxation times.

5.4. Determination of Model Parameters by Proposed Characterization Method

In Chapter 4, a procedure for characterization of response based on three measurements at a certain temperature was outlined. Applicability of the proposed method to the measured data is discussed below.

For evaluation of model constants using the proposed method, the measured values of storage and loss moduli at a temperature of 25° C, and frequencies of 0.6283, 6.283 and 62.830 rad/s were used. The selected frequencies are equally spaced on a logarithmic scale. The storage and loss moduli were substituted in equations (4. 5) and (4. 6), respectively, to obtain two systems of three simultaneous equations. The systems of

Table 5.5. Results of *t* Test for Relaxation Spectra

Binder	$\bar{d}$	*s*	*t*	Binder	$\bar{d}$	*s*	*t*
AUC2	-0.0479	0.1615	-1.899	**ARD3**	0.0051	0.1269	0.257
AUC3	-0.0314	0.1535	-1.310	**ARD4**	-0.0126	0.1094	-0.737
AUC4	-0.0211	0.1139	-1.186	**ARD5**	-0.0208	0.0998	-1.335
ARC2	-0.0207	0.1704	-0.778	**AUS3**	0.0153	0.1218	0.804
ARC3	-0.0295	0.1304	-1.449	**AUS4**	-0.0266	0.0840	-2.028
ARC4	-0.0228	0.1055	-1.384	**AUS5**	0.0009	0.0616	0.094
AUP3	-0.0508	0.1782	-1.826	**ARS3**	-0.0081	0.0990	-0.524
AUP4	-0.0336	0.1520	-1.416	**ARS4**	-0.0123	0.0831	-0.948
AUP5	-0.0341	0.1324	-1.650	**ARS5**	-0.0133	0.0574	-1.485
ARP3	-0.0309	0.1339	-1.477	**AUG3**	-0.0166	0.1602	-0.663
ARP4	-0.0179	0.1263	-0.907	**AUG4**	-0.0194	0.1022	-1.215
ARP5	-0.0043	0.1262	-0.218	**AUG5**	-0.0028	0.0740	-0.242
AUD3	-0.0262	0.1510	-1.111	**ARG3**	-0.0023	0.1323	-0.111
AUD4	-0.0099	0.1366	-0.464	**ARG4**	0.0006	0.1044	0.037
AUD5	-0.0723	0.1601	-2.892	**ARG5**	-0.0056	0.0677	-0.529

Table 5.5. Results of t Test for Relaxation Spectra (continued)

Binder	$\bar{d}$	s	t
AUX3	-0.0046	0.0954	-0.309
AUX4	-0.0014	0.0826	-0.109
AUX5	-0.0102	0.0872	-0.749
ARX3	-0.0273	0.1028	-1.701
ARX4	-0.0106	0.1029	-0.660
ARX5	-0.0259	0.0907	-1.829
AUN3	-0.0296	0.0952	-1.992
AUN4	0.0014	0.0773	0.116
AUN5	0.0210	0.0598	2.247
ARN3	-0.0331	0.1151	-1.8418
ARN4	-0.0114	0.0709	-1.029
ARN5	0.0199	0.0707	1.803
AU00	-0.0168	0.2810	-0.383
AR00	-0.0084	0.1888	-0.285

equations were then solved for values of coefficients. The results of this analysis are summarized in Tables 5.6 and 5.7. Table 5.6 contains the measured storage moduli at three pre-described frequencies, and the resulting parameters l, p, and $\log G_g$. The observed loss moduli at the same frequencies, as well as solution of system of equations for $\log G''_{max}$, d, and $\log \omega_d$, are presented in Table 5.7.

The model constants derived from the proposed system as shown in Tables 5.6 and 5.7 may be compared to those estimated from non-linear least squares previously presented in Tables 5.1 and 5.2. Although in most cases the estimated parameters from two different methods are fairly close, for some modified binders differences are more appreciable. It is not certain how the simultaneous variations of three constants can affect the overall value of modulus derived from the equation. Therefore, comparisons are more reasonable to be made between the resulting moduli rather than the estimated coefficients. This subject is discussed in the next section.

5.5. Prediction of Moduli by Proposed Characterization Procedure

To further examine the accuracy of proposed models and characterization method, comparisons were made between the measured moduli and those predicted by the proposed method. The estimated model parameters as described in the previous section were used to compute the storage and loss moduli at a frequency of 6.283 rad/s using

Table 5.6. Derivation of Parameters of Storage Modulus Model from the Proposed Characterization Method

Binder	Log Measured Storage Modulus @			l	p	log G_g
	.6283 rad/s	6.283 rad/s	62.83 rad/s	(1/rad/s)		(Pa)
AUC2	4.439	5.382	6.243	3.882	0.105	13.852
AUC3	4.507	5.431	6.279	4.065	0.098	14.322
AUC4	4.529	5.417	6.243	4.356	0.081	15.597
ARC2	4.982	5.815	6.561	4.318	0.138	11.477
ARC3	4.980	5.816	6.555	4.464	0.123	12.168
ARC4	4.940	5.753	6.500	4.937	0.093	13.667
AUP3	4.584	5.519	6.344	3.837	0.125	12.519
AUP4	4.698	5.591	6.387	4.129	0.115	12.904
AUP5	4.754	5.623	6.398	4.261	0.115	12.776
ARP3	5.124	5.926	6.652	4.683	0.122	11.992
ARP4	5.057	5.885	6.602	4.470	0.137	11.386
ARP5	5.117	5.927	6.625	4.394	0.149	10.869
AUD3	4.700	5.540	6.338	4.025	0.137	11.322
AUD4	4.708	5.522	6.312	4.223	0.126	11.858
AUD5	4.826	5.615	6.367	4.439	0.138	10.927

Table 5.6. Derivation of Parameters of Storage Modulus Model from the Proposed Characterization Method (continued)

Binder	Log Measured Storage Modulus @			l	p	log G_g
	.6283 rad/s	6.283 rad/s	62.83 rad/s	(1/rad/s)		(Pa)
ARD3	5.127	5.910	6.626	4.649	0.141	10.963
ARD4	5.146	5.912	6.603	4.659	0.152	10.435
ARD5	5.155	5.897	6.576	4.862	0.145	10.558
AUS3	4.907	5.721	6.461	4.580	0.122	11.840
AUS4	5.013	5.785	6.525	4.929	0.114	11.989
AUS5	5.117	5.857	6.539	5.518	0.095	13.040
ARS3	5.367	6.100	6.763	5.146	0.140	10.793
ARS4	5.365	6.083	6.732	5.291	0.137	10.755
ARS5	5.430	6.124	6.751	5.791	0.114	11.554
AUG3	4.942	5.744	6.520	4.380	0.135	11.410
AUG4	5.152	5.882	6.598	5.047	0.123	11.397
AUG5	5.322	6.021	6.698	5.364	0.134	10.791
ARG3	5.375	6.114	6.796	4.919	0.153	10.487
ARG4	5.502	6.207	6.845	5.199	0.155	10.240
ARG5	5.677	6.301	6.901	5.724	0.148	10.152

Table 5.6. Derivation of Parameters of Storage Modulus Model from the Proposed Characterization Method (continued)

Binder	Log Measured Storage Modulus @			l	p	log G_g
	.6283 rad/s	6.283 rad/s	62.83 rad/s	(1/rad/s)		(Pa)
AUX3	5.033	5.792	6.547	5.292	0.082	14.649
AUX4	5.185	5.929	6.650	5.436	0.098	12.963
AUX5	5.248	5.954	6.656	5.701	0.092	13.266
ARX3	5.427	6.137	6.813	5.390	0.130	11.019
ARX4	5.544	6.230	6.882	5.361	0.153	10.191
ARX5	5.575	6.260	6.909	5.698	0.137	10.641
AUN3	4.884	5.677	6.438	4.803	0.107	12.560
AUN4	5.076	5.823	6.540	5.671	0.081	14.263
AUN5	5.276	5.999	6.648	6.012	0.091	12.934
ARN3	5.301	6.041	6.723	4.944	0.155	10.166
ARN4	5.418	6.127	6.764	5.471	0.133	10.836
ARN5	5.549	6.225	6.840	6.140	0.102	12.303
AU00	4.425	5.396	6.267	3.638	0.120	13.027
AR00	5.064	5.908	6.662	4.213	0.154	10.995

Table 5.7. Derivation of Parameters of Loss Modulus Model from the Proposed Characterization Method

Binder	Log Measured Loss Modulus @			d	$\log\omega_d$	$\log G''_{max}$
	.6283 rad/s	6.283 rad/s	62.83 rad/s	(Pa)	(rad/s)	(Pa)
AUC2	5.025	5.823	6.524	2.933	4.203	7.384
AUC3	5.072	5.857	6.545	3.135	4.290	7.415
AUC4	5.049	5.825	6.515	3.611	4.758	7.573
ARC2	5.403	6.111	6.721	4.295	4.618	7.564
ARC3	5.396	6.104	6.712	4.222	4.546	7.527
ARC4	5.342	6.041	6.652	4.861	5.062	7.646
AUP3	5.134	5.916	6.594	3.011	4.096	7.370
AUP4	5.204	5.960	6.607	3.263	4.086	7.329
AUP5	5.225	5.959	6.589	3.641	4.323	7.435
ARP3	5.509	6.196	6.780	4.422	4.493	7.536
ARP4	5.455	6.149	6.739	4.286	4.444	7.489
ARP5	5.497	6.170	6.747	4.912	4.780	7.582
AUD3	5.155	5.914	6.582	3.731	4.664	7.555
AUD4	5.130	5.878	6.547	4.407	5.279	7.755
AUD5	5.210	5.936	6.573	4.359	4.914	7.572

Table 5.7. Derivation of Parameters of Loss Modulus Model from the Proposed Characterization Method (continued)

Binder	Log Measured Loss Modulus @			d	$\log\omega_d$	$\log G''_{max}$
	.6283 rad/s	6.283 rad/s	62.83 rad/s	(Pa)	(rad/s)	(Pa)
ARD3	5.487	6.170	6.760	4.891	4.884	7.652
ARD4	5.474	6.143	6.723	5.313	5.092	7.662
ARD5	5.459	6.117	6.685	5.441	5.063	7.589
AUS3	5.297	6.021	6.647	4.050	4.564	7.501
AUS4	5.365	6.076	6.689	4.249	4.609	7.535
AUS5	5.420	6.090	6.657	4.665	4.522	7.394
ARS3	5.653	6.286	6.828	5.785	5.039	7.674
ARS4	5.639	6.262	6.792	5.828	4.950	7.590
ARS5	5.673	6.279	6.795	6.267	5.082	7.604
AUG3	5.350	6.072	6.718	5.069	5.600	7.986
AUG4	5.458	6.130	6.719	5.597	5.388	7.771
AUG5	5.574	6.225	6.783	5.396	4.937	7.629
ARG3	5.664	6.316	6.877	5.484	5.025	7.756
ARG4	5.746	6.367	6.885	5.351	4.549	7.550
ARG5	5.840	6.413	6.903	7.291	5.404	7.746

Table 5.7. Derivation of Parameters of Loss Modulus Model from the Proposed Characterization Method (continued)

Binder	Log Measured Loss Modulus @			d	$\log\omega_d$	$\log G''_{max}$
	.6283 rad/s	6.283 rad/s	62.83 rad/s	(Pa)	(rad/s)	(Pa)
AUX3	5.378	6.086	6.719	5.408	5.732	7.998
AUX4	5.493	6.179	6.778	5.132	5.149	7.775
AUX5	5.517	6.190	6.777	5.407	5.230	7.774
ARX3	5.692	6.326	6.870	5.827	5.085	7.733
ARX4	5.780	6.387	6.917	7.200	5.806	7.958
ARX5	5.794	6.412	6.939	6.020	5.040	7.757
AUN3	5.272	5.997	6.635	4.461	5.008	7.670
AUN4	5.398	6.086	6.680	4.766	4.831	7.563
AUN5	5.538	6.182	6.722	4.990	4.511	7.412
ARN3	5.609	6.253	6.807	5.667	5.079	7.688
ARN4	5.676	6.286	6.807	6.268	5.133	7.639
ARN5	5.773	6.350	6.849	7.649	5.710	7.791
AU00	5.045	5.848	6.554	2.856	4.167	7.408
AR00	5.494	6.201	6.805	4.133	4.445	7.579

equations (4. 5) and (4. 6). For all asphalt-polymer combinations, the computed moduli were then compared to the measured data.

In Figure 5.2 the predicted values of storage modulus are compared to the experimental data. An equality line is provided as a means for comparison. The agreement is quite good and no specific trend or bias in prediction can be observed. Figure 5.3 illustrates a similar comparison for the values of loss modulus. In general, the predictive capability of the analytical expression for loss modulus using the proposed characterization method appears to be higher than that of storage modulus equation. This may be attributed to the difficulties involved with the estimation of parameters of equation (4. 5) using numerical methods in contrast to exact solution to the system of equations generated by equation (4. 6).

Although Figures 5.2 and 5.3 represent the entire modified binders in both aged and unaged conditions, they are restricted to a single frequency, i.e., 6.283 rad/s. In order to examine the accuracy of models and proposed procedure at other frequencies, Figures 5.4 and 5.5 are presented. In Figure 5.4 the predicted values of storage modulus at seventeen frequencies within the range of reduced frequencies of experimental master curves are plotted. The measured data points are shown on the same graph. The moduli correspond to three distinct binders with different polymer types, concentration levels and aging conditions, i.e., three representative samples. A similar presentation for predicted and measured values of loss modulus of the same binders is made in Figure 5.6.

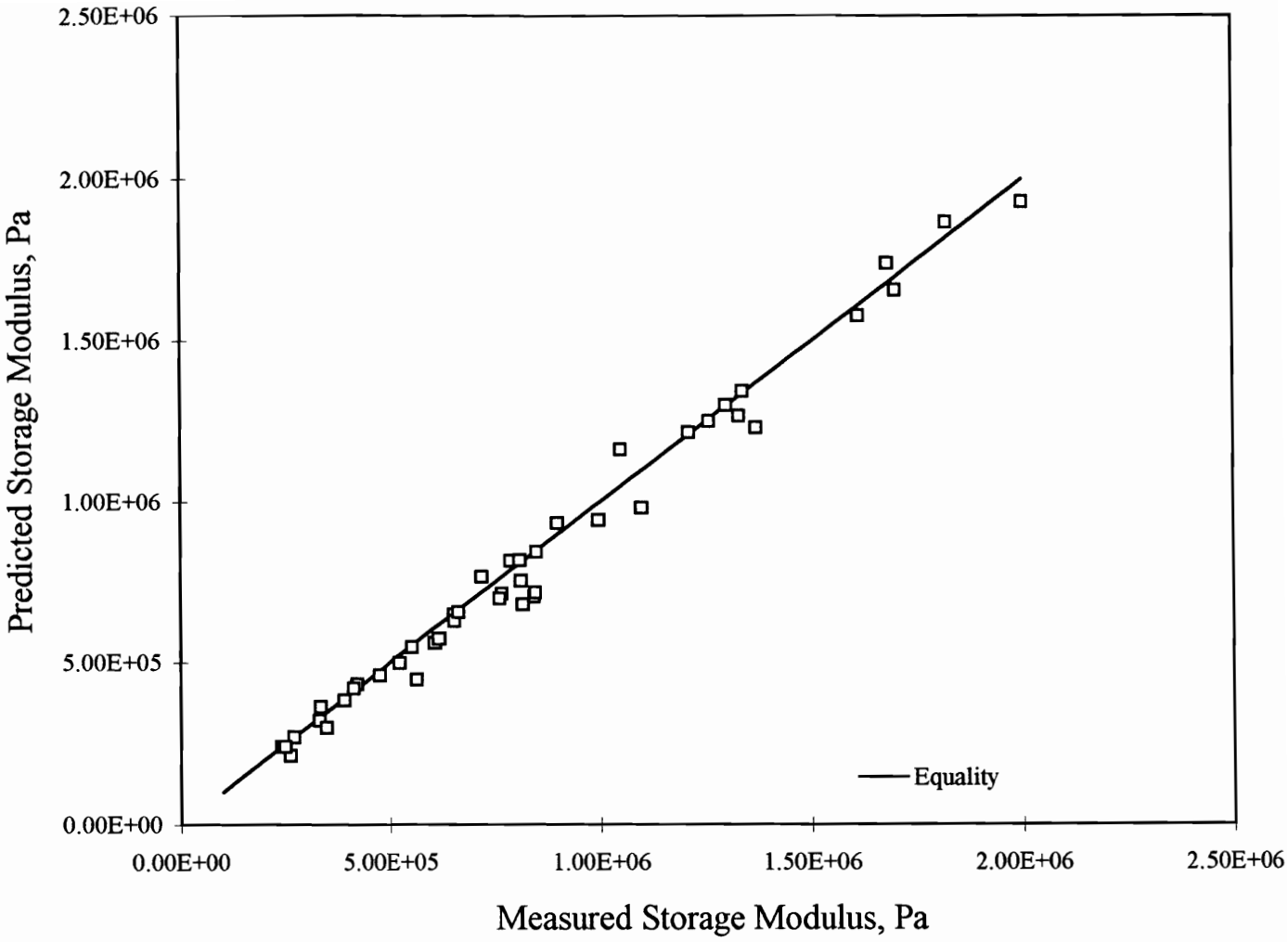

Figure 5.2. Predicted Storage Modulus from the Proposed Method Versus Measured Data for All Modified Binders at 6.283 rad/s

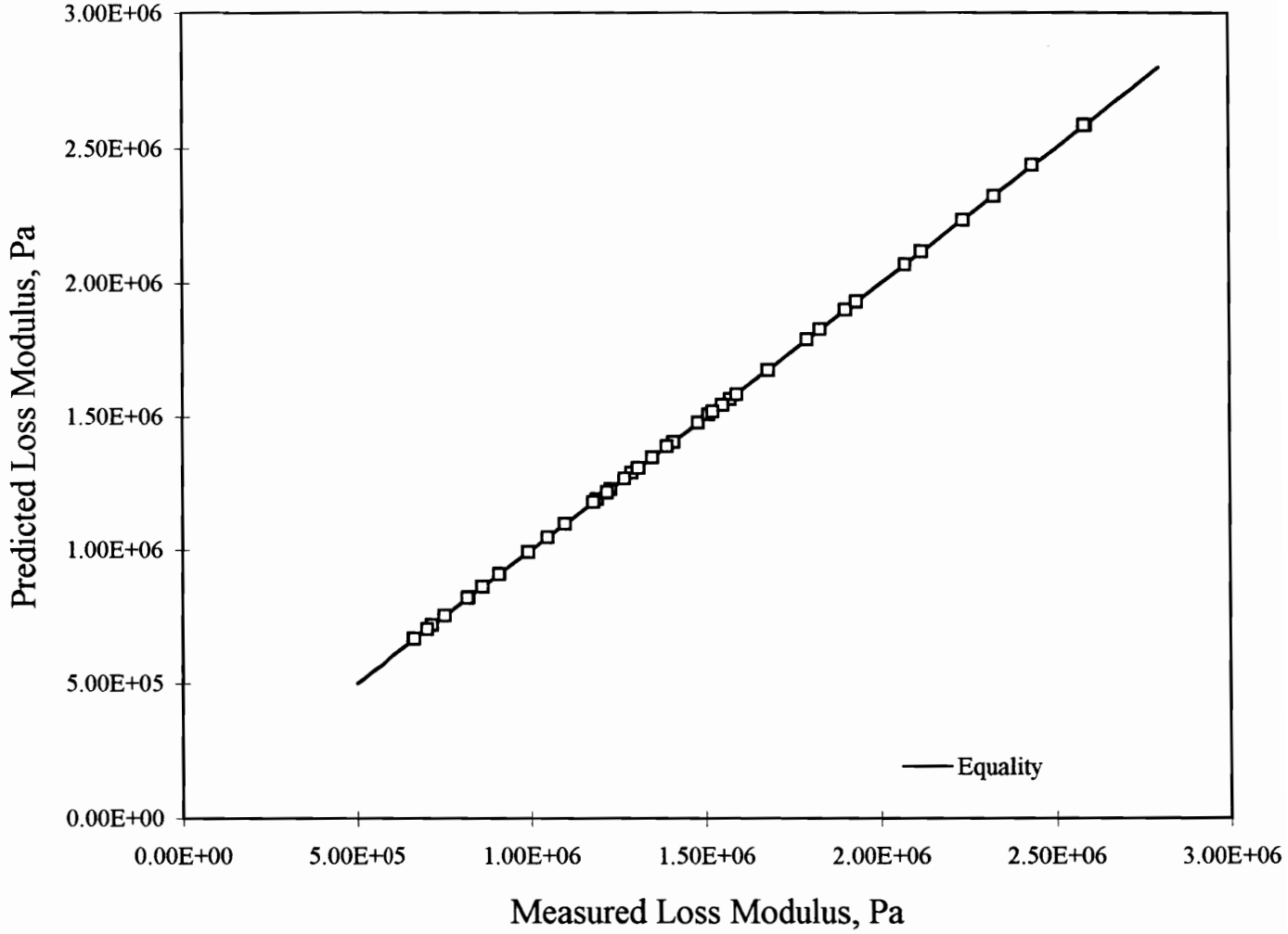

Figure 5.3. Predicted Loss Modulus from the Proposed Method Versus Measured Data for All Modified Binders at 6.283 rad/s

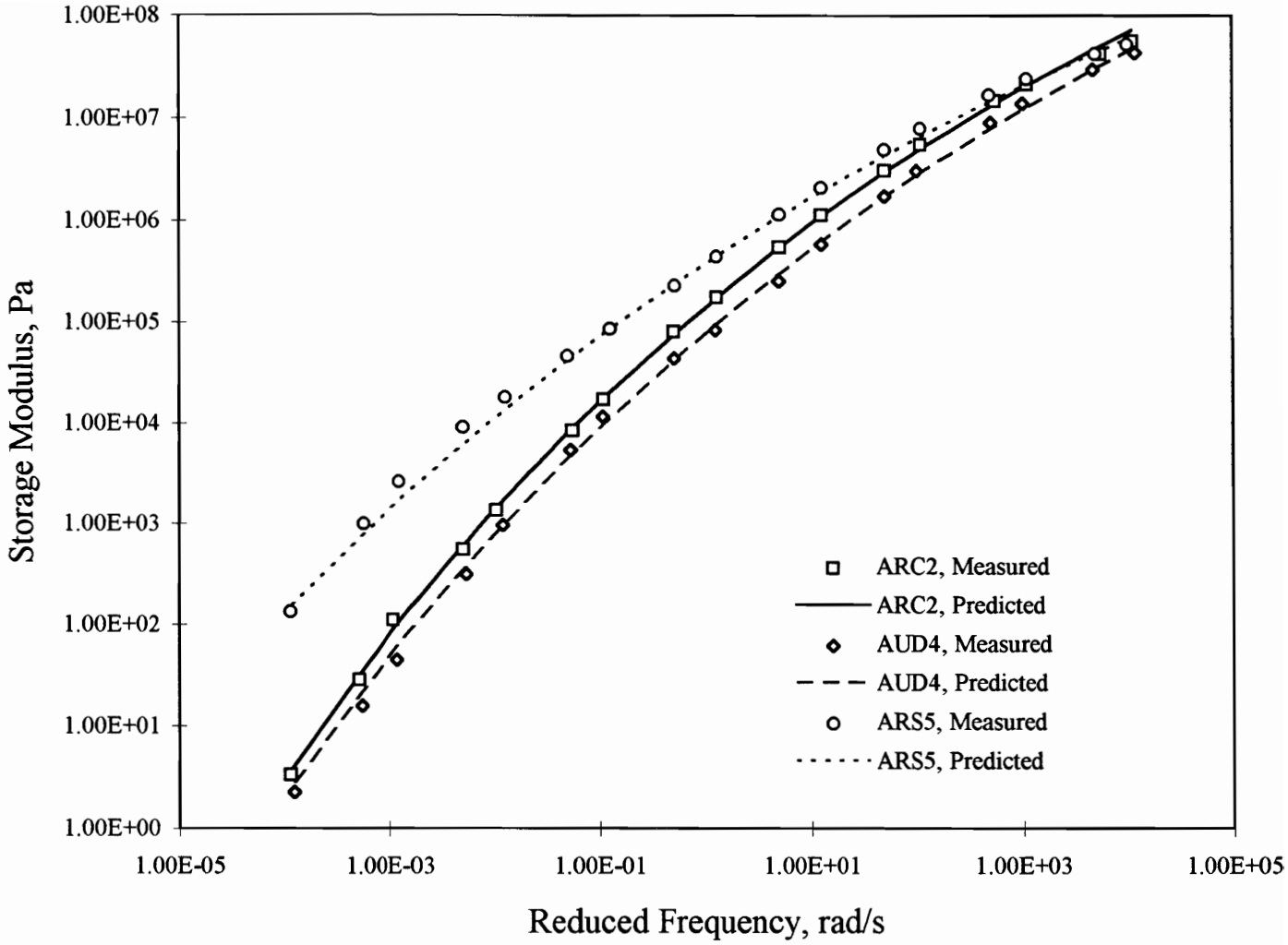

Figure 5.4. Comparison between Measured and Predicted Storage Modulus for ARC2, AUD4, and ARS5

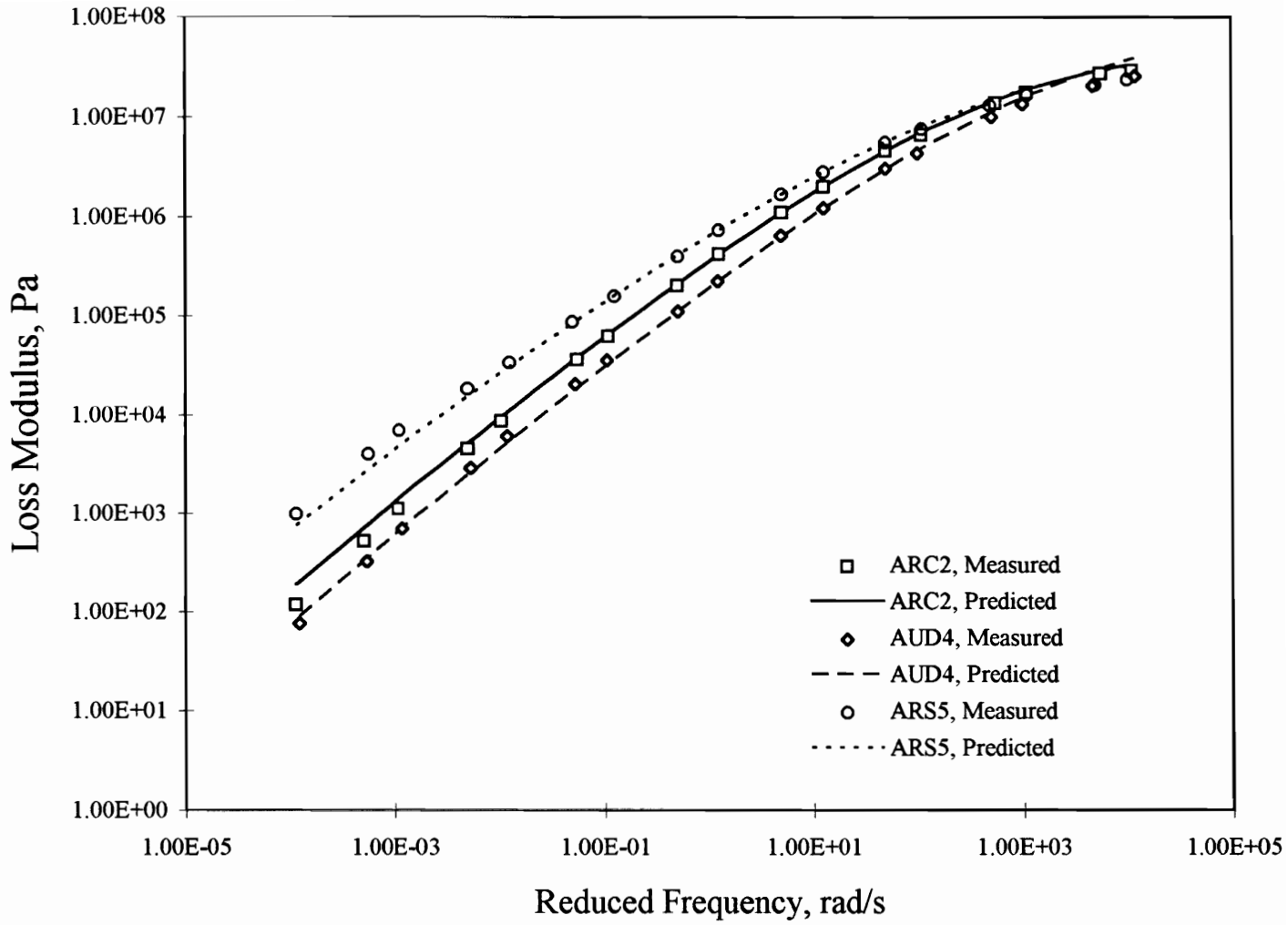

Figure 5.5. Comparison between Measured and Predicted Loss Modulus for ARC2, AUD4, and ARS5

Figures 5.5 and 5.6 clearly prove the adequacy of proposed models and characterization procedure over the entire range of reduced frequencies.

5.6. Determination of Reference Temperature in WLF Equation

The measured shift factor data were fit to the WLF equation with universal constants using non-linear least squares and the values of reference temperature for all modified binders were determined. In performing the least squares analysis, the observed shift factors from both independent replicas were used simultaneously. The reason for using replicate observations is to provide a means for evaluating the fit by lack of fit analysis which is discussed in the following section. As an example, the SAS input and output data files for non-linear least squares fit of the shift factors of ARP5 to WLF equation are presented in Appendix E.

The results of least squares analysis are summarized in Table 5.8. In this table, in addition to the estimated reference temperature for each binder, the values of asymptotic standard error, coefficient of determination, mean squared error and total degrees of freedom are presented. The adequacy of fit is discussed in Section 5.7. As a graphical example of agreement between the WLF fit and measured data, Figure 5.6 is provided. In this Figure, the observed shift factor data for AUC4 resulted from two independent replicas are plotted and compared to the WLF fit to the same data set. Despite slight

Table 5.8. Estimated Reference Temperatures in WLF Equation from Least Squares

Binder	T_s (°C)	$s(T_s)$ (°C)	r^2	MSE	DF
AUC2	36.6	0.63	0.9974	0.0128	16
AUC3	36.7	0.60	0.9977	0.0117	16
AUC4	36.1	0.57	0.9980	0.0101	16
ARC2	36.9	0.75	0.9963	0.0208	16
ARC3	38.8	0.77	0.9960	0.0219	16
ARC4	38.5	0.72	0.9966	0.0187	16
AUP3	36.9	0.63	0.9975	0.0130	16
AUP4	37.4	0.72	0.9967	0.0174	16
AUP5	37.7	0.69	0.9970	0.0160	16
ARP3	39.2	0.82	0.9955	0.0256	16
ARP4	39.0	0.80	0.9962	0.0239	16
ARP5	39.0	0.74	0.9962	0.0206	16
AUD3	37.8	0.65	0.9973	0.0143	16
AUD4	37.1	0.66	0.9972	0.0144	16
AUD5	37.3	0.67	0.9971	0.0148	16

Table 5.8. Estimated Reference Temperatures in WLF Equation from Least Squares (continued)

Binder	T_S (°C)	$s(T_S)$ (°C)	r^2	MSE	DF
ARD3	39.5	0.88	0.9948	0.0301	16
ARD4	38.8	0.81	0.9956	0.0241	16
ARD5	39.4	0.81	0.9956	0.0253	16
AUS3	38.2	0.67	0.9971	0.0159	16
AUS4	38.5	0.75	0.9964	0.0201	16
AUS5	39.3	0.79	0.9957	0.0240	16
ARS3	40.7	0.95	0.9938	0.0378	16
ARS4	40.6	0.90	0.9944	0.0338	16
ARS5	41.2	0.93	0.9940	0.0374	16
AUG3	38.9	0.69	0.9968	0.0177	16
AUG4	39.6	0.83	0.9954	0.0268	16
AUG5	40.3	0.83	0.9952	0.0283	16
ARG3	40.7	0.88	0.9946	0.0327	16
ARG4	41.4	0.97	0.9934	0.0415	16
ARG5	42.4	1.01	0.9926	0.0482	16

Table 5.8. Estimated Reference Temperatures in WLF Equation from Least Squares (continued)

Binder	T_s (°C)	$s(T_s)$ (°C)	r^2	MSE	DF
AUX3	38.9	0.74	0.9963	0.0206	16
AUX4	39.6	0.81	0.9955	0.0257	16
AUX5	39.8	0.79	0.9958	0.0246	16
ARX3	41.2	0.98	0.9933	0.0417	16
ARX4	41.6	1.01	0.9928	0.0456	16
ARX5	41.8	1.05	0.9922	0.0503	16
AUN3	38.2	0.73	0.9966	0.0188	16
AUN4	39.0	0.76	0.9962	0.0217	16
AUN5	40.2	0.89	0.9946	0.0323	16
ARN3	40.6	0.91	0.9943	0.0341	16
ARN4	40.7	0.96	0.9936	0.0382	16
ARN5	41.7	0.99	0.9930	0.0440	16
AU00	36.7	0.68	0.9970	0.0148	16
AR00	39.4	0.84	0.9953	0.0271	16

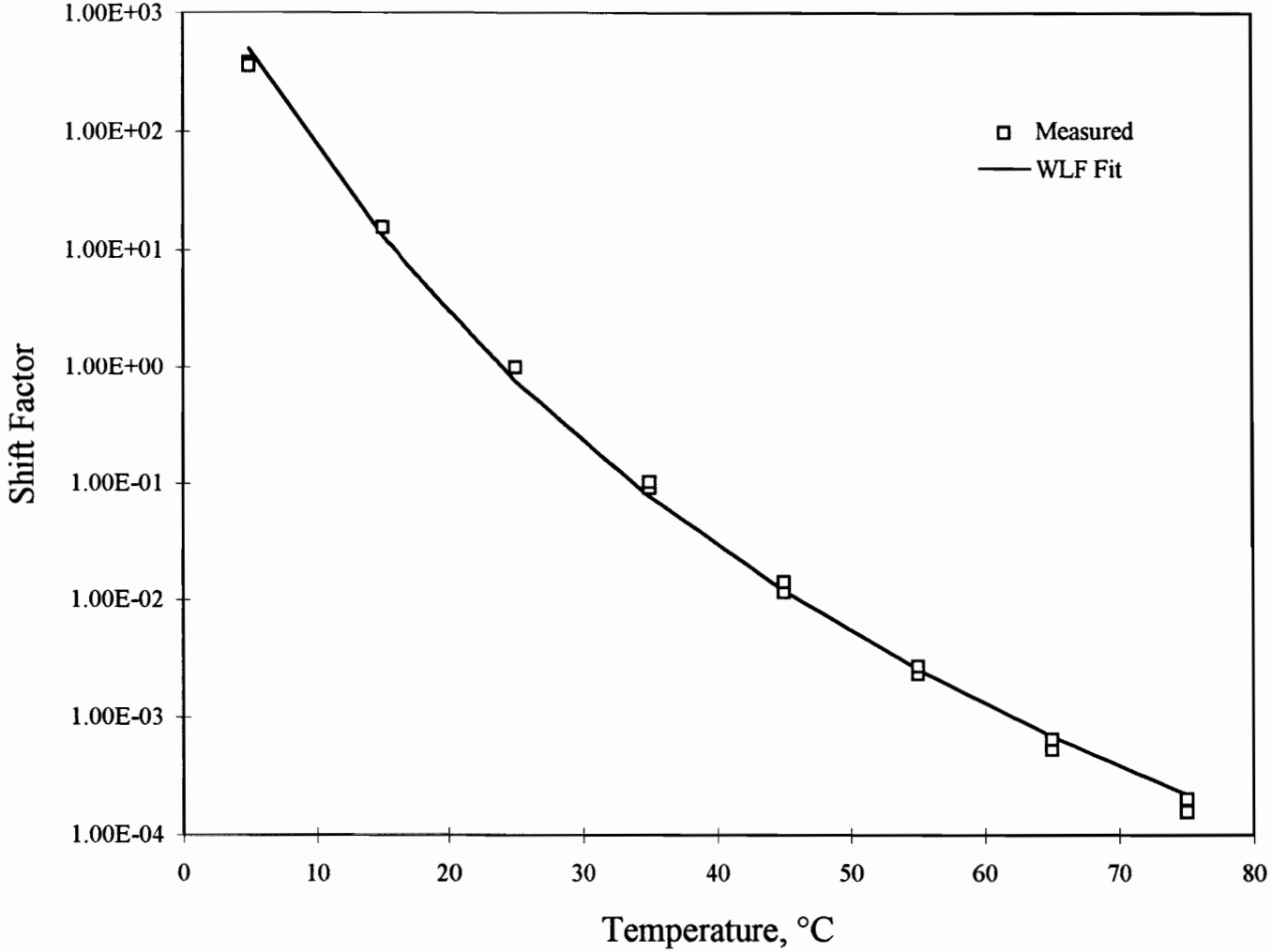

Figure 5.6. Comparison between Measured Shift Factors and WLF Fit for AUC4

deviations at some temperatures, the fit is reasonably good and representative of the experimental data.

5.7. Lack of Fit Analysis for the WLF Fit

To evaluate the accuracy of WLF equation in describing the temperature dependence of modified binders, a lack of fit analysis was performed. Lack of fit test requires replicate observations (shift factors) at each independent variable (temperature) level. This test assumes that observations at each level are independent and normally distributed. In general, the procedure involves evaluation of a component of mean squared error which is solely due to lack of fit of the model, through excluding the pure error (Neter *et al.*, 1990). Therefore, it is an effective approach to assess the adequacy of model.

To perform the lack of fit test, first the pure error sum of squares (SSPE) is computed according to the following equation:

$$SSPE = \sum_{j=1}^{c}\sum_{i=1}^{m}\left(\log a_{T_{ij}} - mean(\log a_{T_j})\right)^2 \qquad (5.4)$$

where,

a_T = shift factor,

c = number of observations in each replica = 8, and

m = number of replicas = 2.

Therefore, SSPE can be simply defined as the sum of squares of differences between each replicate shift factor and the mean value of the paired replicas.

The lack of fit sum of squares (SSLF) is computed next by subtracting the SSPE from error sum of squares (SSE), the latter being determined during the least squares analysis:

$$SSLF = SSE - SSPE \tag{5. 5}$$

Regarding the fact that number of parameters in the WLF equation is equal to two, the degrees of freedom associated with SSLF is DF(SSLF) = 8-2 = 6, and that of SSPE is DF(SSPE) = 16-8 = 8. The mean squared lack of fit error (MSLF) and mean squared pure error (MSPE) can then be computed according to the following equations:

$$MSLF = \frac{SSLF}{DF(SSLF)} = \frac{SSLF}{6} \tag{5. 6}$$

$$MSPE = \frac{SSPE}{DF(SSPE)} = \frac{SSPE}{8} \tag{5. 7}$$

The results of analysis of lack of fit for WLF equation are given in Table 5.9. Included in the table are the values of SSE, SSPE, SSLF, MSPE, and MSLF for each binder. The small values of MSLF in all cases are another indication of the appropriateness of fit. It can be concluded that the WLF equation with universal constants is indeed adequate to characterize the temperature dependence of response of modified binders.

Table 5.9. Results of Lack of Fit Analysis for WLF Equation

Binder	SSE	SSPE	SSLF	MSPE	MSLF
AUC2	0.178564	0.007543	0.171021	0.000943	0.028504
AUC3	0.163658	0.002295	0.161363	0.000287	0.026894
AUC4	0.141263	0.020574	0.120689	0.002572	0.020115
ARC2	0.291404	0.002927	0.288478	0.000366	0.048080
ARC3	0.306177	0.001384	0.304793	0.000173	0.050799
ARC4	0.262244	0.017688	0.244556	0.002211	0.040759
AUP3	0.181941	0.001259	0.180682	0.000157	0.030114
AUP4	0.243901	0.004232	0.239669	0.000529	0.039945
AUP5	0.224438	0.003580	0.220858	0.000448	0.036810
ARP3	0.358086	0.010922	0.347165	0.001365	0.057861
ARP4	0.333711	0.002190	0.331521	0.000274	0.055254
ARP5	0.288914	0.000996	0.287919	0.000124	0.047986
AUD3	0.200662	0.001800	0.198862	0.000225	0.033144
AUD4	0.202273	0.003331	0.198943	0.000416	0.033157
AUD5	0.207662	0.002988	0.204674	0.000374	0.034112

Table 5.9. Results of Lack of Fit Analysis for WLF Equation (continued)

Binder	SSE	SSPE	SSLF	MSPE	MSLF
ARD3	0.421932	0.011104	0.410828	0.001388	0.068471
ARD4	0.336729	0.000872	0.335857	0.000109	0.055976
ARD5	0.354763	0.007110	0.347653	0.000889	0.057942
AUS3	0.223206	0.003886	0.219320	0.000486	0.036553
AUS4	0.281231	0.000950	0.280281	0.000119	0.046714
AUS5	0.335338	0.003272	0.232067	0.000409	0.055344
ARS3	0.528667	0.000940	0.527727	0.000118	0.087955
ARS4	0.473410	0.001487	0.471924	0.000186	0.078654
ARS5	0.523738	0.000759	0.522980	0.000095	0.087163
AUG3	0.247651	0.011948	0.235703	0.001494	0.039284
AUG4	0.374507	0.000483	0.374024	0.000060	0.062337
AUG5	0.396052	0.003432	0.392620	0.000429	0.065437
ARG3	0.457586	0.006665	0.450922	0.000833	0.075154
ARG4	0.581627	0.004512	0.577115	0.000564	0.096186
ARG5	0.675129	0.005479	0.669650	0.000685	0.111608

Table 5.9. Results of Lack of Fit Analysis for WLF Equation (continued)

Binder	SSE	SSPE	SSLF	MSPE	MSLF
AUX3	0.287969	0.003709	0.284260	0.000464	0.047377
AUX4	0.360035	0.001450	0.358585	0.000181	0.059764
AUX5	0.344554	0.000654	0.343900	0.000082	0.057317
ARX3	0.583327	0.012182	0.571145	0.001523	0.095191
ARX4	0.638793	0.000787	0.638006	0.000098	0.106334
ARX5	0.703826	0.006735	0.697092	0.000842	0.116182
AUN3	0.262758	0.000781	0.261978	0.000098	0.043663
AUN4	0.304287	0.001402	0.302885	0.000175	0.050481
AUN5	0.451559	0.001708	0.449852	0.000213	0.074975
ARN3	0.477945	0.001946	0.475999	0.000243	0.079333
ARN4	0.535211	0.002695	0.532516	0.000337	0.088753
ARN5	0.615884	0.002080	0.613805	0.000260	0.102301
AU00	0.206959	0.014275	0.192685	0.001784	0.032114
AR00	0.379128	0.004083	0.375045	0.000510	0.062507

Chapter 6
Summary, Findings, Conclusions, and Recommendations

6.1. Summary

This study aimed at characterizing the linear viscoelastic response of polymer modified asphalt binders at intermediate and high service temperatures. Effects of random copolymers and thermoplastic block copolymers on the rheological properties of asphalt were studied. Dynamic mechanical analysis was conducted on modified binders at temperatures between 5 and 75° C and frequencies ranging from 0.06 to 188.5 rad/s. The results of dynamic tests were reduced to dynamic master curves of moduli. By interpretation of the dynamic master curves, effects of several variables on the response were evaluated. Applicability of a number of analytical expressions previously derived for straight asphalts, to the frequency dependence of response of modified binders was investigated. Two mathematical models were proposed to describe the variations of storage shear modulus and loss shear modulus of polymer modified binders with respect to frequency. Furthermore, using the collected shift factor data, temperature dependency of response was studied and applicability of a classical model was investigated. Based on the overall results, a procedure was developed to characterize the viscoelastic response of modified binders over a wide range of frequencies using a limited number of dynamic measurements.

The proposed mathematical models were extensively evaluated through various statistical methods. Applicability of the proposed method of characterization to practical problems was assessed as well.

6.2. Findings

Findings of this study can be listed as follows:

- Repeatability of dynamic measurements on polymer modified asphalt binders is significantly affected by temperature, steric hardening, specimen preparation method, and testing procedure.

- Dynamic moduli of asphalt binders are highly sensitive to temperature variations. Temperature fluctuations as low as 0.5° C can result in up to 15% change in the measured dynamic moduli.

- Prefabrication of binder specimens tends to increase the variability of results of dynamic tests. This is most likely due to lack of sufficient bond between the specimen prepared by this method and confining plates.

- Trimming the elastomerically modified binder between two confining plates is a major source of variability in results of dynamic measurements.

- Identifying an exact border between the linear and non-linear ranges of viscoelastic response of polymer modified asphalts is not possible. This is due to slight variations of moduli with respect to increasing applied stresses (or strains). Therefore, the dividing line between the two regions of response should be defined based on an appropriate arbitrary criterion.

- Linear range of response is a function of temperature. At higher temperatures, the binder can withstand higher strains while remaining in the linear viscoelastic region.

- Polymer modified asphalts are heterophase systems and thermorheologically complex in nature. However, their isothermal response curves admit simple time-temperature superposition without any complications. This may be attributed to domination of temperature dependence of asphalt phase in the asphalt-polymer blend. Another possibility is an undetectable lack of superposition which stems from the smallness of experimental window compared to the wide separation of the two dominant viscoelastic transitions.

- Loss tangent master curves of asphalts modified by thermoplastic block copolymers exhibit a plateau region at intermediate frequencies. This phenomenon can be attributed to formation of a polymeric network within the binder.

- Approximate interrelationships between viscoelastic functions used in previous studies on straight asphalts fail to represent the response of modified binders.

- For block copolymer modified binders, transition to glassy modulus takes place at a higher rate than SBR modified asphalts. The polymer concentration level, however, does not appear to influence this rate appreciably.

- Short term aging of modified binders accelerates the rate of approaching the glassy state of response.

- The peak value of loss modulus is a characteristic of the base asphalt. Addition of polymer, and aging treatment do not appreciably affect this value.

- The frequency corresponding to the peak loss modulus increases with polymer content and decreases with aging treatment. This value for blends with block copolymers is generally higher than that of blends containing random copolymers.

- In blends containing block copolymers, transition between the viscous asymptote and peak loss modulus is more gradual than those containing random copolymers. A similar trend can be observed due to increasing concentration levels for both category of polymers.

- Short term aging of modified binders leads to a wider transition from the viscous asymptote to the peak loss modulus.

- Larger dispersion in the relaxation process due to addition of polymer is well manifested in the relaxation spectrum curves. Increasing polymer contents result in broader spectra, i.e., extending the relaxation phenomenon to larger periods of time.

- Temperature dependence of polymer modified binders appears to be predominantly affected by the base asphalt . Variations of shift factor data conform to a WLF shape with no abrupt change due to addition of polymer.

- The estimated reference temperatures in WLF equation exhibit a slight increase with increasing polymer contents.

- Short term aging of modified binders tends to increase the estimated reference temperature in WLF equation.

- The reference temperature in WLF equation is evidently correlated with the glass transition temperature of binder.

6.3. Conclusions

Based on this study, the following conclusions can be drawn:

- Mathematical models for frequency dependence found in literature, are generally incapable of characterizing the viscoelastic response of polymer modified asphalt binders. This is partly due to the fact that these models, have all been developed based on dynamic mechanical data on straight asphalts.

- Two new mathematical models for frequency dependence of response of polymer modified asphalt binders at intermediate and high service temperatures were developed. The storage shear modulus and loss shear modulus can be characterized by the following equations, respectively:

$$\log G'(\omega) = \log G_g\left[1 - \exp(-p(\log\omega + l))\right]$$

$$\log G''(\omega) = (\log G''_{\max} + d) - \sqrt{(\log\omega - \log\omega_d)^2 + d^2}$$

- The proposed mathematical model for storage modulus can predict the moduli below 10^8 Pa accurately. Above this value, the model tends to overestimate the actual moduli.

- The proposed model for frequency dependence of loss modulus is highly accurate in predicting the moduli between the viscous state and peak modulus. Beyond the peak, applicability of the equation is not certain.

- The loss tangent function resulting from the proposed equations is capable of representing the experimental data.

- Within the specified range of temperatures, the WLF equation with universal constants is adequate to characterize the temperature dependence of response of polymer modified binders.

- Using the proposed equations for storage and loss moduli, characterization of the response of modified binders at a certain temperature and over a wide range of frequencies is possible by taking three dynamic measurements at three different frequencies. For evaluating the response at other temperatures, taking a single modulus measurement will suffice.

6.4. Recommendations

Based on the findings and conclusions of the present study, the following guidelines for further research are recommended:

- Establishing a correlation between the glass transition temperature of modified binders and reference temperature in WLF equation is necessary. This can be accomplished through dilatometric glass transition temperature measurements, and will help to better understand the temperature dependence of polymer modified asphalt binders.

- Applicability of the proposed mathematical models to viscoelastic response of plastomerically modified binders and crumb rubber modified asphalts needs to be investigated.

- In depth study of the relationships between the various model constants and physical and mechanical properties of asphalts and polymers can result in more efficient application of the proposed models.

- Evaluation of the long term aging effects on the rheological properties of modified binders is needed. This can be accomplished by experimental study of PAV residuum of modified asphalts.

- Applicability of the proposed models to dynamic mechanical data on blends with higher polymer contents (up to 10%) needs further investigation.

References

AASHTO Provisional Standards. (1994), "AASHTO PP1, Standard Practice for Accelerated Aging of Asphalt Binder Using a Pressurized Aging Vessel (PAV)," Washington, D.C.

AASHTO Provisional Standards. (1994), "AASHTO TP5, Standard Test Method for Determining the Rheological Properties of Asphalt Binder Using a Dynamic Shear Rheometer (DSR)," Washington, D.C.

Al Dhalaan, M., Balghunaim, F., Al Dhubaib, I., and Noureldin, A. S. (1992), "Field Trials with Polymer Modified Asphalts in Saudi Arabia," *Polymer Modified Asphalt Binders*, STP 1108, Wardlaw, K. R., and Shuler, S., Editors, ASTM, Philadelphia, PA, pp. 203-223.

Amoco Oil Company. (1995), *Technical Data Sheets*, Naperville, IL.

Anderson, D. A., Christensen, D. W., and Bahia, H. (1991), "Physical Properties of Asphalt Cement and the Development of Performance Related Specifications," *Journal of the Association of Asphalt Paving Technologists*, Vol. 60, pp. 437-475.

Anderson, D. A., Christensen, D. W., Roque, and R., Robyak, R. A. (1992), "Rheological Properties of Polymer Modified Emulsion Residue," *Polymer Modified Asphalt Binders*, STP 1108, Wardlaw, K. R. and Shuler, S., Editorsr, ASTM, Philadelphia, PA, pp. 20-34.

Andrews, R. D., Hofman-Bang, N., and Tobolosky, A. V. (1948), "Elastoviscous Properties of Polyisobutylene. I. Relaxation of Stress in Whole Polymers of Different Molecular Weights at Eleavated Temperatures," *Journal of Polymer Science*, Vol. 3, No. 5, pp. 669-692.

Annual Book of ASTM Standards. (1991), "ASTM D 1754-87, Standard Test Method for Effect of Heat and Air on Asphaltic Materials (Thin-Film Oven Test)," Vol. 04.03, Philadelphia, PA, pp. 231-233.

Annual Book of ASTM Standards. (1991), "ASTM D 2872-88, Standard Test Method for Effect of Heat and Air on a Moving Film of Asphalt (Rolling Thin Film Oven Test)," Vol. 04.03, Philadelphia, PA, pp. 315-318.

Annual Book of ASTM Standards. (1991), "ASTM D 2170-85, Standard Test Method for Kinematic Viscosity of Asphalts (Bitumens)," Vol. 04.03, Philadelphia, PA, pp. 260-268.

Annual Book of ASTM Standards. (1991), "ASTM D 5-86, Standard Test Method for Penetration of Bituminous Materials," Vol. 04.03, Philadelphia, PA, pp. 71-73.

Annual Book of ASTM Standards. (1991), "ASTM D 36-86, Standard Test Method for Softening Point of Bitumen (Ring-and-Ball Apparatus)," Vol. 04.04, Philadelphia, PA, pp. 9-12.

Annual Book of ASTM Standards. (1991), "ASTM D 2171-88, Standard Test Method for Viscosity of Asphalts by Vacuum Capillary Viscometer," Vol. 04.03, Philadelphia, PA, pp. 269-275.

Bishop, E. T. and Davison, S. (1969) "Network Characteristics of the Thermoplastic Elastomers," *Journal of Polymer Science*, Part C, No. 26, pp. 59-79.

Bohlin Inc. (1990), *Bohlin CS Reference Guide*, Cranbury, NJ.

Booij, H. C. and Palmen, J. H. M. (1982), "Some Aspects of Linear and Nonlinear Viscoelastic Behavior of Polymer Melts in Shear," *Rheologica Acta*, Vol. 21, pp. 376-387.

Booij, H. C. and Thoone, G. P. J. M. (1982), "Generalization of Kramers-Kronig Transforms and Some Approximations of Relations between Viscoelastic Quantities," *Rheologica Acta*, Vol. 21, pp. 15-24.

Brodnyan, J. G., Gaskins, F. H., Philippoff, W., and Thelen, E. (1960), "The Rheology of Asphalt, III. Dynamic Mechanical Properties of Asphalt," *Transactions of the Society of Rheology*, Vol. 4, pp. 279-296.

Brown, E. R., Parker, F., and Smith, M. R. (1992), "Study of the Effectiveness of Styrene-Butadiene Rubber Latex in Hot Mix Asphalt Mixes," *Asphalt and Asphalt Additives*, Transportation Research Record No. 1342, Transportation Research Board, Washington, D.C., pp. 85-91.

Christensen, D. W., and Anderson, D. A. (1992), "Interpretation of Dynamic Mechanical Test Data for Paving Grade Asphalt Cements," *Journal of the Association of Asphalt Paving Technologists*, Vol. 61, pp. 67-115.

Cohen, R. E. and Tschoegl, N. W. (1973), "Dynamic Mechanical Properties of Block Copolymer Blends - A Study of the Effects of Terminal Chains in Elastomeric Materials," *International Journal of Polymeric Materials*, Vol. 2, No. 3, pp. 205-223.

Cohen, R. E. and Tschoegl, N. W. (1976), "Comparison of the Dynamic Mechanical Properties of Two Styrene-Butadiene-Styrene Triblock Copolymers with 1,2- and 1,4-Polybutadiene Center Blocks," *Transactions of the Society of Rheology*, Vol. 20, Issue 1, pp. 153-169.

Collins, J. H. and Bouldin, M. G. (1992), "Stability of Straight and Polymer Modified Asphalts," *Asphalt and Asphalt Additives*, Transportation Research Record No. 1342, Transportation Research Board, Washington, D.C., pp. 92-100.

Collins, J. H., Bouldin, M. G., Gelles, R., and Berker, A. (1991), "Improved Performance of Paving Asphalts by Polymer Modification," *Journal of the Association of Asphalt Paving Technologists*, Vol. 60, pp. 43-79.

Collins, J. H. and Mikols, W. J. (1985), "Block Copolymer Modification of Asphalt Intended for Surface Dressing Applications," *Journal of the Association of Asphalt Paving Technologists*, Vol. 54, pp. 1-17.

Corbett, L. W. (1969), "Composition of Asphalt Based on Generic Fractionation Using Solvent Deasphaltening, Elution-Adsorption Chromatography, and Densimetric Characterization," *Analytical Chemistry*, Vol. 41, pp. 576-579.

Dickinson, E. J. and Witt., H. P. (1974), "The Dynamic Shear Modulus of Paving Asphalts as a function of Frequency," *Transactions of the Society of Rheology*, Vol. 18, No. 4, pp. 591-606.

Dobson, G. R. (1969), "The Dynamic Mechanical Properties of Bitumen," *Proceedings of the Association of Asphalt Paving Technologists*, Vol. 38, pp. 123-139.

Doolittle, A. K. and Doolittle, D. B. (1957), "Studies in Newtonian Flow. V. Further Verification of the Free-Space Viscosity Equation," *Journal of Applied Physics*, Vol. 28, No. 8, pp.901-905.

Federal Highway Administration. (1990), *Highway Statistics*, U.S. Department of Transportation, Washington, D.C.

Ferry, J. D. (1980), *Viscoelastic Properties of Polymers*, 3rd Edition, John Wiley & Sons, Inc., New York, NY.

Fesko, D. J. and Tschoegl, N. W. (1971), "Time-Temperature Superposition in Thermorheologically Complex Materials," *Journal of Polymer Science*, Part C, No. 35, Viscoelastic Relaxation in Polymers, pp. 51-69.

Fesko, D. J. and Tschoegl, N. W. (1974), "Time-Temperature Superposition in Styrene/Butadiene/Styrene Block Copolymers," *International Journal of Polymeric Materials*, Vol. 31, No. 1, pp. 51-79.

Fleckenstein, L. J., Mahboub, K., and Allen, D. L. (1992) "Performance of Polymer Modified Asphalt Mixes in Kentucky," *Polymer Modified Asphalt Binders*, STP 1108, Wardlaw, K. R. and Shuler, S., Editors, ASTM, Philadelphia, PA, pp. 173-185.

Goodrich, J. L. (1991), "Asphalt Binder Rheology, Asphalt Concrete Rheology, and Asphalt Concrete Mix Properties," *Journal of the Association of Asphalt Paving Technologists*, Vol. 60, pp. 80-120.

Goodrich, J. L. (1988), "Asphalt and Polymer Modified Asphalt Properties Related to the Performance of Asphalt Concrete Mixes," *Proceedings of the Association of Asphalt Paving Technologists*, Vol. 57, pp. 116-175.

Halstead, W. J. (1985), "Relation of Asphalt Chemistry to Physical Properties and Specifications," *Proceedings of the Association of Asphalt Paving Technologists*, Vol. 54, pp. 91-117.

Holden, G., Bishop, E. T., and Legge, N. R. (1969), "Thermoplastic Elastomers," *Journal of Polymer Science*, Part C, No. 26, pp. 37-57.

Jacobs, F. A. (1981), "Hot Rolled Asphalt: Effect of Binder Properties on Resistance to Deformation," *TRRL Lab Report*, No. 1003, Birmingham, U.K.

Jew, P., Shimizu, J. A., Suazic, M., and Woodhams, R. T. (1986), "Polyethylene Modified Bitumen for Paving Applications," *Journal of Applied Polymer Science*, Vol. 31, pp. 2685-2704.

Jew, P. and Woodhams, R. T. (1986), "Polyethylene Modified Bitumens for Paving Applications," *Proceedings of the Association of Asphalt Paving Technologists*, Vol. 55, pp. 541-563.

Jongepier, R. and Kuilman, B. (1969), "Characteristics of the Rheology of Bitumen," *Proceedings of the Association of Asphalt Paving Technologists*, Vol. 38, pp. 99-122.

Jongepier, R. and Kuilman, B. (1970), "The Dynamic Shear Modulus of Bitumens as a Function of Frequency and Temperature," *Rheologica Acta*, Vol. 9, No. 1, pp. 102-111.

Kaplan, D. and Tschoegl, N. W. (1974), "Time-Temperature Superposition in Two-Phase Blends," *Polymer Science and Technology*, Vol. 4, Recent Advances in Polymer Blends, Grafts, and Blocks, pp. 415-430.

Khosla, N. P. (1991), "Effects of Modifiers on Performance of Asphaltic Pavements," *Asphalt Mixtures: Design, Testing and Evaluation*, Transportation Research Record No. 1317, Transportation Research Board, Washington, D.C., pp. 10-22.

King, G. N. and King, H. W. (1986), "Polymer Modified Asphalts, an Overview," *Solutions for Pavement Rehabilitation Problems*, Lahue, S. P., Editor, ASCE, New York, NY, pp. 240-254.

King, G. N., King, H. W., Harders, O., Arand, W., and Planche, P. P. (1993), "Influence of Asphalt Grade and Polymer Concentration on the Low Temperature Performance of Polymer Modified Asphalt," *Journal of the Association of Asphalt Paving Technologists*, Vol. 62, pp. 1-22.

Kramers, H. A. (1927), *Resoconto del Congresso dei Fisici*, Como, II, 35.

Kraus, G. and Hall, D. S. (1983), "Applications of Elastomeric Diene-Styrene Block Copolymers," *Block Copolymers, Science and Technology*, MMI Press Symposium Series, Vol. 3, Harwood Academic Publishers, New York, NY, pp. 167-195.

Krebs, R. D. and Walker, R. D. (1971), *Highway Materials*, Mc-Graw Hill, New York, NY.

Kronig, R. de L. (1926), in *Journal of Optical Society of America*, 12., p. 547.

Lewandowski, L. H. (1994), "Polymer Modification of Paving Asphalt Binders," *Rubber Chemistry and Technology*, Vol. 67, No. 3, pp. 447-480.

Lim, C. K., Cohen, R. E., and Tschoegl, N. W. (1971), "Time-Temperature Superposition in Block Copolymers," *Advances in Chemistry Series*, No. 99, Multicomponent Polymer Systems, American Chemical Society Publications, pp. 397-417.

Little, D. N. (1992), "Analysis of the Influence of Low Density Polyethylene Modification (Novophalt) of Asphalt Concrete on Mixture Shear Strength and Creep Deformation,"

Polymer Modified Asphalt Binders, STP 1108, Wardlaw, K. R., and Shuler, S., Editors, ASTM, Philadelphia, PA, pp. 186-202.

Leaderman, H. (1943), "Elasic and Creep Properties of Filamentous Materials and Other High Polymers," *The Textile Foundation Inc.*, Washington, D. C., p.175.

Mitscherlich, E. A. (1909), "Das Gesetz des Minimums und das Gestez des Abnehmenden Bodenertrages," *Landw. Jahrb.*, Vol. 38, pp. 537-552.

Muncy, H. W., King, G. N., and Prudhomme, J. B. (1987), "Improved Rheological Properties of Polymer-Modified Asphalts," *Asphalt Rheology, Relationship to Mixture*, STP 941, Briscoe, O. E., Editor, ASTM, Philadelphia, PA, pp. 146-165.

Nellensteyn, F. G. (1923), *Bereiding en Constitutie van Asphalt (Manufacture and Constitution of Asphaltic Bitumen)*, Dissertaite Technische Hoogeschool, Delft, Netherlands.

Netter, J., Wasserman, W., and Kunter, M. H. (1990), *Applied Linear Statistical Models - Regression, Analysis of Variance, and Experimental Designs*, 3rd Edition, Richard D. Irwin Inc., Homewood, IL.

Ninomiya, K. and Ferry, J. D. (1959), "Some Approximate Equations Useful in the Phenomenological Treatment of Linear Viscoelastic Data," *Journal of Colloid Science*, Vol. 14, pp. 36-48.

Noshay, A. and McGrath, J. E. (1977), *Block Copolymers, Overview and Critical Survey*, Academic Press, Inc., New York, NY.

Petersen, J. C., Robertson, R. E., Branthaver, J. F., and Anderson, D. A. (1992), *SHRP A-002A: Binder Characterization and Evaluation*, Draft Final Report, Strategic Highway Research Program, Washington D. C.

Rawlings, J. O. (1988), *Applied Regression Analysis: A Research Tool*, Wadsworth & Brooks/Cole Advanced Books & Software, Pacific Grove, CA.

Roberts, F. L., Kandhal, P. S., Brown, E. R., Lee, D. Y., and Kennedy, T. W. (1991), *Hot Mix Asphalt, Mixture Design and Construction*, NAPA Education Foundation, Lanham, MD.

Schmidt, R. J. and Santucci, L. E. (1966), "A Practical Method for Determining the Glass Transition Temperature of Asphalts and Calculation of Their Low Temperature Viscosities," *Proceedings of the Association of Asphalt Paving Technologists*, Vol. 35, pp. 61-91.

Schwarzl, F. and Sraverman, A. J. (1952), "Time-Temperature Dependence of Linear Viscoelastic Behavior," *Journal of Applied Physics*, Vol. 23, No. 8, pp. 838-843.

Serfass, J. P., Joly, A., and Sammons, J. (1992), "SBS-Modified Asphalt for Surface Dressing - A Comparison between Hot-Applied and Emulsified Binders," *Polymer Modified Asphalt Binders*, STP 1108, Wardlaw, K. R. and Shuler, S., Editors, ASTM, Philadelphia, PA, pp. 281-308.

Shell Chemical Company. (1992), *Kraton Thermoplastic Rubber, Typical Properties*, Chicago, IL.

Strategic Highway Research Program. (1990), *Hypotheses and Models Employed in the SHRP Asphalt Research Program*, SHRP-A/WP-90-008, Washington, D.C.

Shuler, T. S., Collins, J. H., and Kirkpatrick, J. P. (1987), "Polymer Modified Asphalt Properties Related to Asphalt Concrete Performance," *Asphalt Rheology, Relationship to Mixture*, STP 941, Briscoe, O. E. Editor, ASTM, Philadelphia, PA, pp. 179-193.

Speer, H. L., Burnstrum, L. C., Sisko, A. W., Ott, L. E., Evans, R., and Evans, J. V. (1963), "Asphalt Viscosity as Related to Pavement Performance," *Proceedings of the Association of Asphalt Paving Technologists*, Vol. 32 , pp. 236-246.

Srivastava, A., Hopman, P. C., and Molenaar, A. A. (1992), "SBS Polymer Modified Asphalt Binder and Its Implications on Overlay Design," *Polymer Modified Asphalt*

Binders, STP 1108, Wardlaw, K. R. and Shuler, S., Editors, ASTM, Philadelphia, PA, pp. 309-329.

Stock, A. F. and Arand, W. (1993), "Low Temperature Cracking in Polymer Modified Binders," *Journal of the Association of Asphalt Paving Technologists*, Vol. 62 , pp. 23-53.

Tada, H. (1985), "Study on the Prevention of Pavement Flow through Asphalt Viscosity," *Transactions of the Japan Society of Civil Engineers*, Vol. 15, pp. 500-501.

Takayanagi, M. (1965), in *Proceedings of the 4th International Congress on Rheology*, Part 1, Interscience, p. 161.

Tayebali, A. H., Goodrich, J. L., Sousa, J. B., and Monismith, C. L. (1992), "Influence of the Rheological Properties of Modified Asphalt Binders on the Load Deformation Characteristics of the Binder-Aggregate Mixtures," *Polymer Modified Asphalt Binders*, STP 1108, Wardlaw, K. R. and Shuler, S., Editors, ASTM, Philadelphia, PA, pp. 77-98.

Textile Rubber and Chemical Company. (1992), *Ultrapave SBR Latex Polymers*, Dalton, GA.

Thompson, D. C. (1979), in *Bituminous Materials: Asphalt Tars and Pitches*, Robert Krieger Publishing Company, Vol. 1.

Tobolosky, A. V. (1956), "Stress Relaxation Studies of the Viscoelastic Properties of Polymers," *Journal of Applied Physics*, Vol. 27, No.7, pp. 673-685.

Tobolosky, A. V. and Eyring, H. (1943), "Mechanical Properties of Polymeric Materials," *Journal of Chemical Physics*, Vol. 11, No. 3, pp. 125-134.

Tschoegl, N. W. (1989), *The Phenomenological Theory of Linear Viscoelastic Behavior, An Introduction*, Springer-Verlag, New York, NY.

Tschoegl, N. W. and Cohen, R. E. (1978), "The Representation of the Time-Dependent Properties of Heterophase Polymers," *Polymer Reprints*, Vol. 19, No. 1, American Chemical Society, Division of Polymer Chemistry, pp. 49-52.

Wada, Y. and Hirose, H. (1960), "Glass Transition Phenomena and Rheological Properties of Petroleum Asphalt," *Journal of Physical Society of Japan*, Vol. 15, No. 10, pp. 1885-1894.

Williams, M. L., Landel, R. F., and Ferry, J. D. (1955), "The Temperature Dependence of Relaxation Mechanism in Amorphous Polymers and Other Glass-Forming Liquids," *Journal of the American Chemical Society*, Vol. 77, pp. 3701-3706.

Appendix A

Dynamic Master Curves

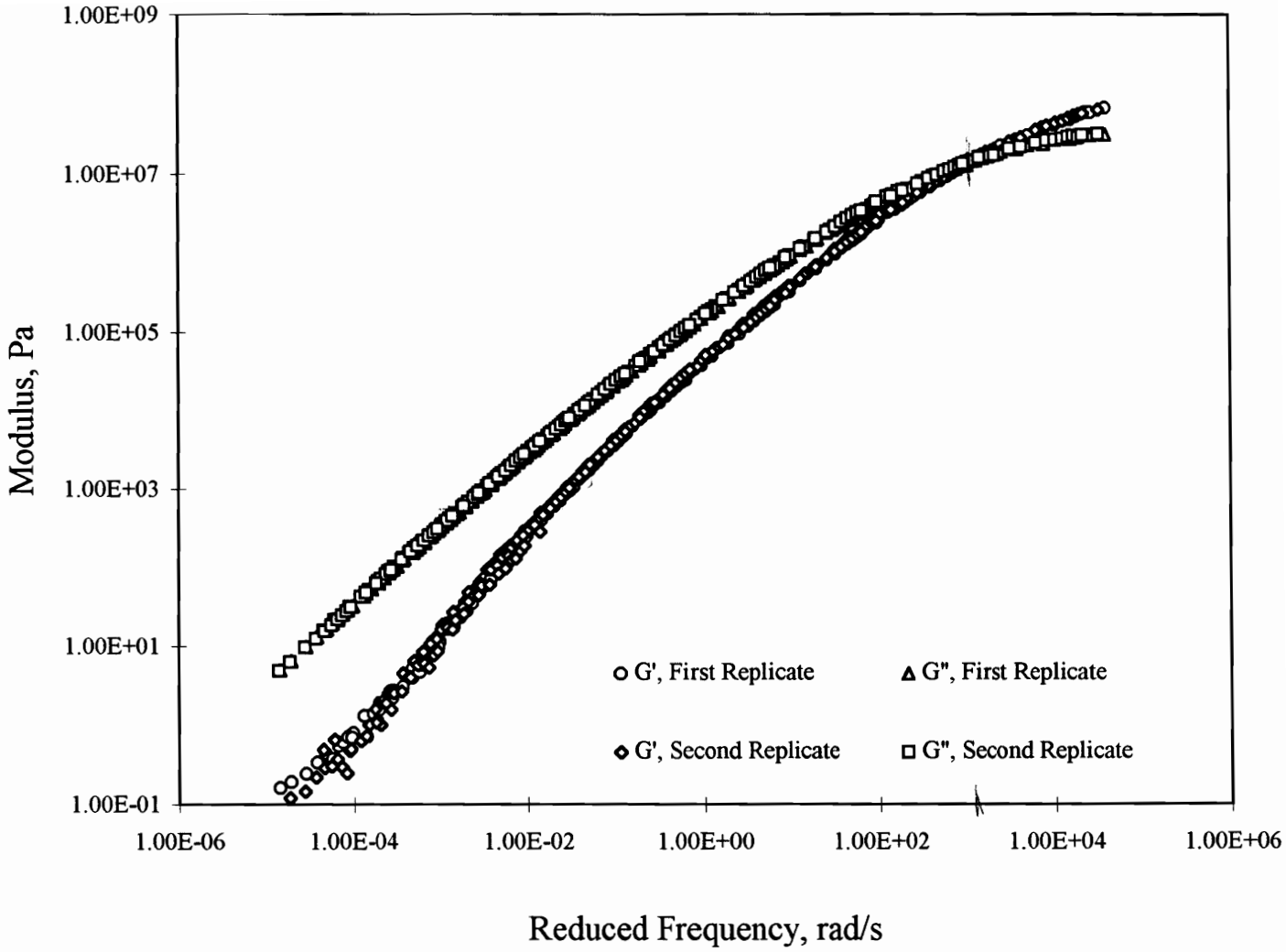

Figure a.1. Dynamic Master Curves for AUC2

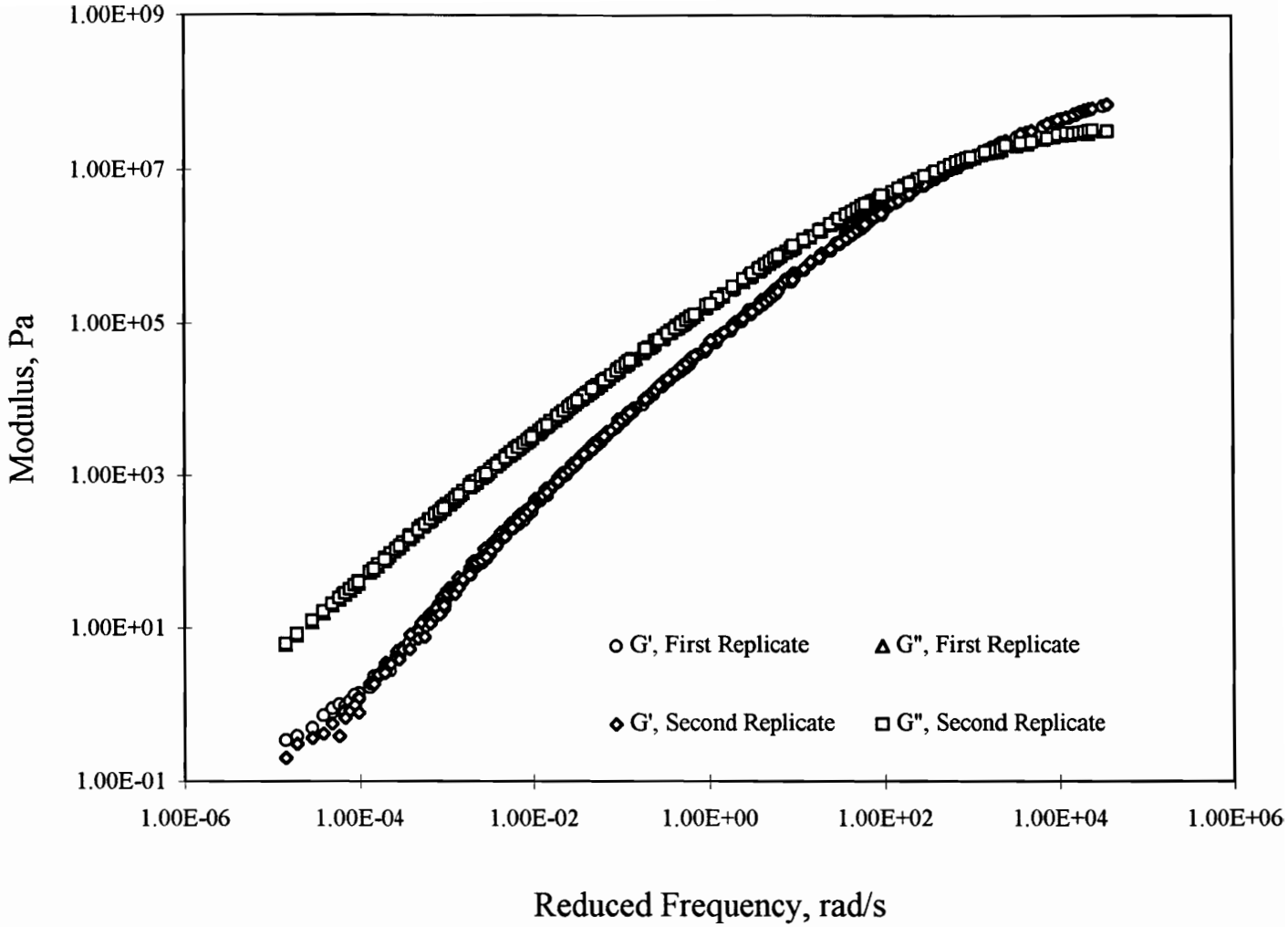

Figure a.2. Dynamic Master Curves for AUC3

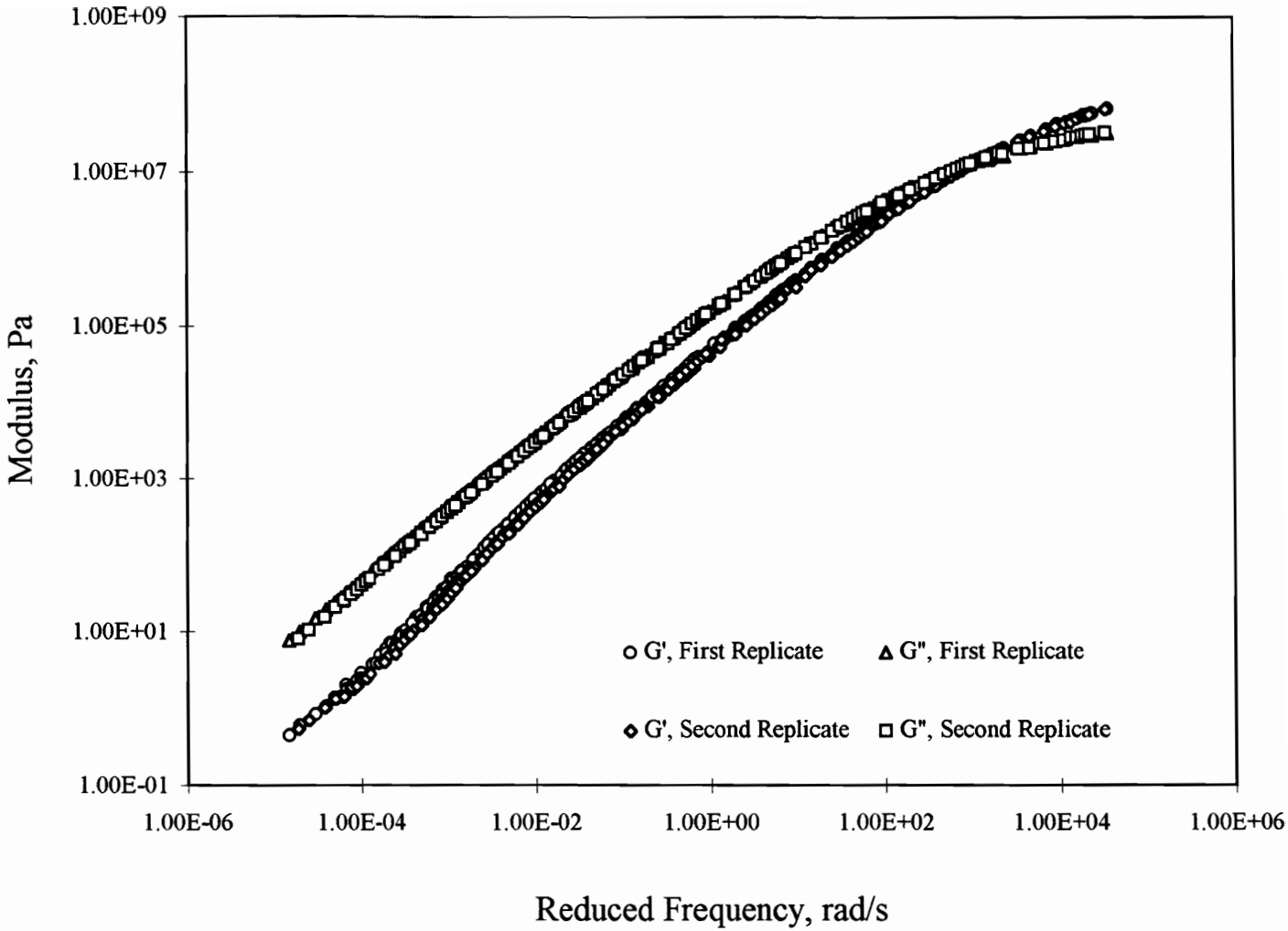

Figure a.3. Dynamic Master Curves for AUC4

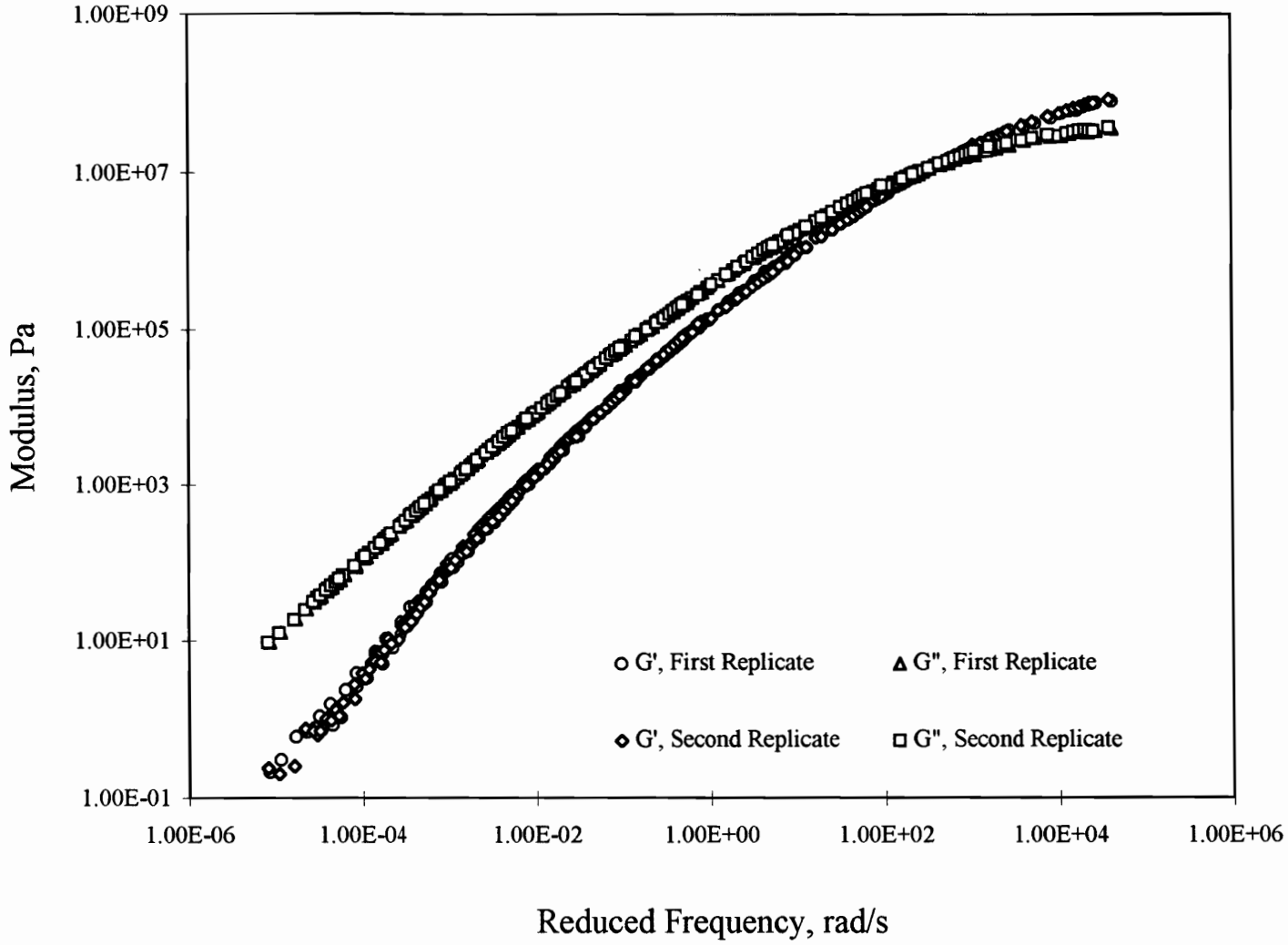

Figure a.4. Dynamic Master Curves for ARC2

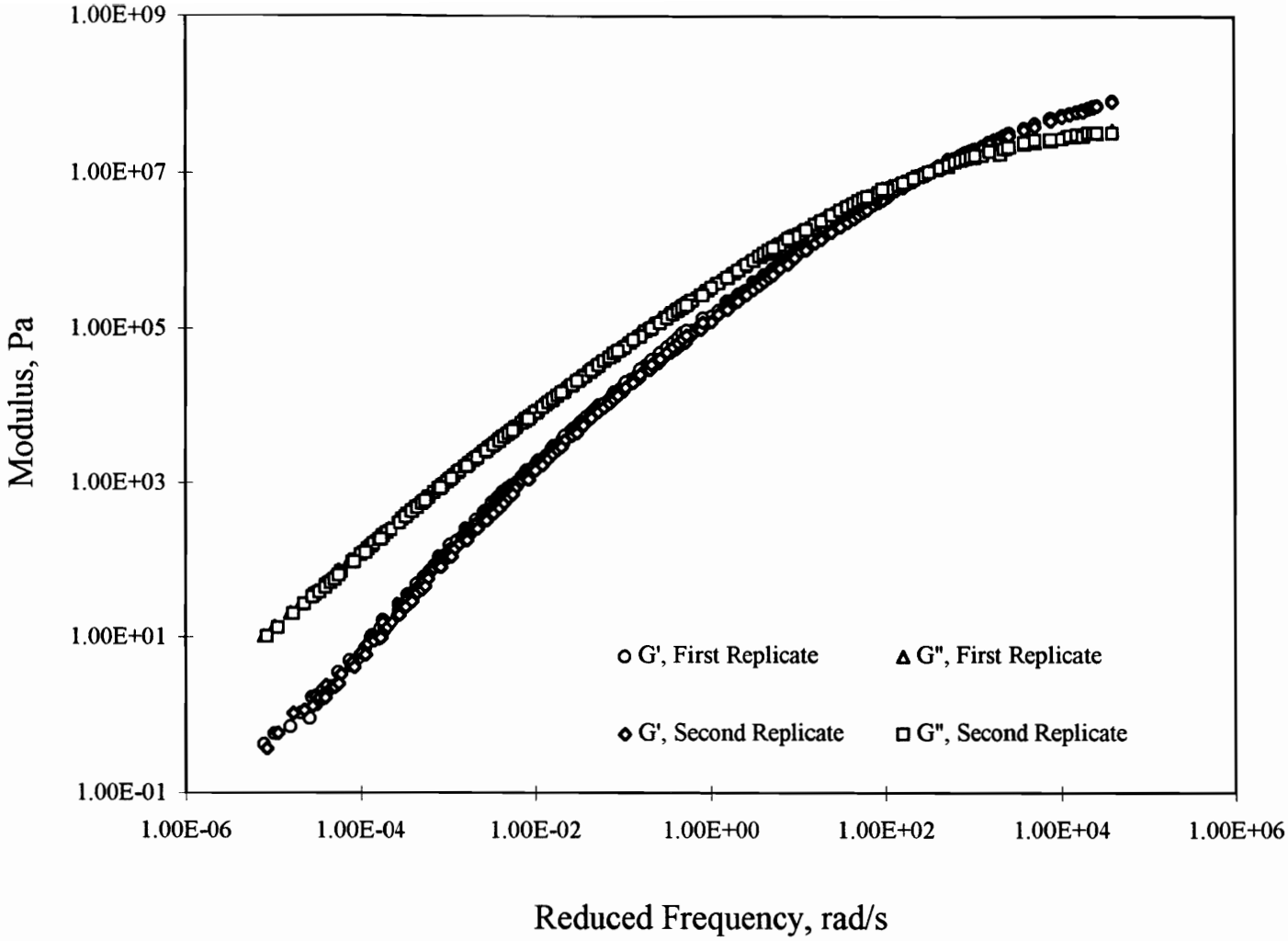

Figure a.5. Dynamic Master Curves for ARC3

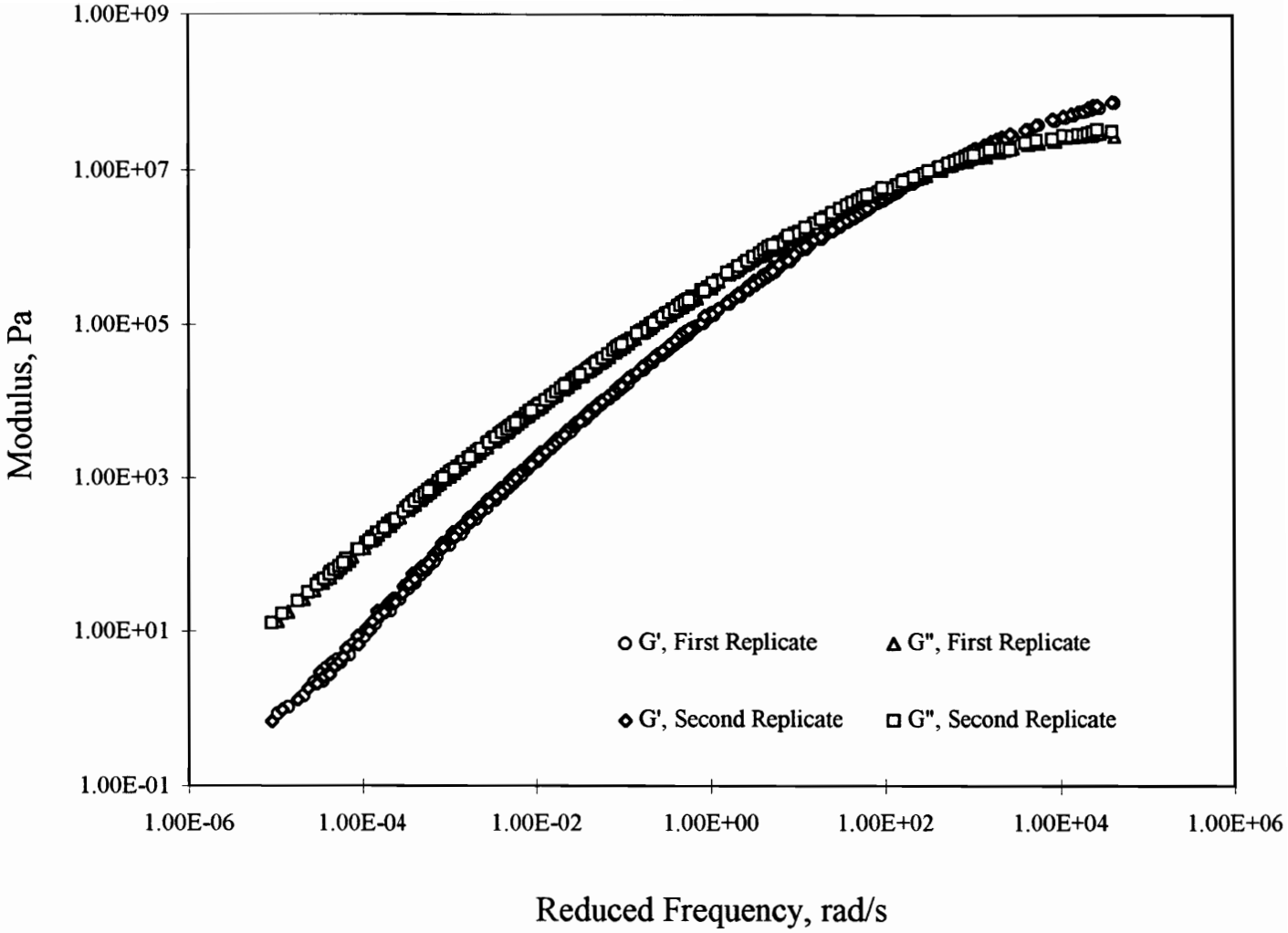

Figure a.6. Dynamic Master Curves for ARC4

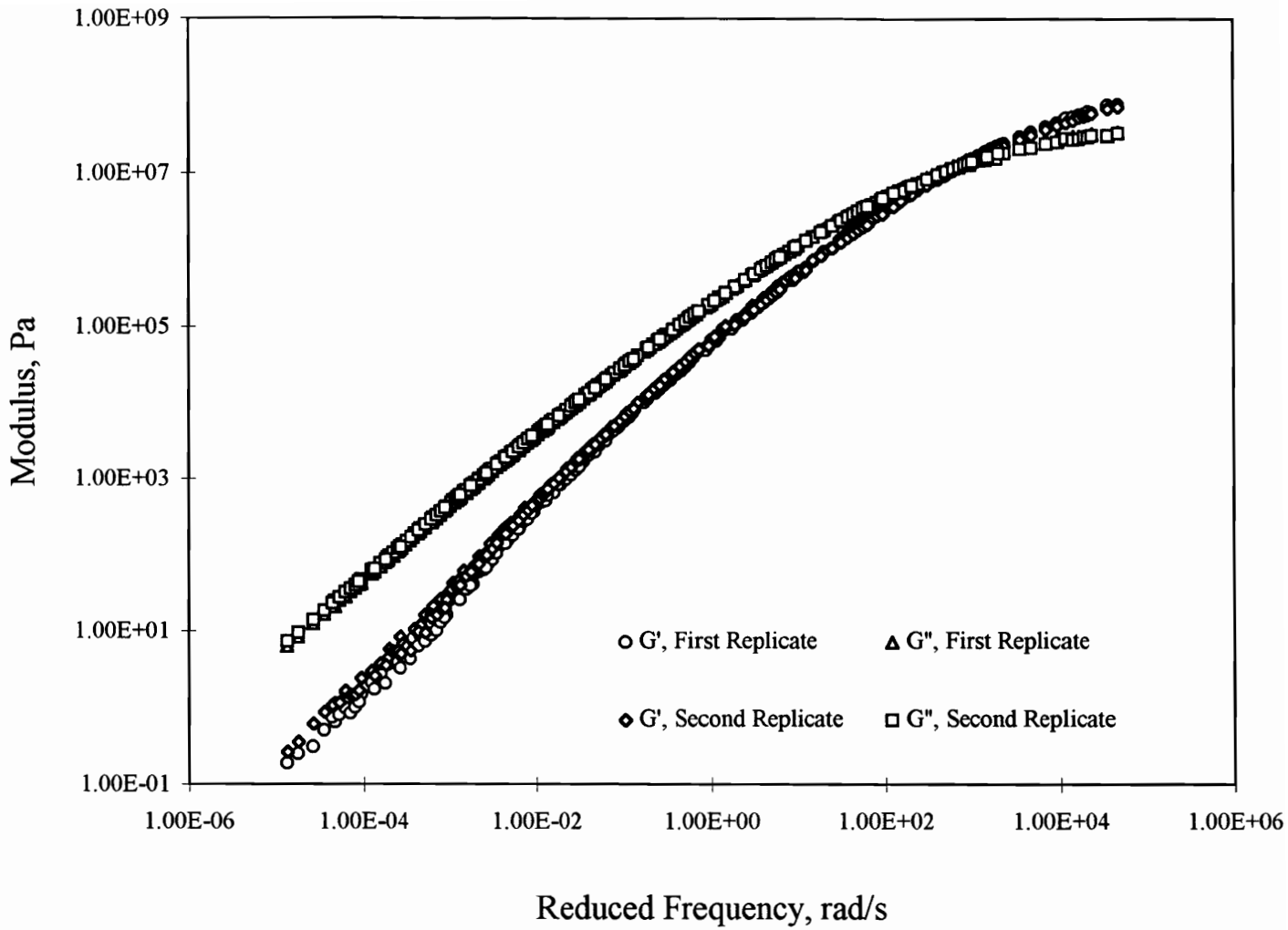

Figure a.7. Dynamic Master Curves for AUP3

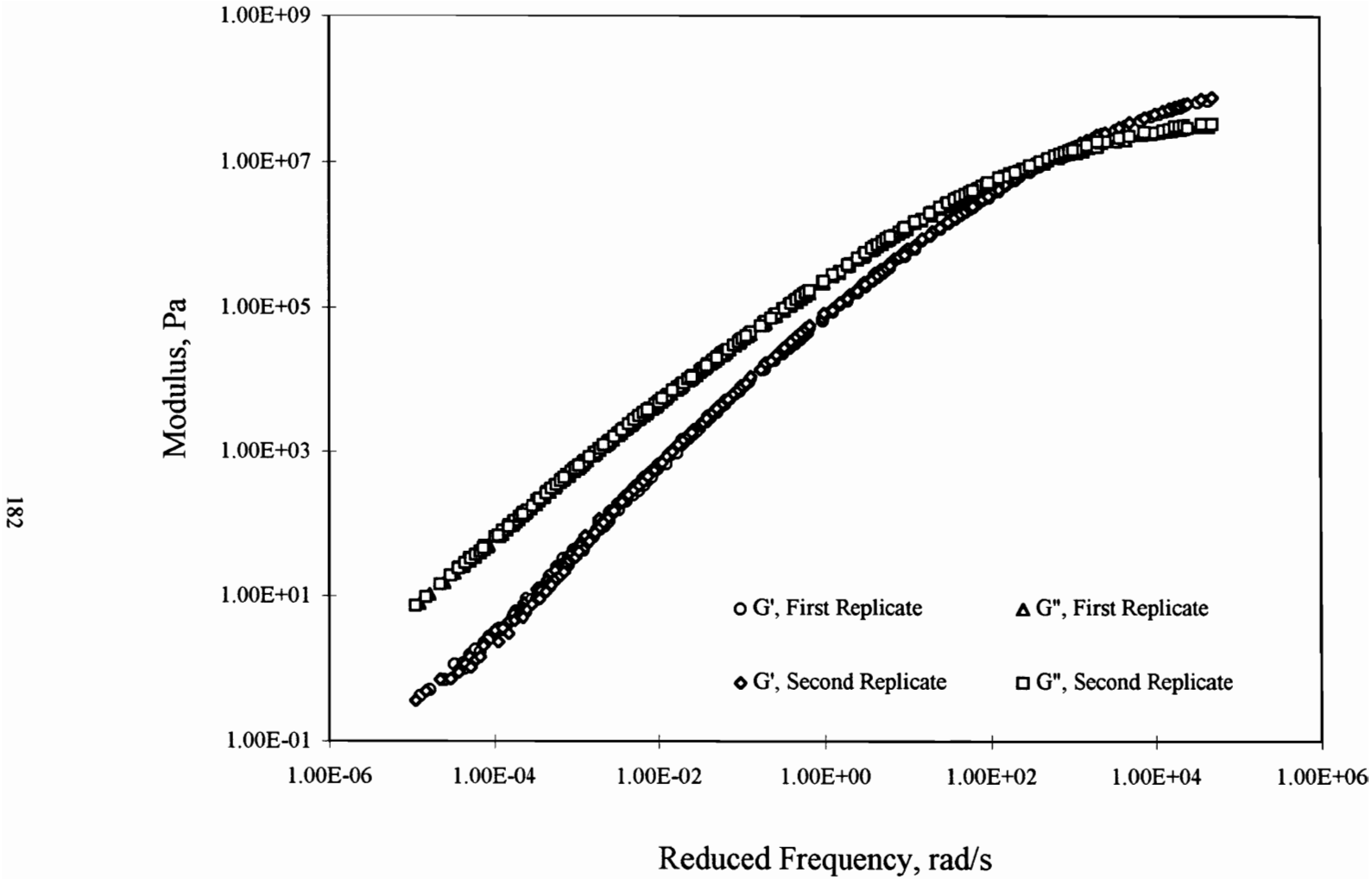

Figure a.8. Dynamic Master Curves for AUP4

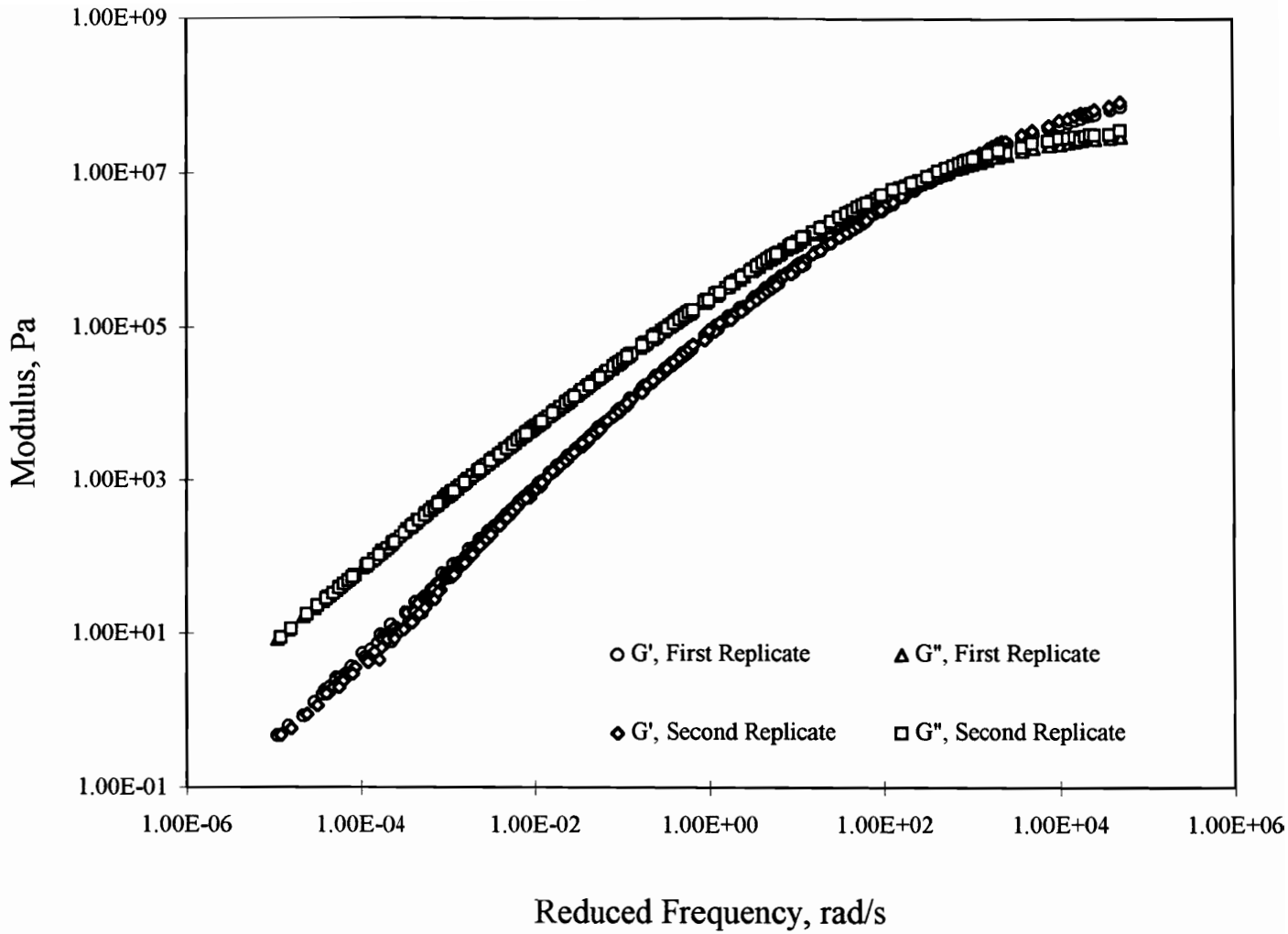

Figure a.9. Dynamic Master Curves for AUP5

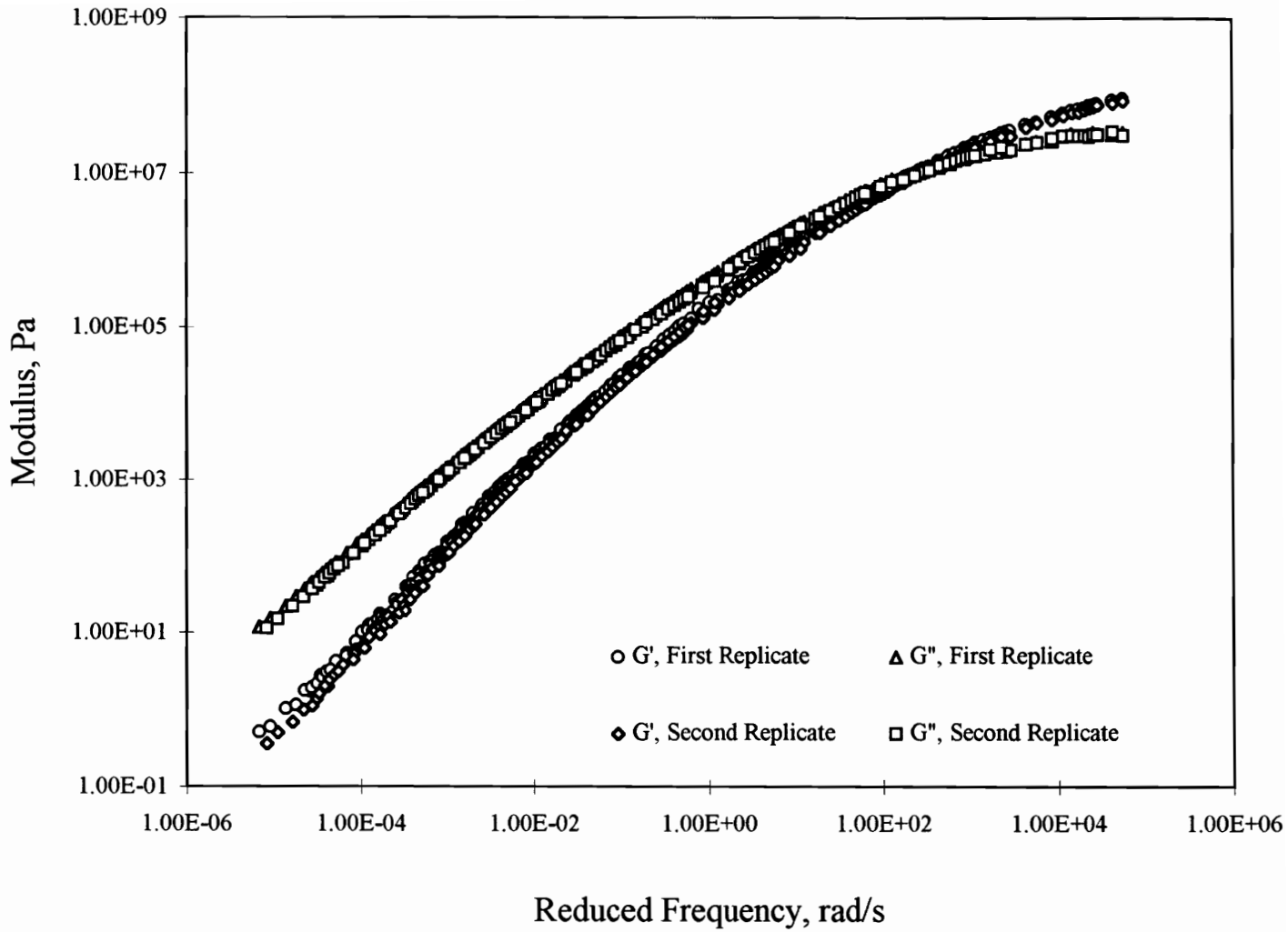

Figure a.10. Dynamic Master Curves for ARP3

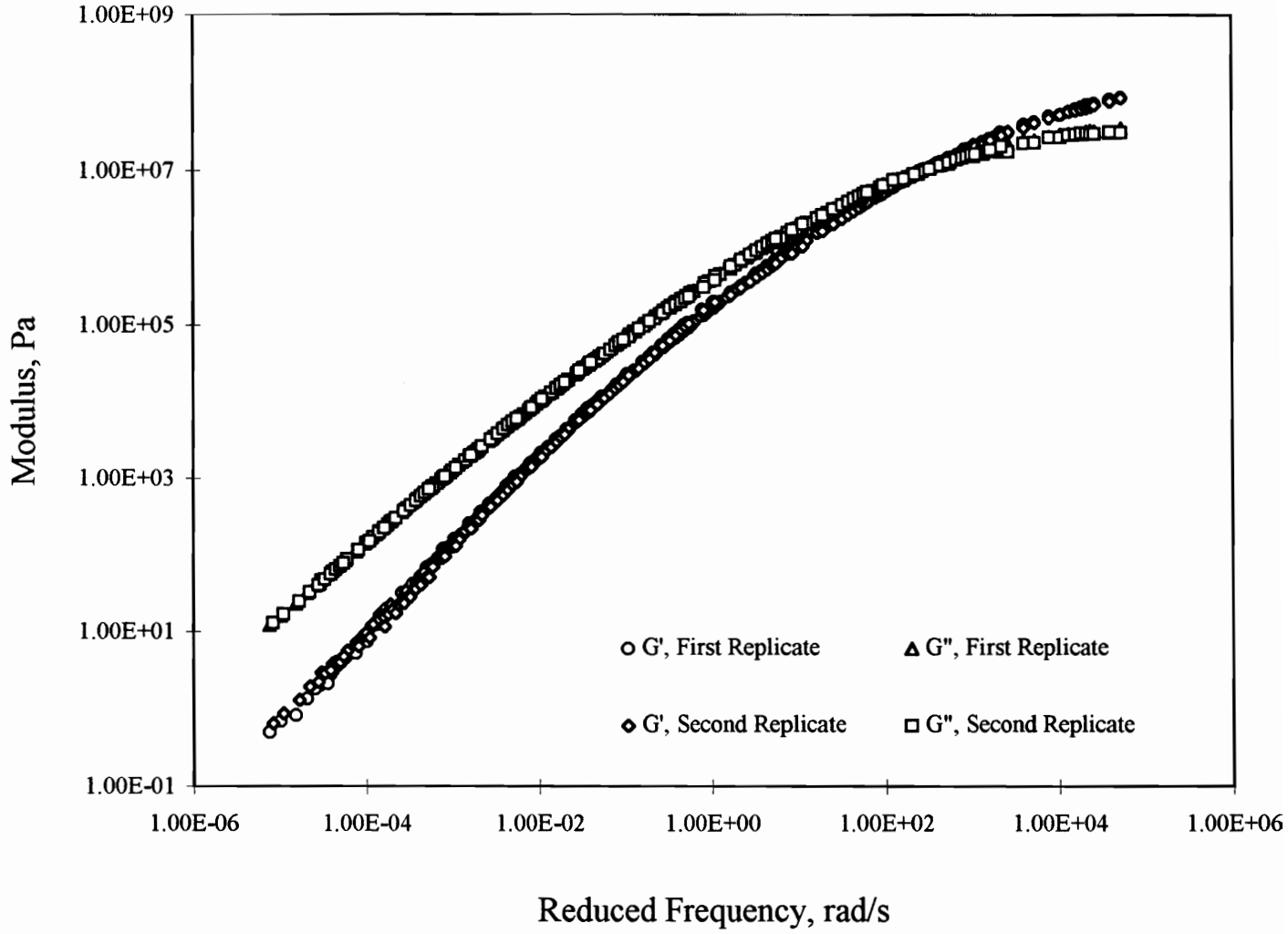

Figure a.11. Dynamic Master Curves for ARP4

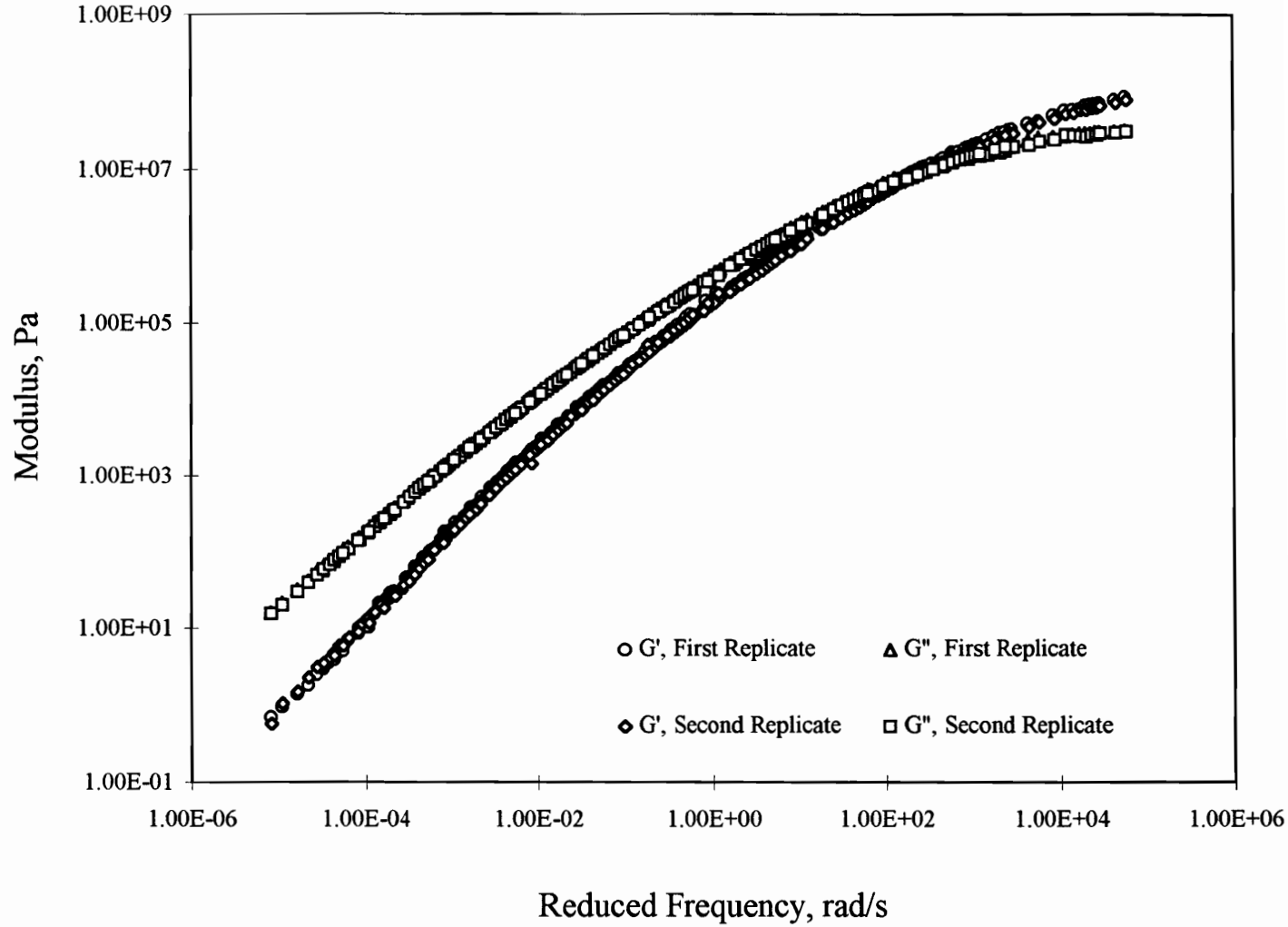

Figure a.12. Dynamic Master Curves for ARP5

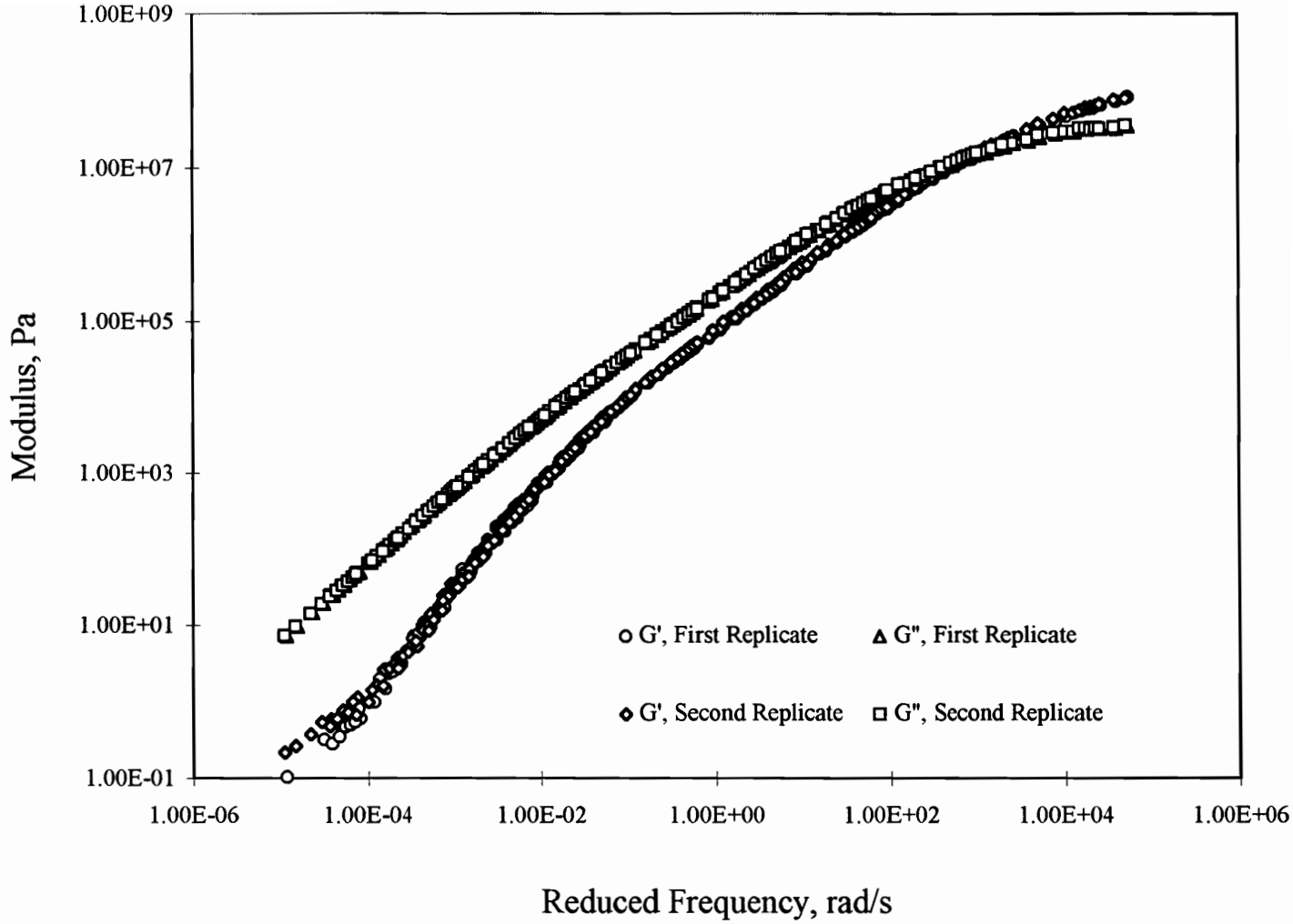

Figure a.13. Dynamic Master Curves for AUD3

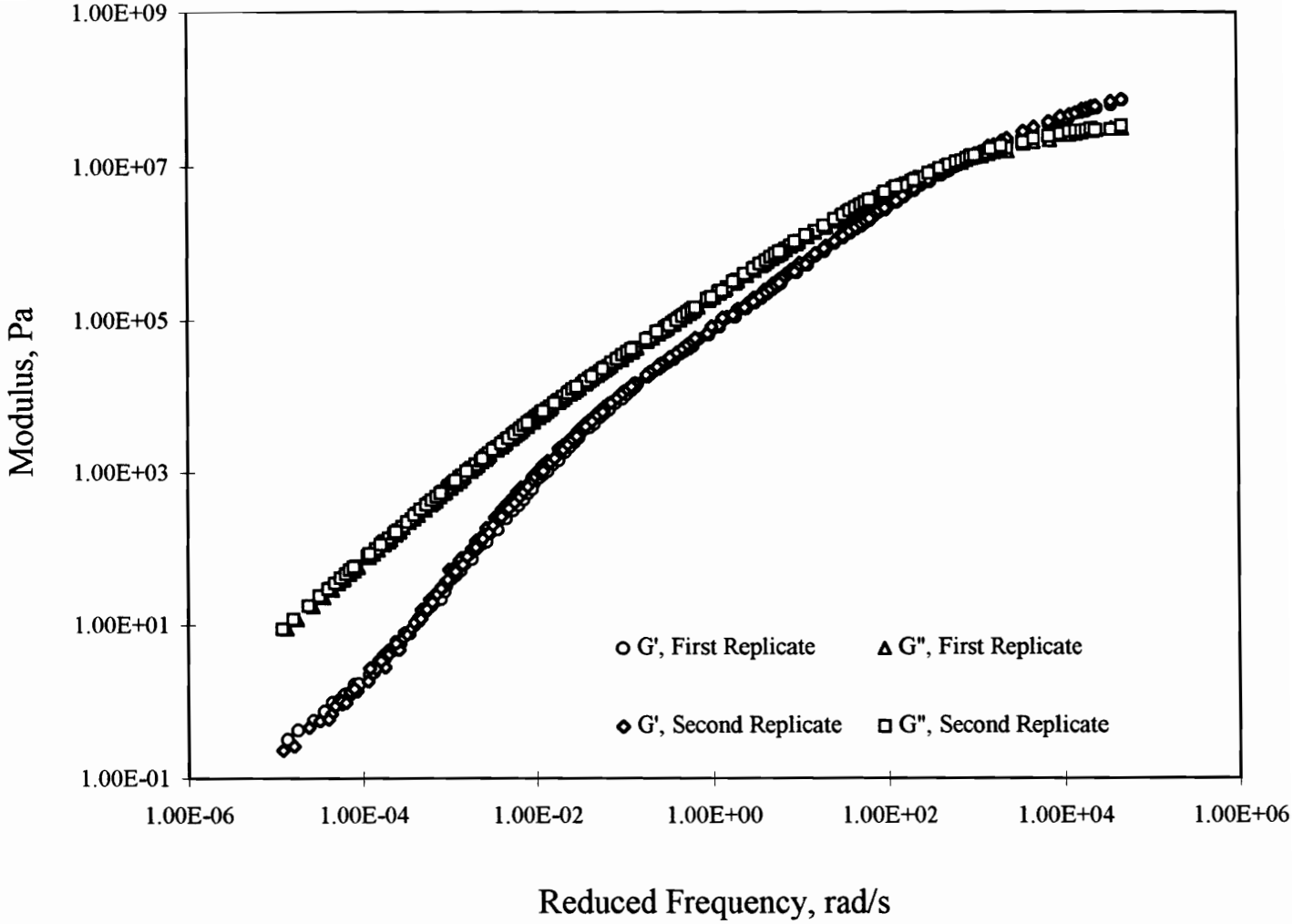

Figure a.14. Dynamic Master Curves for AUD4

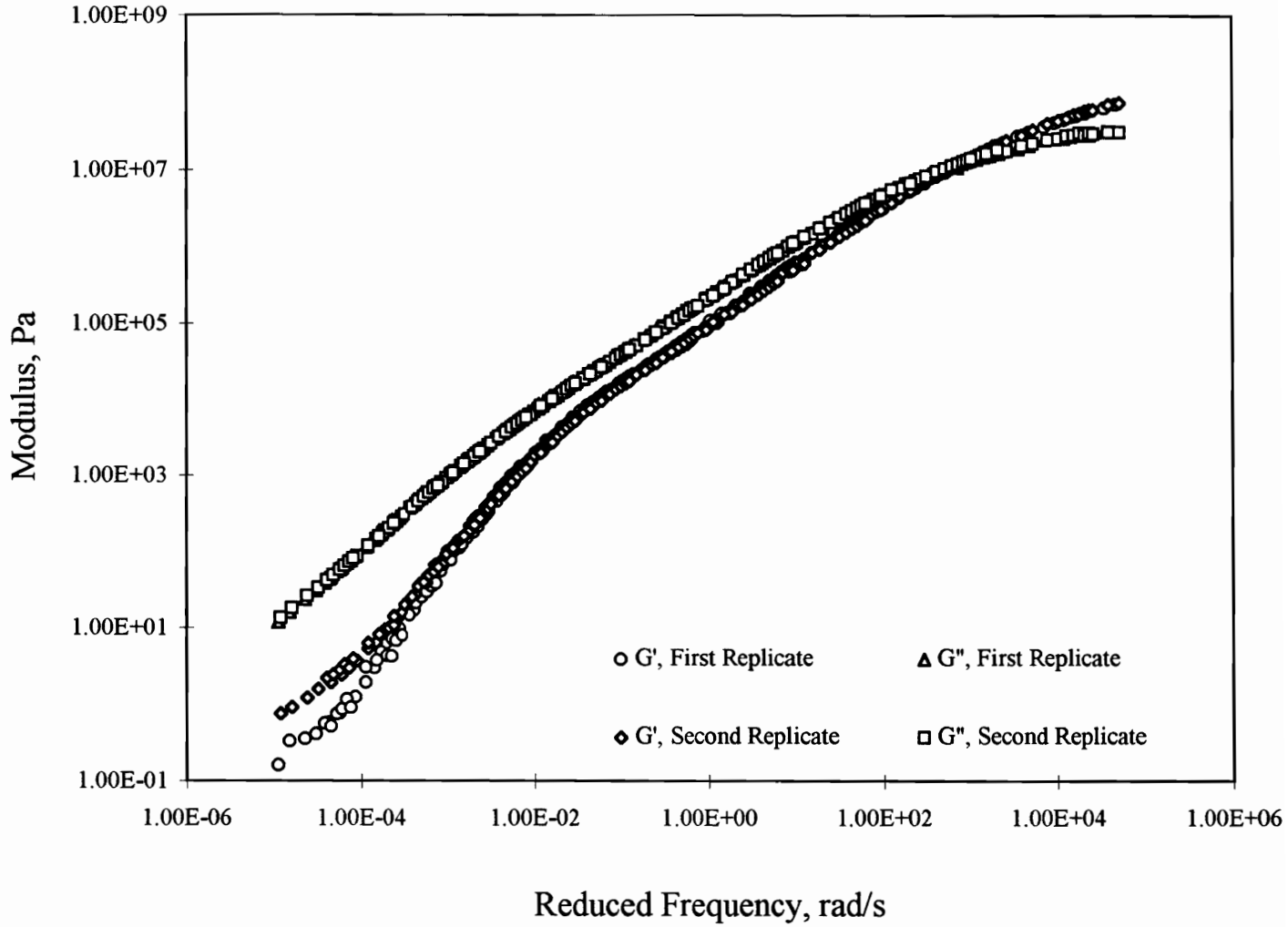

Figure a.15. Dynamic Master Curves for AUD5

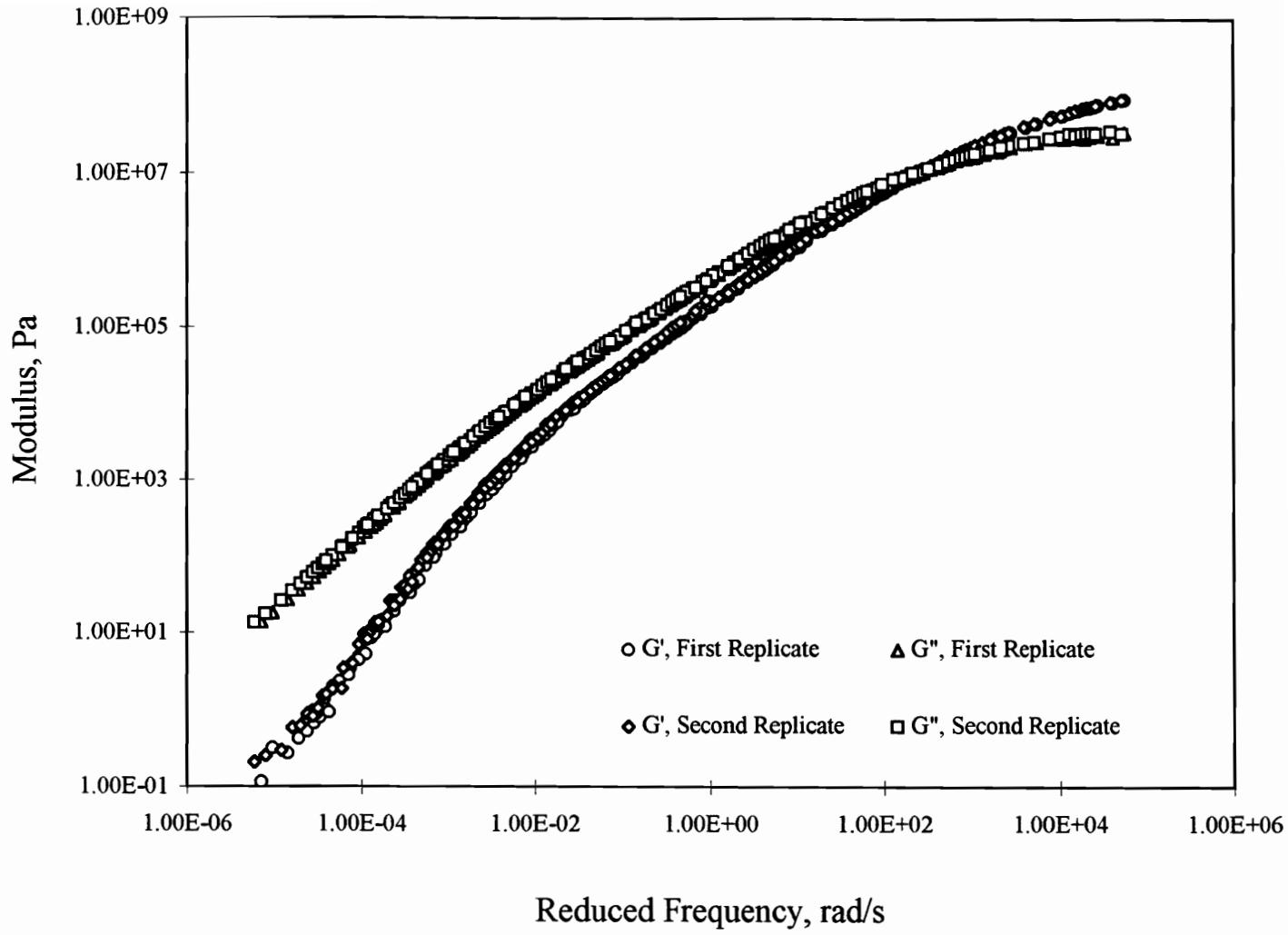

Figure a.16. Dynamic Master Curves for ARD3

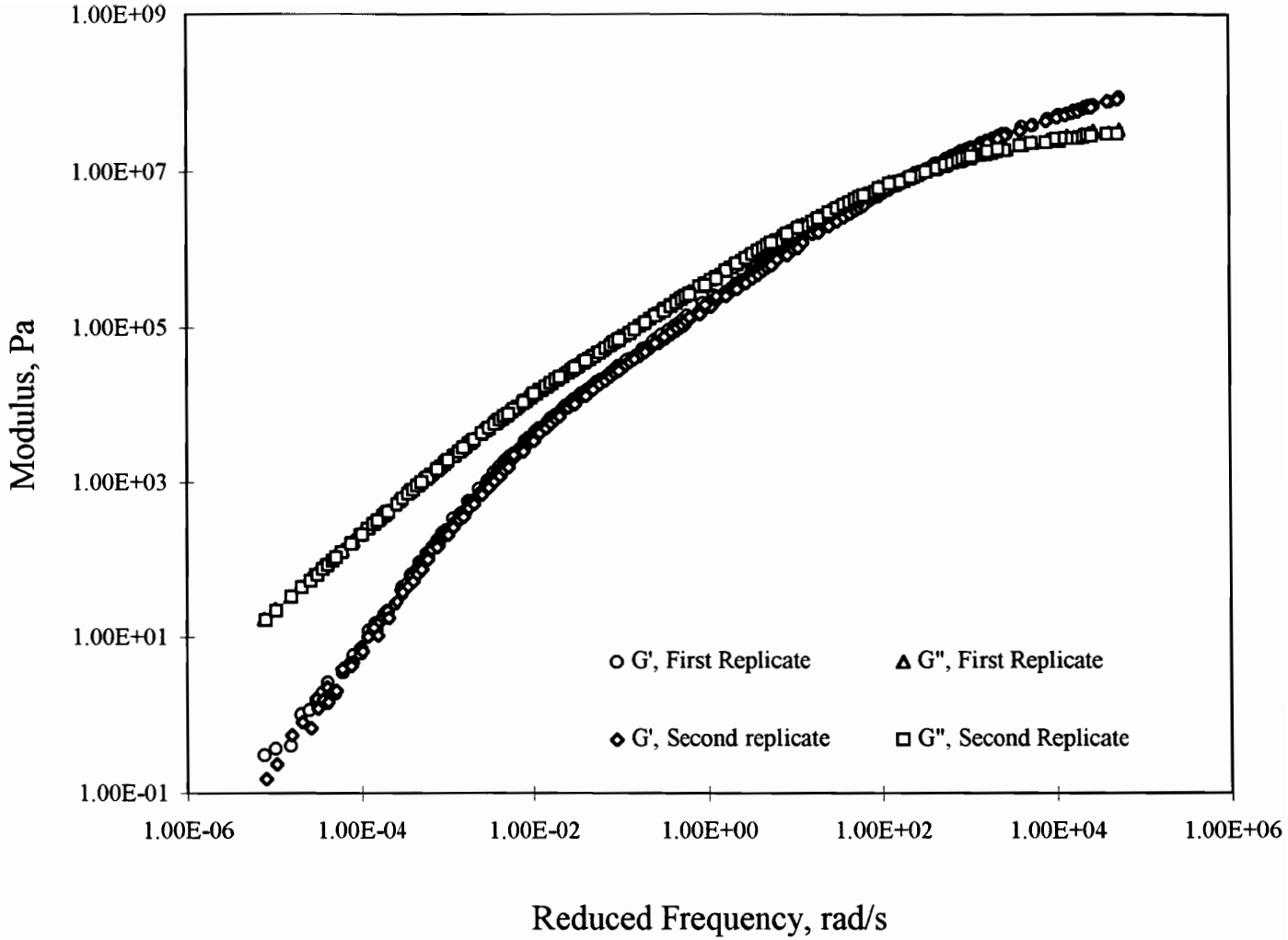

Figure a.17. Dynamic Master Curves for ARD4

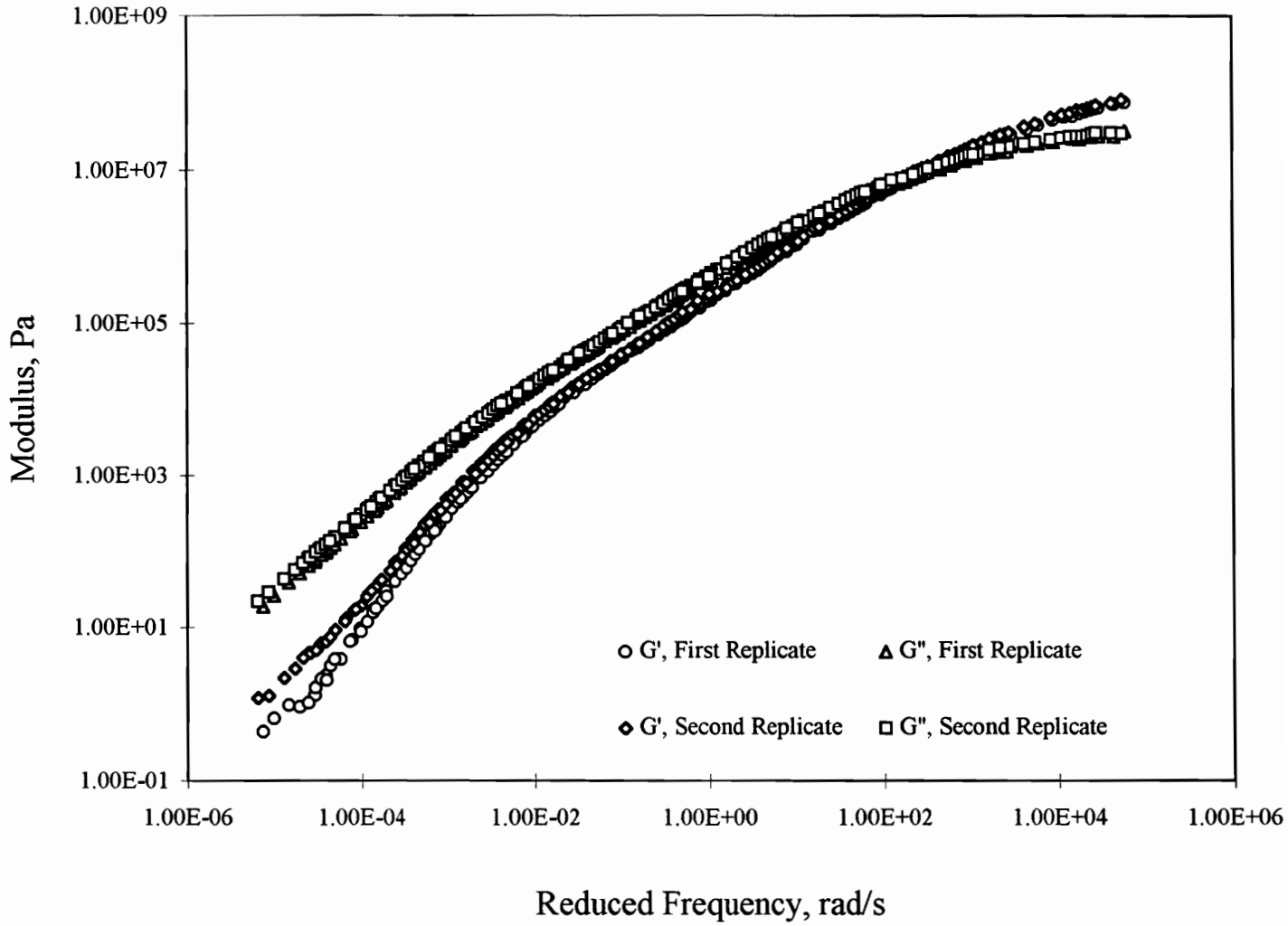

Figure a.18. Dynamic Master Curves for ARD5

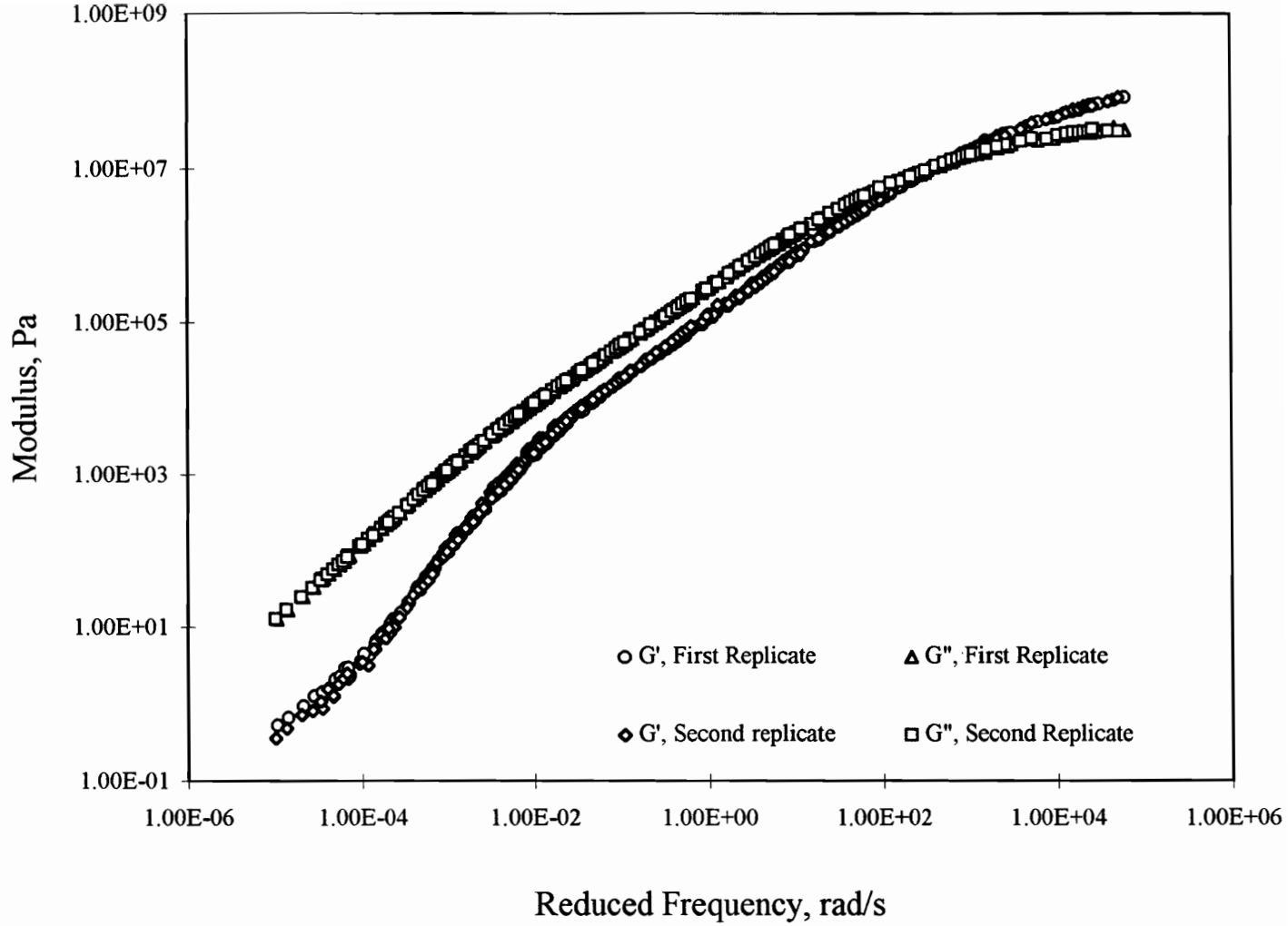

Figure a.19. Dynamic Master Curves for AUS3

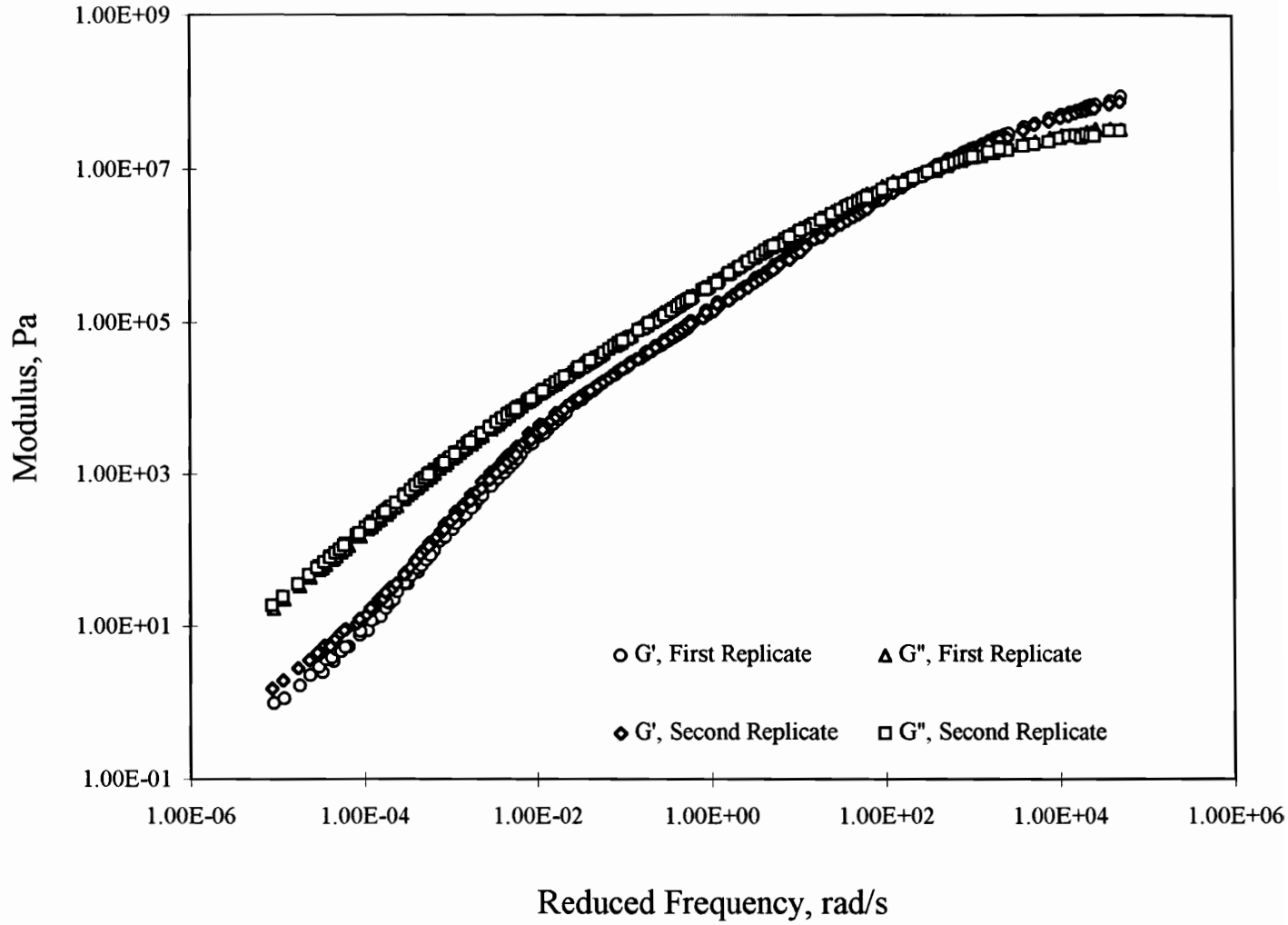

Figure a.20. Dynamic Master Curves for AUS4

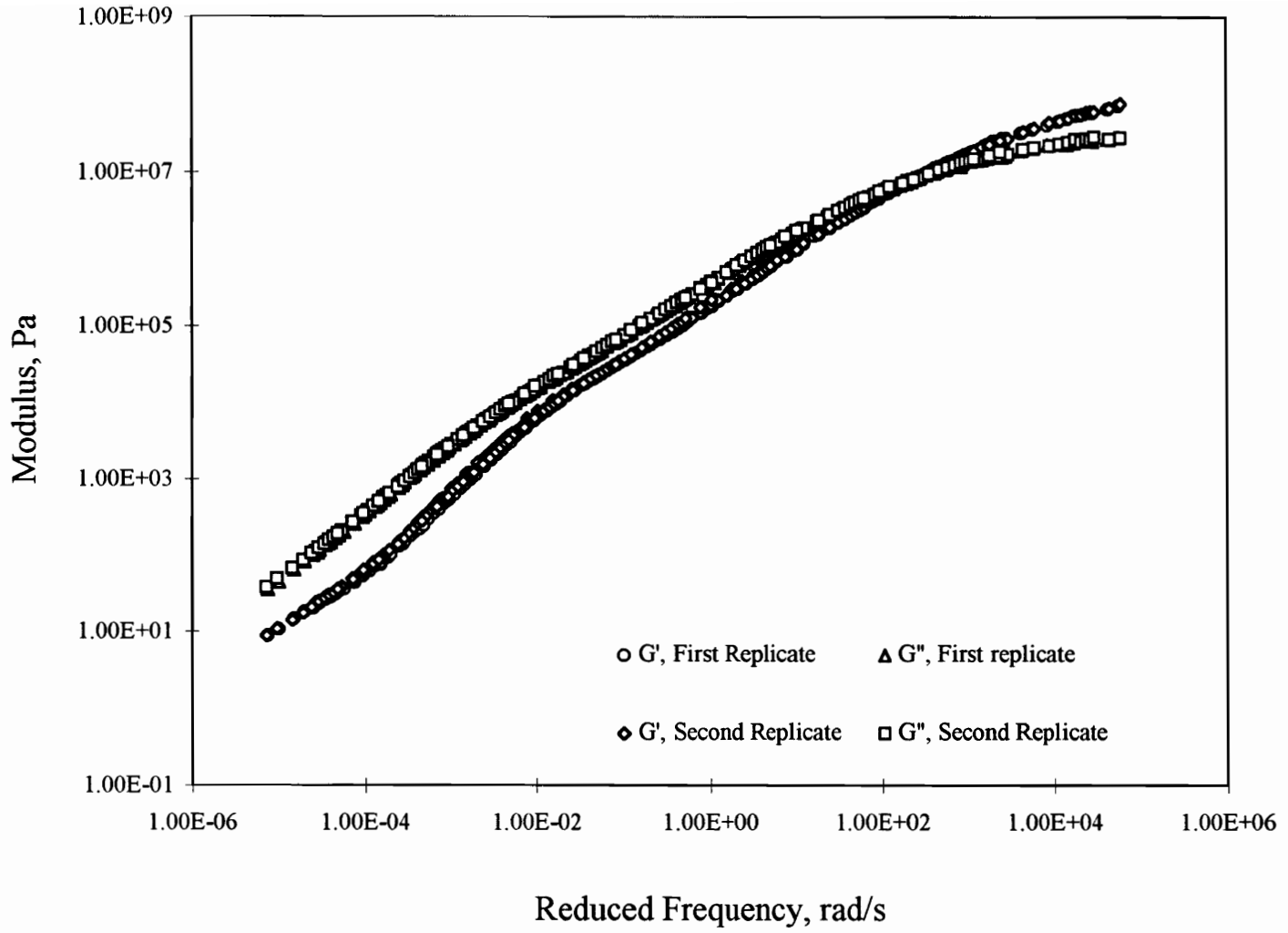

Figure a.21. Dynamic Master Curves for AUS5

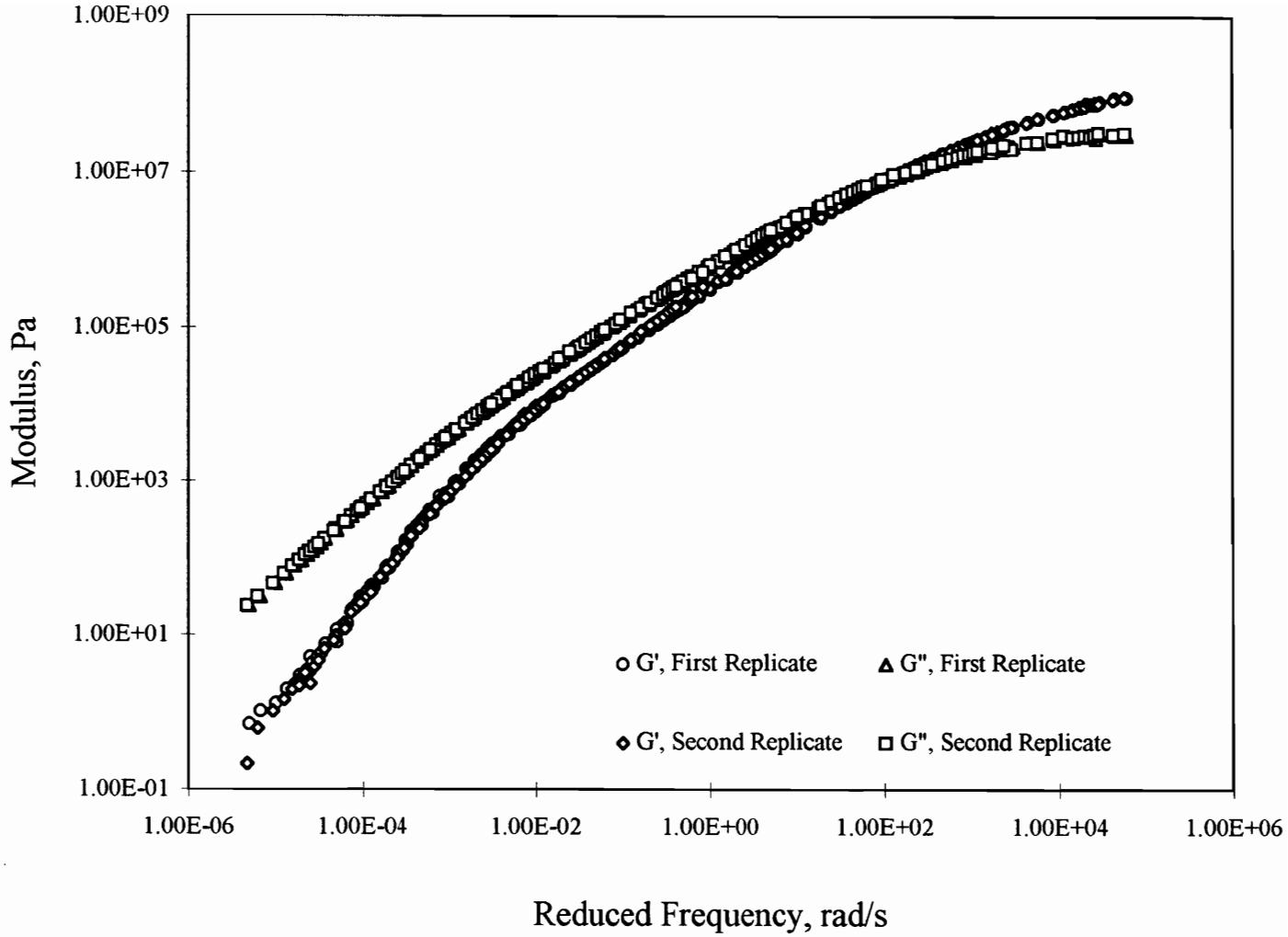

Figure a.22. Dynamic Master Curves for ARS3

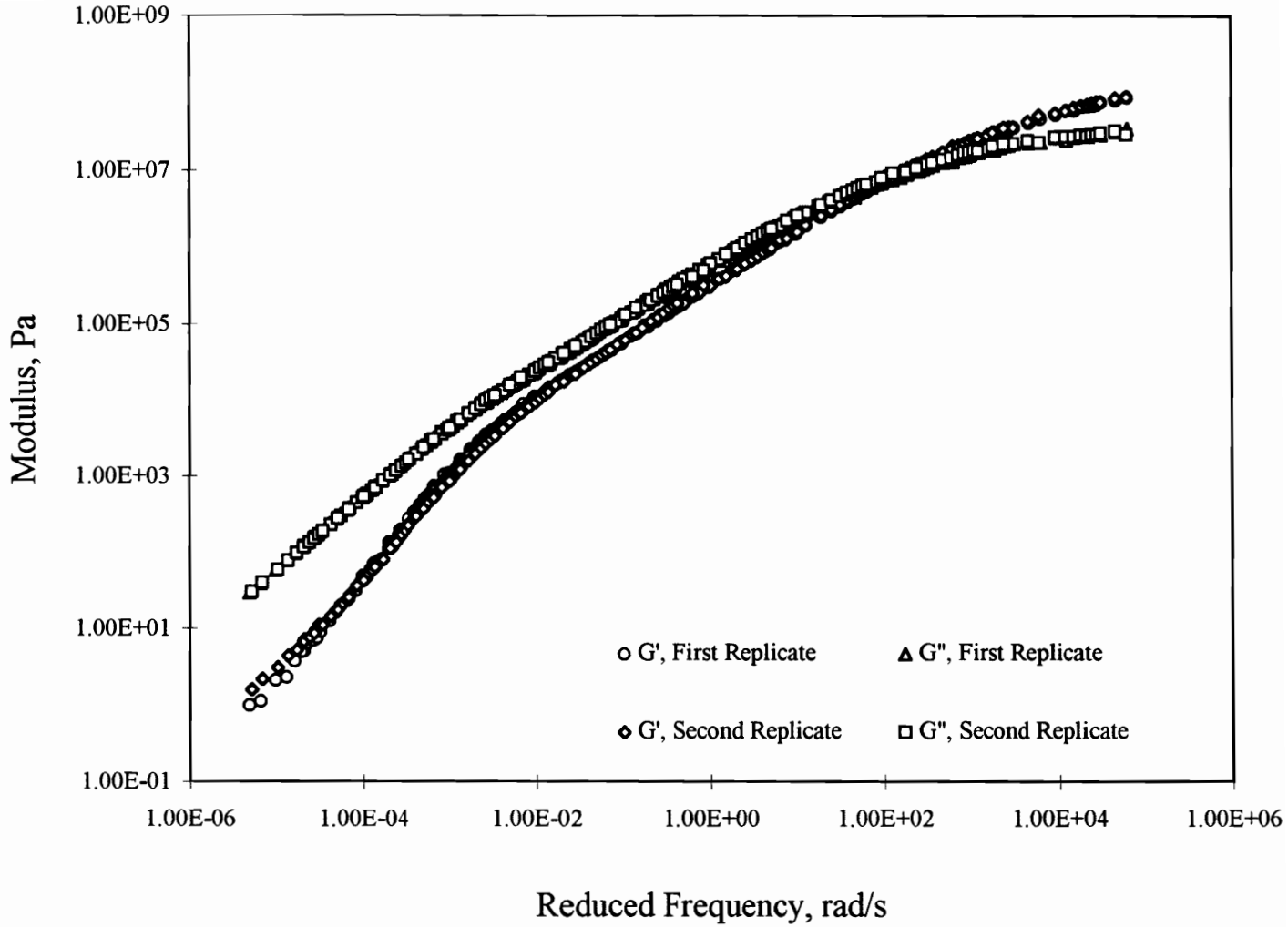

Figure a.23. Dynamic Master Curves for ARS4

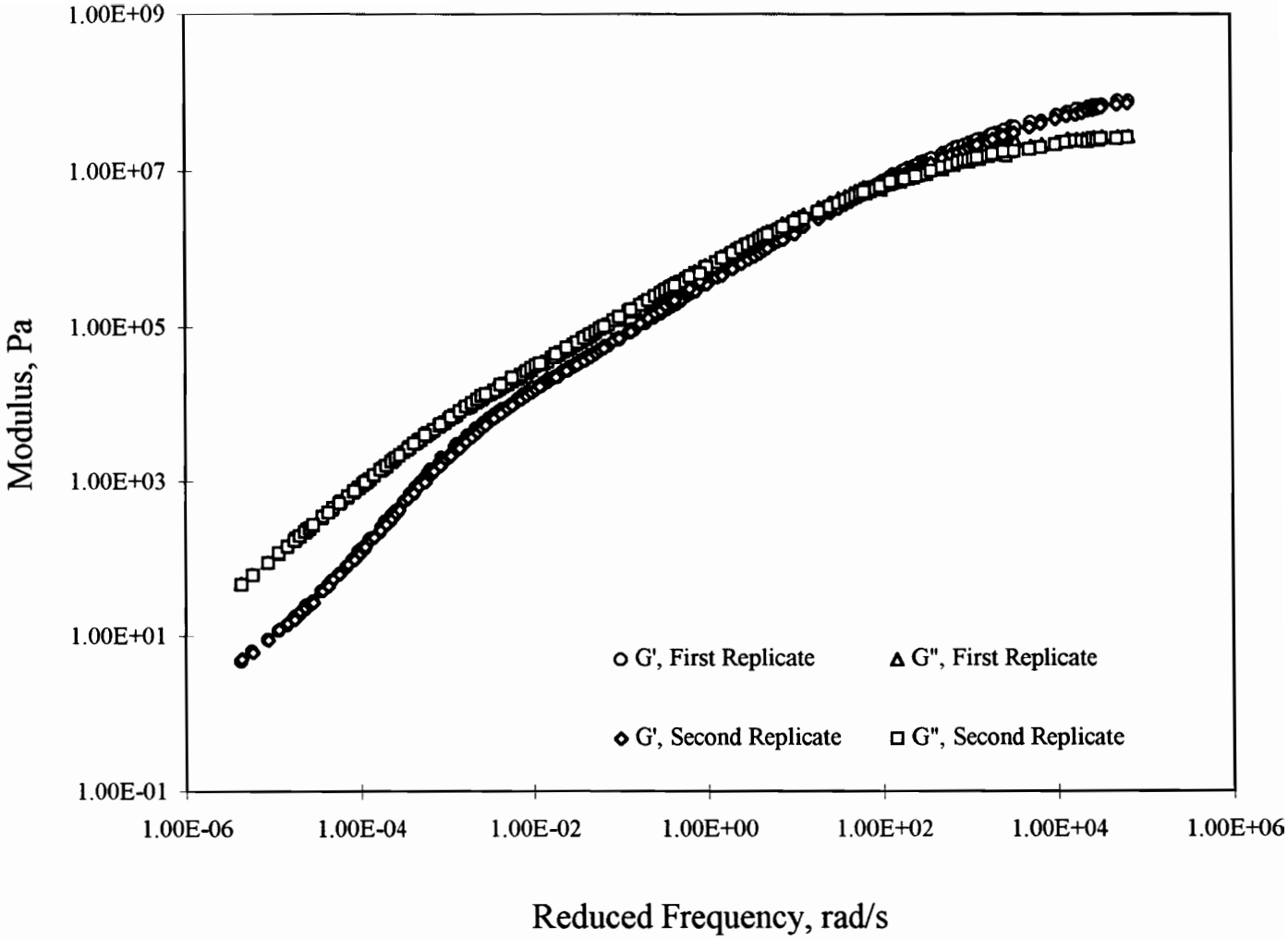

Figure a.24. Dynamic Master Curves for ARS5

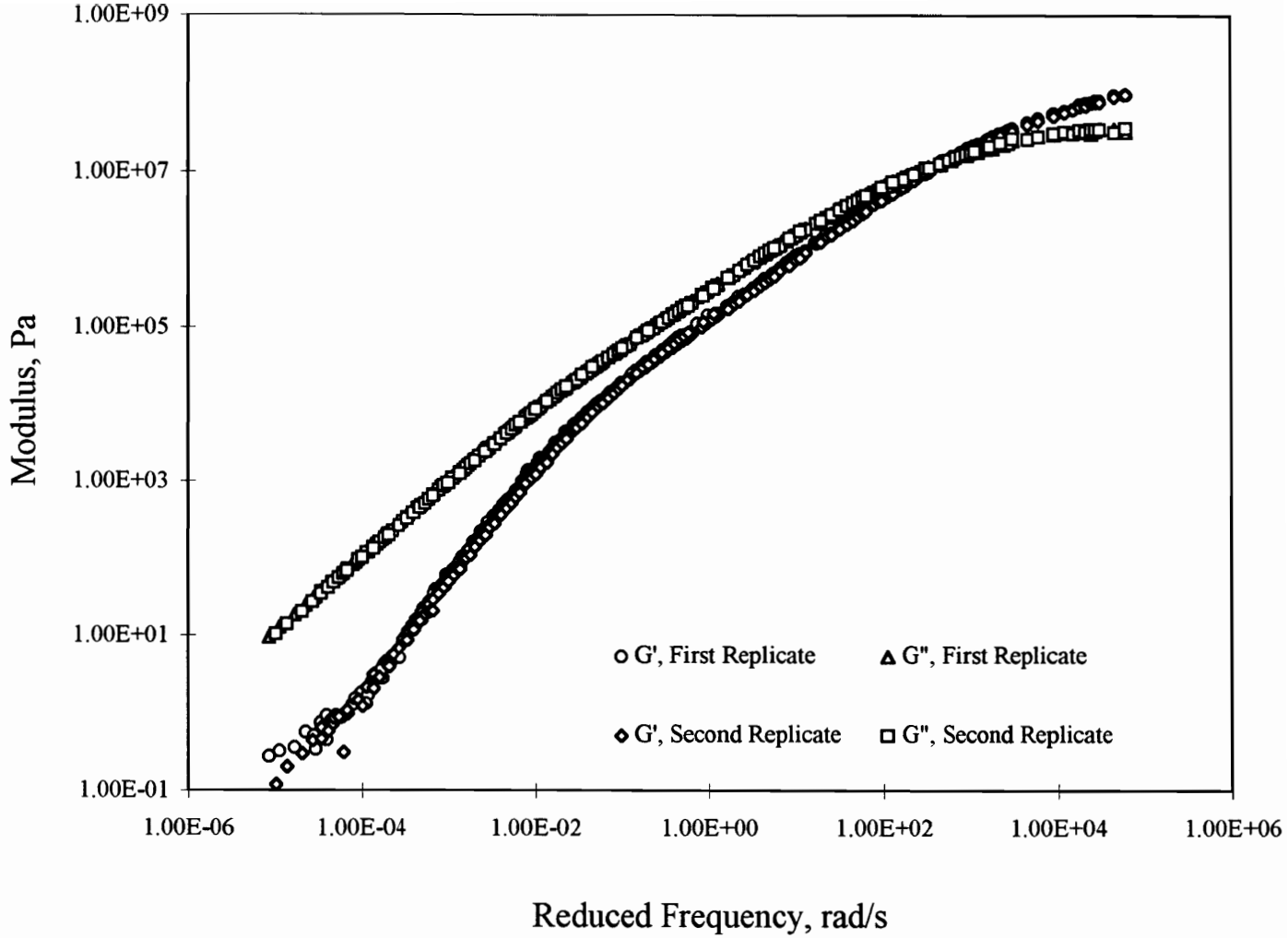

Figure a.25. Dynamic Master Curves for AUG3

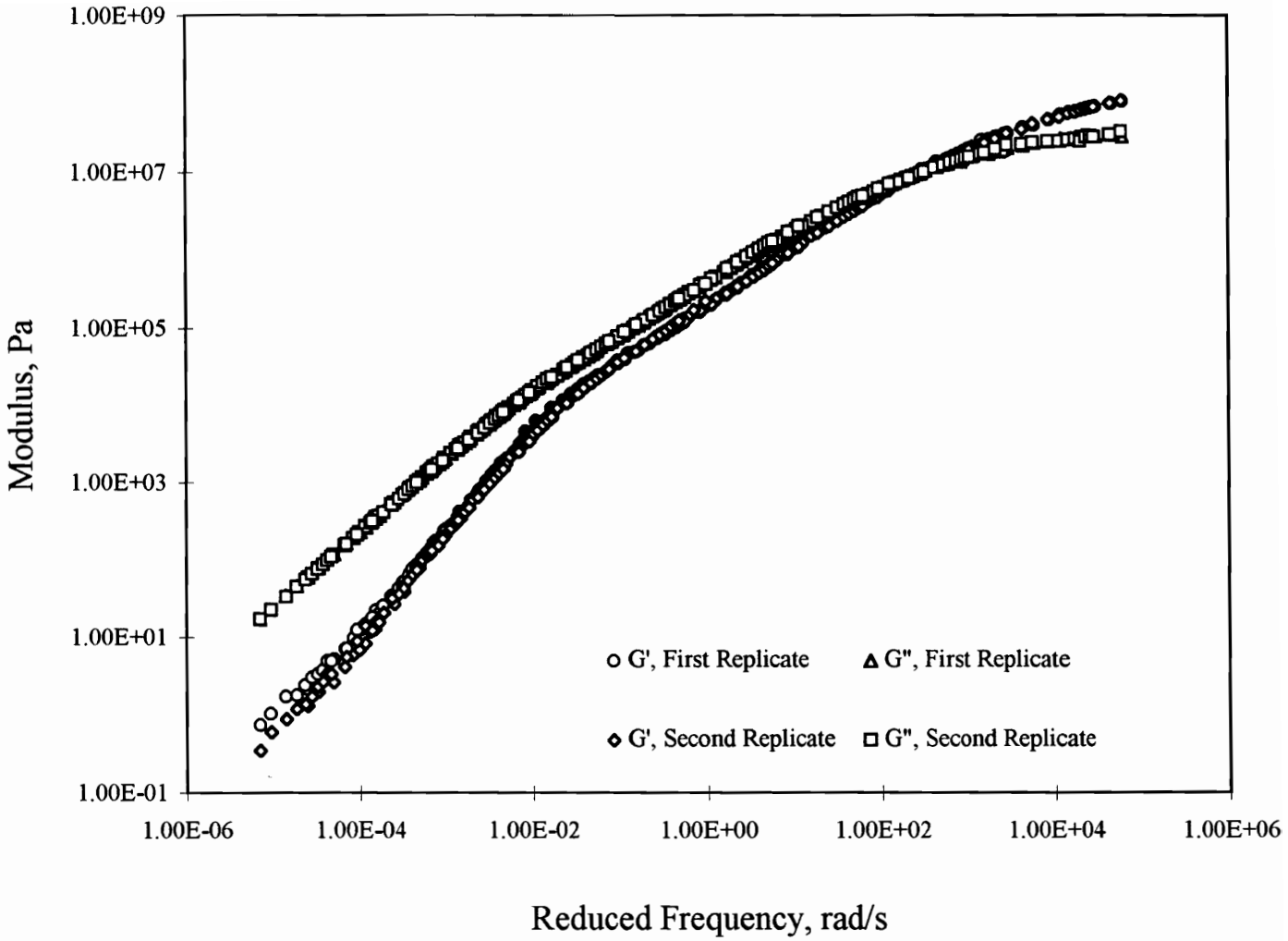

Figure a.26. Dynamic Master Curves for AUG4

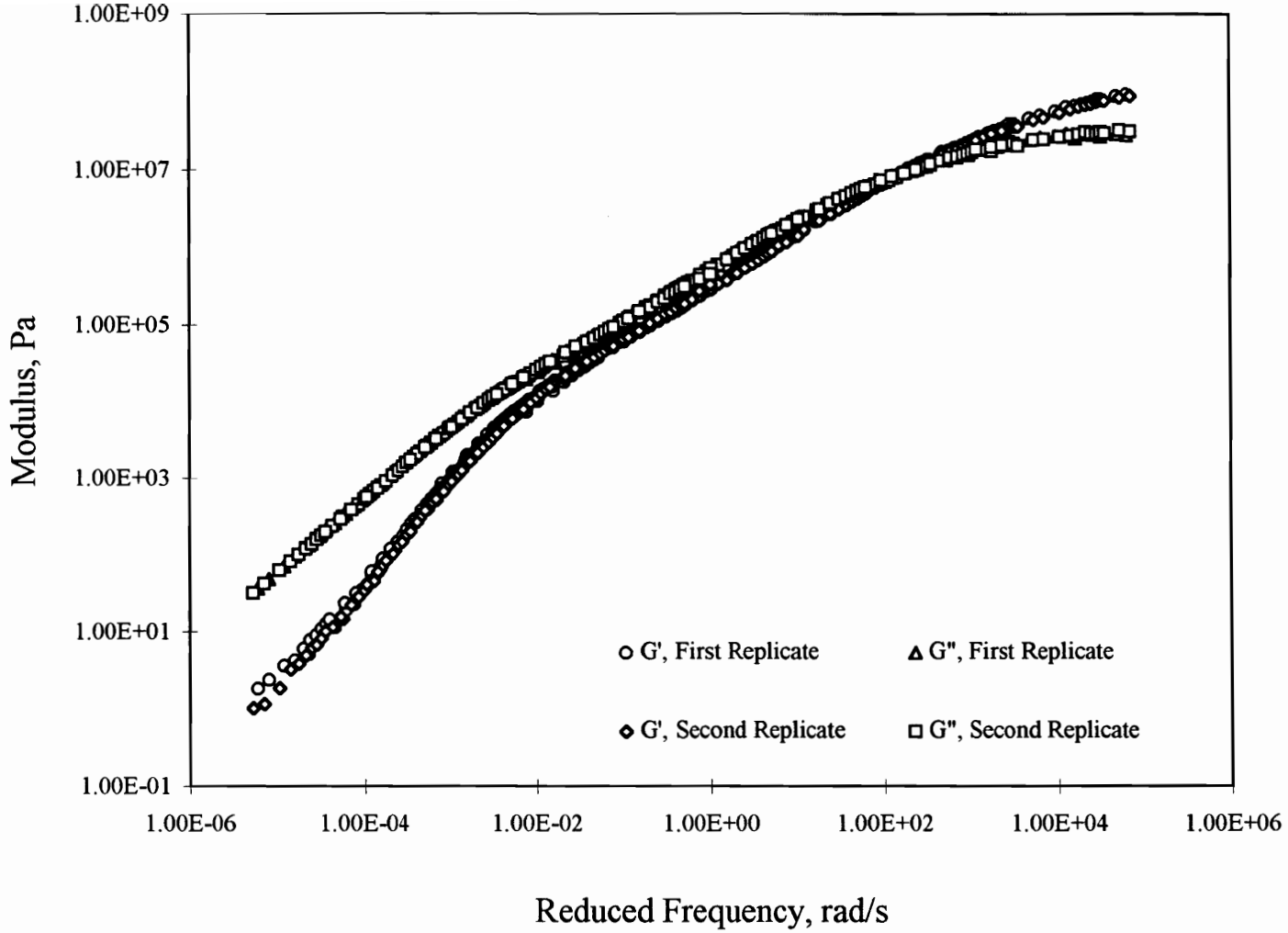

Figure a.27. Dynamic Master Curves for AUG5

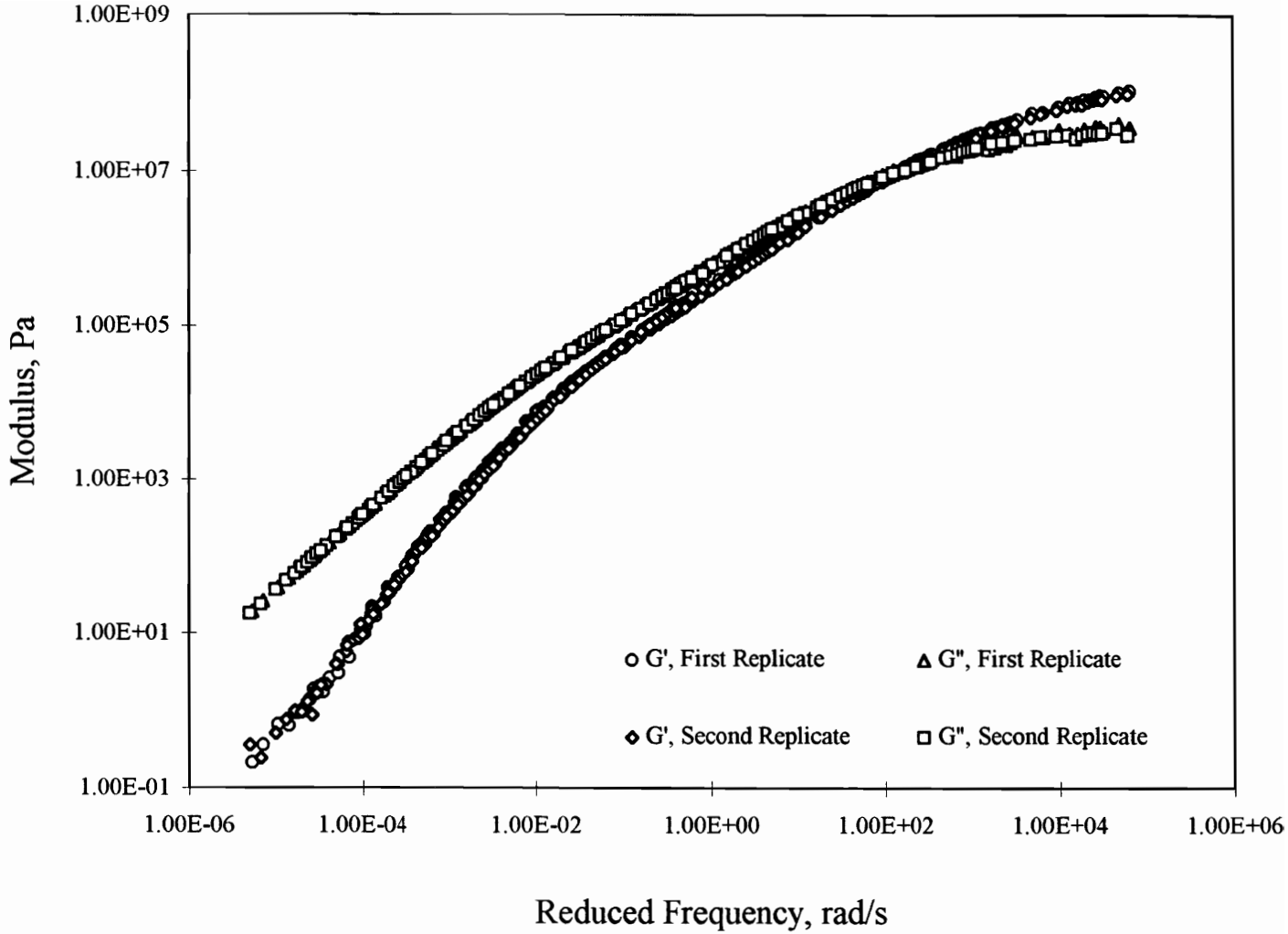

Figure a.28. Dynamic Master Curves for ARG3

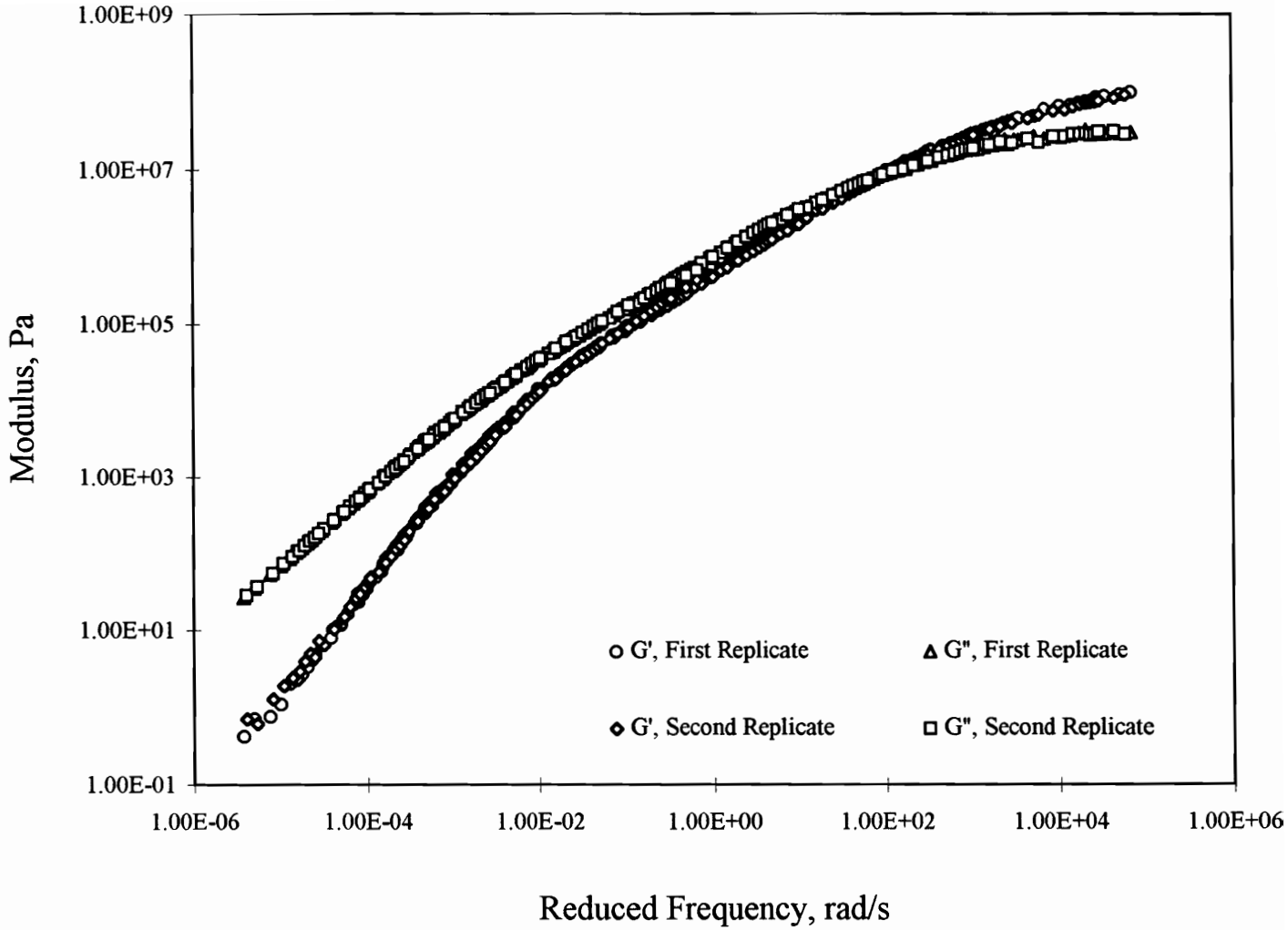

Figure a.29. Dynamic Master Curves for ARG4

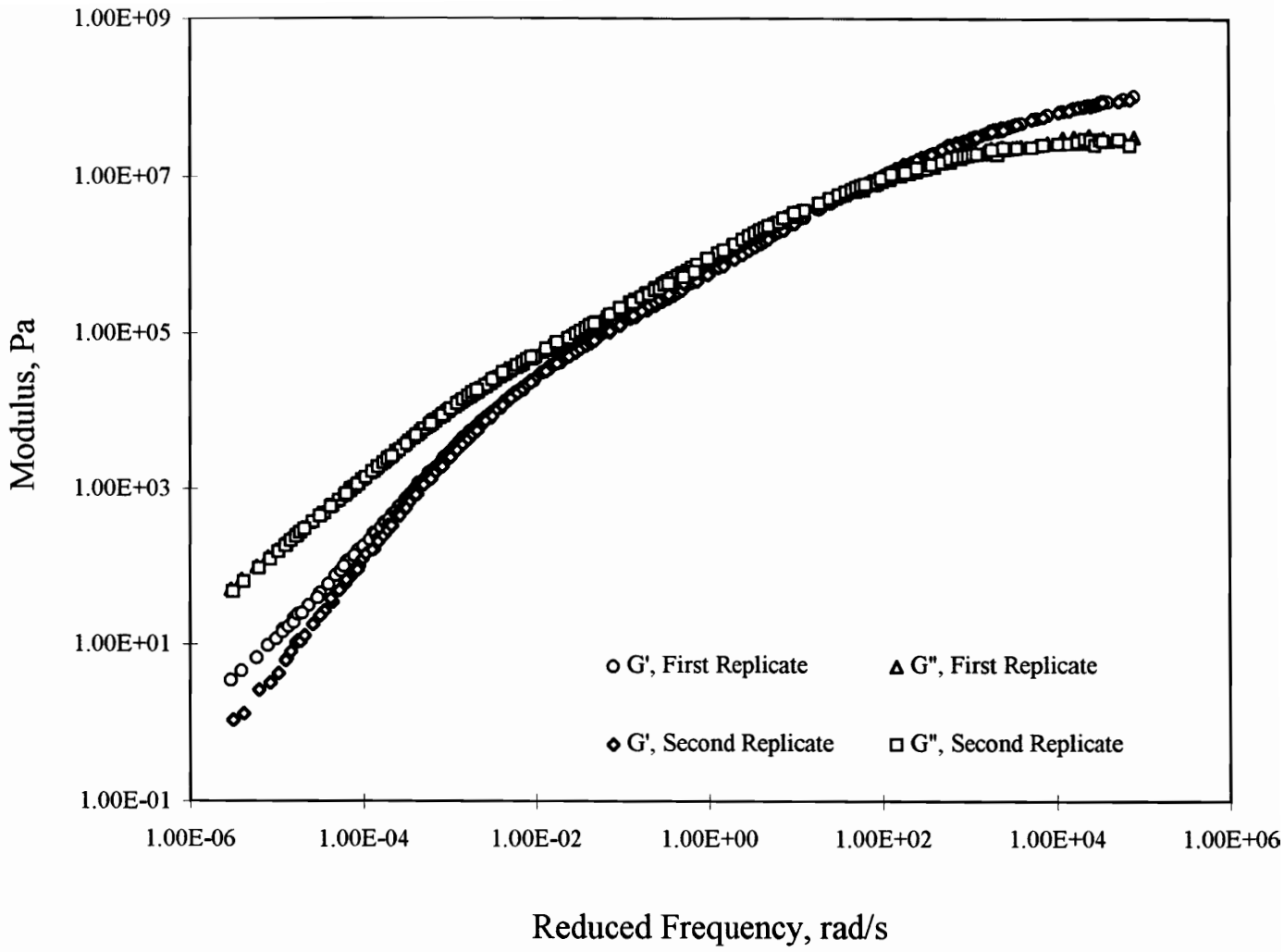

Figure a.30. Dynamic MAster Curves for ARG5

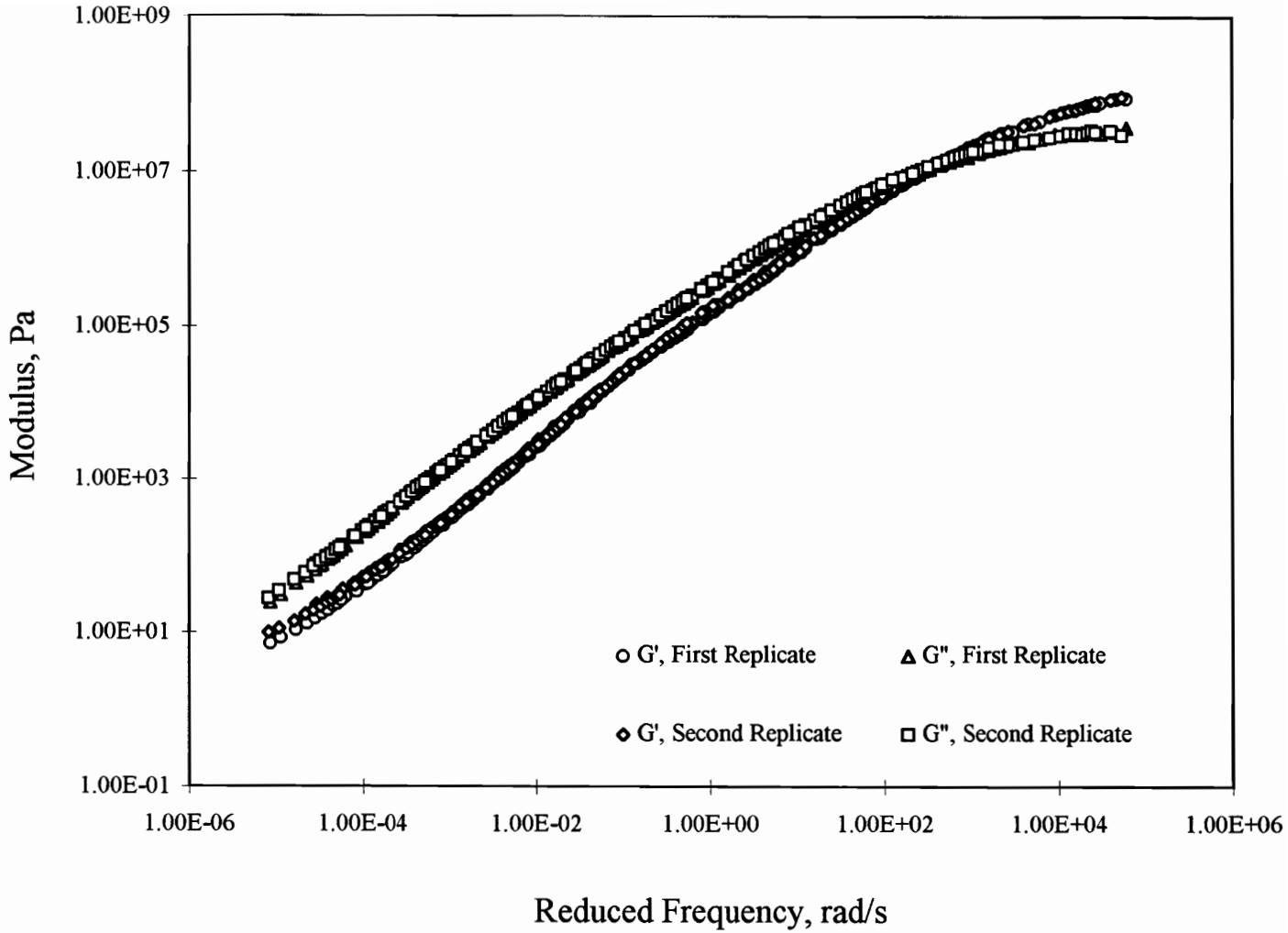

Figure a.31. Dynamic Master Curves for AUX3

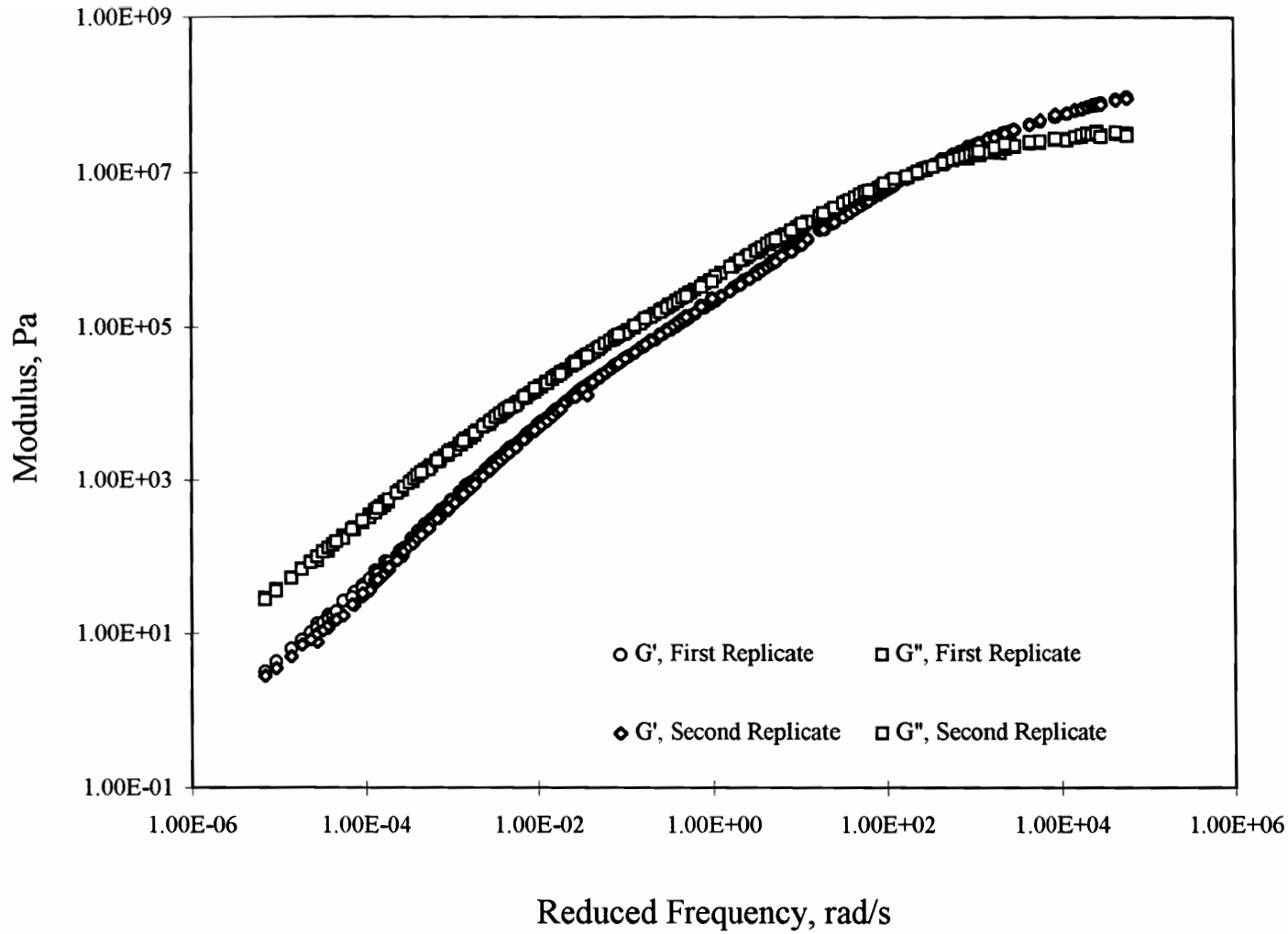

Figure a.32. Dynamic Master Curves for AUX4

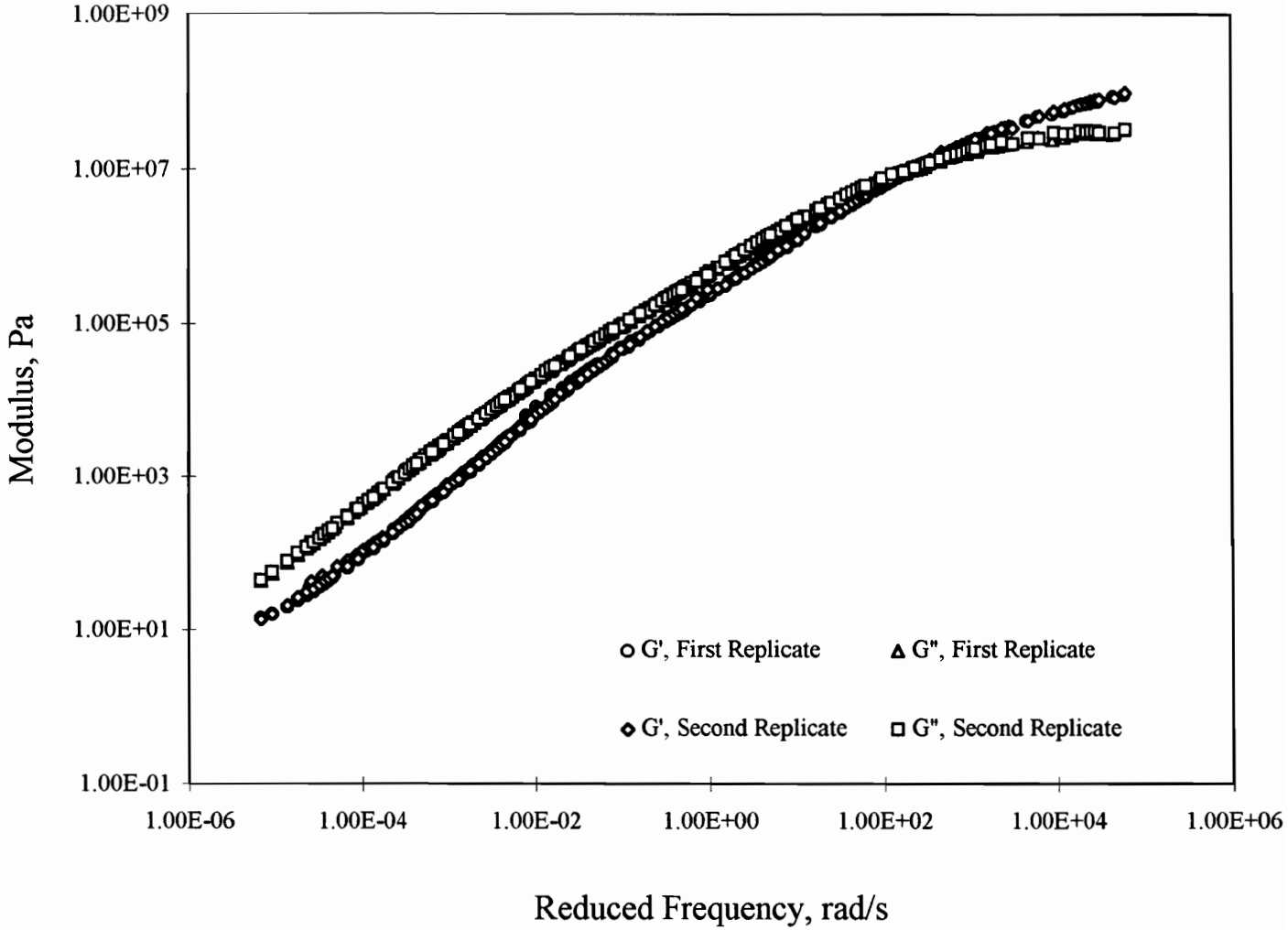

Figure a.33. Dynamic Master Curves for AUX5

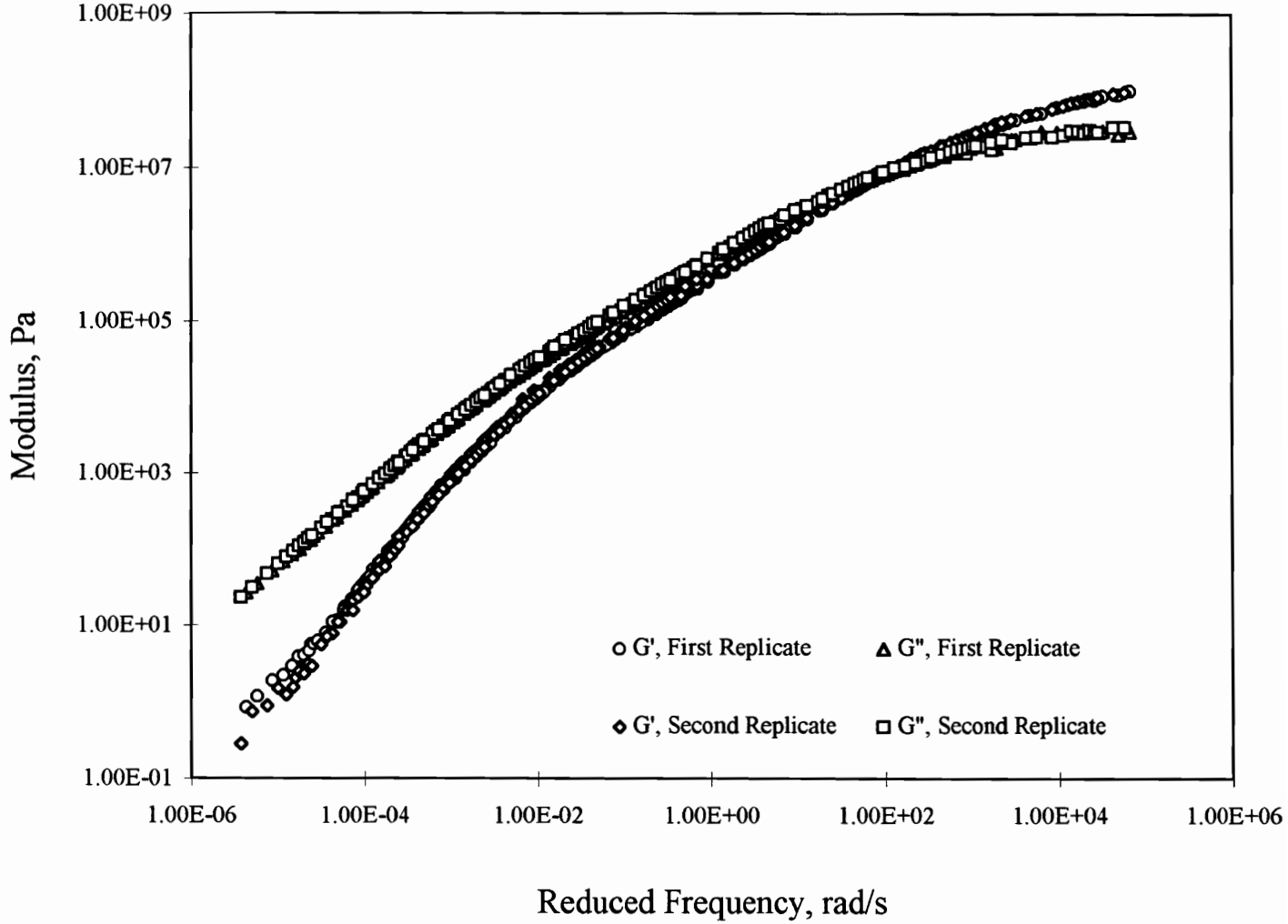

Figure a.34. Dynamic Master Curves for ARX3

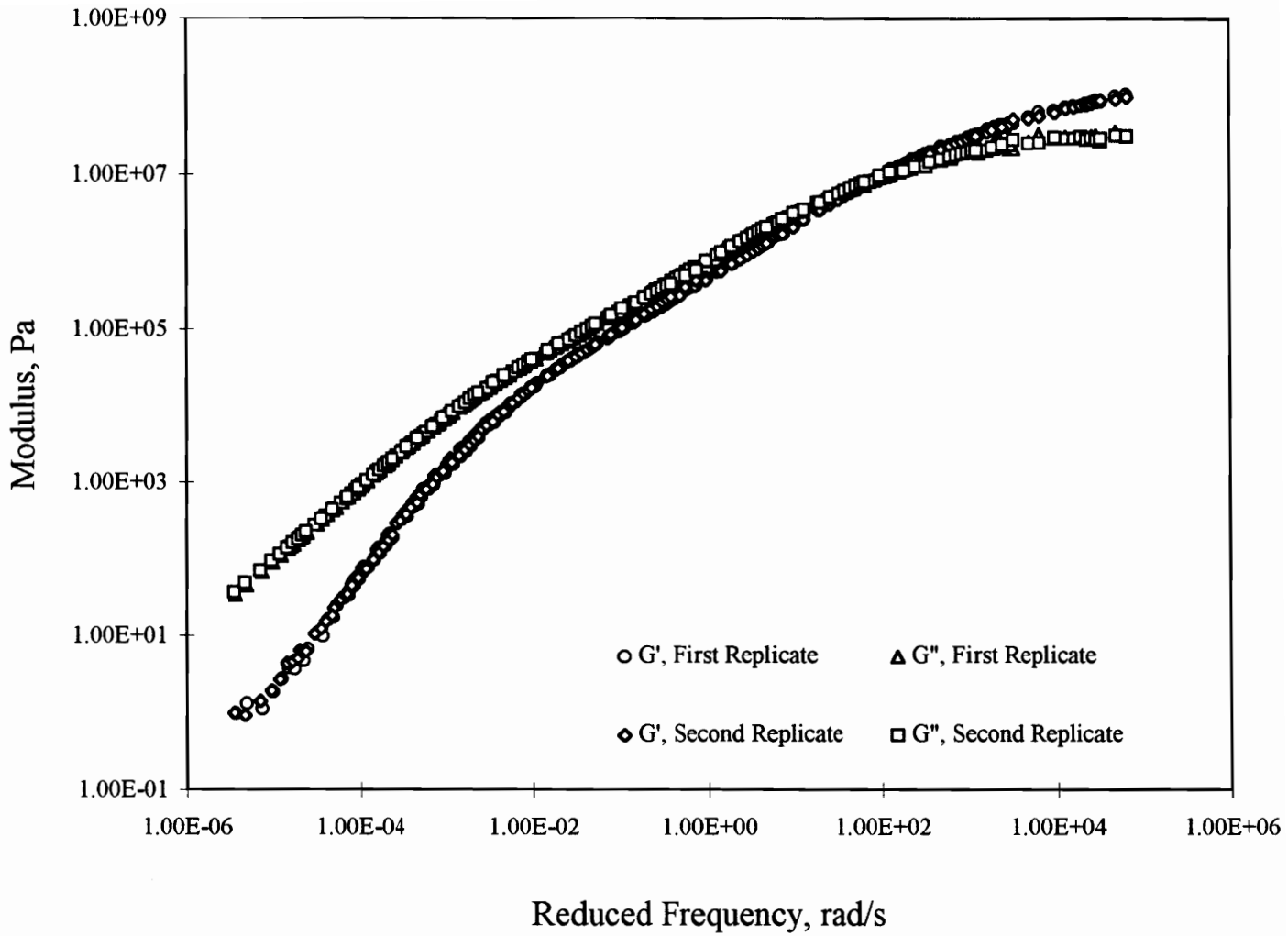

Figure a.35. Dynamic Master Curves for ARX4

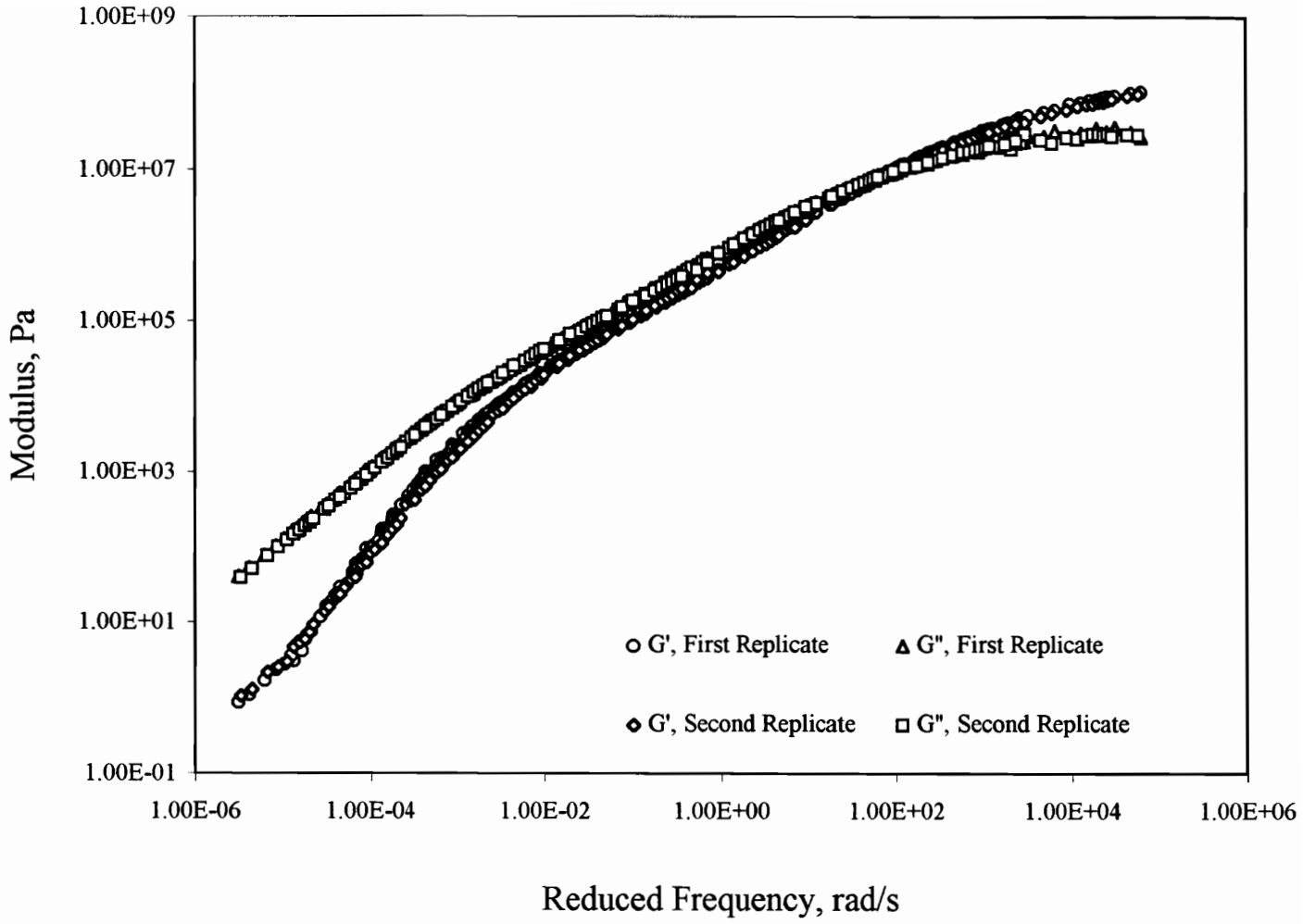

Figure a.36. Dynamic Master Curves for ARX5

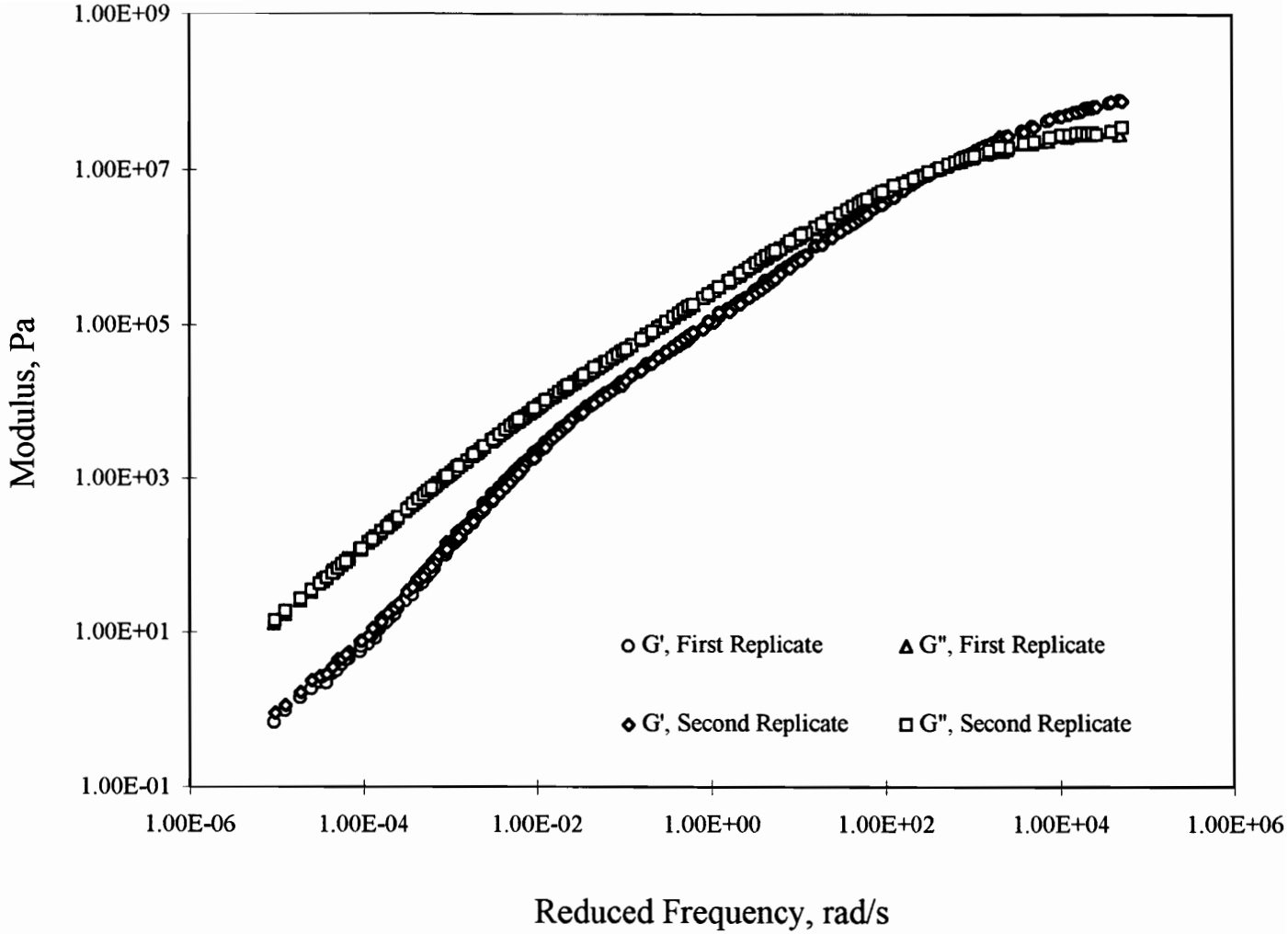

Figure a.37. Dynamic Master Curves for AUN3

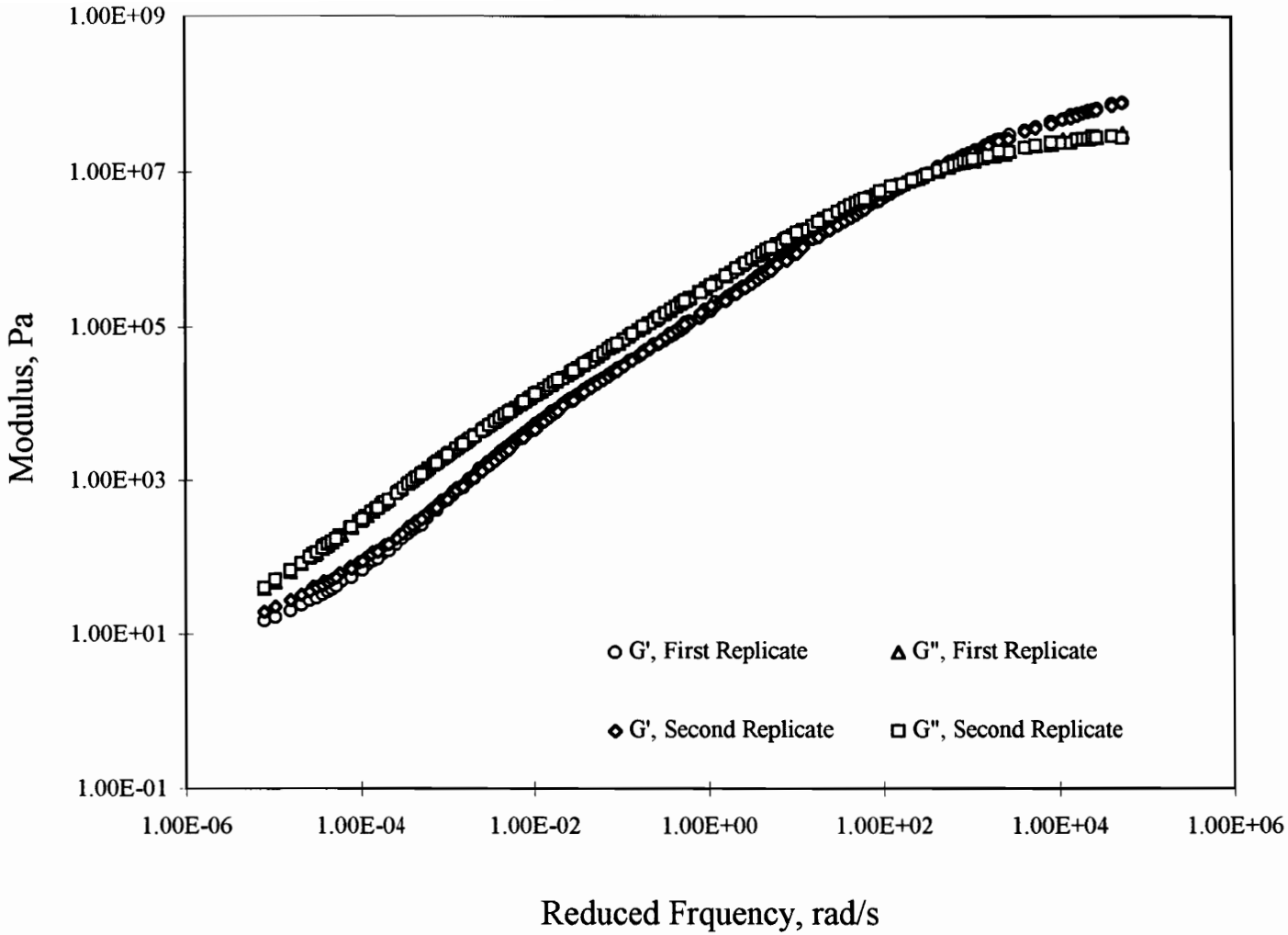

Figure a.38. Dynamic Master Curves for AUN4

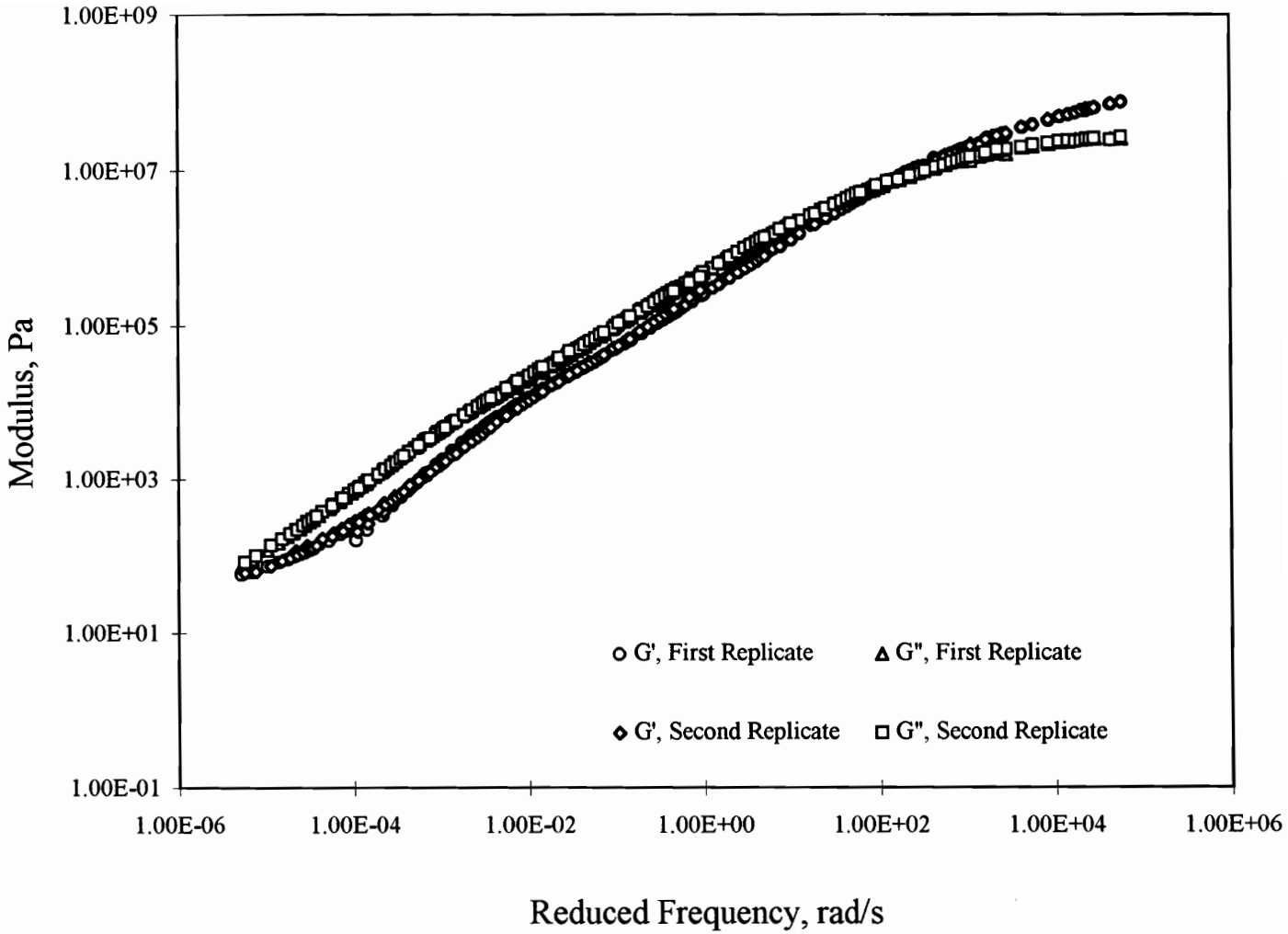

Figure a.39. Dynamic Master Curves for AUN5

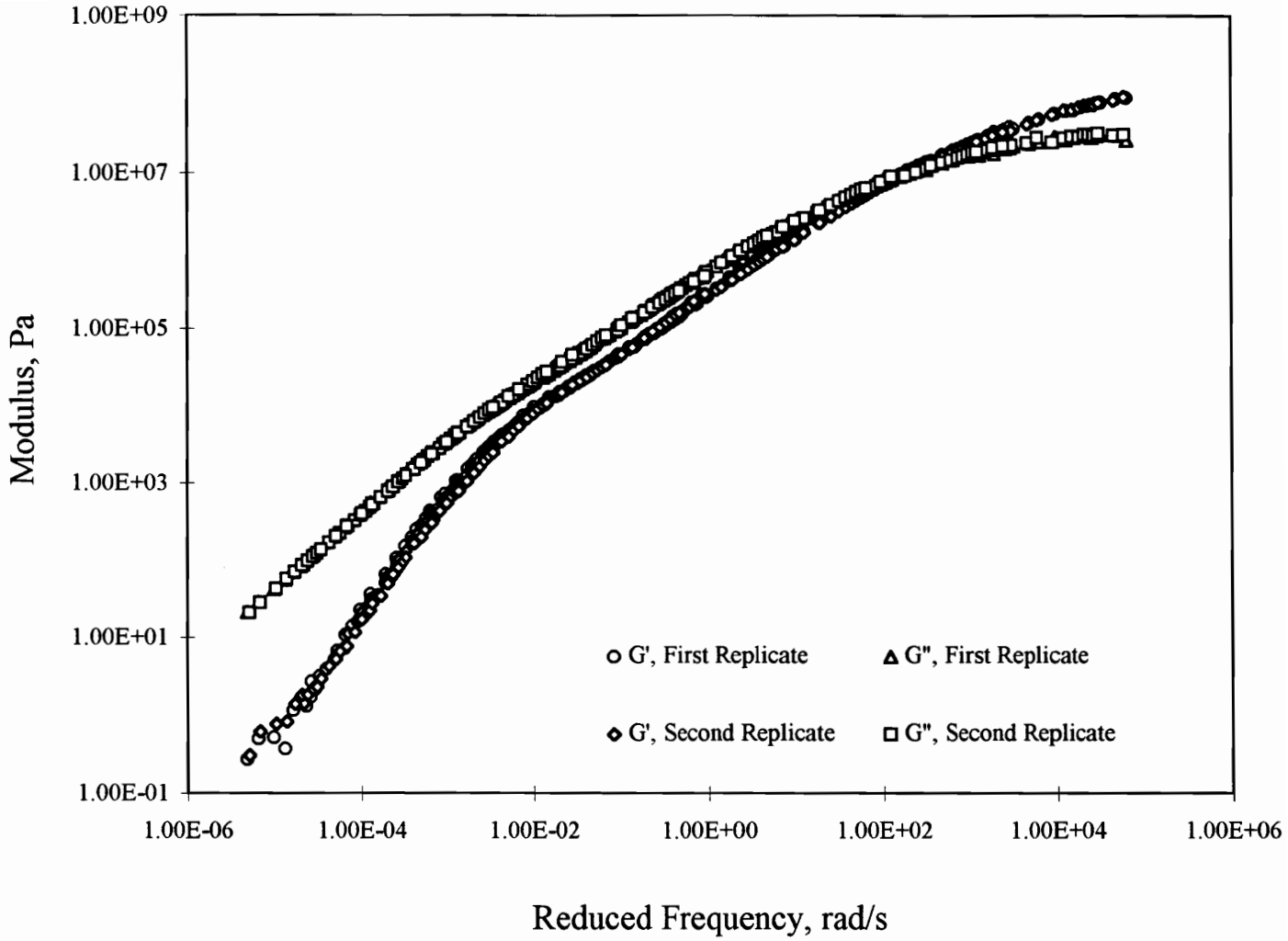

Figure a.40. Dynamic Master Curves for ARN3

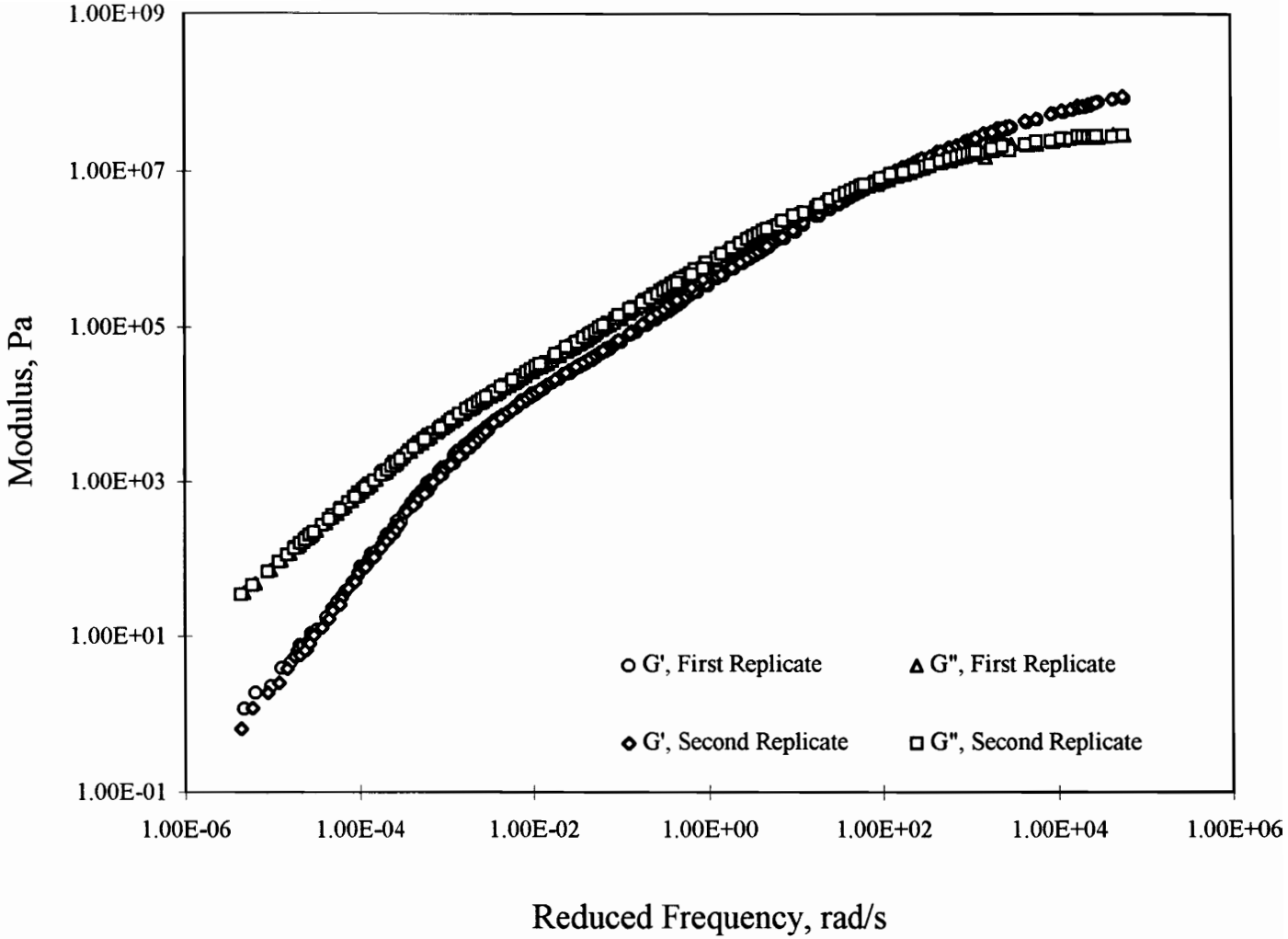

Figure a.41. Dynamic Master Curves for ARN4

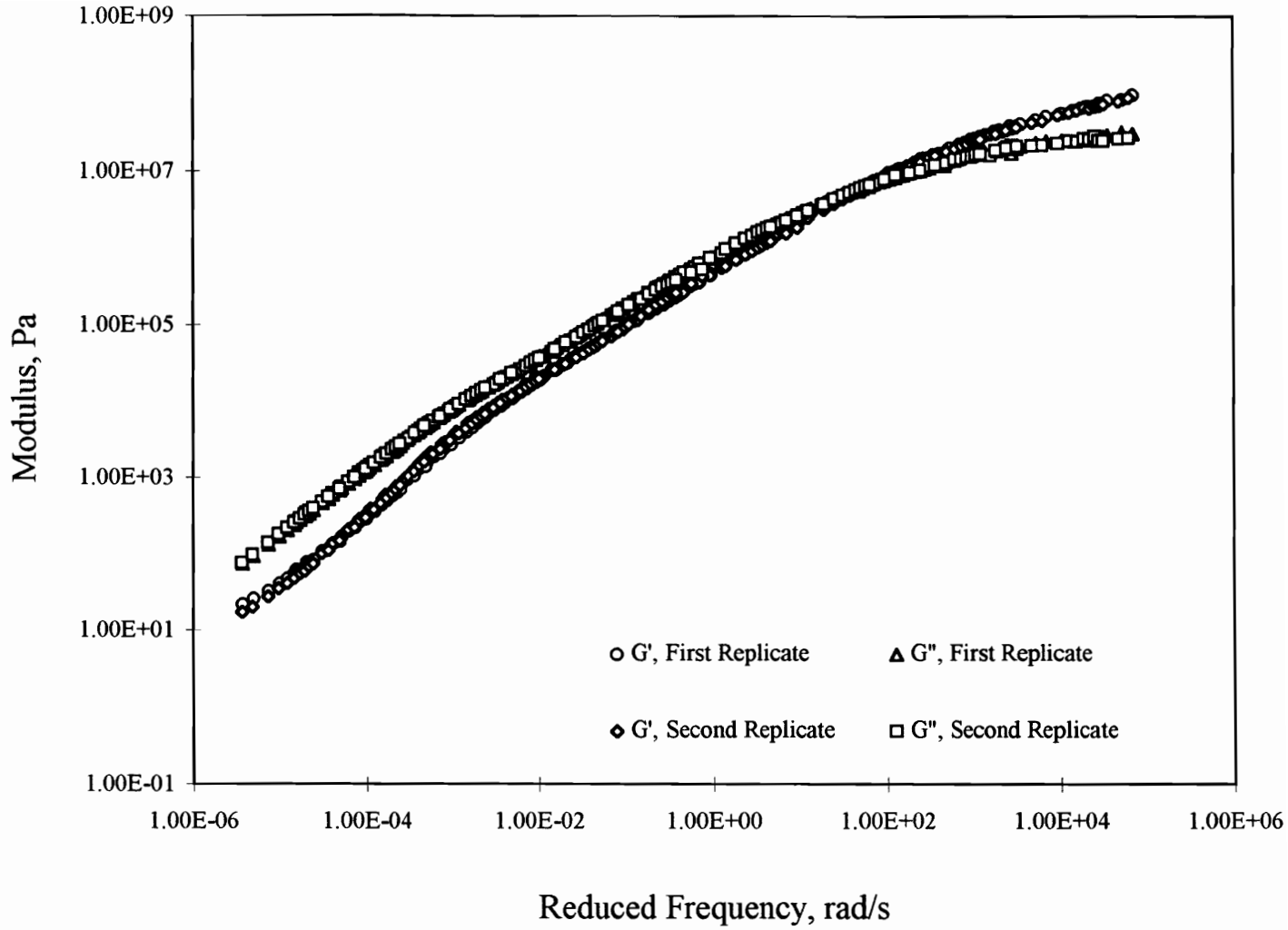

Figure a.42. Dynamic Master Curves for ARN5

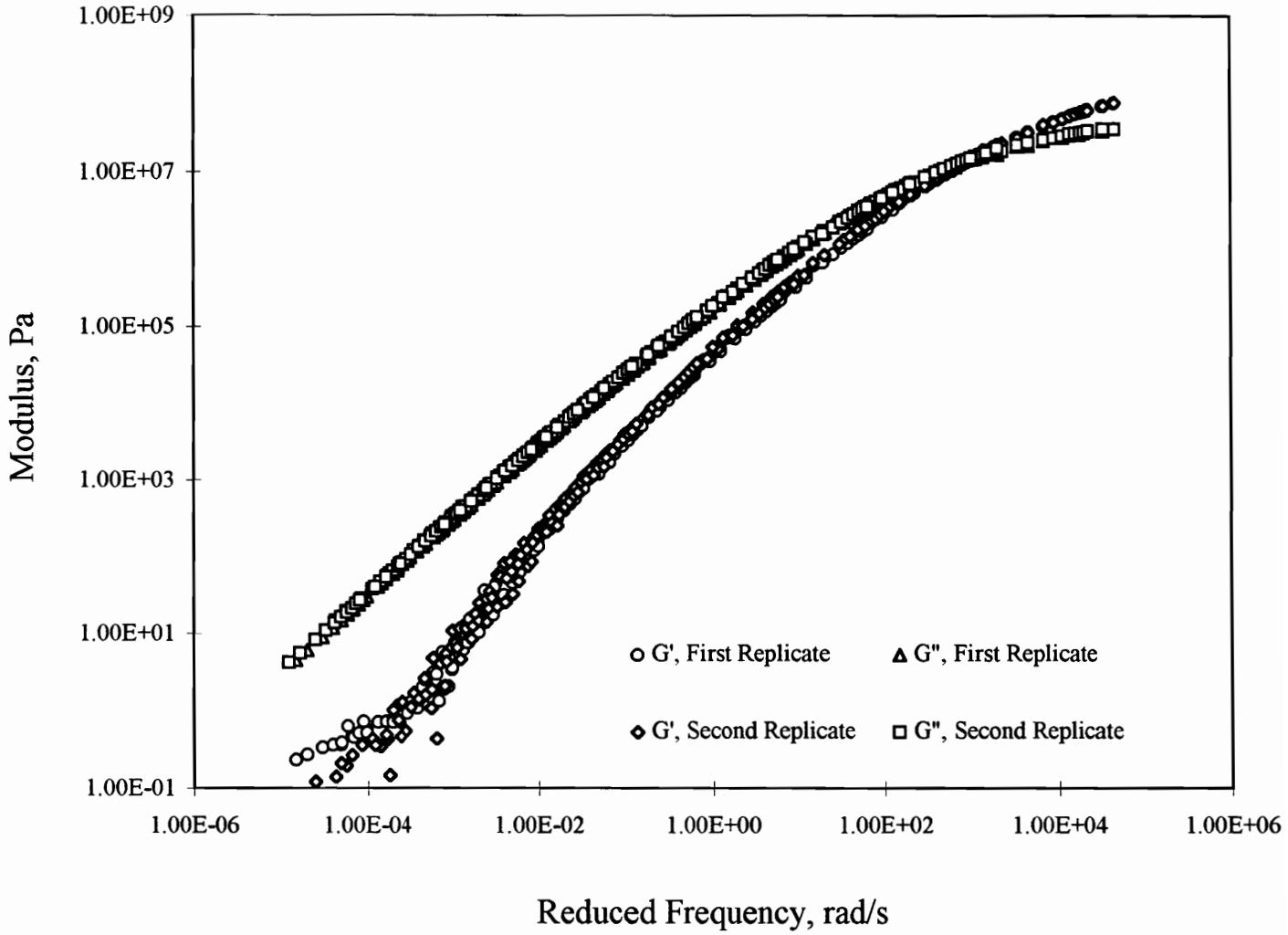

Figure a.43. Dynamic Master Curves for AU00

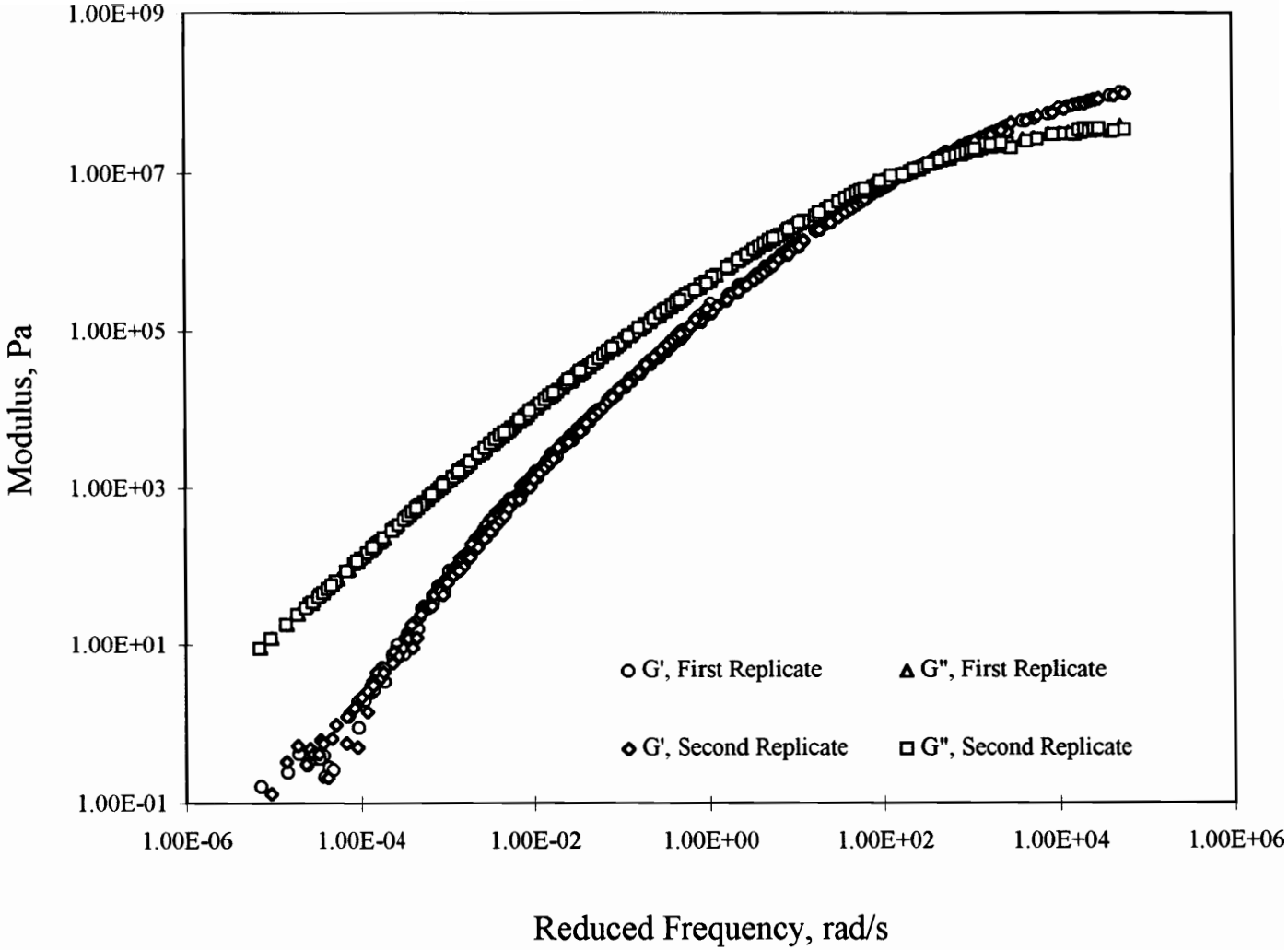

Figure a.44. Dynamic Master Curves for AR00

Appendix B

Shift Factors

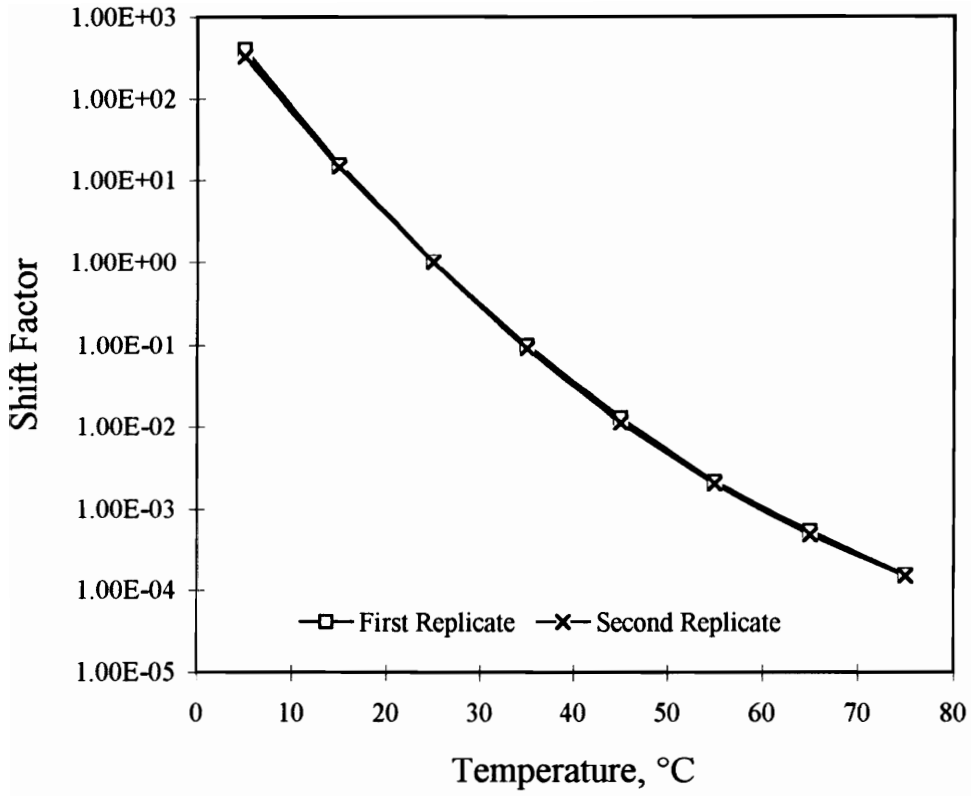

Figure b.1. Shift Factors for AUC2

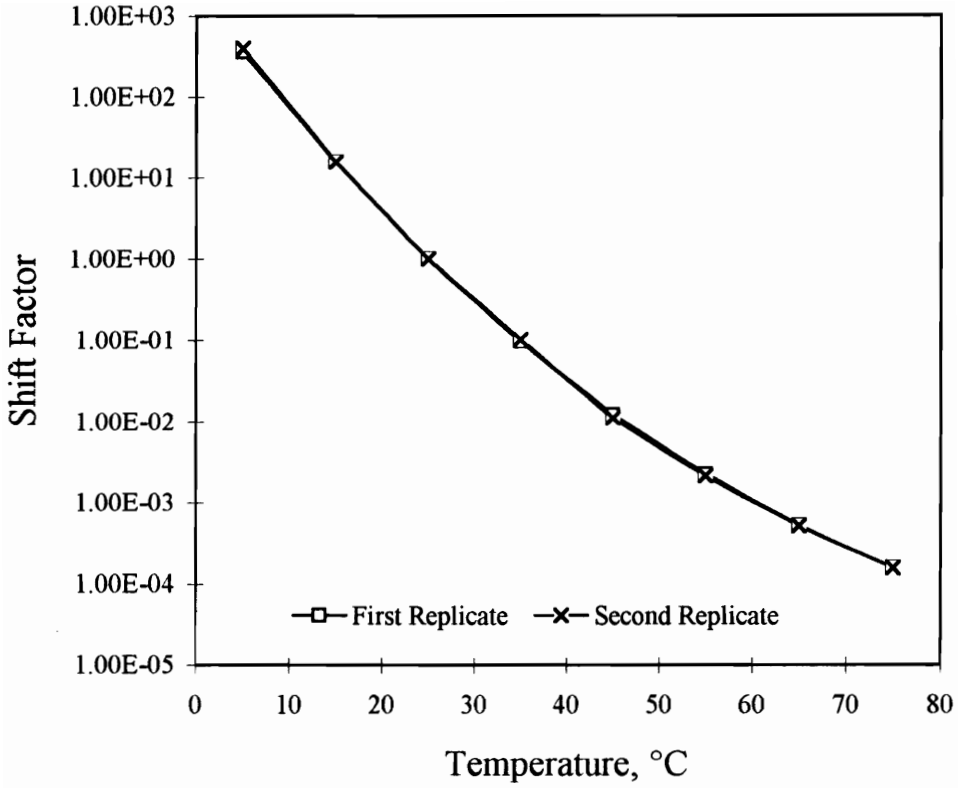

Figure b.2. Shift Factors for AUC3

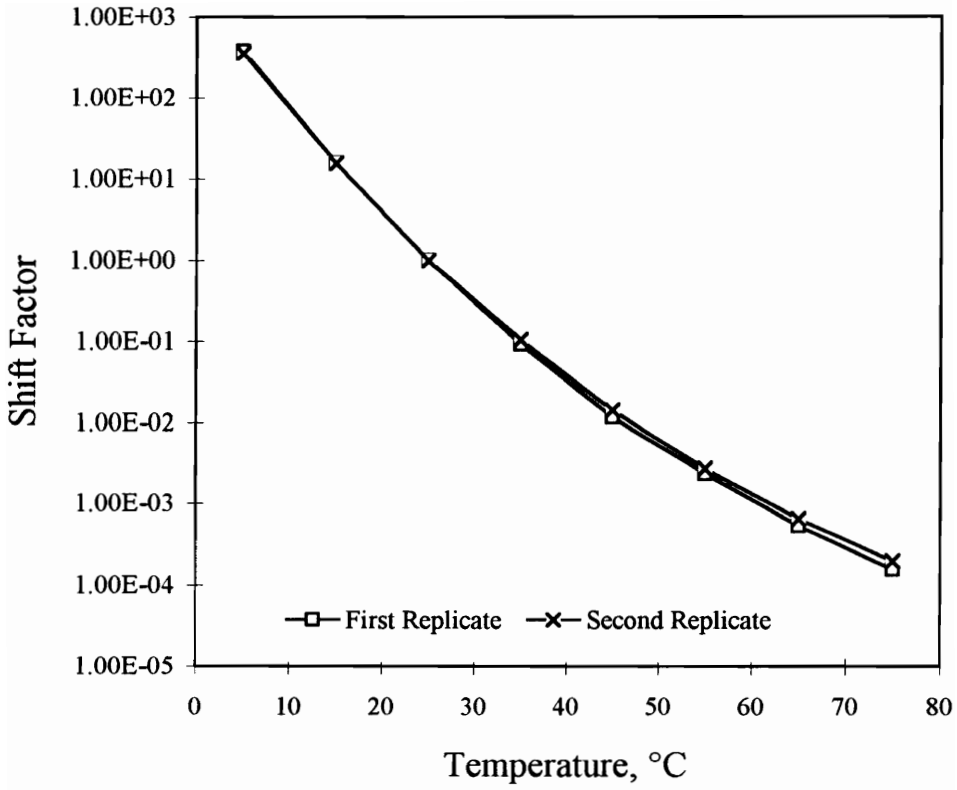

Figure b.3. Shift Factors for AUC4

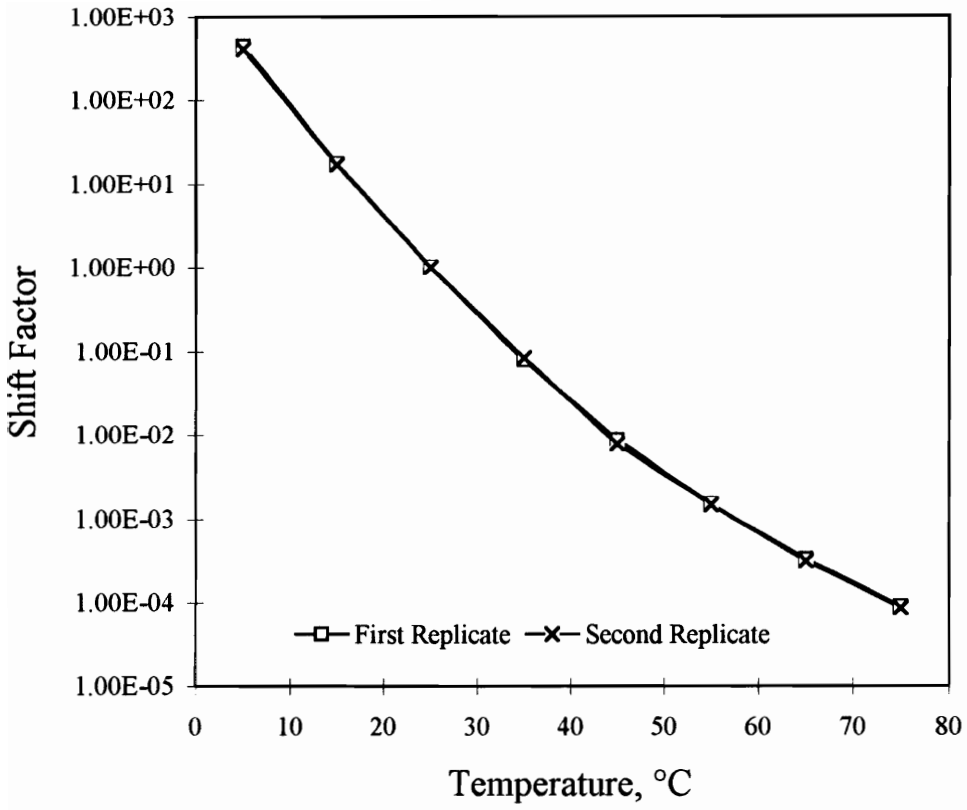

Figure b.4. Shifta Factors for ARC2

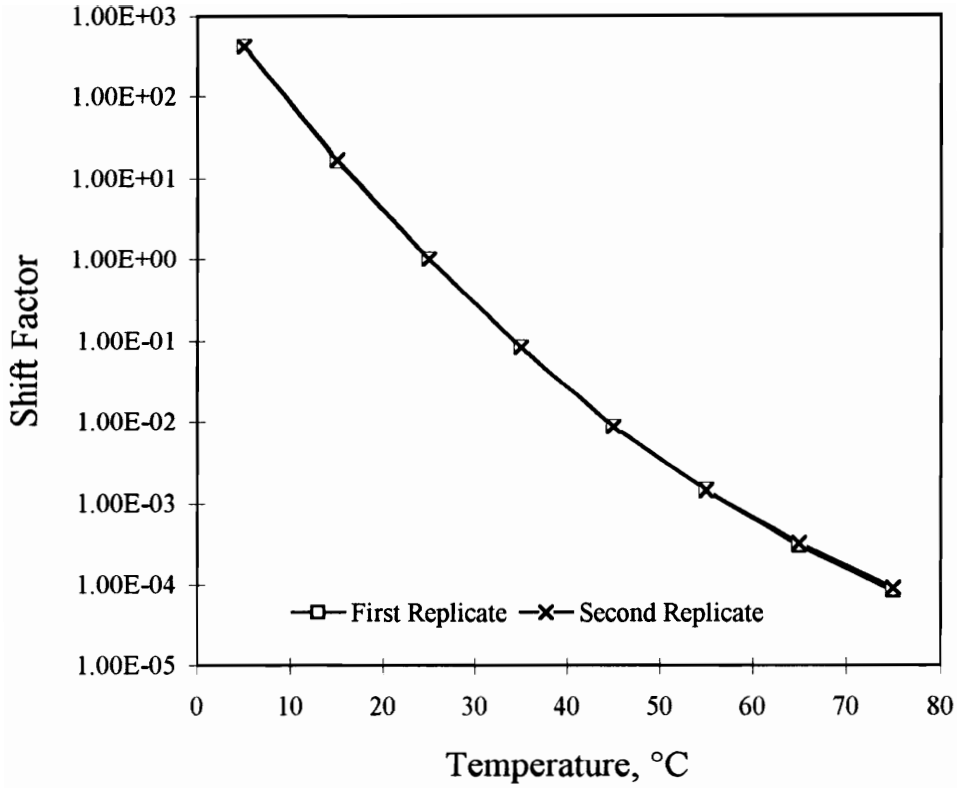

Figure b.5. Shift Factors for ARC3

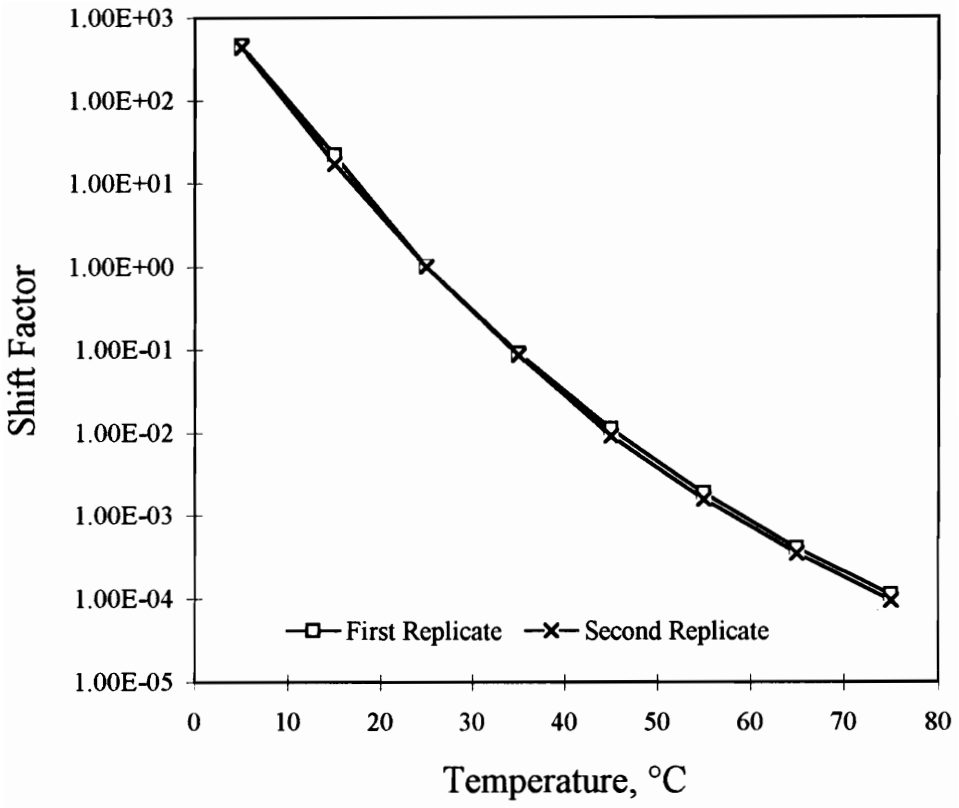

Figure b.6. Shift Factors for ARC4

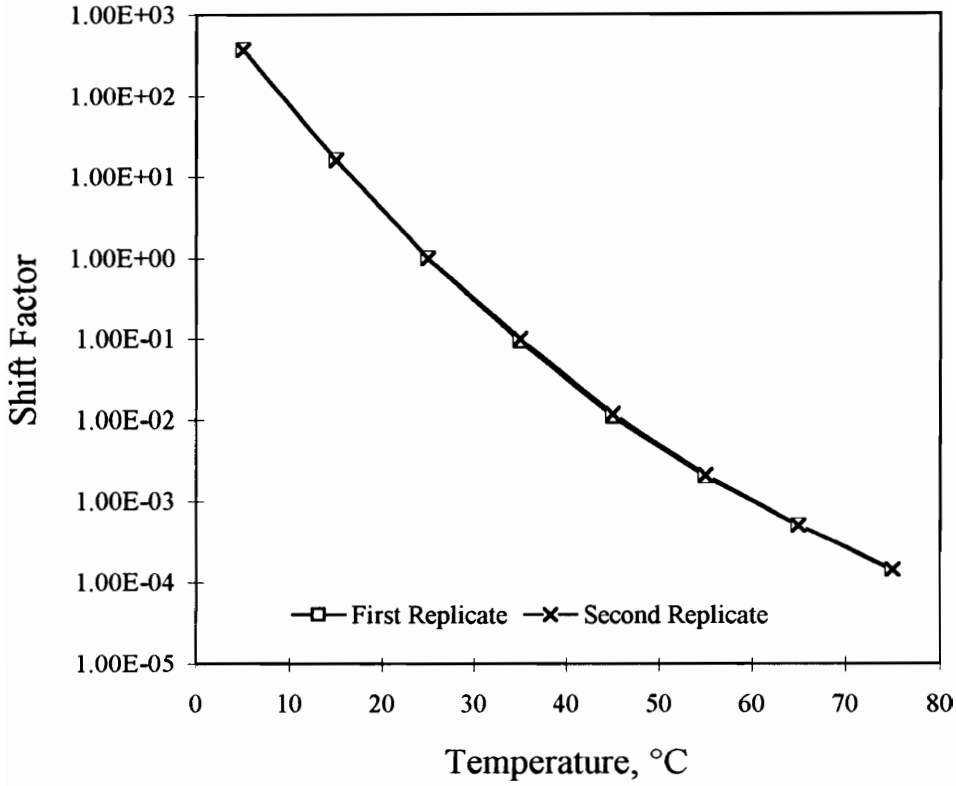

Figure b.7. Shift Factors for AUP3

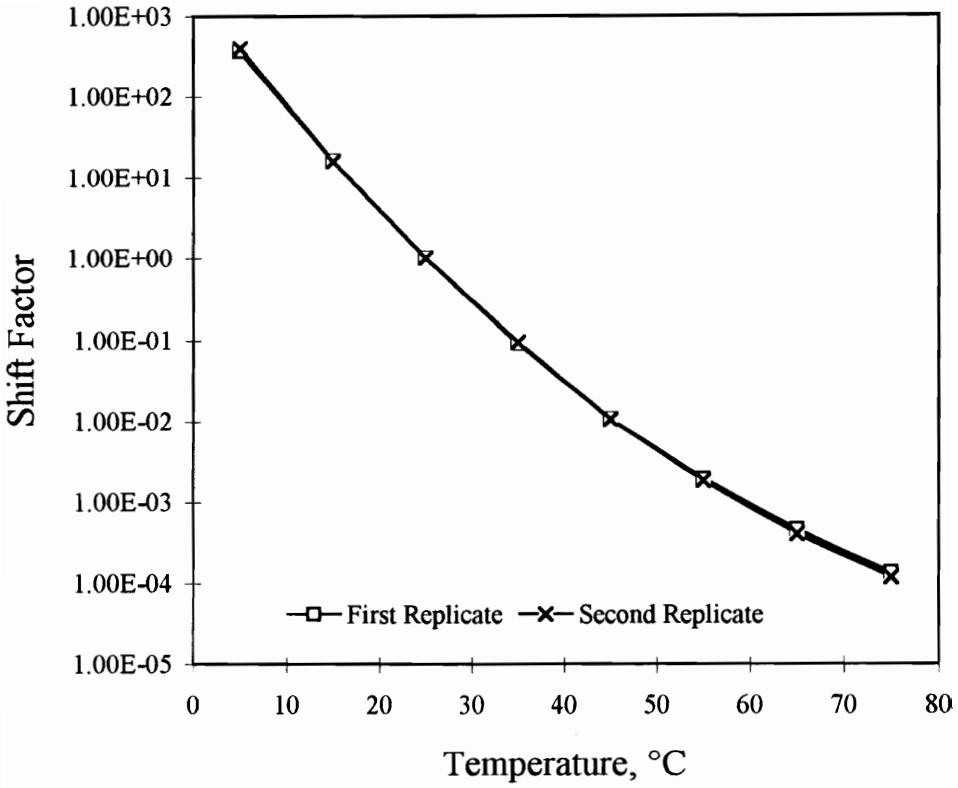

Figure b.8. Shift Factors for AUP4

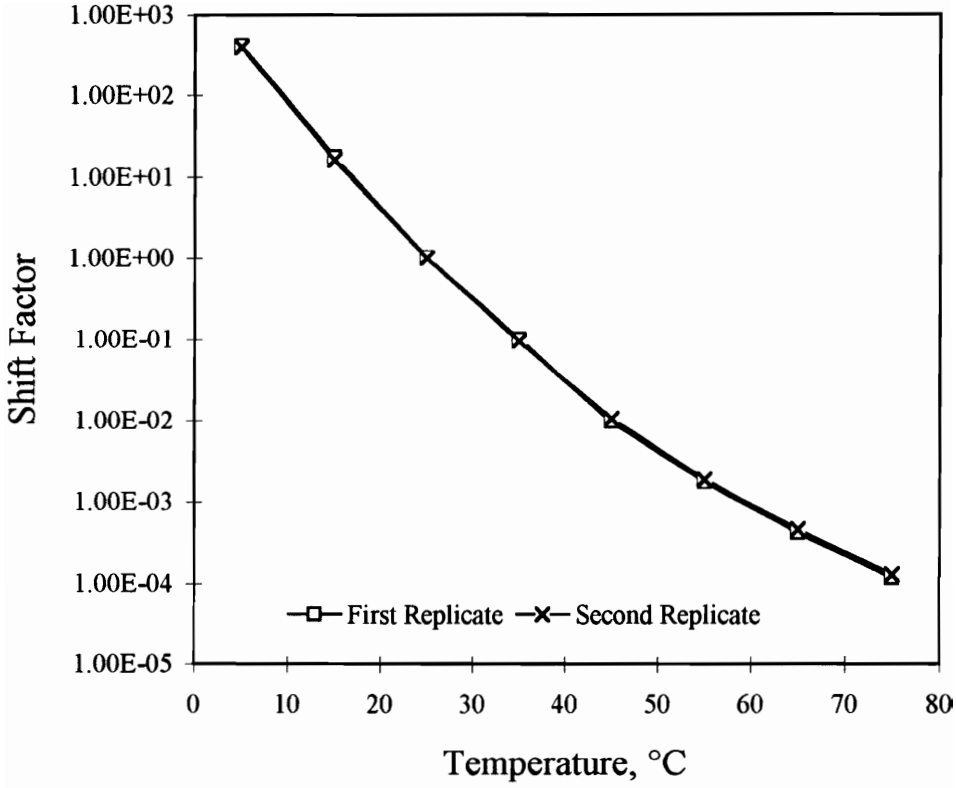

Figure b.9. Shift Factors for AUP5

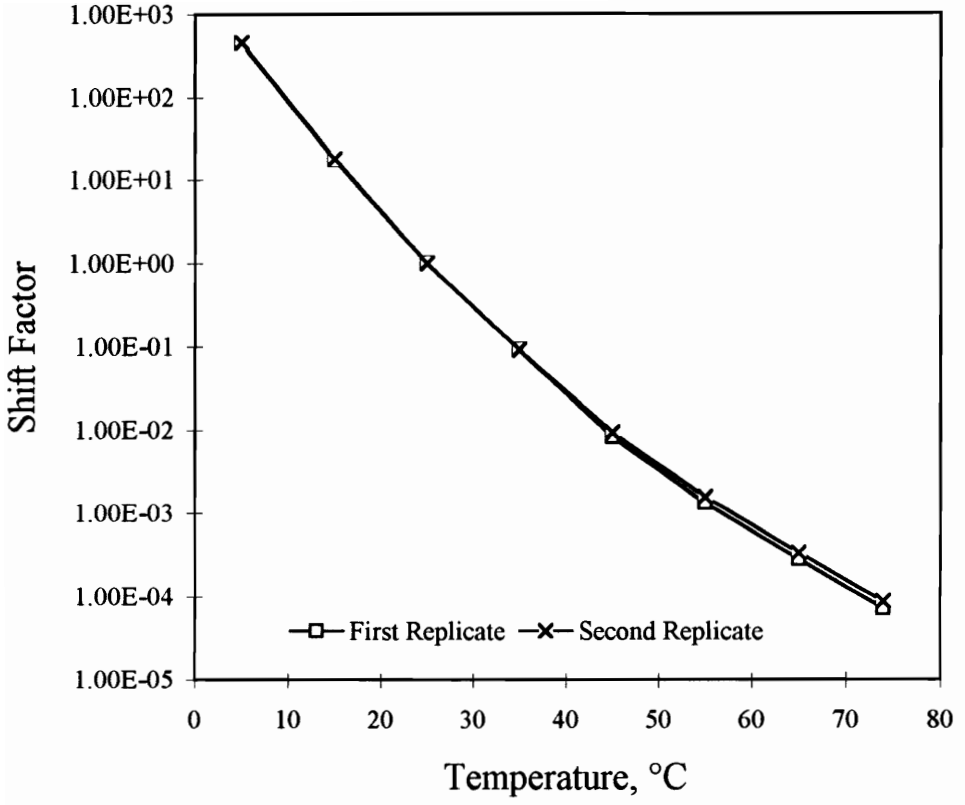

Figure b.10. Shift Factors for ARP3

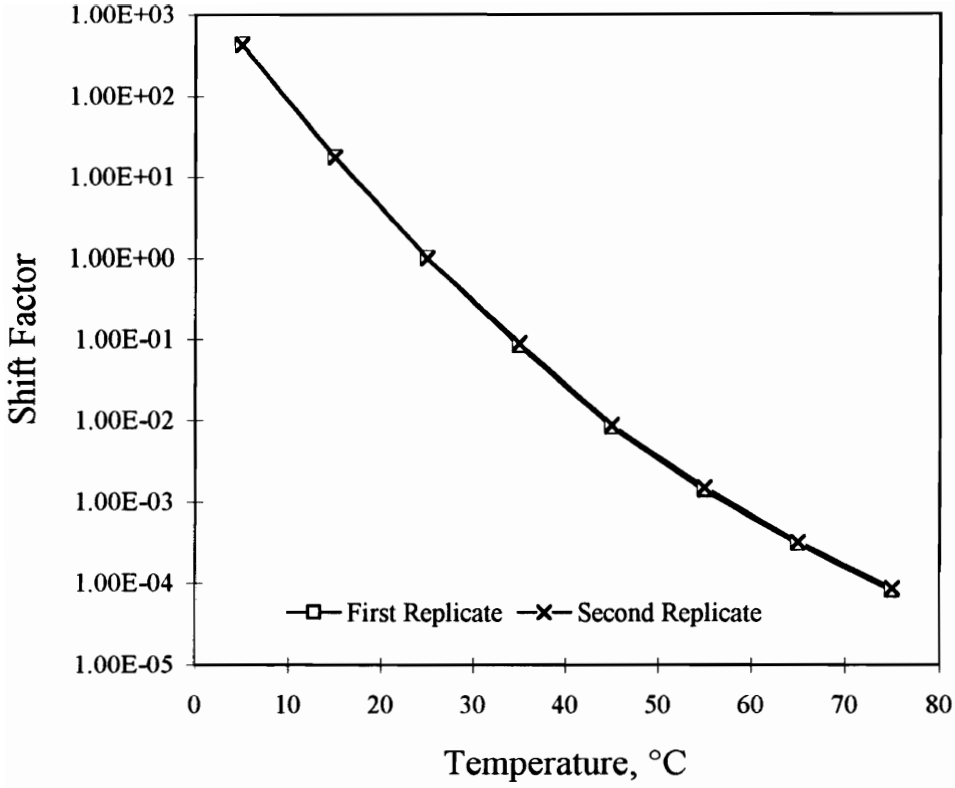

Figure b.11. Shift Factors for ARP4

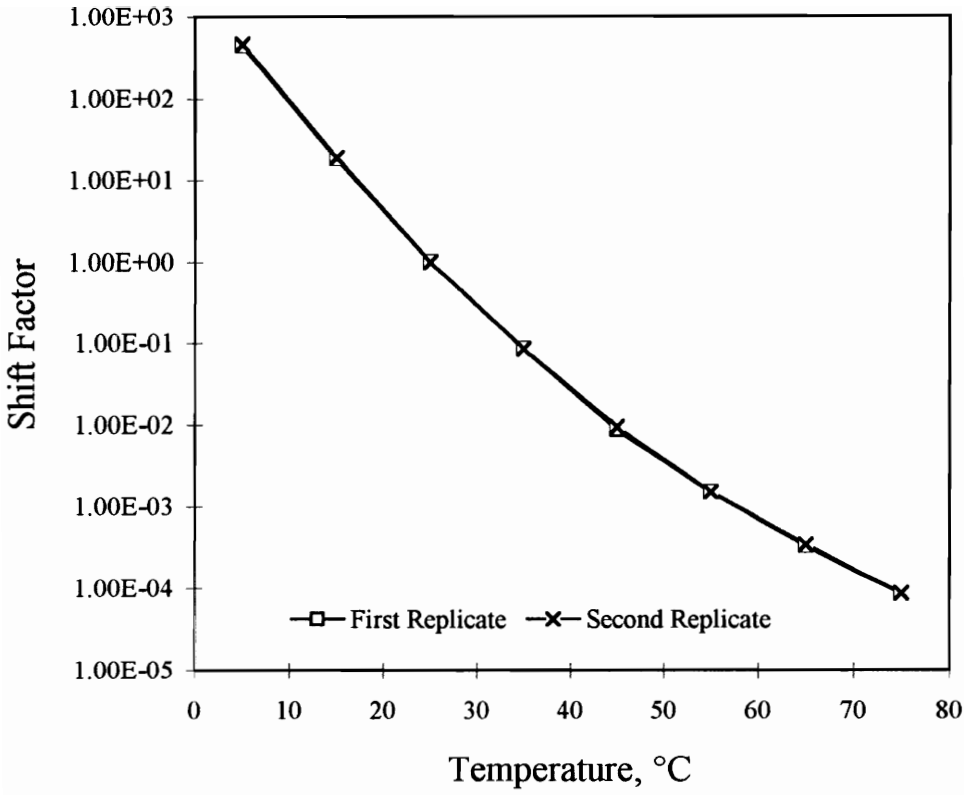

Figure b.12. Shift Factors for ARP5

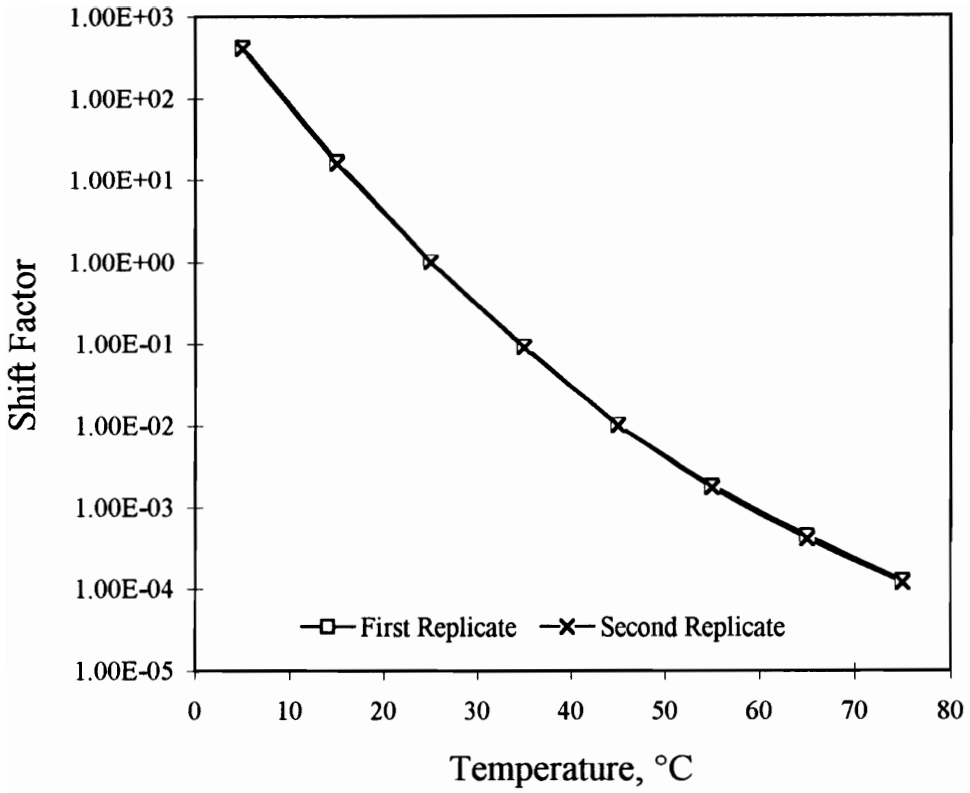

Figure b.13. Shift Factors for AUD3

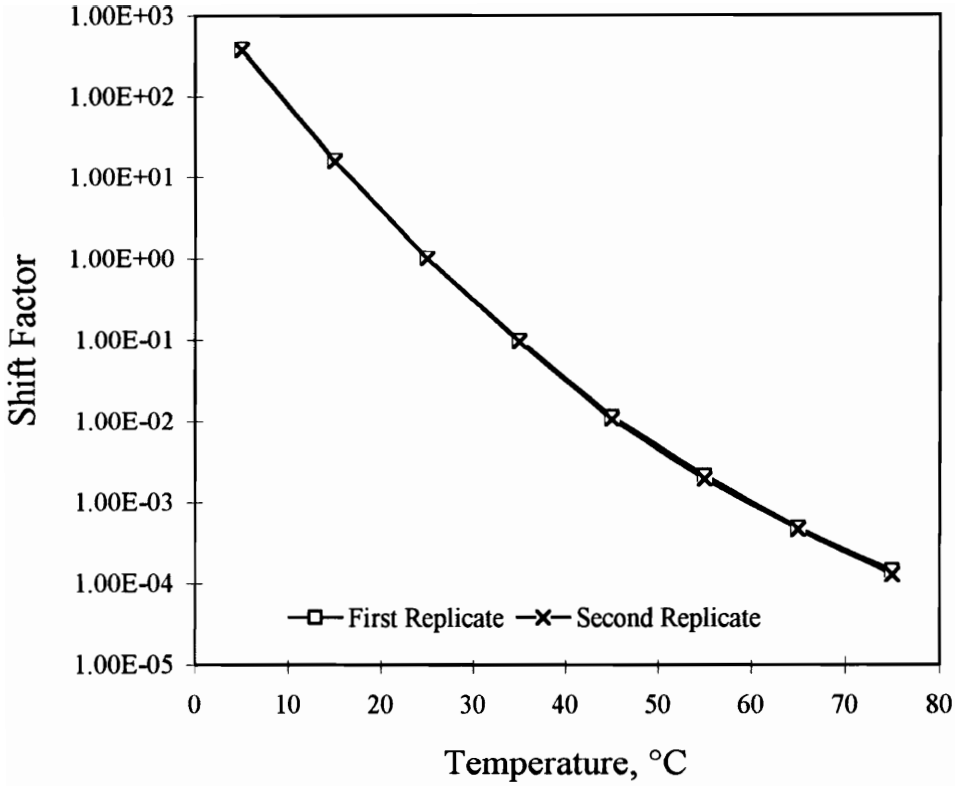

Figure b.14. Shift Factors for AUD4

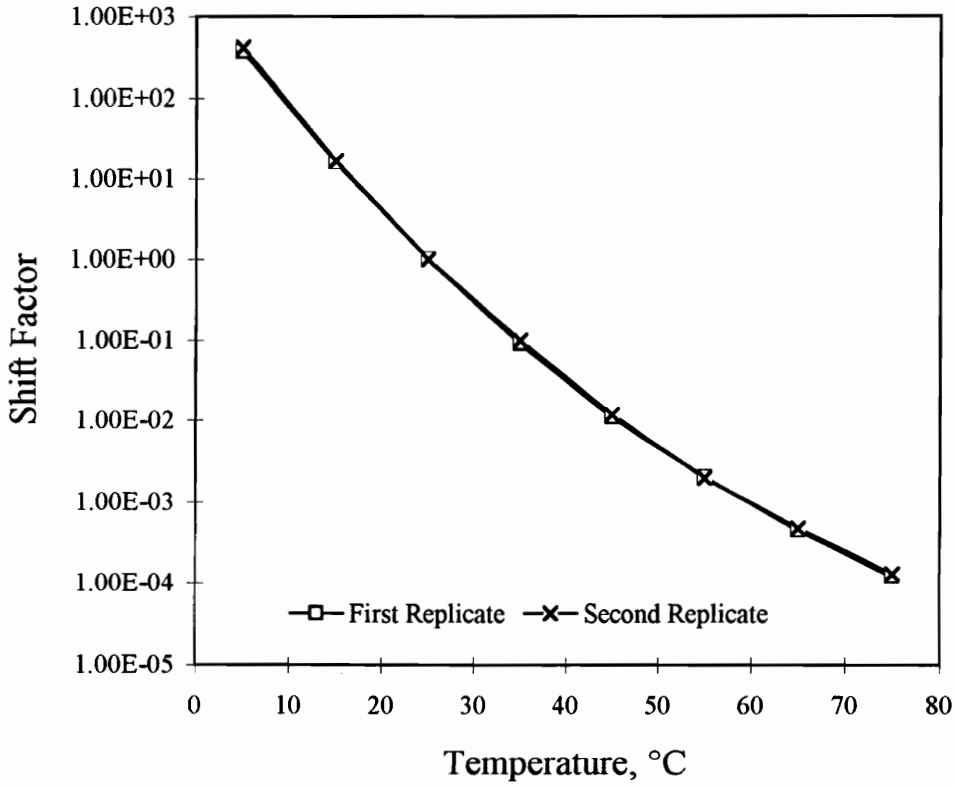

Figure b.15. Shift Factors for AUD5

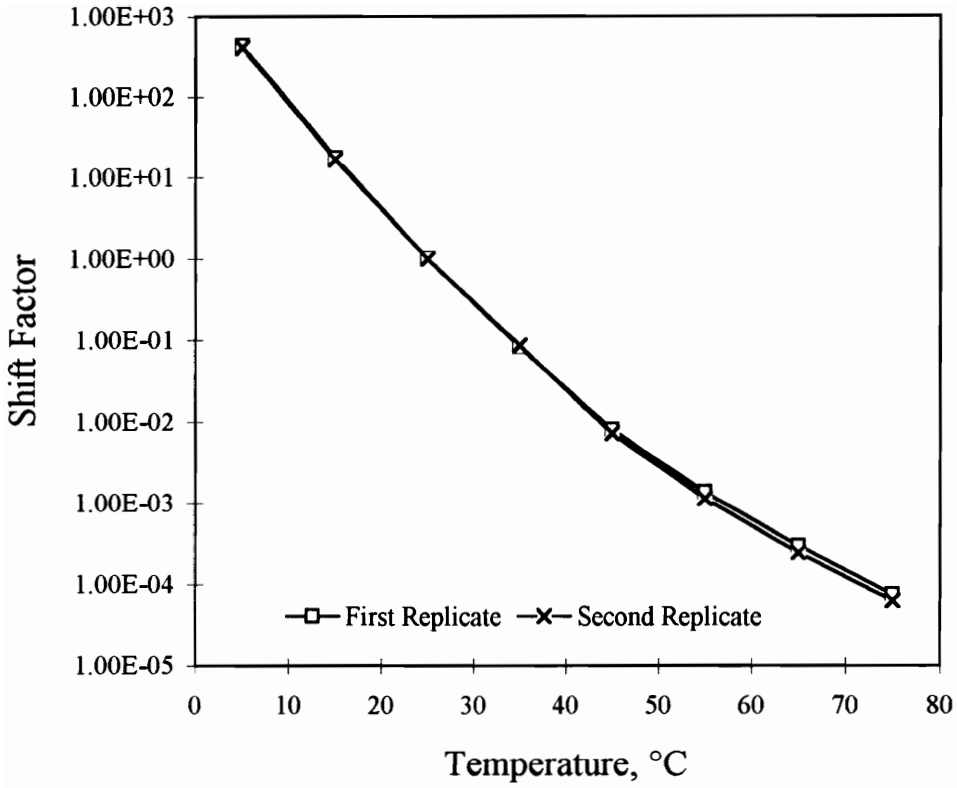

Figure b.16. Shift Factors for ARD3

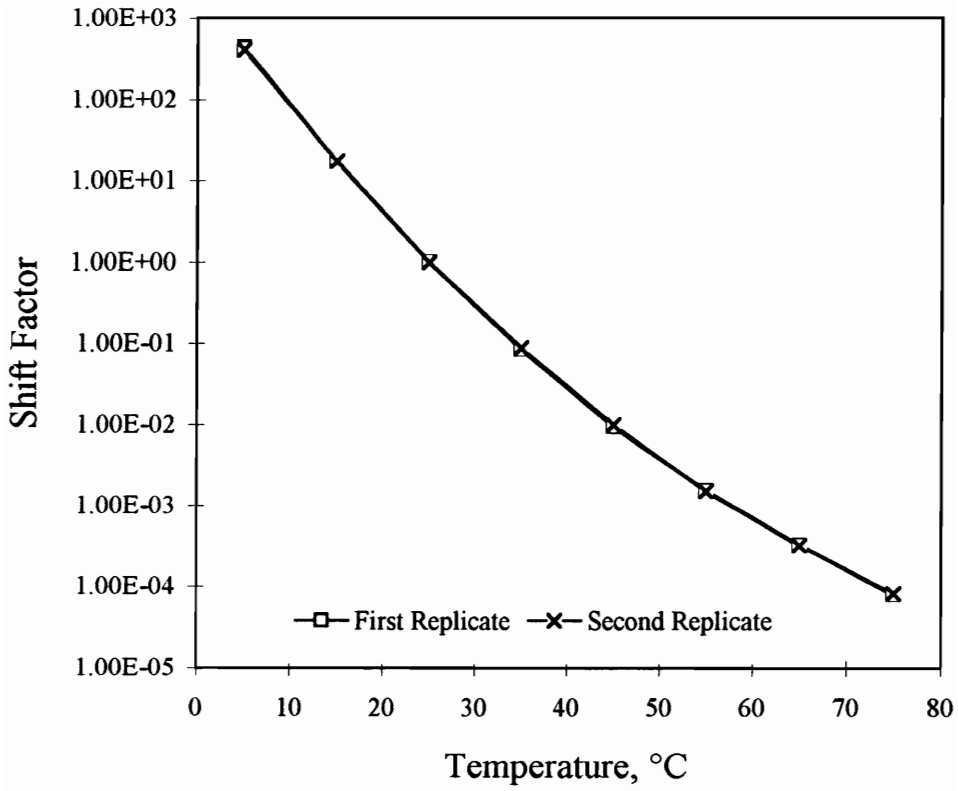

Figure b.17. Shift Factors for ARD4

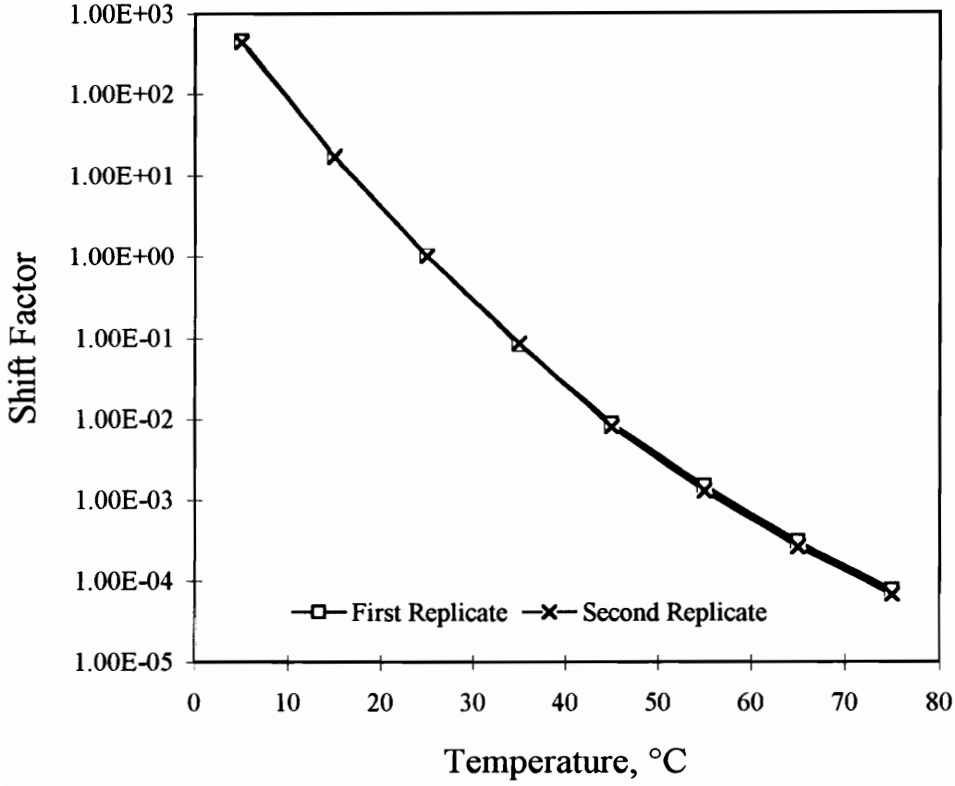

Figure b.18. Shift Factors for ARD5

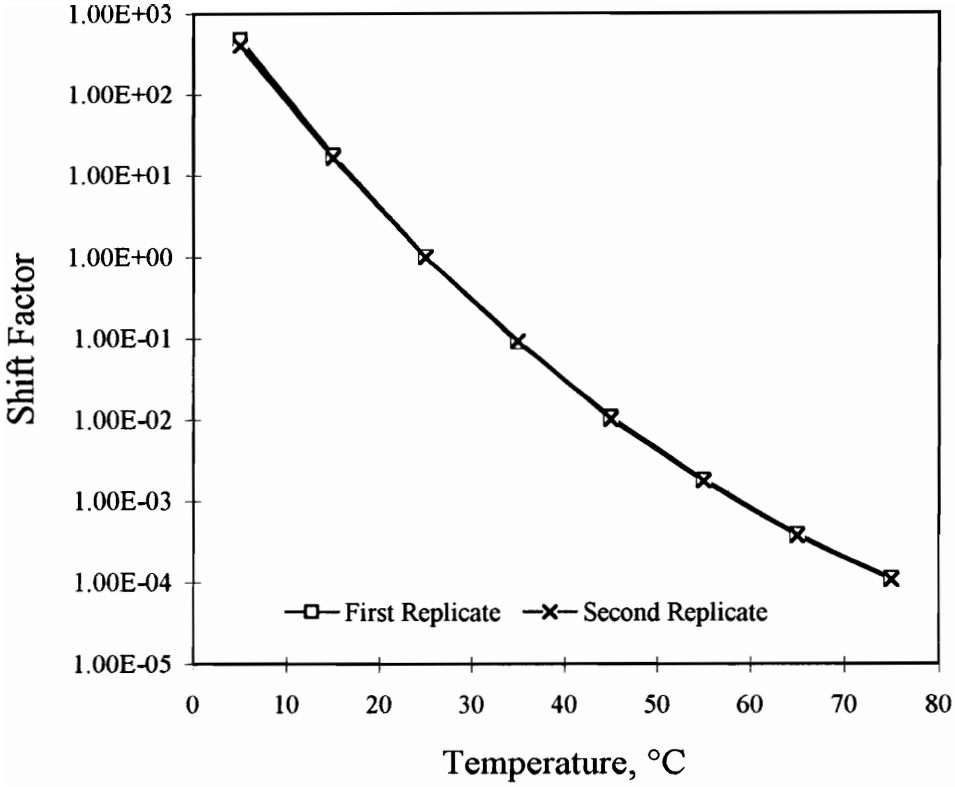

Figure b.19. Shift Factors for AUS3

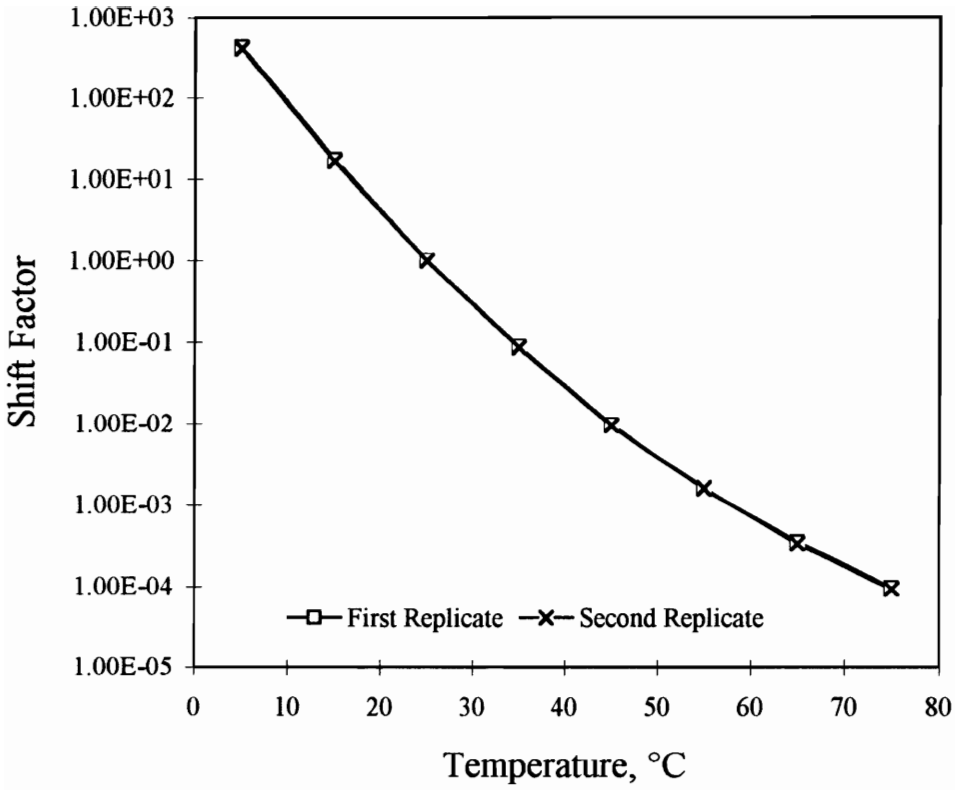

Figure b.20. Shift Factors for AUS4

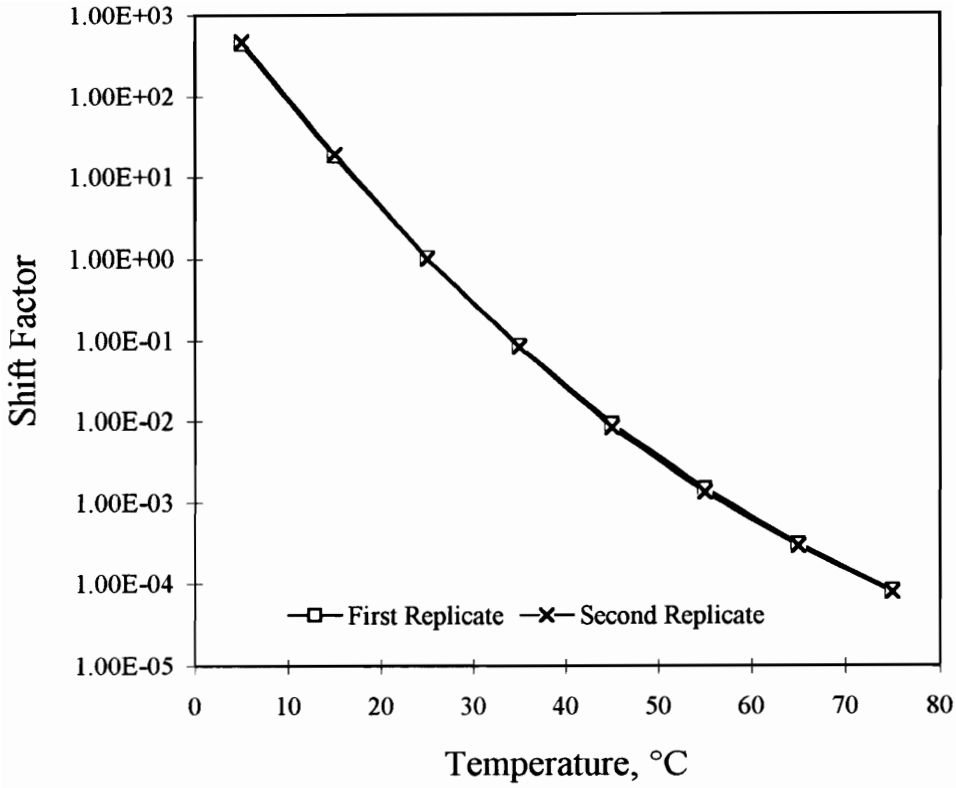

Figure b.21. Shift Factors for AUS5

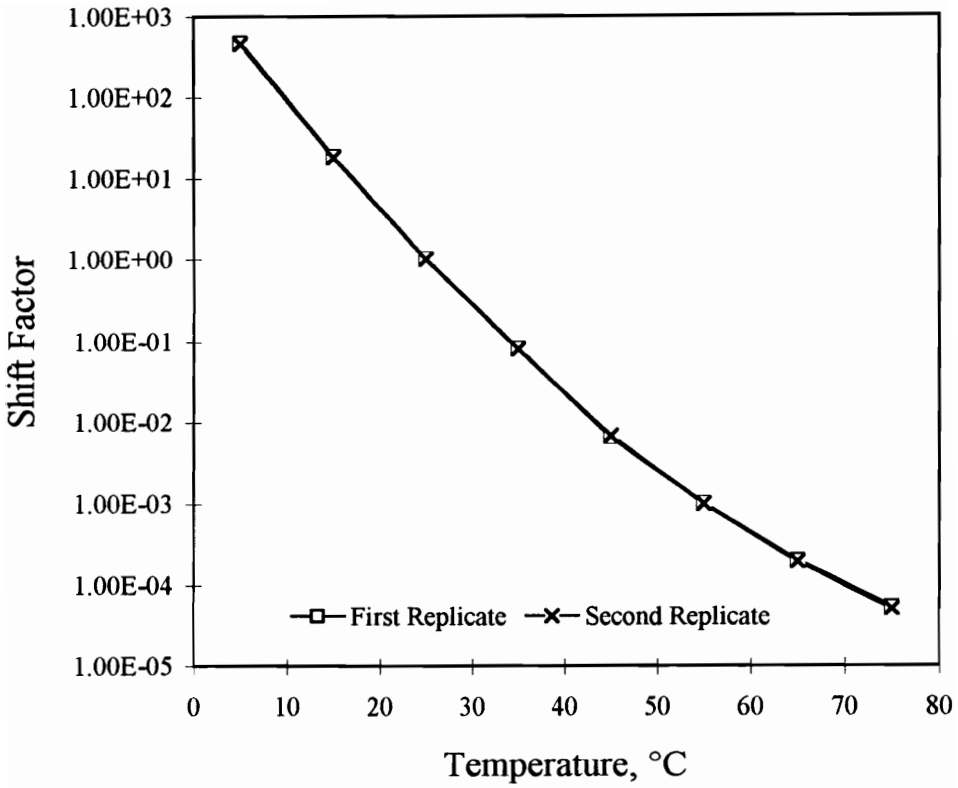

Figure b.22. Shift Factors for ARS3

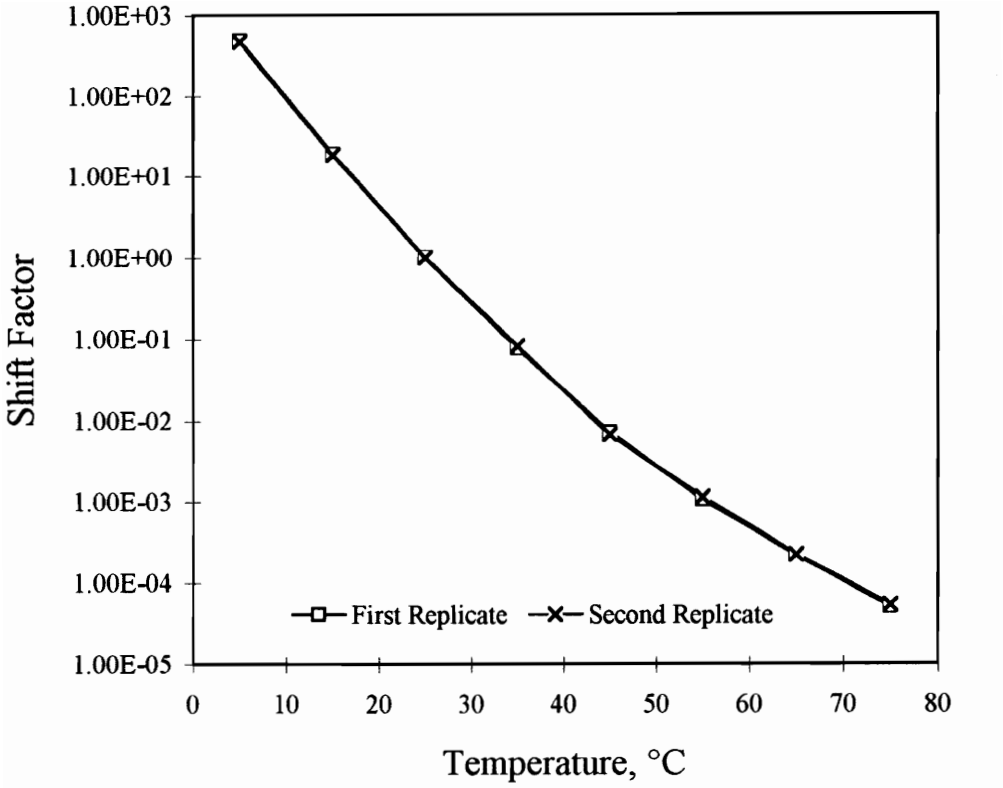

Figure b.23. Shift Factors for ARS4

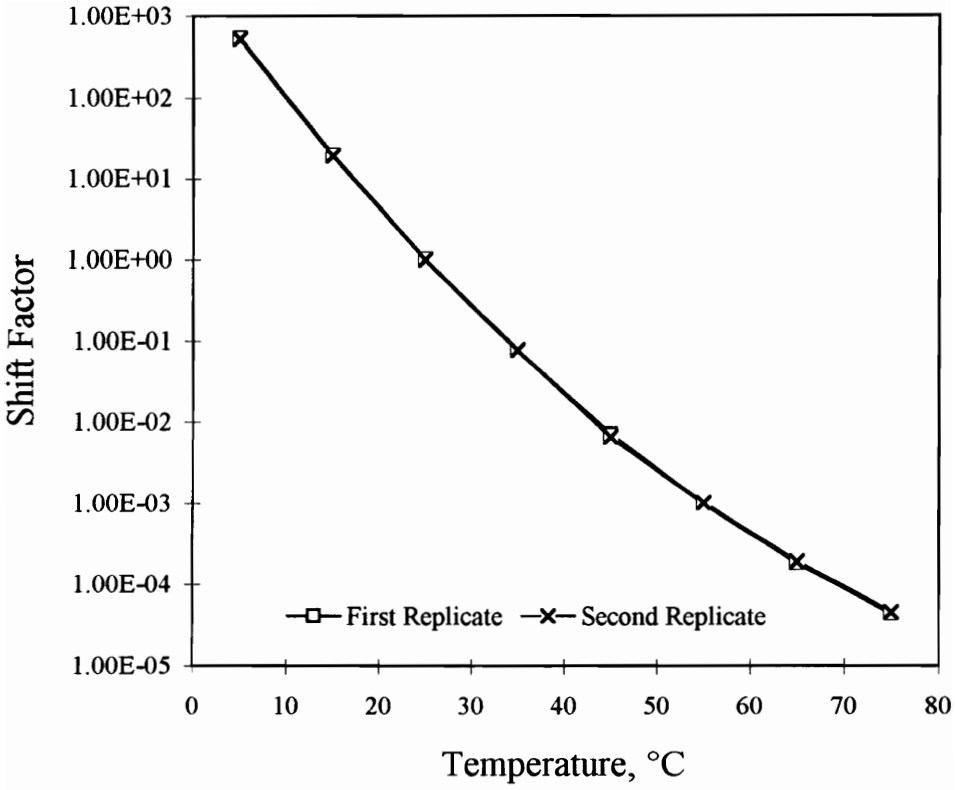

Figure b.24. Shift Factors for ARS5

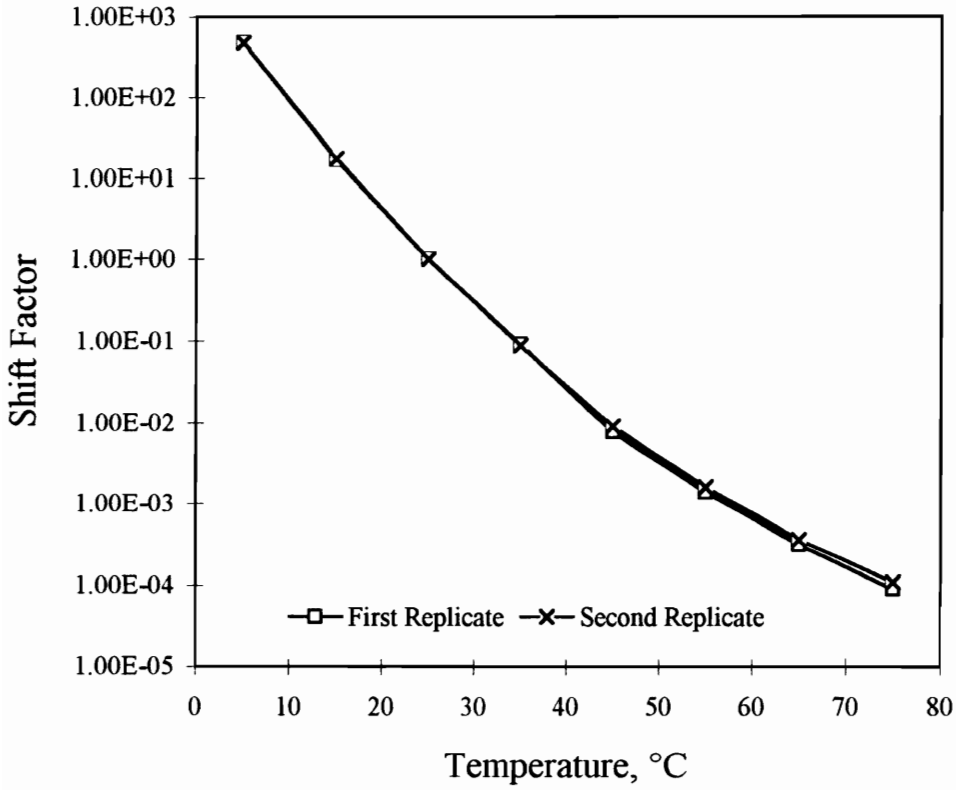

Figure b.25. Shift Factors for AUG3

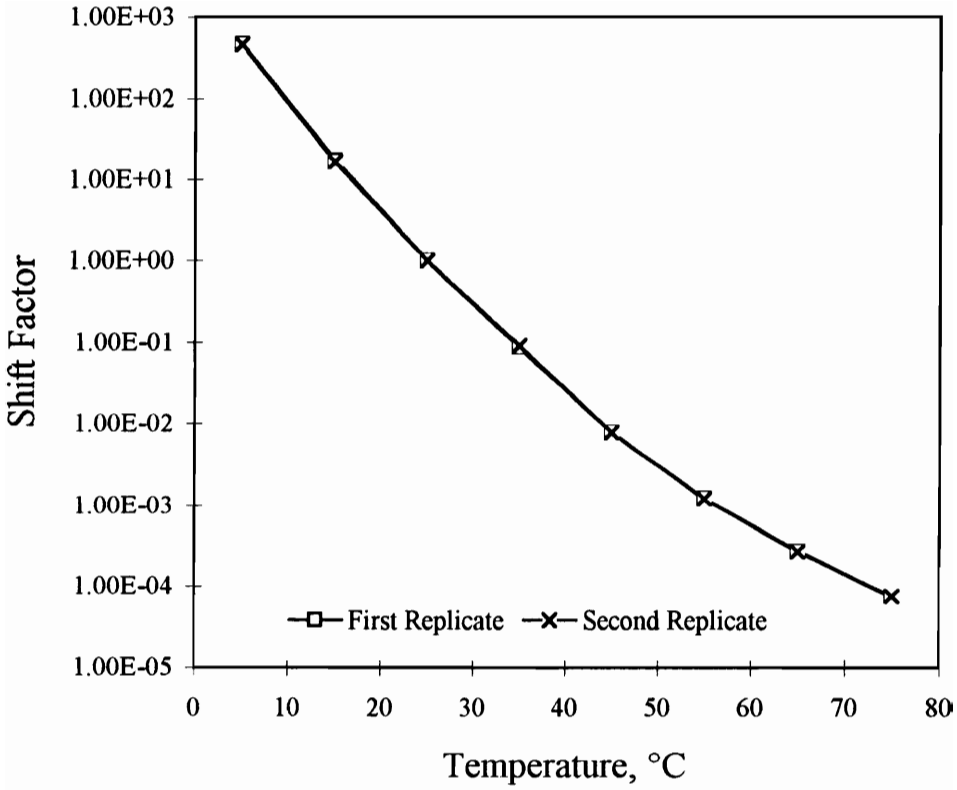

Figure b.26. Shift Factors for AUG4

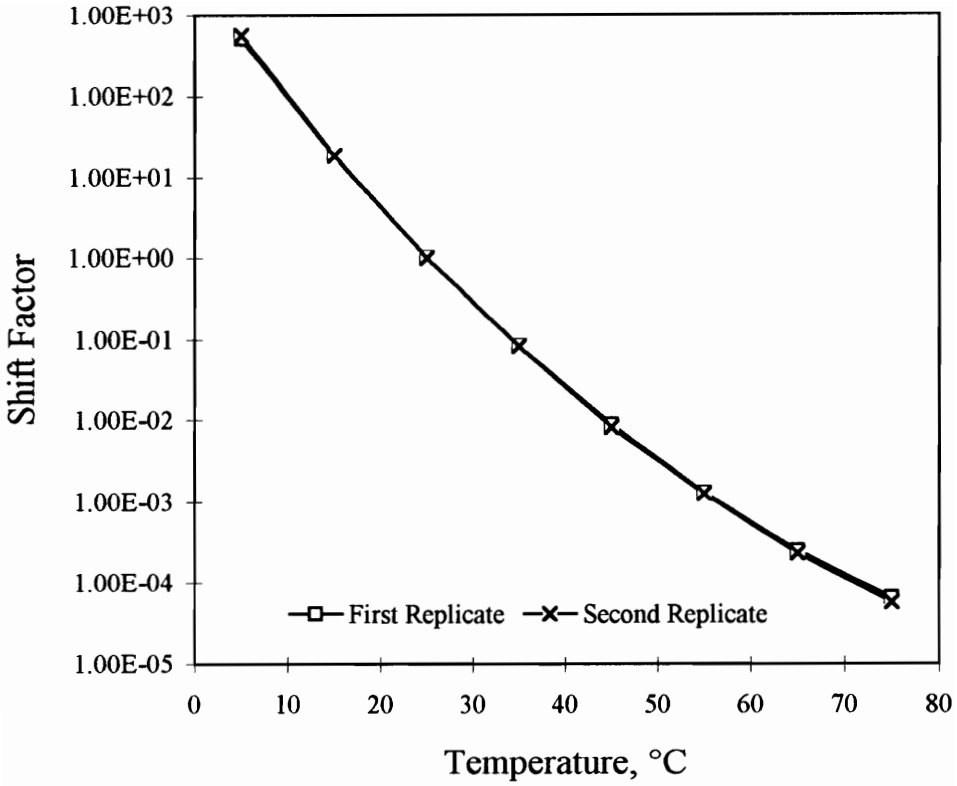

Figure b.27. Shift Factors for AUG5

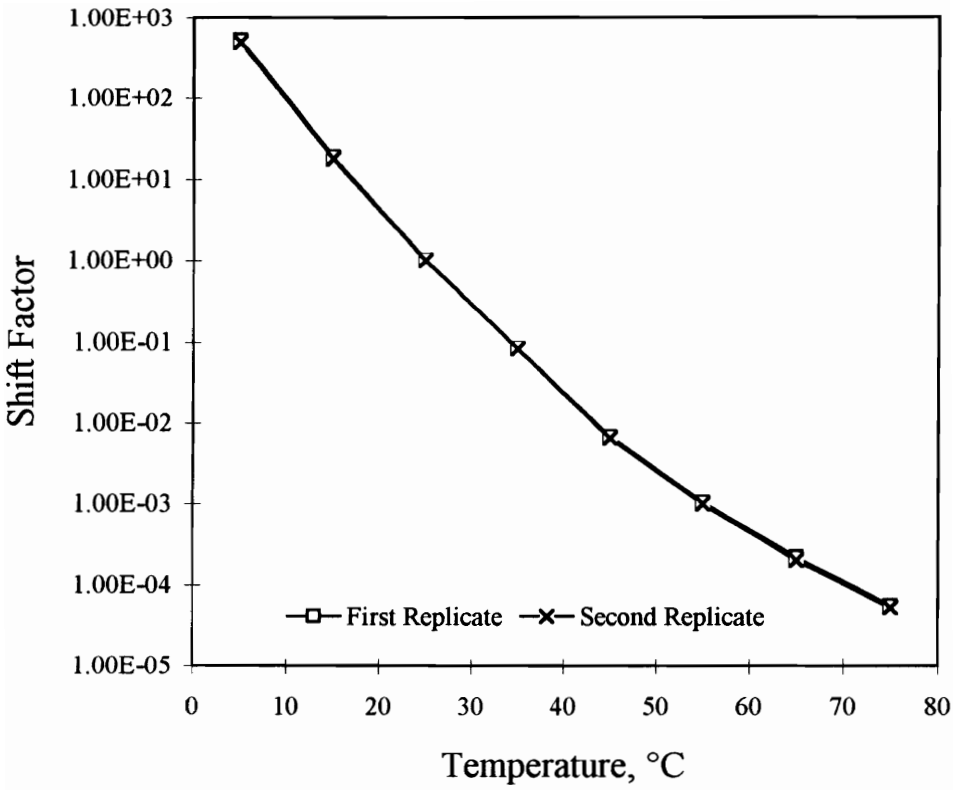

Figure b.28. Shift Factors for ARG3

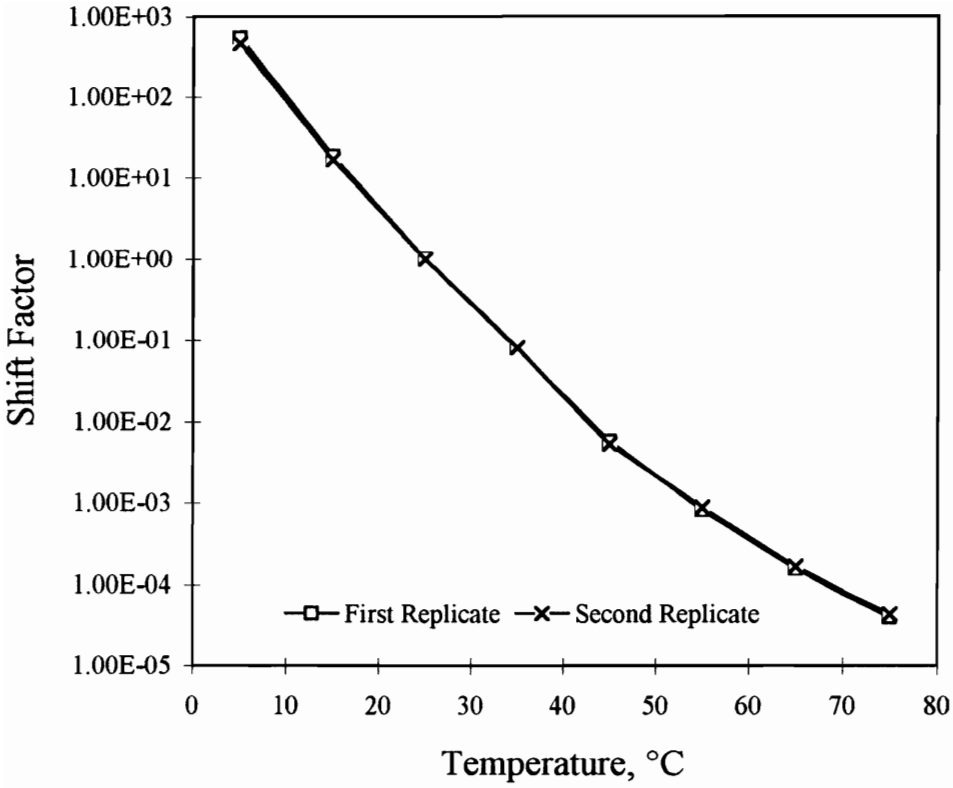

Figure b.29. Shift Factors for ARG4

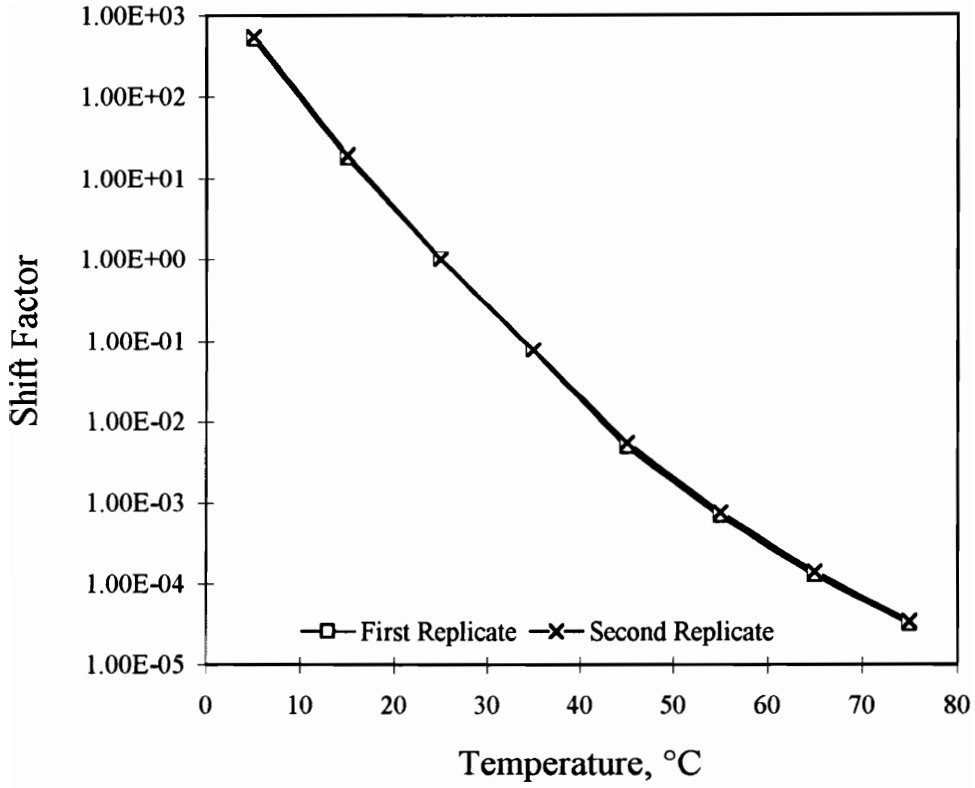

Figure b.30. Shift Factors for ARG5

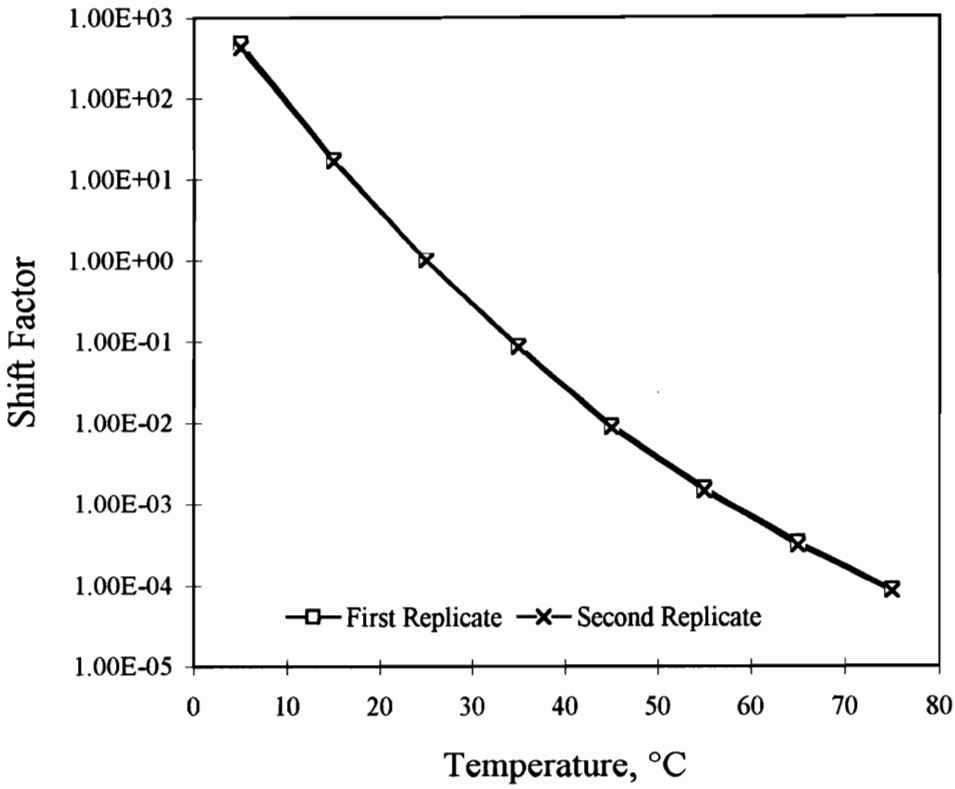

Figure b.31. Shift Factors for AUX3

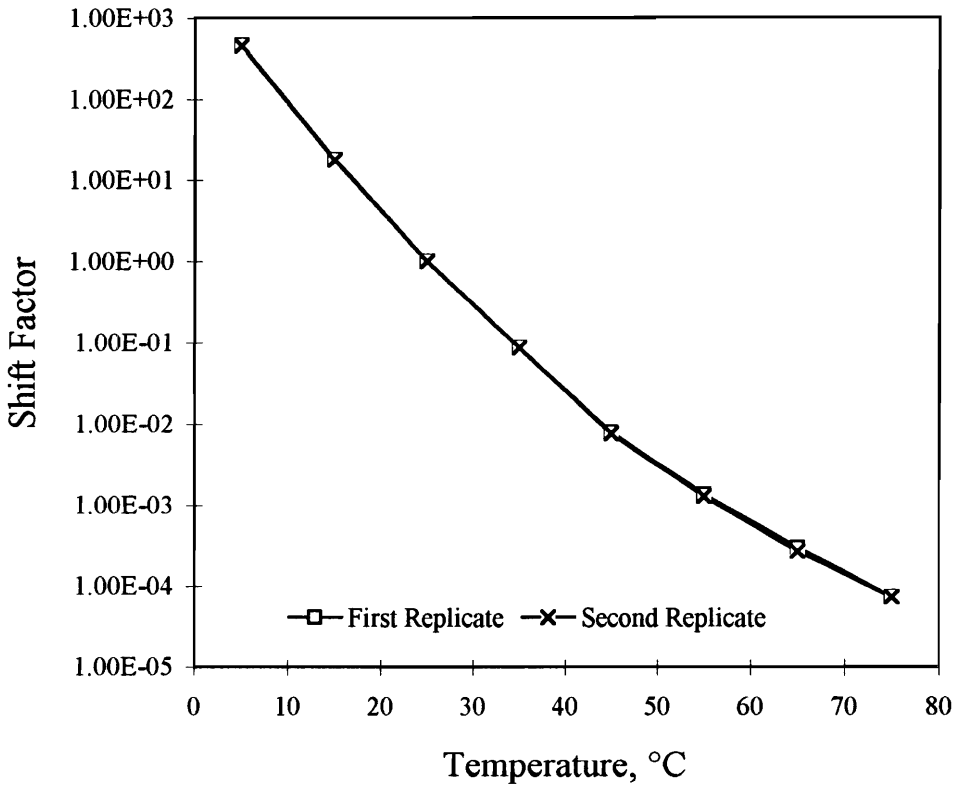

Figure b.32. Shift Factors for AUX4

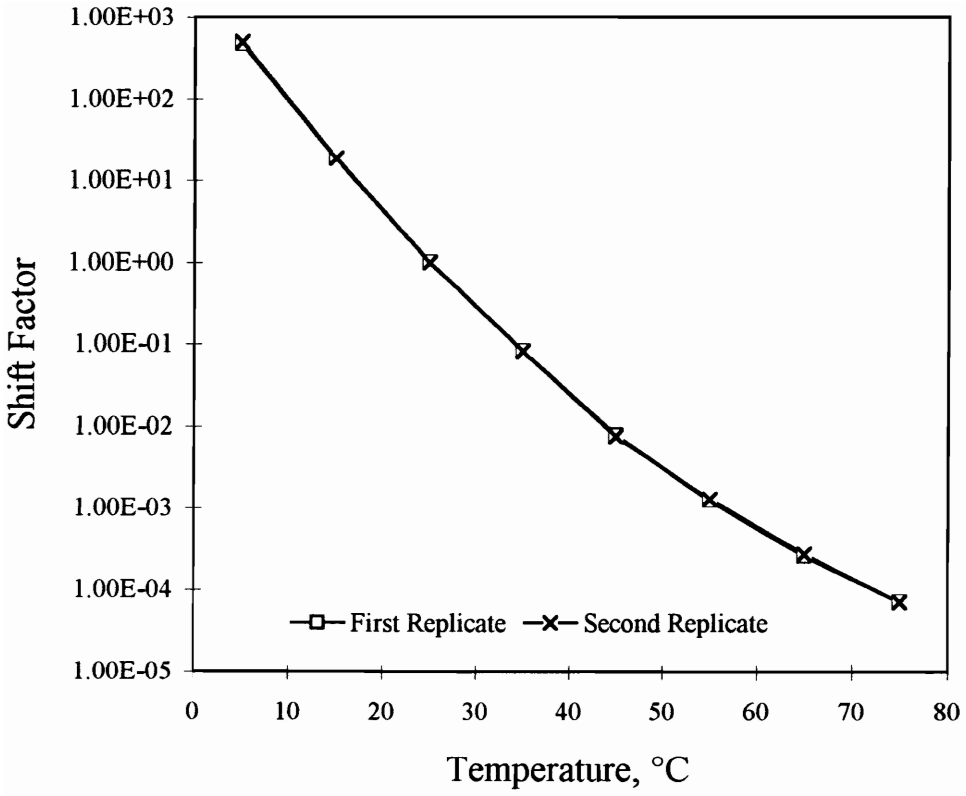

Figure b.33. Shift Factors for AUX5

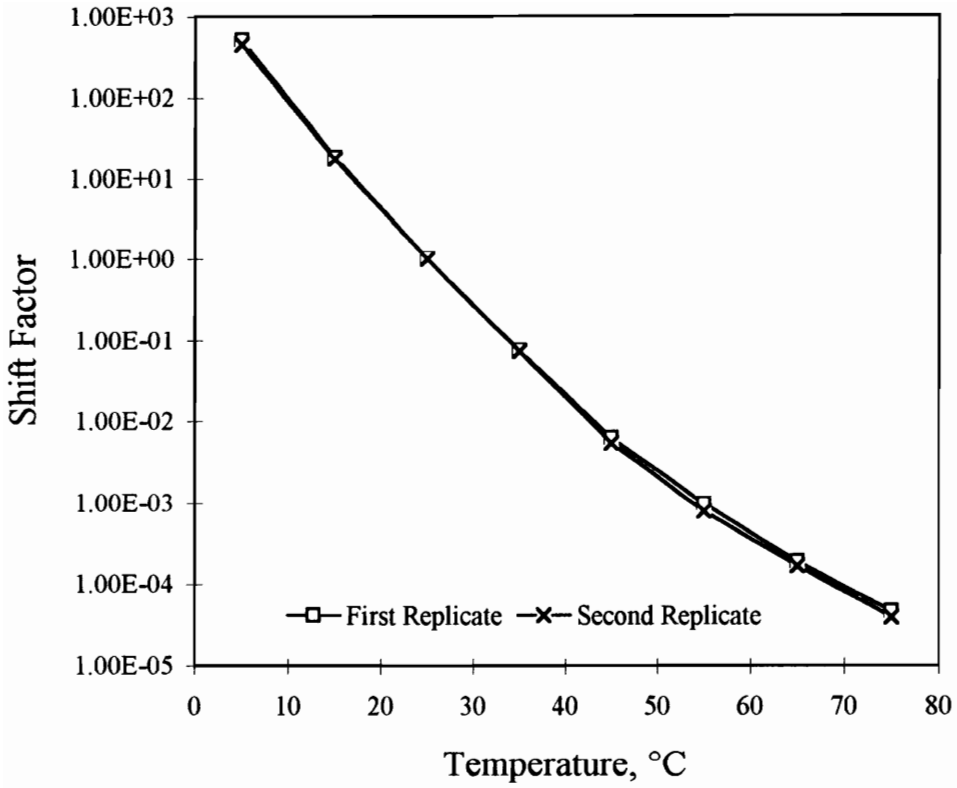

Figure b.34. Shift Factors for ARX3

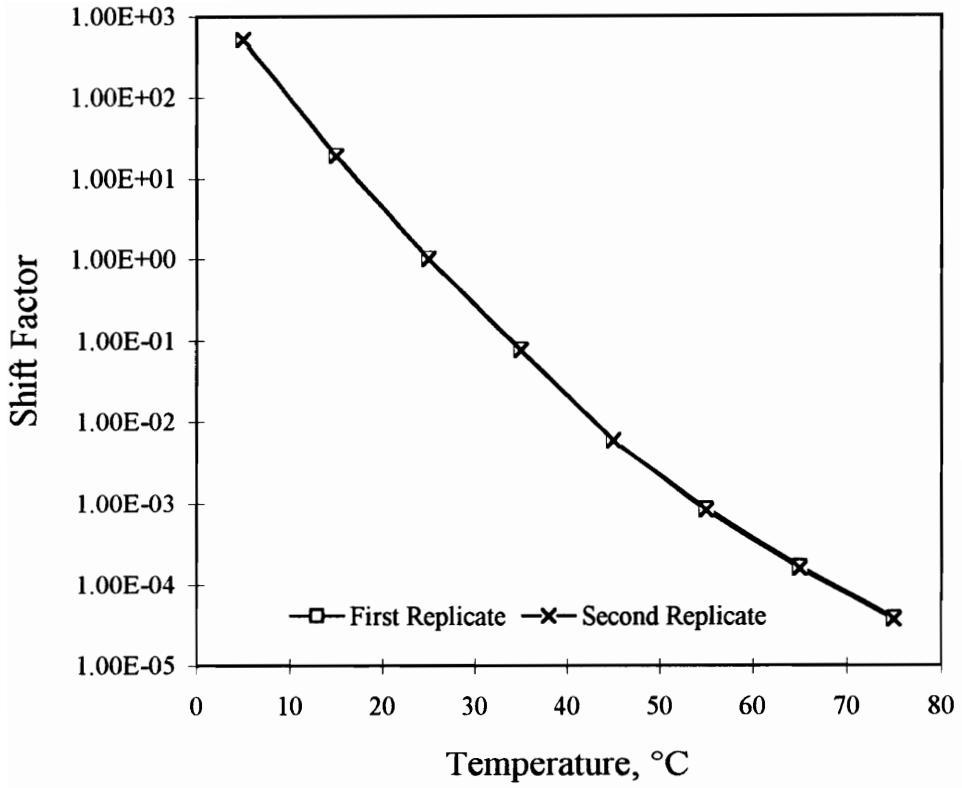

Figure b.35. Shift Factors for ARX4

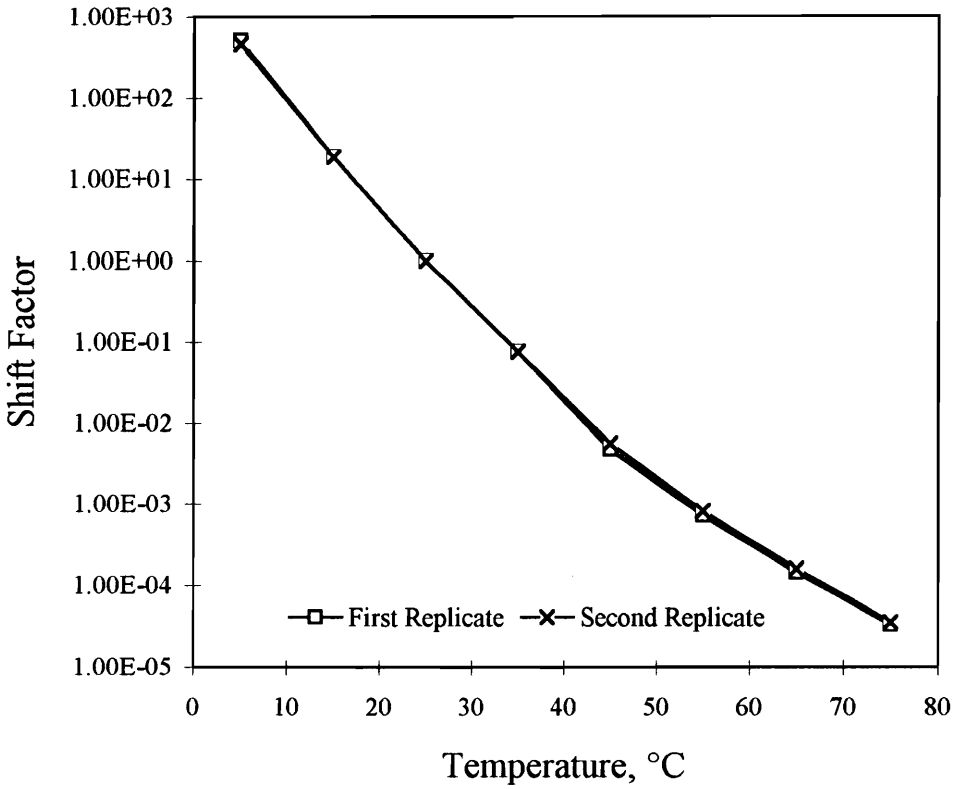

Figure b.36. Shift Factors for ARX5

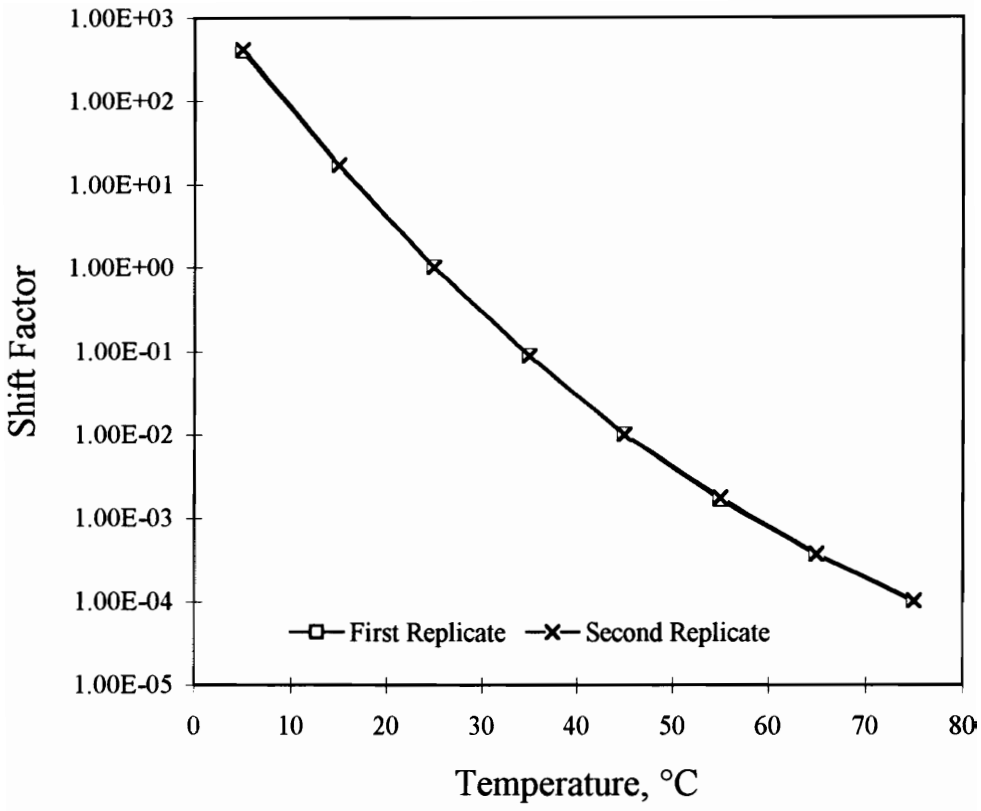

Figure b.37. Shift Factors for AUN3

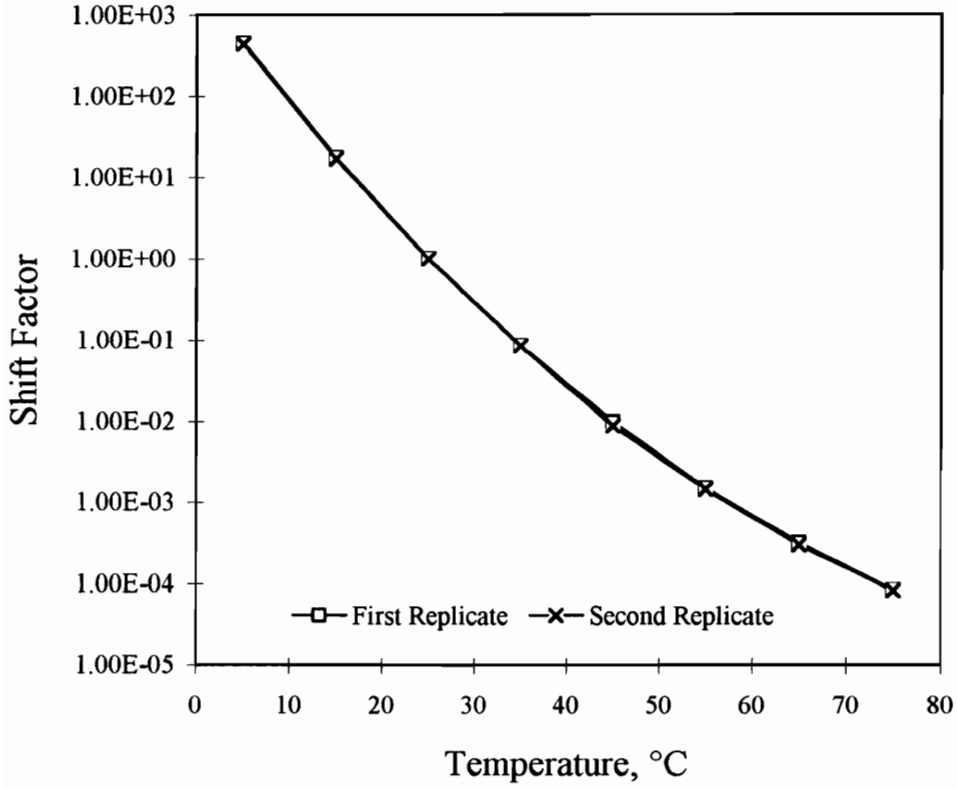

Figure b.38. Shift Factors for AUN4

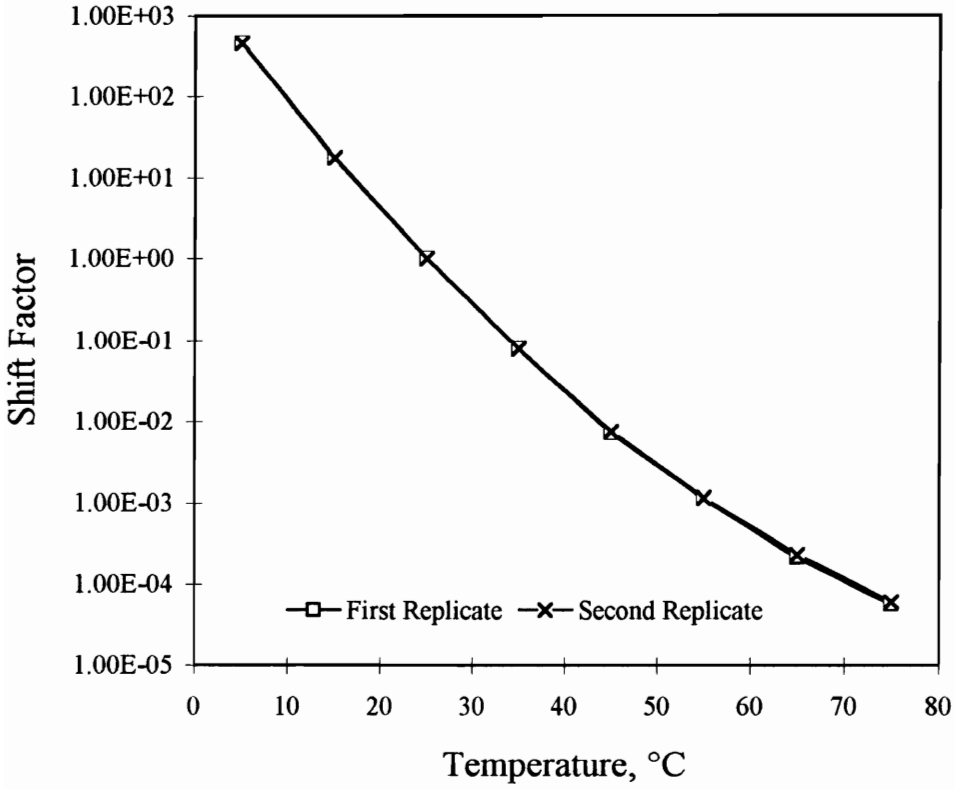

Figure b.39. Shift Factors for AUN5

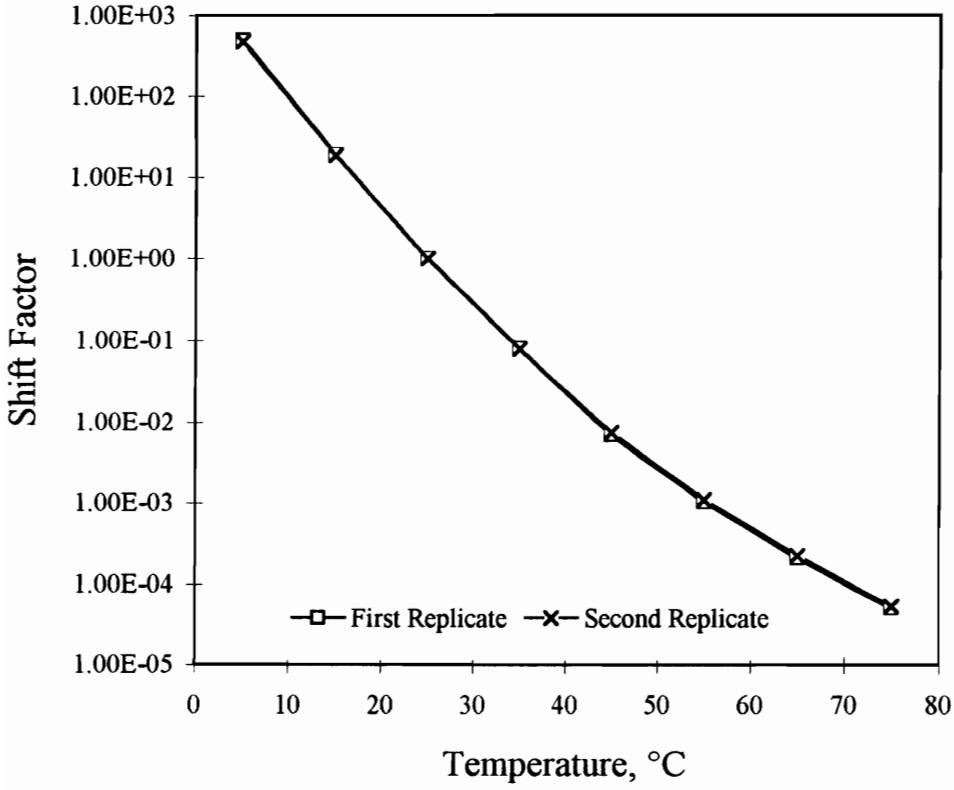

Figure b.40. Shift Factors for ARN3

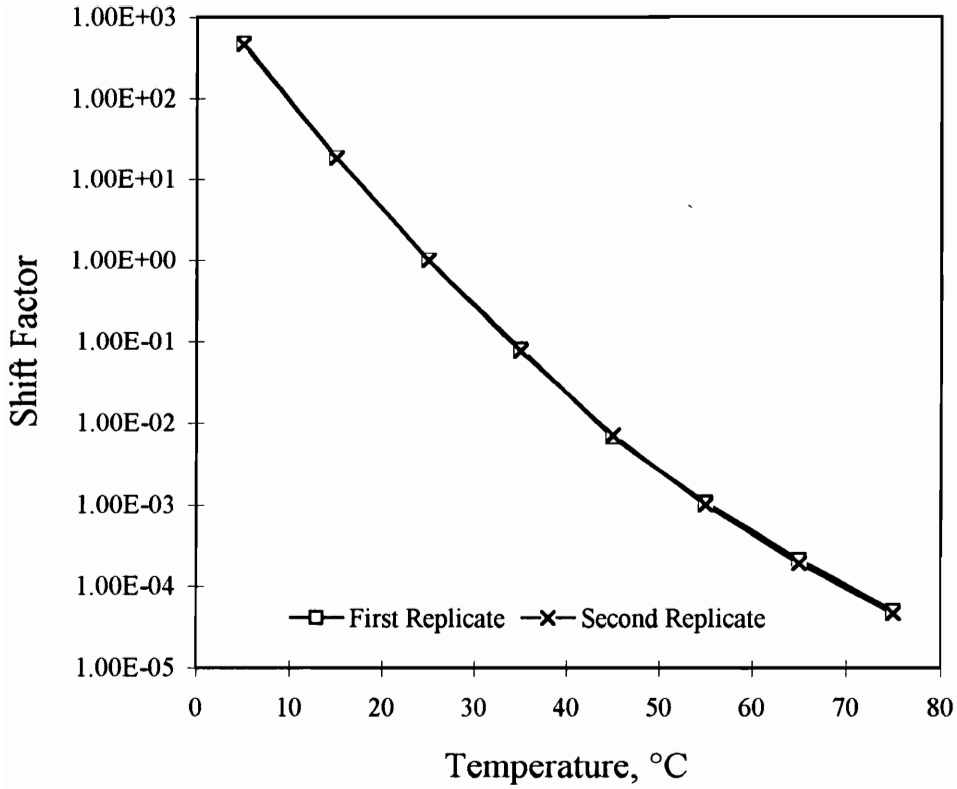

Figure b.41. Shift Factors for ARN4

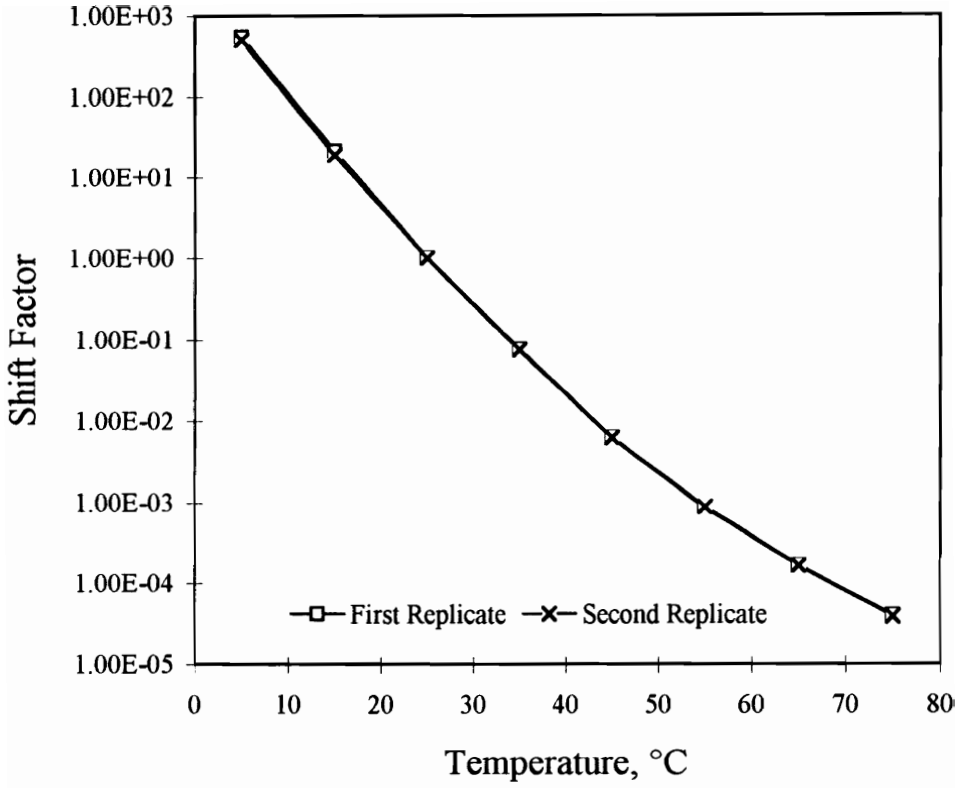

Figure b.42. Shift Factors for ARN5

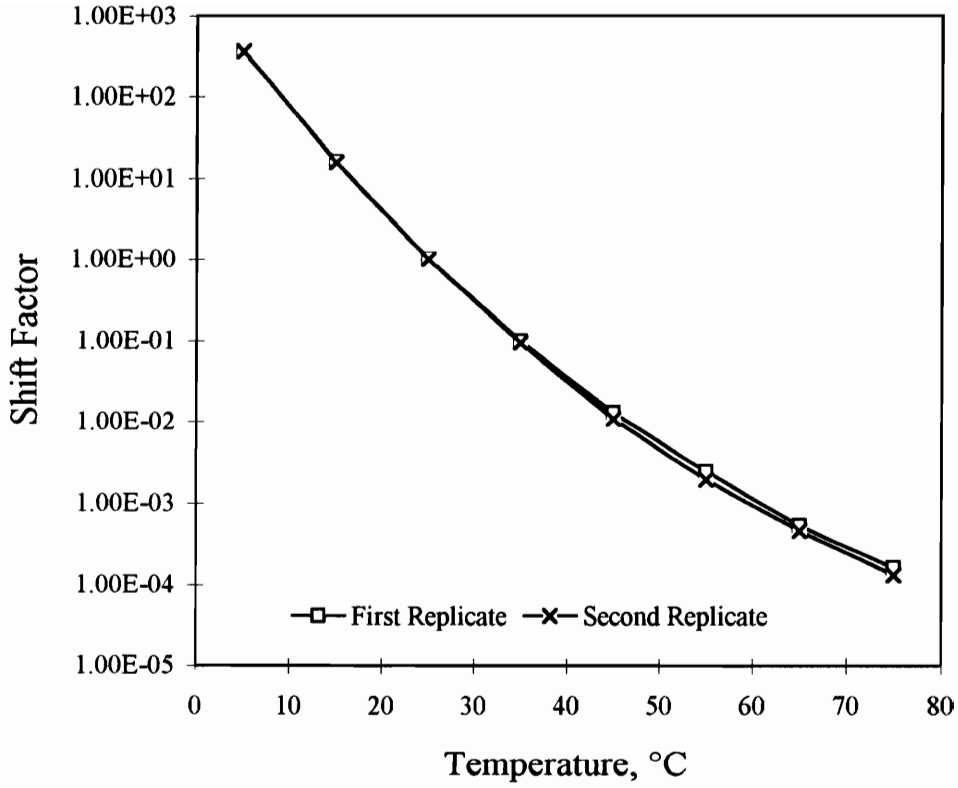

Figure b.43. Shift Factors for AU00

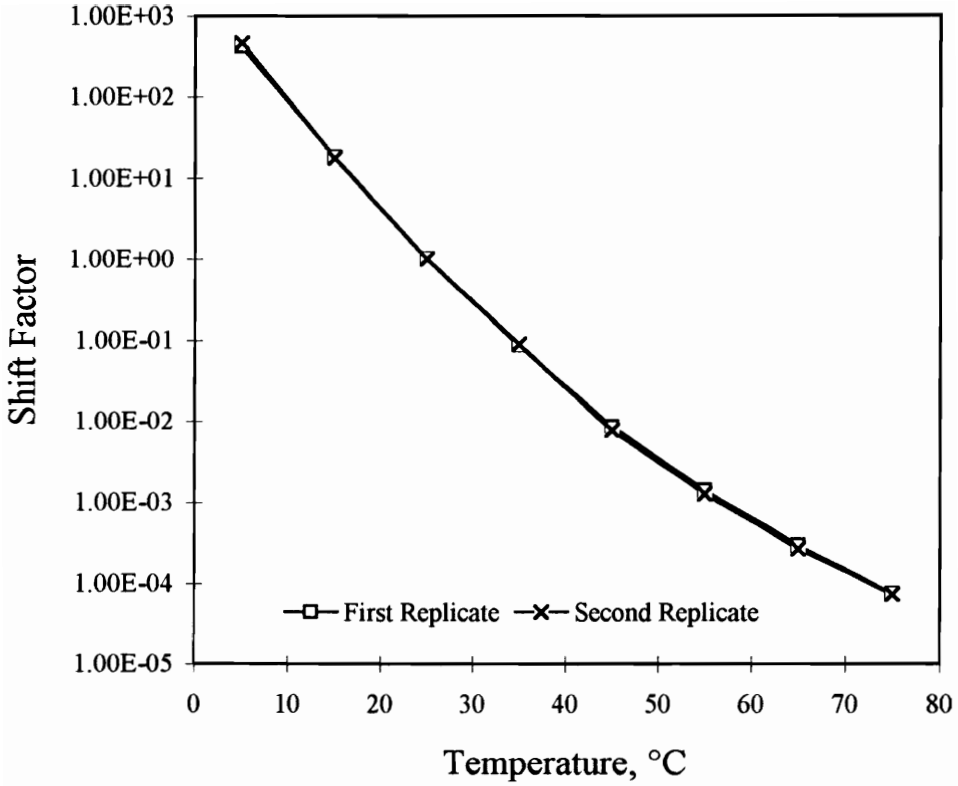

Figure b.44. Shift Factors for AR00

Appendix C

SAS Input and Output Data Files for Non-Linear Least Squares Fit of ARP5 to the Proposed Storage Modulus Equation

INPUT DATA FILE

```
OPTIONS LINESIZE=72;
TITLE 'ARP5 DATA FIT TO PROPOSED STORAGE MODULUS EQUATION';
DATA;
INPUT X Y;
CARDS;
 4.240E+01   3.540E+06
 5.650E+01   4.490E+06
 8.480E+01   5.490E+06
 1.130E+02   6.710E+06
 1.410E+02   7.520E+06
 1.700E+02   8.430E+06
 1.980E+02   9.300E+06
 2.260E+02   1.000E+07
 2.540E+02   1.070E+07
 2.830E+02   1.120E+07
 4.240E+02   1.350E+07
 5.650E+02   1.680E+07
 8.480E+02   1.940E+07
 1.130E+03   2.200E+07
 1.410E+03   2.490E+07
 1.700E+03   2.730E+07
 1.980E+03   3.000E+07
 2.260E+03   3.040E+07
 2.540E+03   3.280E+07
 2.830E+03   3.330E+07
 4.240E+03   3.960E+07
 5.650E+03   4.290E+07
 8.480E+03   5.100E+07
 1.130E+04   5.780E+07
 1.410E+04   5.930E+07
 1.700E+04   6.000E+07
 1.980E+04   6.660E+07
 2.260E+04   6.880E+07
 2.540E+04   7.030E+07
 2.830E+04   7.200E+07
 4.240E+04   7.930E+07
 5.650E+04   8.630E+07
 1.700E+00   3.020E+05
 2.260E+00   3.860E+05
 3.390E+00   5.700E+05
 4.520E+00   6.950E+05
```

5.650E+00	8.160E+05
6.790E+00	9.440E+05
7.920E+00	1.070E+06
9.050E+00	1.150E+06
1.020E+01	1.270E+06
1.130E+01	1.370E+06
1.700E+01	1.820E+06
2.260E+01	2.190E+06
3.390E+01	3.010E+06
4.520E+01	3.590E+06
5.650E+01	4.160E+06
6.790E+01	4.660E+06
7.920E+01	5.250E+06
9.050E+01	5.730E+06
1.020E+02	5.930E+06
1.130E+02	6.430E+06
1.700E+02	8.140E+06
2.260E+02	9.640E+06
3.390E+02	1.210E+07
4.520E+02	1.410E+07
5.650E+02	1.580E+07
6.790E+02	1.720E+07
7.920E+02	1.860E+07
9.050E+02	1.990E+07
1.020E+03	2.100E+07
1.130E+03	2.200E+07
1.700E+03	2.640E+07
2.260E+03	3.040E+07
9.420E-02	2.390E+04
1.260E-01	3.210E+04
1.880E-01	4.570E+04
2.510E-01	5.900E+04
3.140E-01	7.140E+04
3.770E-01	8.450E+04
4.400E-01	9.760E+04
5.030E-01	1.100E+05
5.650E-01	1.210E+05
6.280E-01	1.310E+05
9.420E-01	1.870E+05
1.260E+00	2.410E+05
1.880E+00	3.290E+05
2.510E+00	4.120E+05
3.140E+00	4.940E+05

3.770E+00	5.720E+05
4.400E+00	6.440E+05
5.030E+00	7.130E+05
5.650E+00	7.850E+05
6.280E+00	8.460E+05
9.420E+00	1.140E+06
1.260E+01	1.40E+06
1.880E+01	1.880E+06
2.510E+01	2.290E+06
3.140E+01	2.660E+06
3.770E+01	3.020E+06
4.400E+01	3.350E+06
5.030E+01	3.670E+06
5.650E+01	4.020E+06
6.280E+01	4.220E+06
9.420E+01	5.580E+06
1.260E+02	6.790E+06
8.060E-03	1.920E+03
1.070E-02	2.640E+03
1.610E-02	4.160E+03
2.150E-02	5.470E+03
2.690E-02	6.680E+03
3.220E-02	8.310E+03
3.760E-02	9.970E+03
4.300E-02	1.110E+04
4.830E-02	1.270E+04
5.370E-02	1.380E+04
8.060E-02	2.050E+04
1.070E-01	2.690E+04
1.610E-01	3.880E+04
2.150E-01	5.000E+04
2.690E-01	6.120E+04
3.220E-01	7.180E+04
3.760E-01	8.180E+04
4.300E-01	9.060E+04
4.830E-01	1.020E+05
5.370E-01	1.110E+05
8.060E-01	1.560E+05
1.070E+00	2.010E+05
1.610E+00	2.760E+05
2.150E+00	3.490E+05
2.690E+00	4.170E+05
3.220E+00	4.800E+05

3.760E+00	5.400E+05
4.300E+00	6.000E+05
4.830E+00	6.600E+05
5.370E+00	7.100E+05
8.060E+00	9.680E+05
1.070E+01	1.180E+06
8.340E-04	1.870E+02
1.110E-03	2.470E+02
1.670E-03	3.920E+02
2.220E-03	5.360E+02
2.780E-03	7.100E+02
3.340E-03	8.360E+02
3.890E-03	9.730E+02
4.450E-03	1.170E+03
5.000E-03	1.300E+03
5.560E-03	1.530E+03
8.340E-03	2.240E+03
1.110E-02	3.120E+03
1.670E-02	4.770E+03
2.220E-02	6.130E+03
2.780E-02	8.170E+03
3.340E-02	9.230E+03
3.890E-02	1.110E+04
4.450E-02	1.240E+04
5.000E-02	1.400E+04
5.560E-02	1.580E+04
8.340E-02	2.280E+04
1.110E-01	2.960E+04
1.670E-01	4.360E+04
2.220E-01	5.830E+04
2.780E-01	6.880E+04
3.340E-01	8.360E+04
3.890E-01	9.720E+04
4.450E-01	1.060E+05
5.000E-01	1.240E+05
5.560E-01	1.340E+05
8.340E-01	2.000E+05
1.110E+00	2.530E+05
1.430E-04	2.150E+01
1.900E-04	2.880E+01
2.860E-04	4.560E+01
3.810E-04	6.480E+01
4.760E-04	8.510E+01

5.710E-04	1.040E+02
6.660E-04	1.160E+02
7.620E-04	1.470E+02
8.570E-04	1.720E+02
9.520E-04	1.920E+02
1.430E-03	2.960E+02
1.900E-03	4.120E+02
2.860E-03	6.490E+02
3.810E-03	9.190E+02
4.760E-03	1.140E+03
5.710E-03	1.400E+03
6.660E-03	1.670E+03
7.620E-03	1.960E+03
8.570E-03	2.150E+03
9.520E-03	2.420E+03
1.430E-02	3.780E+03
1.900E-02	5.010E+03
2.860E-02	7.550E+03
3.810E-02	1.010E+04
4.760E-02	1.230E+04
5.710E-02	1.470E+04
6.660E-02	1.720E+04
7.620E-02	1.970E+04
8.570E-02	2.180E+04
9.520E-02	2.390E+04
1.430E-01	3.580E+04
1.900E-01	4.640E+04
3.090E-05	3.100E+00
4.120E-05	3.960E+00
6.180E-05	7.110E+00
8.240E-05	1.010E+01
1.030E-04	1.280E+01
1.240E-04	1.540E+01
1.440E-04	1.950E+01
1.650E-04	2.260E+01
1.850E-04	2.420E+01
2.060E-04	3.000E+01
3.090E-04	4.680E+01
4.120E-04	6.460E+01
6.180E-04	1.090E+02
8.240E-04	1.510E+02
1.030E-03	1.950E+02
1.240E-03	2.450E+02

```
 1.440E-03   2.950E+02
 1.650E-03   3.440E+02
 1.850E-03   3.890E+02
 2.060E-03   4.380E+02
 3.090E-03   7.030E+02
 4.120E-03   9.850E+02
 6.180E-03   1.510E+03
 8.240E-03   2.010E+03
 1.030E-02   2.580E+03
 1.240E-02   3.110E+03
 1.440E-02   3.640E+03
 1.650E-02   4.220E+03
 1.850E-02   4.780E+03
 2.060E-02   5.290E+03
 3.090E-02   7.970E+03
 4.120E-02   1.040E+04
 8.060E-05   8.490E+00
 1.070E-04   1.040E+01
 1.610E-04   1.900E+01
 2.150E-04   2.640E+01
 2.690E-04   3.350E+01
 3.220E-04   4.450E+01
 3.760E-04   5.300E+01
 4.300E-04   6.760E+01
 4.830E-04   7.640E+01
 5.370E-04   8.790E+01
 8.060E-04   1.450E+02
 1.070E-03   2.040E+02
 1.610E-03   3.310E+02
 2.150E-03   4.560E+02
 2.690E-03   5.940E+02
 3.220E-03   7.340E+02
 3.760E-03   8.660E+02
 4.300E-03   1.000E+03
 4.830E-03   1.170E+03
 5.370E-03   1.300E+03
 8.060E-03   1.960E+03
 1.070E-02   2.630E+03
;
X1=LOG10(X);
Y1=LOG10(Y);
PROC NLIN METHOD=DUD;
PARMS P=0.2 L=3 LOGGG=10;
```

```
MODEL Y1=LOGGG*(1-EXP(-P*(X1+L)));
```

OUTPUT DATA FILE

ARP5 DATA FIT TO PROPOSED STORAGE MODULUS EQUATION

Non-Linear Least Squares DUD Initialization Dependent Variable Y1

DUD	P	L	LOGGG	Sum of Squares
-4	0.200000	3.000000	10.000000	574.783481
-3	0.220000	3.000000	10.000000	539.287593
-2	0.200000	3.300000	10.000000	309.745510
-1	0.200000	3.000000	11.000000	532.908576

Non-Linear Least Squares Iterative Phase
Dependent Variable Y1 Method: DUD

Iter	P	L	LOGGG	Sum of Squares
0	0.200000	3.300000	10.000000	309.745510
1	0.153241	4.185701	10.595809	39.302071
2	0.122175	4.831977	11.570378	4.075908
3	0.120193	4.878674	11.722933	2.718625
4	0.120325	4.875611	11.716731	2.716567
5	0.119770	4.899501	11.780349	2.315476
6	0.133724	4.688887	11.307986	0.764458
7	0.132697	4.700913	11.391984	0.599245
8	0.132901	4.704053	11.390361	0.589957
9	0.132962	4.703325	11.385984	0.589736
10	0.132921	4.703697	11.387702	0.589730
11	0.132914	4.703776	11.387918	0.589730
12	0.132913	4.703778	11.387972	0.589730

NOTE: Convergence criterion met.

Non-Linear Least Squares Summary Statistics Dependent Variable Y1

Source	DF	Sum of Squares	Mean Square
Regression	3	6164.3157260	2054.7719087
Residual	243	0.5897295	0.0024269
Uncorrected Total	246	6164.9054555	
(Corrected Total)	245	945.5603539	

Parameter	Estimate	Asymptotic Std. Error	Asymptotic 95 % Confidence Interval	
			Lower	Upper
P	0.13291303	0.00145370963	0.130049510	0.135776543
L	4.70377779	0.00940434703	4.685253108	4.722302463
LOGGG	11.38797158	0.07082177312	11.248466897	11.527476272

Asymptotic Correlation Matrix

Corr	P	L	LOGGG
P	1	-0.826169873	-0.987166098
L	-0.826169873	1	0.74566091
LOGGG	-0.987166098	0.74566091	1

Appendix D

SAS Input and Output Data Files for Non-Linear Least Squares Fit of ARP5 to the Proposed Loss Modulus Equation

INPUT DATA FILE

```
OPTIONS LINESIZE=72;
TITLE 'ARP5 DATA FIT TO PROPOSED LOSS MODULUS EQUATION';
DATA;
INPUT X Y;
CARDS;
 4.240E+01   4.360E+06
 5.650E+01   5.000E+06
 8.480E+01   6.020E+06
 1.130E+02   7.110E+06
 1.410E+02   7.670E+06
 1.700E+02   8.510E+06
 1.980E+02   8.870E+06
 2.260E+02   9.450E+06
 2.540E+02   9.850E+06
 2.830E+02   1.060E+07
 4.240E+02   1.210E+07
 5.650E+02   1.250E+07
 8.480E+02   1.460E+07
 1.130E+03   1.570E+07
 1.410E+03   1.740E+07
 1.700E+03   1.720E+07
 1.980E+03   1.930E+07
 2.260E+03   1.860E+07
 2.540E+03   1.970E+07
 2.830E+03   2.060E+07
 4.240E+03   2.400E+07
 5.650E+03   2.630E+07
 8.480E+03   2.660E+07
 1.130E+04   2.690E+07
 1.410E+04   2.870E+07
 1.700E+04   2.930E+07
 1.980E+04   2.950E+07
 2.260E+04   2.960E+07
 2.540E+04   3.080E+07
 2.830E+04   3.050E+07
 4.240E+04   3.130E+07
 5.650E+04   3.190E+07
 1.700E+00   6.130E+05
 2.260E+00   7.620E+05
 3.390E+00   1.000E+06
 4.520E+00   1.180E+06
```

5.650E+00	1.380E+06
6.790E+00	1.500E+06
7.920E+00	1.710E+06
9.050E+00	1.790E+06
1.020E+01	1.960E+06
1.130E+01	2.070E+06
1.700E+01	2.640E+06
2.260E+01	3.090E+06
3.390E+01	3.920E+06
4.520E+01	4.500E+06
5.650E+01	5.010E+06
6.790E+01	5.480E+06
7.920E+01	5.780E+06
9.050E+01	6.360E+06
1.020E+02	6.600E+06
1.130E+02	7.040E+06
1.700E+02	8.300E+06
2.260E+02	9.440E+06
3.390E+02	1.110E+07
4.520E+02	1.240E+07
5.650E+02	1.360E+07
6.790E+02	1.450E+07
7.920E+02	1.520E+07
9.050E+02	1.600E+07
1.020E+03	1.670E+07
1.130E+03	1.700E+07
1.700E+03	1.900E+07
2.260E+03	2.110E+07
9.420E-02	7.480E+04
1.260E-01	9.370E+04
1.880E-01	1.270E+05
2.510E-01	1.580E+05
3.140E-01	1.870E+05
3.770E-01	2.160E+05
4.400E-01	2.420E+05
5.030E-01	2.680E+05
5.650E-01	2.920E+05
6.280E-01	3.140E+05
9.420E-01	4.200E+05
1.260E+00	5.110E+05
1.880E+00	6.790E+05
2.510E+00	8.290E+05
3.140E+00	9.650E+05

3.770E+00	1.070E+06
4.400E+00	1.190E+06
5.030E+00	1.300E+06
5.650E+00	1.400E+06
6.280E+00	1.480E+06
9.420E+00	1.910E+06
1.260E+01	2.260E+06
1.880E+01	2.870E+06
2.510E+01	3.370E+06
3.140E+01	3.820E+06
3.770E+01	4.200E+06
4.400E+01	4.570E+06
5.030E+01	4.920E+06
5.650E+01	5.270E+06
6.280E+01	5.590E+06
9.420E+01	6.820E+06
1.260E+02	7.850E+06
8.060E-03	1.000E+04
1.070E-02	1.270E+04
1.610E-02	1.790E+04
2.150E-02	2.280E+04
2.690E-02	2.760E+04
3.220E-02	3.190E+04
3.760E-02	3.650E+04
4.300E-02	4.090E+04
4.830E-02	4.500E+04
5.370E-02	4.910E+04
8.060E-02	6.730E+04
1.070E-01	8.460E+04
1.610E-01	1.160E+05
2.150E-01	1.430E+05
2.690E-01	1.700E+05
3.220E-01	1.940E+05
3.760E-01	2.180E+05
4.300E-01	2.400E+05
4.830E-01	2.620E+05
5.370E-01	2.830E+05
8.060E-01	3.780E+05
1.070E+00	4.650E+05
1.610E+00	6.190E+05
2.150E+00	7.550E+05
2.690E+00	8.740E+05
3.220E+00	9.910E+05

3.760E+00	1.090E+06
4.300E+00	1.200E+06
4.830E+00	1.300E+06
5.370E+00	1.380E+06
8.060E+00	1.780E+06
1.070E+01	2.120E+06
8.340E-04	1.390E+03
1.110E-03	1.790E+03
1.670E-03	2.580E+03
2.220E-03	3.350E+03
2.780E-03	4.080E+03
3.340E-03	4.760E+03
3.890E-03	5.490E+03
4.450E-03	6.140E+03
5.000E-03	6.790E+03
5.560E-03	7.480E+03
8.340E-03	1.050E+04
1.110E-02	1.340E+04
1.670E-02	1.870E+04
2.220E-02	2.390E+04
2.780E-02	2.880E+04
3.340E-02	3.320E+04
3.890E-02	3.750E+04
4.450E-02	4.150E+04
5.000E-02	4.580E+04
5.560E-02	5.000E+04
8.340E-02	6.830E+04
1.110E-01	8.520E+04
1.670E-01	1.150E+05
2.220E-01	1.430E+05
2.780E-01	1.690E+05
3.340E-01	1.940E+05
3.890E-01	2.160E+05
4.450E-01	2.400E+05
5.000E-01	2.590E+05
5.560E-01	2.750E+05
8.340E-01	3.630E+05
1.110E+00	4.330E+05
1.430E-04	2.580E+02
1.900E-04	3.370E+02
2.860E-04	4.950E+02
3.810E-04	6.460E+02
4.760E-04	7.970E+02

5.710E-04	9.380E+02
6.660E-04	1.090E+03
7.620E-04	1.230E+03
8.570E-04	1.360E+03
9.520E-04	1.510E+03
1.430E-03	2.180E+03
1.900E-03	2.810E+03
2.860E-03	4.030E+03
3.810E-03	5.240E+03
4.760E-03	6.390E+03
5.710E-03	7.440E+03
6.660E-03	8.590E+03
7.620E-03	9.570E+03
8.570E-03	1.060E+04
9.520E-03	1.160E+04
1.430E-02	1.640E+04
1.900E-02	2.090E+04
2.860E-02	2.900E+04
3.810E-02	3.680E+04
4.760E-02	4.380E+04
5.710E-02	5.070E+04
6.660E-02	5.720E+04
7.620E-02	6.380E+04
8.570E-02	7.050E+04
9.520E-02	7.590E+04
1.430E-01	1.050E+05
1.900E-01	1.310E+05
3.090E-05	5.910E+01
4.120E-05	7.780E+01
6.180E-05	1.170E+02
8.240E-05	1.550E+02
1.030E-04	1.910E+02
1.240E-04	2.280E+02
1.440E-04	2.650E+02
1.650E-04	2.960E+02
1.850E-04	3.300E+02
2.060E-04	3.650E+02
3.090E-04	5.320E+02
4.120E-04	6.990E+02
6.180E-04	1.020E+03
8.240E-04	1.330E+03
1.030E-03	1.640E+03
1.240E-03	1.940E+03

1.440E-03	2.240E+03
1.650E-03	2.520E+03
1.850E-03	2.800E+03
2.060E-03	3.060E+03
3.090E-03	4.400E+03
4.120E-03	5.670E+03
6.180E-03	8.030E+03
8.240E-03	1.030E+04
1.030E-02	1.250E+04
1.240E-02	1.460E+04
1.440E-02	1.660E+04
1.650E-02	1.860E+04
1.850E-02	2.070E+04
2.060E-02	2.240E+04
3.090E-02	3.110E+04
4.120E-02	3.930E+04
8.060E-06	1.610E+01
1.070E-05	2.140E+01
1.610E-05	3.200E+01
2.150E-05	4.210E+01
2.690E-05	5.340E+01
3.220E-05	6.370E+01
3.760E-05	7.230E+01
4.300E-05	8.220E+01
4.830E-05	9.200E+01
5.370E-05	1.010E+02
8.060E-05	1.500E+02
1.070E-04	1.970E+02
1.610E-04	2.910E+02
2.150E-04	3.850E+02
2.690E-04	4.710E+02
3.220E-04	5.620E+02
3.760E-04	6.480E+02
4.300E-04	7.350E+02
4.830E-04	8.230E+02
5.370E-04	9.100E+02
8.060E-04	1.320E+03
1.070E-03	1.720E+03
1.610E-03	2.490E+03
2.150E-03	3.190E+03
2.690E-03	3.920E+03
3.220E-03	4.620E+03
3.760E-03	5.310E+03

```
 4.300E-03   6.010E+03
 4.830E-03   6.740E+03
 5.370E-03   7.310E+03
 8.060E-03   1.040E+04
 1.070E-02   1.320E+04
;
X1=LOG10(X);
Y1=LOG10(Y);
PROC NLIN METHOD=DUD;
PARMS D=4 LOGOMD=4 LOGGMAX=7.5;
MODEL Y1=LOGGMAX+D-SQRT((X1-LOGOMD)**2+D**2);
```

OUTPUT DATA FILE

ARP5 DATA FIT TO PROPOSED LOSS MODULUS EQUATION

Non-Linear Least Squares DUD Initialization Dependent Variable Y1

DUD	D	LOGOMD	LOGGMAX	Sum of Squares
-4	4.000000	4.000000	7.500000	11.734813
-3	4.400000	4.000000	7.500000	31.569994
-2	4.000000	4.400000	7.500000	2.233776
-1	4.000000	4.000000	8.250000	235.202276

Non-Linear Least Squares Iterative Phase
Dependent Variable Y1 Method: DUD

Iter	D	LOGOMD	LOGGMAX	Sum of Squares
0	4.000000	4.400000	7.500000	2.233776
1	4.063378	4.222400	7.426809	0.302686
2	4.073695	4.225381	7.422019	0.299238
3	4.076020	4.227365	7.422682	0.299228
4	4.078130	4.228743	7.422757	0.299218
5	4.078294	4.228756	7.422720	0.299217
6	4.078271	4.228712	7.422706	0.299217
7	4.078132	4.228590	7.422664	0.299217
8	4.078175	4.228632	7.422682	0.299217
9	4.078175	4.228632	7.422682	0.299217

NOTE: Convergence criterion met.

Non-Linear Least Squares Summary Statistics Dependent Variable Y1

Source	DF	Sum of Squares	Mean Square
Regression	3	6924.8312684	2308.2770895
Residual	253	0.2992174	0.0011827
Uncorrected Total	256	6925.1304858	
(Corrected Total)	255	708.0225814	

Parameter	Estimate	Asymptotic Std. Error	Asymptotic 95 % Confidence Interval	
			Lower	Upper
D	4.078175100	0.03593341773	4.0074074599	4.1489427410
LOGOMD	4.228632018	0.02673502260	4.1759797908	4.2812842450
LOGGMAX	7.422682282	0.00842925192	7.4060816273	7.4392829373

Asymptotic Correlation Matrix

Corr	D	LOGOMD	LOGGMAX
D	1	0.9400169754	0.6170517449
LOGOMD	0.9400169754	1	0.8339975648
LOGGMAX	0.6170517449	0.8339975648	1

Appendix E

SAS Input and Output Data Files for Non-Linear Least Squares Fit of ARP5 Shift Factors to WLF Equation

INPUT DATA FILE

```
OPTIONS LINESIZE=72;
TITLE 'ARP5 SHIFT FACTORS FIT TO WLF EQUATION ';
DATA;
INPUT T LOGAT;
CARDS;
5   2.653
15   1.255
25   0
35  -1.068
45  -2.053
55  -2.820
65  -3.484
75  -4.068
5   2.672
15   1.274
25   0
35  -1.068
45  -2.021
55  -2.820
65  -3.470
75  -4.061
;
PROC NLIN METHOD=DUD;
PARMS TS=20 B=1;
MODEL LOGAT=-8.86*(T-TS)/(101.6+T-TS)-B;
```

OUTPUT DATA FILE

ARP5 SHIFT FACTORS FIT TO WLF EQUATION

Non-Linear Least Squares DUD Initialization Dependent Variable LOGAT

DUD	TS	B	Sum of Squares
-3	20.000000	1.000000	23.427404
-2	22.000000	1.000000	18.180287
-1	20.000000	1.100000	26.736909

Non-Linear Least Squares Iterative Phase
Dependent Variable LOGAT Method: DUD

Iter	TS	B	Sum of Squares
0	22.000000	1.000000	18.180287
1	44.984284	1.749505	5.694377
2	36.859088	1.508614	0.726080
3	38.091759	1.558470	0.379988
4	39.315473	1.615938	0.293191
5	39.054460	1.577224	0.292595
6	38.981332	1.584719	0.288914
7	38.982170	1.584716	0.288914
8	38.984035	1.584924	0.288914
9	38.983685	1.584882	0.288914
10	38.983683	1.584882	0.288914

NOTE: Convergence criterion met.

Non-Linear Least Squares Summary Statistics Dependent Variable LOGAT

Source	DF	Sum of Squares	Mean Square
Regression	2	100.79197910	50.39598955
Residual	14	0.28891390	0.02063671
Uncorrected Total	16	101.08089300	
(Corrected Total)	15	78.33037794	

Parameter	Estimate	Asymptotic Std. Error	Asymptotic 95 % Confidence Interval	
			Lower	Upper
TS	38.98368341	0.74427427253	37.387377618	40.579989206

B	1.58488180	0.08294524374	1.406982363	1.762781235

Asymptotic Correlation Matrix

Corr	TS	B
TS	1	0.9014027368
B	0.9014027368	1

Appendix F

Example of Practical Application of Developed Models

The purpose of this appendix is elaborating on the procedure of characterization of response using the proposed mathematical models. This is accomplished through an example for ARC2.

For this binder, the measured values of storage modulus at a temperature of 25° C and arbitrary frequencies of 0.6283, 6.283 and 62.830 rad/s are 9.59×10^4, 6.53×10^5 and 3.64×10^6 Pa, respectively. Substituting these values in equation (4. 5) leads to the following system of simultaneous equations:

$$4.982 = \log G_g\left[1-\exp\left(-p(-0.202+l)\right)\right]$$

$$5.815 = \log G_g\left[1-\exp\left(-p(0.798+l)\right)\right]$$

$$6.561 = \log G_g\left[1-\exp\left(-p(1.798+l)\right)\right] \qquad \text{(f. 1)}$$

The solution to this system of equations is found to be

$l = 4.318$ 1/rad/s $\qquad p = 0.138 \qquad \log G_g = 11.477$ Pa

Therefore, equation (4. 5) is reduced to

$$\log G'(\omega) = 11.477\left[1-\exp\left(-0.138\left(\log\omega+4.318\right)\right)\right] \qquad \text{(f. 2)}$$

The values of storage modulus at any other frequency can then be derived from equation (f. 2). Graph of this equation which represents the analytical storage modulus master curve at a temperature of 25° C is presented in Figure f.1.

The measured loss modulus values at the same temperature and previously stated arbitrary frequencies are 2.53×10^5, 1.29×10^6 and 5.26×10^6 Pa, respectively. Substitution of these values in equation (4. 6) results in the following system of equations:

$$5.403 = \left(\log G''_{\max} + d\right) - \sqrt{\left(-0.202 - \log\omega_d\right)^2 + d^2}$$

$$6.111 = \left(\log G''_{\max} + d\right) - \sqrt{\left(0.708 - \log\omega_d\right)^2 + d^2}$$

$$6.721 = \left(\log G''_{\max} + d\right) - \sqrt{\left(1.798 - \log\omega_d\right)^2 + d^2} \qquad \text{(f. 3)}$$

This system of equations yields the following solutions for the model parameters:

$d = 4.295$ Pa $\qquad \log\omega_d = 4.618$ rad/s $\qquad \log G''_{\max} = 7.564$ Pa

Therefore, the loss modulus values at all frequencies and T = 25° C can be derived from the following equation:

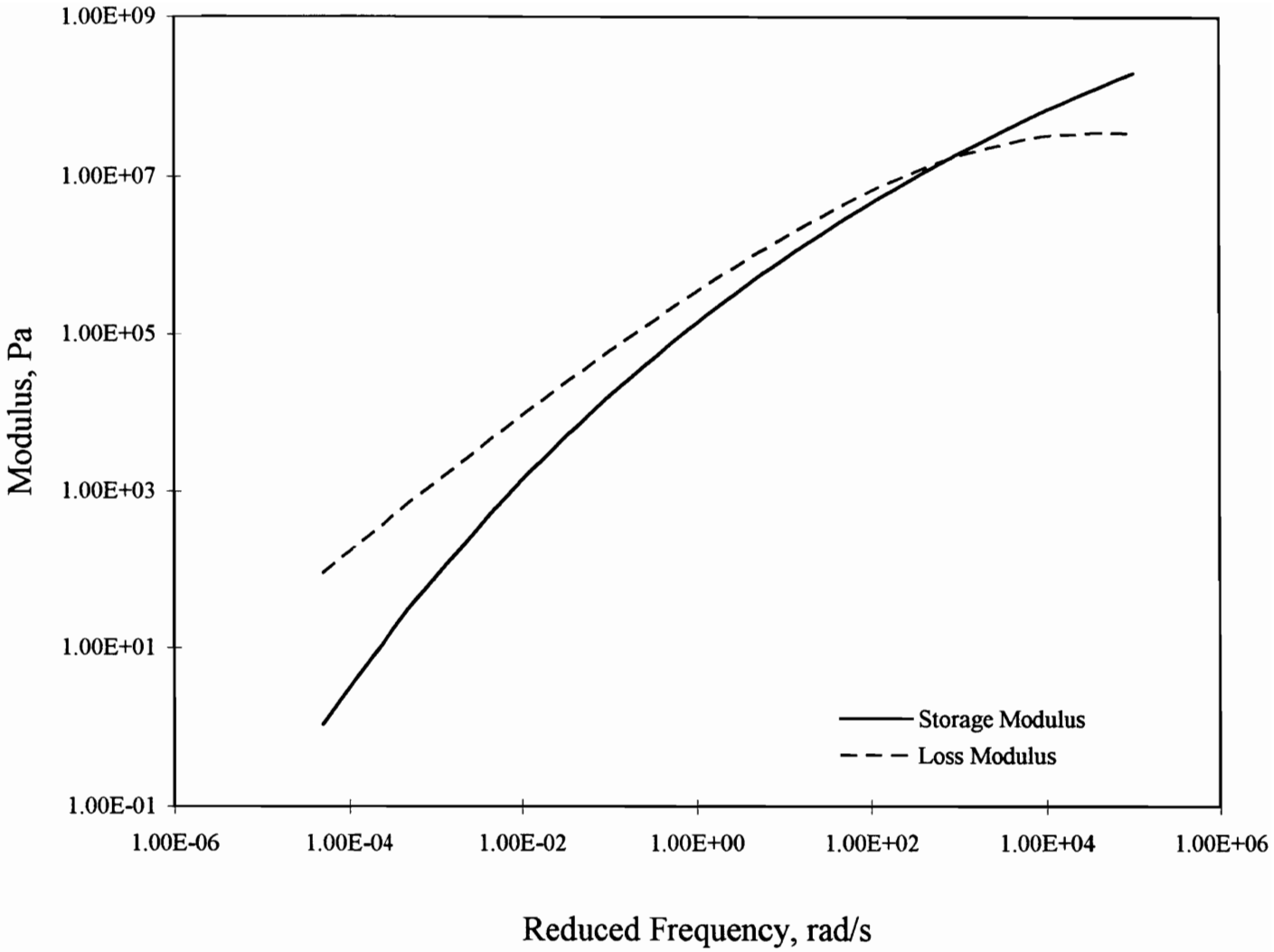

Figure f.1. Analytical Dynamic Master Curves for ARC2 at T=25 C

$$\log G''(\omega) = 11.859 - \sqrt{(\log\omega - 4.618)^2 + 18.447} \qquad \text{(f. 4)}$$

Graph of this equation, i.e., the analytical loss modulus master curve at T = 25° C is shown in Figure f.1.

As stated in Chapter 4, the only temperature dependent coefficients in equations (4. 5) and (4. 6) are location parameters l and $\log\omega_d$. Therefore, in order to characterize the response at any other temperature, the location parameters at that temperature should be evaluated. This can be accomplished by measurement of storage and loss moduli at the desired temperature and at a single arbitrary frequency. For instance, if the response at T = 55° C is desired, and dynamic measurements at ω = 62.830 rad/s have yielded the values of 1.43×10^4 and 5.56×10^4 Pa for storage and loss moduli respectively, one can simply obtain the following from equations (4. 5) and (4. 6):

$$4.155 = 11.477\left[1 - \exp(-0.138(1.798 + l))\right] \qquad \text{(f. 5)}$$

$$4.745 = 11.859 - \sqrt{(1.798 - \log\omega_d)^2 + 18.447} \qquad \text{(f. 6)}$$

Equations (f. 5) and (f. 6) yield the following solutions for the locations parameters at T = 55° C:

l = 1.459 1/rad/s $\qquad\qquad$ $\log\omega_d$ = 7.469 rad/s

Hence, the storage and loss moduli at a temperature of 55° C for all frequencies can be derived from the following equations, respectively:

$$\log G'(\omega) = 11.477\left[1 - \exp\left(-0.138\left(\log\omega + 1.459\right)\right)\right] \qquad \text{(f. 7)}$$

$$\log G''(\omega) = 11.859 - \sqrt{\left(\log\omega - 7.469\right)^2 + 18.447} \qquad \text{(f. 8)}$$

Graphs of these equations which represent the analytical master curves of storage and loss moduli at T = 55° C are shown in Figure f.2.

It should be noted that the difference between location parameters at two temperatures is equal to the shift value between the corresponding master curves along the log frequency axis. Based on parameter *l*, the shift is found to be

$$l|_{T=25} - l|_{T=55} = 4.318 - 1.459 = 2.859,$$

and based on $\log\omega_d$, the shift is derived as

$$\log\omega_d\big|_{T=55} - \log\omega_d\big|_{T=25} = 7.469 - 4.618 = 2.851$$

which is in good agreement with the pervious value.

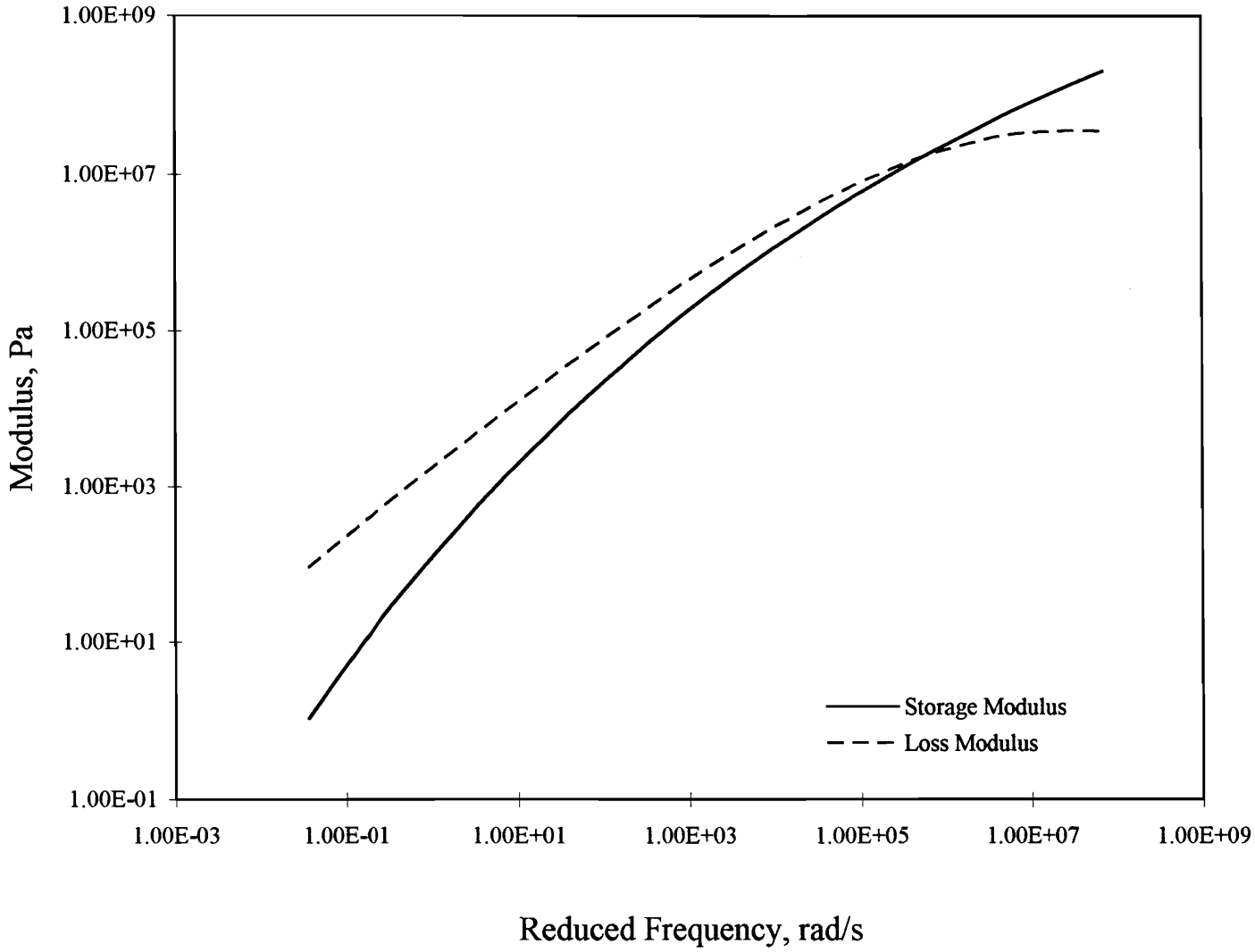

Figure f.2. Analytical Dynamic Master Curves for ARC2 at T=55 C

Vita

The author was born in Tehran, Iran in 1960. After graduating from Kharazmi high school in 1978, he was admitted to the College of Engineering at University of Tehran, where he received a Master of Science in Civil Engineering in 1987. Upon graduation, he worked for a number of consulting firms and construction companies as a structural engineer, and for the Iranian Army Corps of Engineers as part of his military service. He came to Virginia Tech in the spring of 1993 to pursue his Ph.D. in Civil Engineering. He is a member of the American Society of Civil Engineers, Institute of Transportation Engineers, and Chi Epsilon.